

**A LITERATURE REVIEW OF COUPLED  
THERMAL-HYDROLOGIC-  
MECHANICAL-CHEMICAL PROCESSES  
PERTINENT TO THE PROPOSED  
HIGH-LEVEL NUCLEAR WASTE REPOSITORY**

*Prepared for*

**Nuclear Regulatory Commission  
Contract NRC-02-88-005**

*Prepared by*

**Center for Nuclear Waste Regulatory Analyses  
San Antonio, Texas**

**August 1992**



**A LITERATURE REVIEW OF COUPLED  
THERMAL-HYDROLOGIC-MECHANICAL-  
CHEMICAL PROCESSES PERTINENT TO THE  
PROPOSED HIGH-LEVEL NUCLEAR WASTE  
REPOSITORY**

*Prepared for*

**Nuclear Regulatory Commission  
Contract NRC-02-88-005**

*Prepared by*

**Randall D. Manteufel  
Mikko P. Ahola  
David R. Turner  
Asadul H. Chowdhury**

**Center for Nuclear Waste Regulatory Analyses  
San Antonio, Texas**

**August 1992**

## ABSTRACT

A comprehensive literature review has been conducted to determine the state of knowledge available in the modeling of coupled thermal (T), hydrologic (H), mechanical (M), and chemical (C) processes relevant to design and performance of the proposed high-level waste (HLW) repository at Yucca Mountain, Nevada. The review focuses on identifying coupling mechanisms between individual processes, and assessing their importance (i.e., if the coupling is either important, potentially important, or negligible). The significance of considering THMC coupled processes lies in whether or not the processes impact the design and performance objectives of the repository. While some of the coupled processes are relatively well known, many warrant further investigation.

Computer codes will be used extensively to perform coupled analyses for design and performance assessment of the geologic repository. A number of codes can model coupled processes involving two or three processes, however, they frequently have many limitations. Most codes are for continuous medium and significant uncertainties arise with the introduction of fractures. Similarly, significant uncertainties arise in geochemistry, as it has predominately been studied at low temperatures ( $< 100$  °C). Most of these codes are only partially verified against analytical solutions or experimental data. It is expected that reliable prediction of coupled behavior will require numerical predictions using computer codes which have been verified and validated. Hence, the development of adequate mathematical models as well as controlled experimental studies are desirable.

Based on the literature study, processes and their coupled effects are identified as requiring further research and development in relation to the proposed Yucca Mountain repository. A review of the literature, such as reported here, is considered useful in identifying potential coupling mechanisms, assessing their importance, and focusing future research objectives.

# CONTENTS

Section	Page
FIGURES .....	x
TABLES .....	xiii
ACKNOWLEDGEMENTS .....	xv
1 INTRODUCTION .....	1-1
1.1 STATE OF COUPLING IN HLW REPOSITORY ENVIRONMENT .....	1-1
1.2 SINGLE PROCESSES IN THE HLW REPOSITORY ENVIRONMENT .....	1-2
1.3 DESIGN AND PERFORMANCE ISSUES OF THE HLW .....	1-5
1.4 OBJECTIVE AND SCOPE .....	1-5
1.5 SUMMARY OF LITERATURE SEARCH .....	1-6
1.6 STRUCTURE OF REPORT .....	1-7
2 TWO-WAY COUPLING MECHANISMS .....	2-1
2.1 THERMAL -> HYDROLOGIC .....	2-1
2.1.1 Vaporization and Condensation .....	2-1
2.1.2 Dripping in Fractures/Networks .....	2-5
2.1.3 Nonisothermal Enhancement of Vapor Diffusion .....	2-8
2.1.4 Buoyancy Driven Natural Convection .....	2-8
2.1.5 Computer Codes .....	2-13
2.1.5.1 TOUGH .....	2-13
2.1.5.2 VTOUGH .....	2-13
2.1.5.3 PORFLOW .....	2-13
2.1.5.4 FEHMN .....	2-13
2.1.5.5 NORIA and PETROS .....	2-14
2.1.5.6 FRAC-UNIX .....	2-14
2.1.5.7 GEOTHER .....	2-14
2.1.6 Summary and Conclusions .....	2-14
2.2 HYDROLOGIC -> THERMAL .....	2-15
2.2.1 Heat Pipe .....	2-15
2.2.2 Condensate Dripping in Fractures, Boiling Zone .....	2-17
2.2.3 Natural Convection .....	2-20
2.2.4 Material Properties .....	2-24
2.2.5 Summary and Conclusions .....	2-26
2.3 THERMAL -> MECHANICAL .....	2-27
2.3.1 Mechanical Properties and Material Strength .....	2-27
2.3.2 Thermally-Induced Stresses .....	2-27
2.3.3 Computer Codes .....	2-30
2.3.3.1 UDEC, 3DEC .....	2-32
2.3.3.2 SPECTROM-32 .....	2-32
2.3.3.3 STRES3D .....	2-32
2.3.3.4 FLAC .....	2-33
2.3.4 Summary and Conclusions .....	2-33
2.4 MECHANICAL -> THERMAL .....	2-33

## CONTENTS (Cont'd)

Section		Page
2.5	THERMAL -> CHEMICAL . . . . .	2-34
2.5.1	Thermal Effects on Equilibrium Chemistry . . . . .	2-34
2.5.1.1	Equilibrium Constants (Log K) . . . . .	2-34
2.5.1.2	Activity Coefficients . . . . .	2-36
2.5.2	Temperature Effects on Nonequilibrium Chemistry . . . . .	2-37
2.5.3	Computer Codes . . . . .	2-37
2.5.3.1	SUPCRT . . . . .	2-38
2.5.3.2	PHREEQE . . . . .	2-38
2.5.3.3	WATEQ . . . . .	2-39
2.5.3.4	EQ3/EQ6 . . . . .	2-39
2.5.3.5	MINTEQ . . . . .	2-40
2.5.3.6	GEOCHEM . . . . .	2-40
2.5.3.7	ECHEM . . . . .	2-40
2.5.3.8	HYDRAQL . . . . .	2-41
2.5.4	Summary and Conclusions . . . . .	2-41
2.6	CHEMICAL -> THERMAL . . . . .	2-42
2.6.1	Material Properties . . . . .	2-42
2.6.2	Exothermic or Endothermic Reactions . . . . .	2-42
2.6.3	Summary and Conclusions . . . . .	2-43
2.7	HYDROLOGIC -> MECHANICAL . . . . .	2-43
2.7.1	Mechanical Properties . . . . .	2-43
2.7.2	Buffer Swelling . . . . .	2-44
2.7.3	Summary and Conclusions . . . . .	2-44
2.8	MECHANICAL -> HYDROLOGICAL . . . . .	2-44
2.8.1	Effective Hydraulic Conductivity . . . . .	2-45
2.8.2	Seismic Pumping . . . . .	2-48
2.8.3	Summary and Conclusions . . . . .	2-50
2.9	HYDROLOGIC -> CHEMICAL . . . . .	2-50
2.9.1	Equilibrium Solute Transport . . . . .	2-51
2.9.2	Nonequilibrium Solute Transport . . . . .	2-54
2.9.2.1	Two-Region Transport . . . . .	2-54
2.9.2.2	Two-Site Transport . . . . .	2-56
2.9.2.3	Stochastic Models . . . . .	2-57
2.9.3	Computer Codes . . . . .	2-57
2.9.3.1	HYDROGEOCHEM . . . . .	2-59
2.9.3.2	DYNAMIX . . . . .	2-59
2.9.3.3	CHEQMATE . . . . .	2-60
2.9.3.4	TRANQL . . . . .	2-60
2.9.3.5	FASTCHEM . . . . .	2-60
2.9.3.6	CTM . . . . .	2-61
2.9.3.7	CHEMTRN . . . . .	2-61
2.9.3.8	CHMTRNS . . . . .	2-61
2.9.3.9	NEFTRAN and TRACR3D . . . . .	2-62

## CONTENTS (Cont'd)

Section		Page
2.9.4	Summary and Conclusions .....	2-62
2.10	CHEMICAL -> HYDROLOGIC .....	2-62
2.10.1	Mineralogy of Fracture Surfaces .....	2-62
2.10.2	Fracture Healing .....	2-63
2.10.3	Chemical Osmosis .....	2-63
2.10.4	Fluid Properties .....	2-64
2.10.5	Summary and Conclusions .....	2-71
2.11	MECHANICAL -> CHEMICAL .....	2-71
2.11.1	Pressure Effects on Chemical Equilibrium .....	2-72
2.11.2	Pressure Effects on Nonequilibrium Chemistry .....	2-74
2.11.3	Pressure Solution .....	2-74
2.11.4	Computer Codes .....	2-75
2.11.4.1	SUPCRT .....	2-75
2.11.4.2	EQ3/EQ6 .....	2-75
2.11.5	Summary and Conclusions .....	2-75
2.12	CHEMICAL -> MECHANICAL .....	2-76
2.12.1	Chemical Effects on Rock Fracture Propagation .....	2-76
2.12.2	Degradation of Mechanical Properties Due to Chemical Action .....	2-77
2.12.3	Stress Corrosion Cracking .....	2-79
2.12.4	Summary and Conclusions .....	2-83
3	THREE-WAY COUPLED PROCESSES .....	3-1
3.1	THERMAL-HYDROLOGIC-MECHANICAL COUPLING .....	3-1
3.1.1	DECOVALEX International Project .....	3-2
3.1.2	Computer Codes for THM Modeling .....	3-5
3.1.2.1	ROCMAS .....	3-5
3.1.2.2	GENASYS .....	3-5
3.1.2.3	THAMES .....	3-8
3.1.2.4	FEHMS .....	3-8
3.1.3	Summary and Conclusions .....	3-8
3.2	THERMAL-HYDROLOGIC-CHEMICAL COUPLING .....	3-8
3.2.1	Effects of Coupling on Material Properties and Media Characteristics .....	3-9
3.2.2	Onsager's Coupled Processes .....	3-11
3.2.3	Computer Codes .....	3-12
3.2.3.1	CHMTRNS .....	3-13
3.2.3.2	THCC .....	3-13
3.2.3.3	Codell and Murphy (1992) .....	3-13
3.2.3.4	HYDROGEOCHEM .....	3-13
3.2.3.5	Cline et al. (1992) .....	3-14
3.2.4	Summary and Conclusions .....	3-14
4	FOUR-WAY COUPLED PROCESSES .....	4-1
4.1	PERFORMANCE OBJECTIVES .....	4-1

## CONTENTS (Cont'd)

Section	Page
4.2	4-1
4.3	4-6
5	5-1
5.1	5-1
5.2	5-2
5.3	5-2
6	6-1
APPENDIX A. THERMAL PROCESSES	A-1
A.1	A-2
A.1.1	A-2
A.1.2	A-3
A.2	A-6
A.2.1	A-6
A.2.2	A-8
A.3	A-9
A.4	A-11
APPENDIX B. HYDROLOGIC PROCESSES	B-1
B.1	B-2
B.1.1	B-2
B.1.2	B-3
B.1.3	B-5
B.2	B-5
B.3	B-8
B.4	B-12
APPENDIX C. MECHANICAL PROCESSES	C-1
C.1	C-2
C.2	C-4
C.3	C-6
C.3.1	C-6
C.3.2	C-7
C.3.3	C-8
C.4	C-8

## CONTENTS (Cont'd)

Section		Page
	APPENDIX D. CHEMICAL PROCESSES .....	D-1
D.1	EQUILIBRIUM CHEMICAL PROCESSES .....	D-2
D.2	NONEQUILIBRIUM CHEMICAL PROCESSES .....	D-5
D.3	REACTION PROGRESS MODELS .....	D-7
D.4	THERMODYNAMIC DATABASES .....	D-8
D.5	COUPLING WITH OTHER PROCESSES .....	D-8

## FIGURES

Figure	Page
2-1 An Axisymmetric Model of a Geologic Repository . . . . .	2-3
2-2 A Two-Dimensional, Cartesian Model of a Geologic Repository . . . . .	2-3
2-3 Saturation and Temperature Distributions Through the Center of a Repository from Ground Surface (depth = 0 m) to Water Table (depth = 500 m) at Time = (10,50,100,200,1000) Years . . . . .	2-4
2-4 Illustration of a Drift with Vertical Emplacement of a Waste Canister in a Fractured Porous Medium . . . . .	2-6
2-5 Illustration of a Dry Zone and a Condensation Zone with Condensate Dripping in Fractures for Short Times (above) and Longer Times (below) . . . . .	2-7
2-6 Buoyancy Driven Convection Patterns Around a Saturated Repository . . . . .	2-10
2-7 Illustration of Convective Circulation Pattern for the Gas Phase . . . . .	2-10
2-8 Critical Rayleigh Number (for the Benard Problem) Versus Dimensionless Permeability from Darcy's Limit to the Viscous Fluid Limit . . . . .	2-11
2-9 Gas Flux at 100 Years After Waste Emplacement Showing Flow Away from Repository Primarily Due to Diffusion of Water Vapor . . . . .	2-12
2-10 Gas Flux at 100 Years After Waste Emplacement Neglecting Molecular Diffusion of Water Vapor . . . . .	2-12
2-11 Schematic of Heat-Transfer Regimes in a Plane Perpendicular to the Axis of the Waste Package (not to scale) . . . . .	2-16
2-12 Numerically-Simulated Saturation, Pressure, Temperature, and Air-Mole-Fraction Profiles at Various Times. A Heat Pipe is Evident by a Temperature "Plateau." . . . .	2-18
2-13 Temperature Profiles Showing a Lack of a Plateau Near 100 °C, Hence the Absence of a Heat Pipe. Calculations Based on an Explicit Fracture Model and an Effective Continuum Model Using Hydrologic Properties Representative of Topopah Spring Densely Welded Tuff. . . . .	2-19
2-14 Location of Thermocouples, Major Fractures, and Heater in G-Tunnel Heater Tests . . .	2-21
2-15 Temperature History of Selected Thermocouples Below the Heater . . . . .	2-22
2-16 Temperature History of Selected Thermocouples Above the Heater . . . . .	2-22
2-17 Two-Dimensional Model of the Overlying Medium at a Geologic Repository . . . . .	2-23
2-18 Experimental Results Which Reflect Repository Conditions for a Saturated, Homogeneous, Isotropic Medium . . . . .	2-23
2-19 Experimental Apparatus Used to Measure the Thermal Conductivity of Apache Leap Tuff as a Function of Water Content . . . . .	2-25
2-20 Thermally Induced Normal Fracture Displacement (a) for Horizontal Fracture Zone Just Beneath the Repository and (b) of Vertical Fracture Zone Intersecting Repository. A Positive Sign Indicates Opening Displacement. . . . .	2-29
2-21 Thermomechanical Environment in the Vicinity of (a) Waste Emplacement Drift and (b) Tuff Main Access Drift at the Proposed Repository Beneath Yucca Mountain . . . . .	2-31
2-22 Illustration of Axial, Radial, and Circumferential Fractures Around a Circular Excavation . . . . .	2-46
2-23 Illustration of Normal Stresses in the Circumferential ( $\sigma_{\theta\theta}$ ) and Radial ( $\sigma_{rr}$ ) Orientation Around a Circular Excavation . . . . .	2-47

## FIGURES (Cont'd)

Figure		Page
2-24	Water-Table Response for Isotropic Permeability and for Local Vertical Permeability Enhancement ( $10$ to $10^3$ ) Within 100-m-Wide Anisotropic Region Centered on Normal Fault Simulating Zone of Vertical Fracturing . . . . .	2-49
2-25	Water Density as a Function of Temperature for Different Salinities ( $m$ = moles NaCl/kg $H_2O$ ) at a Constant Pressure of 10 MPa $\approx$ 100 atm . . . . .	2-65
2-26	Dynamic Viscosity of Water as a Function of Salinity for Constant $P = 10$ MPa $\approx$ 100 atm . . . . .	2-66
2-27	Shifting of the Vapor-Liquid Line for Pure Water (Solid Line) with the Addition of 10 wt% NaCl (Dotted Line) and 25 wt% NaCl (Dashed Line). The Critical Points are also Shown. The Straight Lines are Isochores Representing Constant Density Fluids with P-T. The Numbers Represent the Density in $g/cm^3$ . . . . .	2-67
2-28	P-T Plot of Isocompositional Curves for the Gas Phase in Equilibrium with the Liquid Phase for the System $H_2O-CO_2$ . The Critical Curve for the System Extends from the Critical Point for Water ( $374$ °C and 220 bars) to Lower Temperatures and Higher Pressures. The Minimum Critical Temperature Occurs at Approximately $266$ °C and about 2150 bars. . . . .	2-69
2-29	Soil Water Diffusivity as a Function of Water Content and Sodium Adsorption Ratio (SAR) at Different Electrolyte Concentrations ( $C = 20$ to 250 meq/l). SAR is a Measure of Total Solution $Na^+$ Concentration Relative to $Ca^{++} + Mg^{++}$ (i.e. $SAR = C_{Na}/[C_{Mg} + C_{Ca}]^{1/2}$ ). The Salinity Effect Increases with Increasing SAR. . .	2-70
2-30	Crack Propagation Stress of Synthetic and Natural Quartz Samples Plotted Versus Chemical Environment . . . . .	2-78
2-31	Resistance to SCC as a Function of Applied Stress. Metals are Commercial Stainless Steel in Boiling 42% $MgCl_2$ at $154$ °C . . . . .	2-80
2-32	Crack Growth Rate (m/s) as a Function of Stress Intensity (MPa $m^{1/2}$ ) for Type 304 Stainless Steel . . . . .	2-81
2-33	Susceptibility of Fe-18Cr-xNi Alloys to SCC in Boiling 42% $MgCl_2$ as a Function of Nickel Content . . . . .	2-82
3-1	Coupled Thermo-Hydrologic-Mechanical (THM) Bench-Mark Problem for DECOVALEX. (a) Block Geometry Showing Locations of Monitoring Points and Applied Heat Flux (b) Zone Discretization for Discrete Element Code UDEC. . . . .	3-3
3-2	Coupled THM Bench-Mark Problem for DECOVALEX. (a) Temperature Contours Assuming Only Conduction Heat Transfer through the Rock Medium. (b) Temperature Contours Taking into Account Conduction as well as the Effect of Forced Convection through the Horizontal Fractures. . . . .	3-4
3-3	Coupled Thermal-Hydraulic-Mechanical Analyses Using ROCMAS Showing (a) Finite Element Model of the Source Environment and (b) Variation of Fluid Inflow to the Heater Borehole as a Function of Time after Heater is Turned on . . . . .	3-6
3-4	Pressure and Aperture Profiles in the Fracture Generated by ROCMAS for Various Durations, and Temperature Profiles Along Heater Midplane . . . . .	3-7

## FIGURES (Cont'd)

Figure	Page
4-1	Illustration of the Important Processes and Couplings During the Operation, Containment, and Isolation Periods for Anticipated Processes and Events at the Proposed Repository. The Right Column is a Subset of the Left Where only Primary Couplings Which Feed into the Processes of Primary Regulatory Interest are Shown . . . .
	4-5
A-1	Relative Thermal Power of HLW Showing the Importance of Fission Products at Short Times and Actinides at Long Times . . . . .
	A-5
A-2	Typical Temperature Histories of Waste Package Components and Host Rock near Emplaced Spent Fuel Canister . . . . .
	A-7
A-3	Comparison of Experimental Measurements of the Emissivity of Oxidized Zircaloy (spent fuel rods) . . . . .
	A-10
B-1	East-West Cross-Sectional Illustration Highlighting the Different Hydrogeologic Units in the Unsaturated Zone at Yucca Mountain . . . . .
	B-6
B-2	Effective Continuum Permeability as a Function of Saturation Showing Influences of Matrix and Fracture Flow . . . . .
	B-10
B-3	Comparison of Calculated and Measured Liquid Saturation Profiles for Various Steady-State, One-Dimensional Recharge Fluxes. Calculated Values Based on an Effective Continuum Model and Measured Values are from the Reference Information Base (RIB) . . . . .
	B-11
D-1	Distinctions Between Classes of Chemical Reactions . . . . .
	D-3

## TABLES

Table		Page
1-1	Diagrams of Uncoupled and Coupled Processes . . . . .	1-3
1-2	Types of Coupled Processes . . . . .	1-4
1-3	Databases Searched for Articles on Coupled Thermal-Hydrologic-Mechanical-Chemical Processes . . . . .	1-8
1-4	List of Journals Explicitly Reviewed for 1991 and 1992 . . . . .	1-9
3-1	Summary of Driving Potentials, Fluid Pressure, Temperature, and Species Concentration, and How They are Expected to Generate a Flux of Fluid, Heat or Species . . . . .	3-12
4-1	Assessment of the Importance of Coupled THMC Processes for Anticipated Processes and Events, for Performance Objectives Associated with the Operations Time Period of the Proposed HLW Repository (10 CFR 60.111) . . . . .	4-2
4-2	Assessment of the Importance of Coupled THMC Processes for Anticipated Processes and Events, for Performance Objectives Associated with the Containment Time Period at the Proposed HLW Repository (10 CFR 60.113) . . . . .	4-2
4-3	Assessment of the Importance of Coupled THMC Processes for Anticipated Processes and Events, for Performance Objectives Associated with the Isolation Time Period at the Proposed HLW Repository (10 CFR 60.112) . . . . .	4-2
B-1	Summary of Hydrogeologic Properties Relevant to Yucca Mountain . . . . .	B-7
D-1	Examples of Tabulations of Thermodynamic Data . . . . .	D-9

## ACKNOWLEDGEMENTS

The authors would like to thank Simon M. Hsiung, Budhi Sagar, Amvrossios C. Bagtzoglou, Bret W. Leslie, Gustavo A. Cragnolino, and Robert G. Baca for their technical reviews of this document. The authors are also thankful to Cathy Garcia and Cathy Cudd, for skillful typing and formatting of the report, and to Curtis Gray and Don Moore, who provided a full range of expert editorial services in the preparation of the final document.

This report was prepared to document work performed by the Center for Nuclear Waste Regulatory Analyses (CNWRA) for the NRC under Contract No. NRC-02-88-005. The activities reported here were performed on behalf of the NRC Office of Nuclear Material Safety and Safeguards, Division of High-Level Waste Management. The report is an independent product of the CNWRA and does not necessarily reflect the views or regulatory position of the NRC.

# 1 INTRODUCTION

## 1.1 STATE OF COUPLING IN HLW REPOSITORY ENVIRONMENT

Despite the similarity between an underground mine and a mined geologic repository system, substantial differences exist in the analysis and design practice of underground openings of these two types of facilities. These are because the considerations for repository design are different from the underground mine design considerations; these include factors such as the thermal load of heat-generating waste, the time and space scales required for effective waste isolation, and the legal and regulatory environment in which waste isolation is to be engineered and managed.

Yucca Mountain in southern Nevada has been designated by the United States Congress for characterization as a potential repository site for nuclear waste disposal. The geomechanical conditions at the site are characterized by a highly-fractured rock material with prominent vertical and sub-vertical jointing, and faults which transgress the site environs. One unique feature of the proposed site is that the host rock is partially saturated and is several hundred meters above the groundwater table. This feature is substantially different from proposed high-level waste repositories in other countries, all of which are located in saturated environments (i.e., below the water table). Inevitably, in the partially saturated condition, gas and/or vapor phases will be introduced into the system, consequently making the already complicated system even more complicated.

The emplacement of radioactive waste in a partially saturated geologic repository will cause a major perturbation of the system involving thermal (T), hydrologic (H), mechanical (M), and chemical (C) processes. The fractured rock mass will be perturbed in two ways (Tsang, 1987). First, the construction of the repository results in large cavities in the fractured rock mass, which changes the original stress distribution. This stress redistribution causes mechanical deformation of the rock, causing the closing or opening of existing fractures. Fracture opening or closing affects fluid flow and solute transport in the rock mass, which are particularly important to the performance of a geologic nuclear waste repository and its environment. Second, the nuclear waste represents a heat source which is active over an extended period of time. As stated by Tsang (1987), this thermal input induces buoyant fluid flow (convection) and rock expansion, which directly depend not only on the magnitude of temperature rise but also on the integrated heat input into the system. The rock expansion will cause the dilation, closure, shear, and propagation of fractures. The hydraulic conductivity of both rock matrix and rock fracture may also change. The thermal load may also cause the degradation of mechanical properties of rock, the healing of rock fractures, and changes of the chemical sorption and retardation capabilities (Lin, et al., 1989).

There appears to be a general consensus in the literature concerning the importance of couplings. For example, thermal processes are expected to influence the performance objectives of the proposed repository underground facility so that thermal loads are specifically referenced as being important to consider in the regulations [(10 CFR 60.133(i)] for mechanical processes (T->M) and groundwater flow (T->H).

The presence of heat in a partially saturated geologic repository induces coupled thermal-hydrologic-mechanical-chemical processes that can be complex. Coupling of the thermal, hydrologic, mechanical, and chemical processes implies that one process affects the initiation and progress of another.

Therefore, under the coupled condition, the behavior of the repository cannot be predicted by considering each process independently.

Tsang (1987) discusses the distinction between different degrees of coupling in order to clarify what is meant by coupled processes. Table 1-1 displays schematically several possible interactions between processes. The fully uncoupled processes conceptually have negligible influence or effect on one another and, therefore, can be evaluated independently. The sequential case implies that one process depends on the final state of another, so that the order in which they are evaluated becomes important. The one-way coupled processes reflect a continuing effect of one or more processes on the others, so that their mutual influences change over time. The two-way coupling (or feedback coupling) reveals a continuing reciprocal interaction between two different processes and represents, in general, the most complex form of coupling. Any combination of one-way and two-way couplings between three or more processes is called three-way or more couplings, respectively. In this report, the term coupled phenomenon refers to one-way or more couplings among the processes.

Among the four processes, there can be only six two-way couplings, four three-way couplings, and one four-way coupling. These can be combined to have only 11 types of possible couplings of various levels of importance (Tsang, 1987), as listed in Table 1-2. Besides displaying the various types of possible coupling among the four processes, Table 1-2 also indicates the stronger coupling (shown as double lines) and weaker ones (shown as single lines). Such a distinction is based on 1987 knowledge primarily on saturated systems and may have to be modified as new data and information emerge.

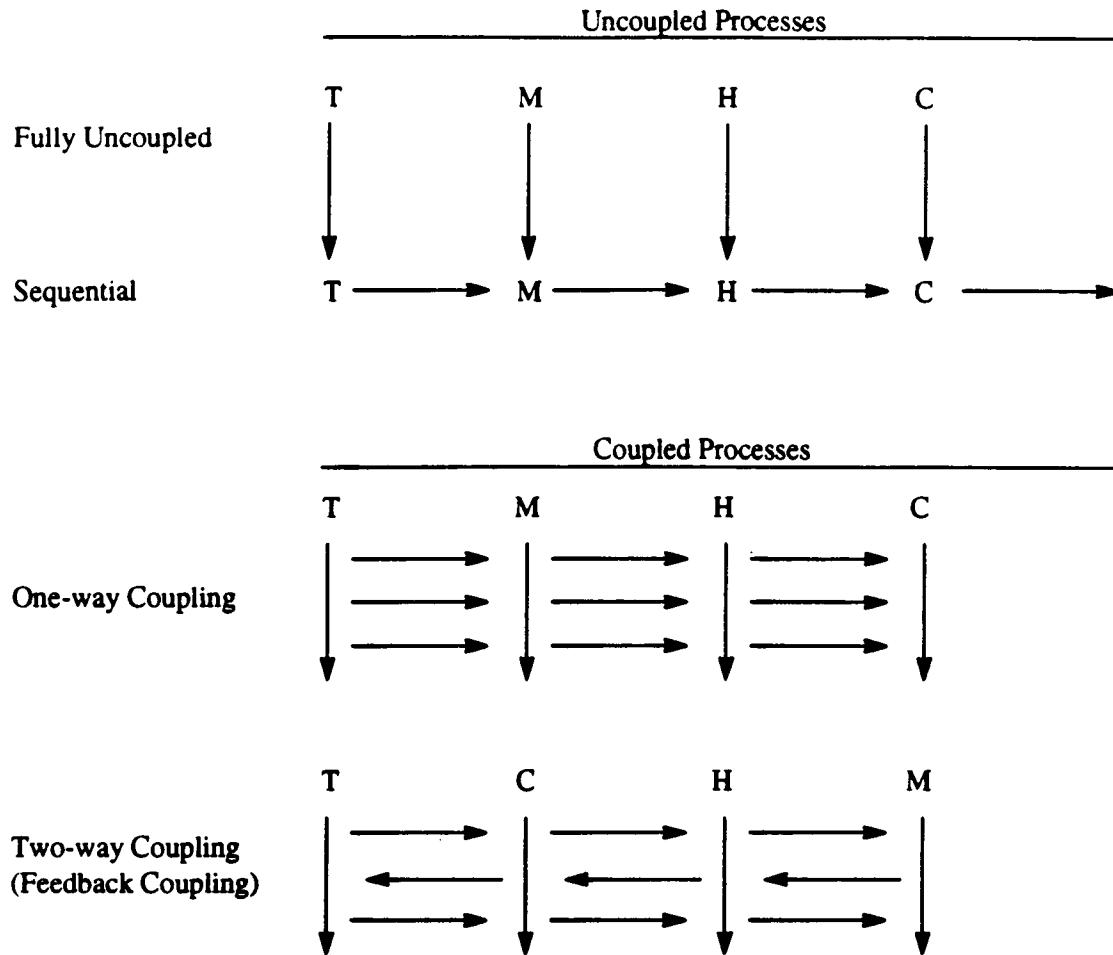
In the nuclear waste geologic repository there are several time and geometric scales. The major time scales are preclosure construction and retrievability period, postclosure containment period, and postclosure isolation period (U.S. Code of Federal Regulations, 1992). The major geometric scales include canister, drift, and repository scales. The temperature and consequently the importance of various couplings will depend upon the design of the engineered barriers, properties of the geologic medium, and the scale (both temporal and spatial) at which these phenomena are of interest.

## **1.2 SINGLE PROCESSES IN THE HLW REPOSITORY ENVIRONMENT**

The mathematical formulations of individual thermal, hydrologic, mechanical, and chemical processes are summarized in Appendices A, B, C, and D and are briefly discussed here. In the appendices, it is noted that the processes are well understood for some conditions but not for many pertinent conditions. For example, the mathematical models for hydrologic processes in a homogeneous and isotropic saturated porous medium are better understood than that for a fractured, partially saturated medium which is expected to be the condition at the proposed repository. Characterization of fractures and fracture networks provides one major difficulty in predicting hydrologic processes. Although effective porous medium models for fractured media seem to be promising, this approach is accurate as long as the hydrologic processes are sufficiently slow so that the fracture and matrix are in hydrologic equilibrium. Effective continuum models may not be appropriate in low permeability units where episodic, fracture-dominated flow may dominate the hydrology.

Heat conduction is expected to be the dominant heat transfer mechanism in the geologic medium at the proposed repository site, and can be predicted through well established mathematical models. However, the effective thermal conductivity can be influenced by rock joint separation (mechanical processes) in addition to being influenced by the degree of saturation of the medium (hydrologic

**Table 1-1. Diagrams of Uncoupled and Coupled Processes (Tsang, 1987)**



Note: T = Thermal, M = Mechanical, H = Hydrologic, C = Chemical.

**Table 1-2. Types of Coupled Processes (Tsang, 1987)**

No.	Type	Example
1.	T = C	phase changes
2.	T = H	buoyancy flow
3.	T = M	thermally induced fractures
4.	H = C	solution and precipitation
5.	H = M	hydraulic fracturing
6.	C - M	stress corrosion
7.		chemical reactions and transport in hydrothermal systems
8.		thermomechanical effects with change of mechanical strengths due to thermochemical transformation
9.		thermally induced hydromechanical behavior of fractured rocks
10.		hydromechanical effects (in fractures) that may influence chemical transport
11.		chemical reactions and transport in fractures under thermal and hydraulic loading

Note: T = Thermal, M = Mechanical, H = Hydrologic, C = Chemical. A single line indicates weak coupling; a double line indicates strong coupling.

processes). In the waste package, the heat transfer may be due to a combination of conduction, natural convection, and thermal radiation. Natural convection is probably the most difficult heat transfer mechanism to characterize for a wide range of conditions. This is because natural convection is strongly influenced by the geometry and the temperature boundary conditions which can be complex in the waste package.

The behavior of continuous medium under mechanical processes has been covered in the literature. However, the mechanical modeling technique for discontinuous medium (such as a fractured rock mass) is at an early stage of development. This may be further complicated by thermal stresses (thermal processes) and changes in joint properties due to the degree of saturation (hydrologic processes) and chemical alterations (chemical processes).

The chemical processes pertinent to the proposed HLW repository at Yucca Mountain may be described by both equilibrium and kinetic chemical processes depending on the processes and the time scale of interest. The modeling of equilibrium chemistry of aqueous systems in a continuous medium at ambient temperatures (i.e., 20 °C) has been well developed. However, the presence of heat sources and discontinuities in the geologic medium provide complexities which are not well understood for modeling of equilibrium chemical processes. The kinetic chemical processes are less understood at this time and accurate modeling techniques are needed.

### **1.3 DESIGN AND PERFORMANCE ISSUES OF THE HLW**

The waste isolation concept for the repository consists of both engineered and natural barriers that act to safely isolate the waste. The engineered barrier system (EBS) consists of the waste package and the underground structure, and is designed to contain the waste for a period of 300 to 1,000 years following permanent closure. During the containment time period, the radiation and thermal levels are high, and the waste packages within the EBS should provide containment of the waste and gradual release of radionuclides. The geologic setting of the site should also isolate the waste from the accessible environment. An important feature of the geologic setting is that it may experience changes due to seismicity, volcanism, and thermal loads during the long period of waste isolation. Furthermore, the geologic repository operations area (GROA), consisting of both surface and subsurface areas, shall be designed for loads due to *in situ* stresses, natural phenomena, and thermally induced phenomena. The design should preserve the option of waste retrieval during the retrievability period, and limit the radiation exposures and releases of radioactive materials to unrestricted areas until permanent closure has been completed.

### **1.4 OBJECTIVE AND SCOPE**

The objective of this literature review is to determine the state of the art in the area of modeling of coupled thermal, hydrologic, mechanical, and chemical processes relevant to the proposed repository at Yucca Mountain, Nevada. Literature reviewed in this document have been selected primarily to enable the CNWRA, and therefore the NRC, to develop the technical capability to review and/or independently verify the Department of Energy (DOE) submittals to the NRC for thermal effects on repository design and preclosure and postclosure performance.

Only a selected number of one-way and multiple-way coupled analysis computer codes that could be utilized with or without modifications have been described herein. No attempt has been made

to provide an exhaustive list of coupled analysis computer codes. In addition, only a few of the codes have been used by the authors, and the summary of a code is based largely on the reported capabilities.

## 1.5 SUMMARY OF LITERATURE SEARCH

A literature search was performed to determine the state of the art in the area of modeling coupled thermal-hydrologic-mechanical-chemical processes in porous, fractured rock as it is pertinent to the proposed HLW repository. The electronic databases used in the search are listed in Table 1-3. Four partially independent searches were conducted to cover each of the four areas with coupling to the remaining three areas. For example, a search was conducted with thermal as the primary topic. Another search used chemical as the primary topic. Because the number of citations was extremely large for certain categories, the scope for each topic was adaptively adjusted (and two searches are reported for both hydrologic and mechanical processes). The selection of key words used are as follows.

For thermal:

(thermal or heat or geothermal)  
and (multiphase or multi()phase or 2()phase or two()phase)  
and (fluid or fluids or hydraulic or hydrology?)  
and (porous or fract? or rock)

For hydrologic (the first time):

(multiphase or multi()phase or 2()phase or two()phase)  
and (fluid or fluids or hydraulic or hydrology?)  
and (porous or fractur? or rock)  
and (mechanical or elastic? or deformation or matrix or  
stress? or displacement or joint? )

For hydrologic (the second time):

((fluid or fluids) or hydraulic()conductivity or hydrology or hydrologic?)  
and ( porous or fracture? or joint? )  
and rock  
and (deform? or hydromechanical or hydro()mechanical or elastic?)

For mechanical (the first time):

(mechanical or elastic? or deformation or matrix or  
stress? or displacement or joint? )  
and (thermal or heat or geothermal)  
and (multiphase or multi()phase or 2()phase or two()phase)  
and (fluid or fluids or hydraulic or hydrology?)

For mechanical (the second time):

thermal()mechanical and (thermal()conductivity or model?)  
or (thermomechanical or thermo()mechanical) and model?  
or (pressure or stress) and (thermal()conductivity or heat capacity)  
and (rock? or stone or granite or limestone or shale or sandstone)

For chemical:

chemi? and geochemi? and thermochemi?

and (thermal or heat or geothermal or thermo?)

and (hydrology? or hydraulic or hydrogeo? or geohydro? or fluid)

and (porous or fractu? or rock)

and (mechanical or elastic? or deformation or matrix or stress

or displacement or joint)

Over 1000 abstracts were requested and reviewed, with over 200 papers ordered. It should be noted that the authors of this literature search have been involved in related work for which relevant articles had already been acquired and reviewed. In addition to an electronic search of databases, the authors performed a manual search of the current literature for approximately the 1991-92 years in the publications listed in Table 1-4.

## **1.6 STRUCTURE OF REPORT**

This report has five main sections:

- Section 2 introduces the two-way coupling mechanisms between individual processes,
- Section 3 synthesizes the coupling mechanisms to discuss three-way-coupled processes,
- Section 4 synthesizes the coupling mechanisms to discuss four-way coupled processes,
- Section 5 provides summary and recommendations for coupled effects, and
- Appendices summarize the four individual processes.

This report attempts to focus on the proposed repository at Yucca Mountain, Nevada. Throughout this report, summaries and conclusions are presented in order to gauge the importance of a coupling mechanism in light of other coupling mechanisms and uncertainties in the processes. An objective assessment of the state of the art is presented in order to identify future research needs in the area of coupled processes.

**Table 1-3. Databases Searched for Articles on Coupled Thermal-Hydrologic-Mechanical-Chemical Processes**

NTIS (64-91/9112B1)
COMPENDEX PLUS (1970-1991/Nov)
GEOREF (1785-1991/Aug)
GEOARCHIVE (74-91/Sept)
FLUIDEX (73 - 90/Dec)
ISMEC: MECHANICAL ENGINEERING (1973-91/Oct)
CONFERENCE PAPERS INDEX (73-91/Nov)
ENERGY SCIENCE & TECHNOLOGY (74-91/Oct)
ENERGYLINE (70-91/Oct)
GEOBASE (1980-91/Aug)
CHEMABSTRACTS (1967-1991)

**Table 1-4. List of Journals Explicitly Reviewed for 1991 and 1992**

Water Resources Research
Transport in Porous Media
ASME Journal of Heat Transfer
International Journal of Heat and Mass Transfer
Journal of Geophysical Research
International Journal of Rock Mechanics and Mining Sciences and Geomechanics Abstracts
International Journal for Numerical and Analytical Methods in Geomechanics
International Journal for Numerical Methods in Engineering
International Journal of Multiphase Flow
International Journal of Numerical Methods in Fluids
Journal of Fluid Mechanics
Applied Geochemistry
Geochimica et Cosmochimica Acta
American Journal of Science

## 2 TWO-WAY COUPLING MECHANISMS

In this section, the coupling mechanisms between processes are discussed. The material in this section constitutes the "backbone" of the report from which conclusions and recommendations are derived in subsequent sections.

The format for this section is to present all of the possible one-way couplings. In total there are twelve one-way couplings: {T -> H, H -> T, T -> M, M -> T, T -> C, C -> T, H -> M, M -> H, H -> C, C -> H, M -> C, C -> M}. Each one-way coupling is discussed in a part of this section where the discussion focuses on the mechanisms by which one process may influence another process. If a feedback exists, then it is a two-way coupling. That is to say, the two-way T <-> H is discussed as two one-way (T -> H and H -> T) couplings. In combination, two parts of this section cover feedback (two-way) couplings.

### 2.1 THERMAL -> HYDROLOGIC

In this section, the influence of thermal processes on hydrologic processes is discussed. It has been recognized in the literature that thermal-hydrologic processes are expected to be important at the proposed repository and need to be considered in repository design and evaluation of performance objectives (DOE, 1988). As a result of thermal heating, water is expected to move in both the liquid and vapor phase and may influence (i) waste package corrosion, (ii) waste form dissolution, and (iii) radionuclide migration among other processes of interest, .

Thermal processes are primarily described by the temperature field, while hydrologic processes are primarily described by the liquid saturation and relative humidity fields. Hence, our interest is in understanding how a temperature field (and its associated temperature gradient) can effect the liquid saturation and relative humidity profiles in a porous, fractured medium.

Five areas of discussion are included in this section: (i) vaporization and condensation, (ii) dripping in fracture networks, (iii) nonisothermal enhancement of vapor diffusion, (iv) buoyancy driven natural convection, and (v) computer codes.

#### 2.1.1 Vaporization and Condensation

Heat generation from radioactive materials emplaced in a geologic repository is expected to lead to increased temperatures around the waste. The increased temperatures lead to increased vapor pressure of the *in situ* water. Because of increased temperature, the water in the liquid phase will not be in equilibrium with the water in the gas phase. Some of the liquid will be vaporized to increase the partial pressure of water in the gas phase and achieve thermodynamic equilibrium. The temperature and vapor pressure can be related through the Clapeyron equation (Wark, 1983, pg 487).

$$P_v = P_{v,0} \exp \left[ \frac{h_{LG} M_w}{R} \left( \frac{1}{T_0} - \frac{1}{T} \right) \right] \quad (2-1)$$

where

$P_v$	= vapor pressure at temperature $T_0$ [ $N/m^2$ ],
$P_{v,0}$	= reference vapor pressure [ $P_{v,0} \approx 7.4 \times 10^3 N/m^2$ at $40^\circ C$ ],
$h_{LG}$	= heat of vaporization [ $h_{LG} \approx 2400 kJ/kg$ at $40^\circ C$ ],
$M_w$	= molecular weight of water [18.02 g/mole ],
$R$	= ideal gas constant [8.314 J/(mole-K)], and
$T_0$	= reference temperature [ $T_0 = 313 K$ ].

As the porous medium dries, the amount of water in both the liquid and the gas phase decreases. Assuming thermodynamic equilibrium, the amount of water in the gas phase can be related to the potential energy of water in the porous medium. At equilibrium, the potential energy is equal for the water in both the gas and liquid phases. Two physical mechanisms are responsible for holding the water in the porous medium: capillarity and adsorption. As a general rule, capillarity is important at high saturations and adsorption is important at low saturations. The more prominent distinction between capillarity and adsorption is the potential energy measured through the capillary/adsorption pressure,  $P_{CAP/ADS}$ . The  $P_{CAP/ADS}$  is also known as the capillary pressure, suction pressure and matrix potential, among other terms. A relation known as Kelvin's equation (Thomson, 1871), is commonly used to predict the decrease in the partial pressure of water over a porous medium.

$$P_{w,G} = P_v \exp \left( \frac{- M_w P_{CAP/ADS}}{\rho_L R T} \right) \quad (2-2)$$

where

$P_{w,G}$	= partial pressure of water in the gas phase [ $N/m^2$ ], and
$\rho_L$	= density of liquid [ $kg/m^3$ ]

Because of the long times associated with processes at the repository, the water in the porous medium and in the gas phase is normally assumed to be in thermodynamic equilibrium. From Clapeyron's equation and Kelvin's equation, the partial pressure of water in the gas phase can be calculated to be a function of  $T$  and  $P_{CAP/ADS}$ . (Eqs. 2-1 and 2-2 can be combined into the "extended Clapeyron" equation.) A nonuniform temperature field then results in a nonuniform field in  $P_{w,G}$ . Air is expected to be present at the repository hence the gas phase will consist of two components: water vapor and air. The water vapor is expected to travel from hotter regions to cooler regions due to either advection or diffusion. The advection mechanism will result from a gradient in the total gas pressure (Darcy's Law) and the diffusion will result from a gradient in partial pressure of water vapor (Fick's Law). Once the water vapor reaches cooler regions, it will condense. In summary, liquid water is expected to vaporize in regions of higher temperature, flow to regions of lower temperature, and condense.

The geologic repository is commonly approximated as a heat-generating, porous disk in an axisymmetric model as in Figure 2-1, or as a thin source in a two-dimensional, cartesian cross-sectional model as in Figure 2-2. In many analyses, the repository is sufficiently thin compared to geologic length scales to neglect its width. Pollock (1986) performed thermal-hydrologic calculations using the model in Figure 2-2. Results of his calculations indicated a region of increased liquid saturation forming both above and below the repository horizon (see Figure 2-3). Although these calculations are outdated, more recent calculations yield the same trend (Buscheck and Nitao, 1992). The increase in liquid saturation above and below the repository is due primarily to vaporization of water near the heat-generating repository, temperature-gradient driven molecular diffusion of the water vapor, and condensation in cooler regions.

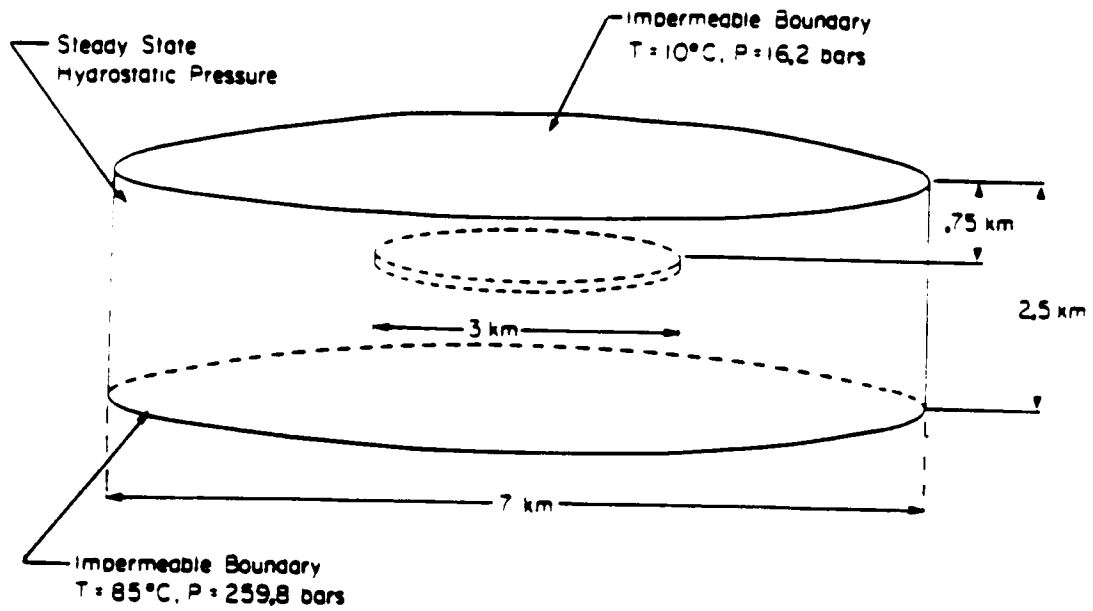


Figure 2-1. An Axisymmetric Model of a Geologic Repository (Verma and Pruess, 1988)

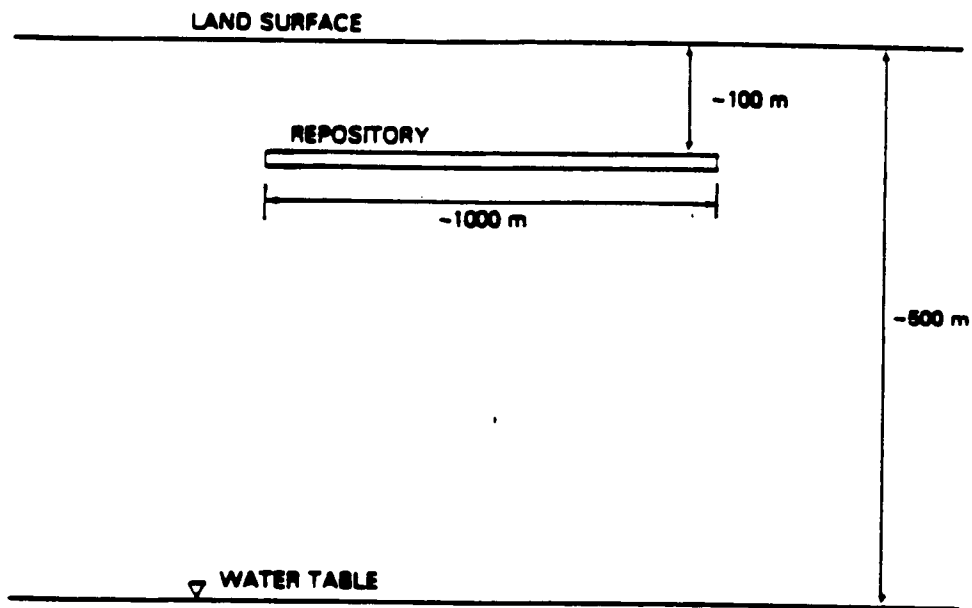


Figure 2-2. A Two-Dimensional, Cartesian Model of a Geologic Repository (Pollock, 1986)

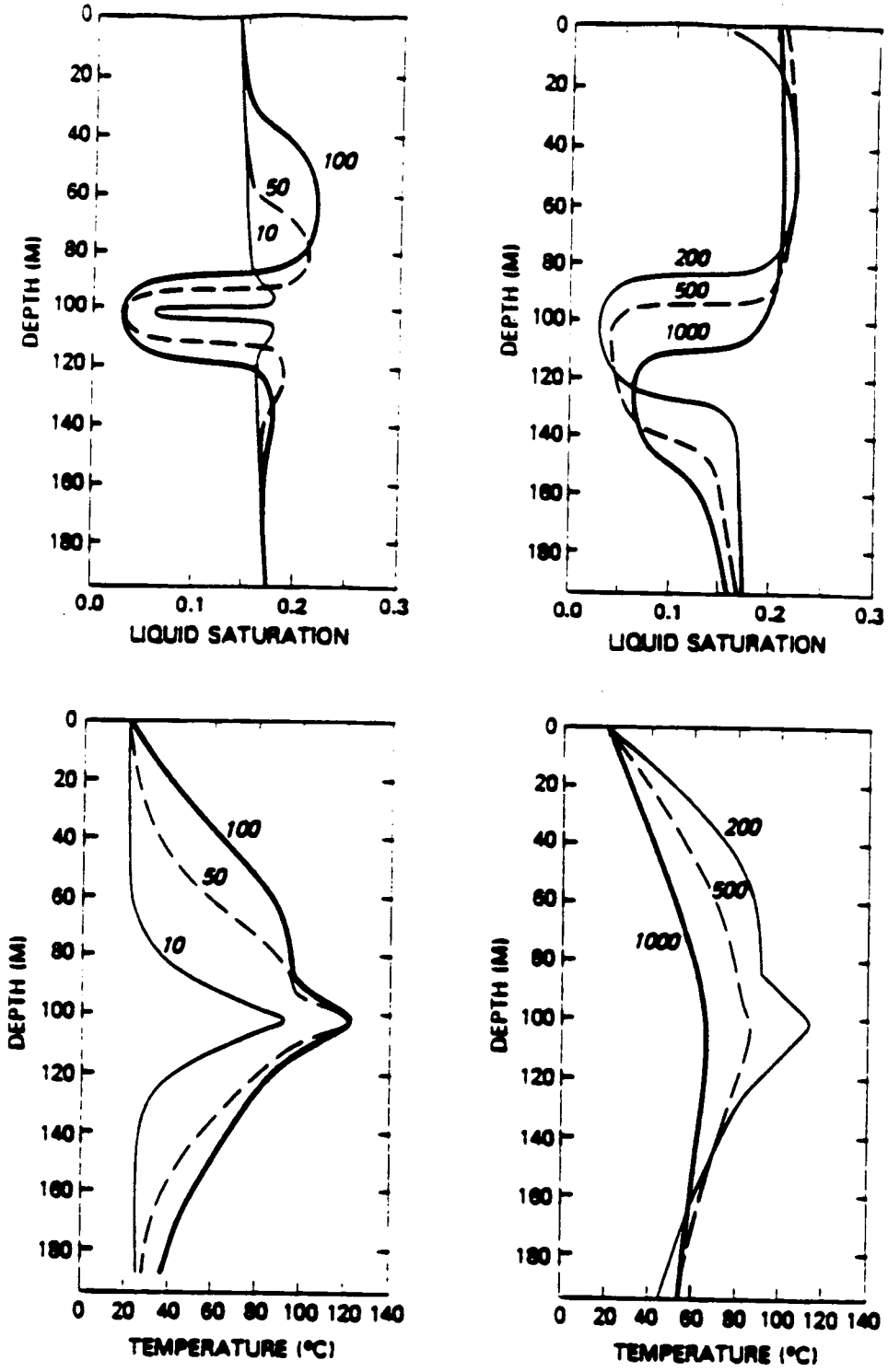


Figure 2-3. Saturation and Temperature Distributions Through the Center of a Repository from Ground Surface (depth = 0 m) to Water Table (depth = 500 m) at Time = (10, 50, 100, 200, 500, 1000) Years, see Figure 2-2 (Pollock, 1986)

Buscheck and Nitao (1988, 1992) among others, have described a "constructive" use of heat where the decay heat may lead to increased (i) water vaporization, (ii) vapor flow away from the hotter waste packages, (iii) condensation in cooler regions, and (iv) liquid imbibition into the matrix. This sequence may keep the waste packages dry for thousands of years for a high repository heat loading (dense package spacing). Optimally, the condensed water will imbibe into the rock or be shed from the waste packages and flow downward by gravity drainage in the fractures. The processes of condensate drainage in fractures has recently attracted much attention since it is expected that drainage may occur over considerable distances before being totally imbibed by the matrix. In this work, condensate drainage is expected to result in dripping in fractures, and is discussed next.

### 2.1.2 Dripping in Fractures/Networks

There are two primary mechanisms whereby liquid water may come into contact with waste packages potentially leading to accelerated corrosion and release of radionuclides: episodic (e.g., incidental series of events) infiltration from the ground surface, and condensate drainage. If liquid flows in fractures, then it is expected to travel greater distances in shorter periods of time. Episodic infiltration is primarily a hydrologic process and does not result from thermal processes, hence it is discussed in Section B.3. Vapor flow, condensation, and dripping are thermally driven, hence, they are discussed here.

Buscheck and Nitao (1992) suggest a repository with a large power density will result in significant rock dry-out in the near-field, and flow of water vapor (primarily through fractures) to cooler regions where it condenses. If the matrix has a low permeability, condensate may drain considerable distances along fractures before being totally imbibed by the matrix. The locations of condensate dripping in fractures and the sizes of liquid flow rates are unresolved issues.

A cross-section of an emplacement drift is shown in Figure 2-4. Here, the drift is assumed to be the traditional dome shape and the waste packages are assumed to be emplaced vertically. The surrounding rock is shown to be highly fractured. The waste package is heat-generating and is expected to create a dry zone, a condensation zone, and regions of condensate dripping as shown in Figure 2-5. For low power densities, the amount of water redistributed in the medium may be small enough so that the condensation is imbibed in the matrix as fast as it is produced. At higher power densities, the rate of growth of the dry zone is faster so that more condensate is created at an increased rate. It is conceivable that under varying conditions, condensate will drain in the fractured medium.

At short times after emplacement, the dry zone is small, hence the amount of liquid in the condensation zone is small, see Figure 2-5. At longer times, the dry zone increases in size, and similarly the amount of liquid in the condensation zone also increases. Current repository design proposals have parallel drifts. At long times, the condensate zones between emplacement drifts may interact, and probably encourage dripping between drifts as shown in Figure 2-5. For a non-fractured, homogeneous, isotropic medium, the condensate above the waste packages would preferentially drain between drifts. However, fractures may be a dominant mechanism which dictate where condensate drains.

It has been hypothesized that the mineralogy of the fracture surfaces may be important in resisting condensate imbibition into the matrix. Gallegos et al. (1992) investigated the effects of low-permeability mineralized layers at the matrix/fracture interface which may substantially reduce matrix imbibition and result in fracture-dominated flow. The mineralized layers on the fracture faces can inhibit

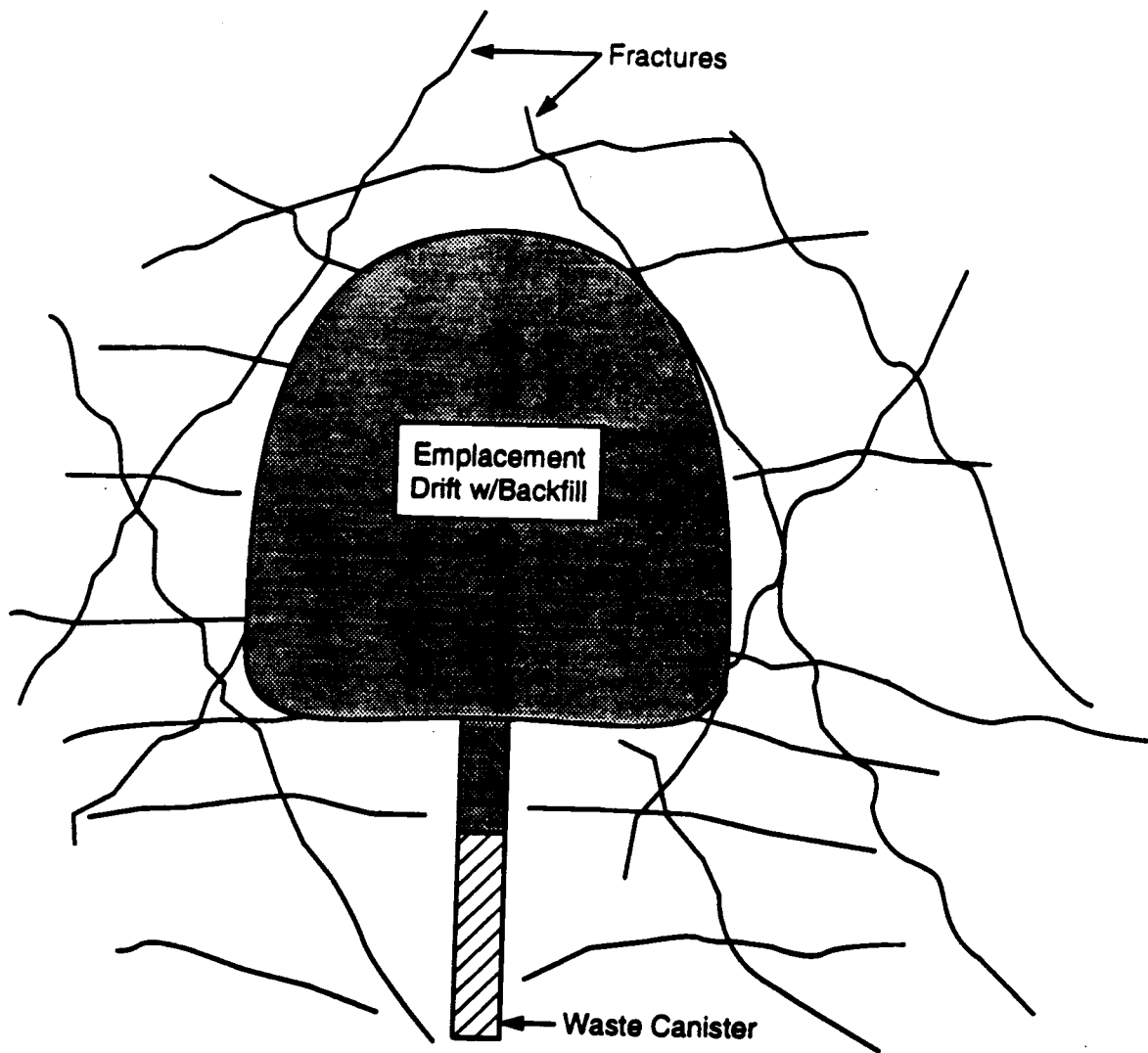


**Figure 2-4. Illustration of a Drift with Vertical Emplacement of a Waste Canister in a Fractured Porous Medium**

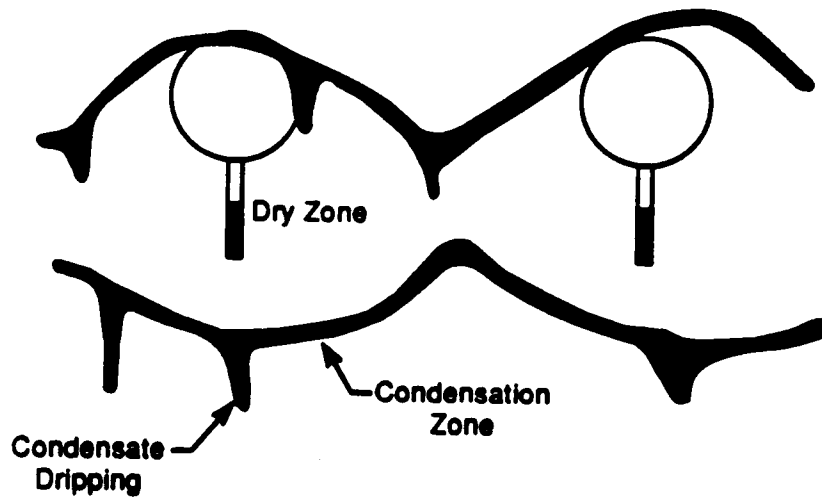
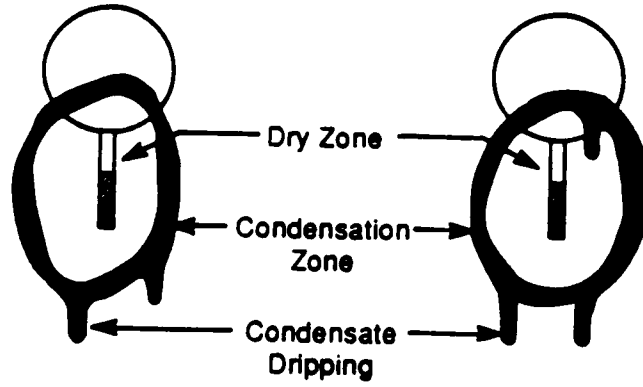


**Figure 2-5. Illustration of a Dry Zone and a Condensation Zone with Condensate Dripping in Fractures for Short Times (above) and Longer Times (below)**

the uptake of water into the adjacent matrix. This effect may invalidate the application of effective continuum models which are based on matrix/fracture equilibrium and typically predict matrix-dominated flows except for extremely large values of liquid saturation (this is discussed in Appendix B.3). Gallegos et al. (1992) conducted laboratory imbibition experiments and have reported that fracture coatings may severely reduce matrix uptake, however these conclusions are based on only four tuff samples and only one of the four samples had a dramatic effect (reduction in imbibition by seven orders of magnitude). Imbibition will also be affected by the continuity and type of mineral coating. At Yucca Mountain, minerals such as zeolites may enhance imbibition and "most fractures are only partially sealed" (DOE, 1988, pg. 4-13).

### 2.1.3 Nonisothermal Enhancement of Vapor Diffusion

Molecular diffusion of water vapor in the fractured, porous medium can be an important transport mechanism, and can be strongly influenced by the temperature field. Philip and de Vries (1957), Pollock (1982), Mulay (1988) and others, have noted that a straightforward application of Fick's law underestimates the molecular diffusion of water vapor in a nonisothermal porous medium. This conclusion is based on comparison with experimental data which has been found to be two to eight times larger than predictions based on Fick's law (Philip and de Vries, 1957). In a dry porous medium, a straightforward application of Fick's law appears valid. In a wet porous medium, the effect of liquid-vapor interaction may be important in the overall rate of vapor transfer. Philip and de Vries (1957) proposed that Fick's law be multiplied with an empirical nonisothermal enhancement factor.

$$\bar{j}_{w,g} = - \eta \tau \phi S_G \rho_G D_{wA,G} \nabla m_{w,g} \quad (2-3)$$

where

- $\bar{j}_{w,g}$  = diffusive flux of water vapor in the gas [kg/(m<sup>2</sup>-s)],
- $\eta$  = nonisothermal diffusion enhancement factor for water [dimensionless],
- $\tau$  = tortuosity [dimensionless],
- $\phi$  = porosity [dimensionless],
- $D_{wA,G}$  = molecular diffusion coefficient of water vapor in air [m<sup>2</sup>/s], and
- $m_{w,g}$  = mass fraction of water vapor in the gas [dimensionless].

Two explanations for nonisothermal enhancement are: (i) coupled gas-liquid transfer, and (ii) increased temperature gradients in the gas phase. The explanations are not discussed here; however, it is noted that not all researchers acknowledge the need for a nonisothermal enhancement factor. Pruess (1987) does not discuss nonisothermal vapor diffusion enhancement, but has adopted a straightforward application of Fick's law ( $\eta = 1$ ). Similarly, Bixler (1985), Forsyth (1990), and Forsyth and Simpson (1991) do not discuss nonisothermal vapor diffusion enhancement. In comparison, Pollock (1982) and Mulay (1988) discussed the importance and necessity of the diffusion enhancement factor. Because of the lack of a solid theoretical basis (although it has been reported experimentally), the nonisothermal diffusion enhancement factor for water vapor is typically neglected.

### 2.1.4 Buoyancy Driven Natural Convection

Many of the earlier studies related to geologic repositories involved saturated media. In a saturated medium, increased fluid motion is expected to accelerate the spread of radionuclides. The emplacement of heat-generating HLW is expected to elevate temperatures at the repository which could

create thermally-driven natural convection currents. Wang and Tsang (1980) studied buoyancy driven natural convection at a hypothetical saturated repository (see Figure 2-6). Here, natural convection increases fluid flow from the repository towards the ground surface.

In addition to saturated medium, natural convection in the gas phase for a partially saturated medium has been studied. Pollock (1986) modeled natural convection circulation in the gas phase at a hypothetical repository as shown in Figure 2-7. In general, the elevated temperature at the repository results in decreased gas density and a natural buoyancy of the lighter gas. Because Yucca Mountain is partially saturated, the more recent studies focus on gas phase buoyancy driven flows.

Temperature-driven natural convection is especially important in modeling gas flow at Yucca Mountain with respect to predicting gaseous transport of volatile and semi-volatile radionuclides such as C-14 in CO<sub>2</sub>, I-129 in I<sub>2</sub>, Cs-135 in Cs, Se-79 in SeO<sub>2</sub>, and Tc-99 in Tc<sub>2</sub>O<sub>7</sub>, (Park, 1991). In early analyses, the release of C-14 has been shown to be near or exceeding regulatory limits (van Konynenburg, 1991). The influence of temperature on the release and gaseous transport of radionuclides is considered important.

For a semi-infinite, saturated porous medium which is heated at the bottom and cooled at the top, there exists a critical Rayleigh number, Ra<sub>c</sub>, below which the fluid remains stagnant and above which the fluid flows (Cheng, 1978; Bejan, 1984; among others). The traditional Rayleigh number is described as the ratio of buoyancy forces to viscous forces

$$Ra = \frac{g \beta \Delta T L^3}{\nu \alpha} \quad (2-4)$$

where

$g$  = gravitational constant,

$\beta$  = thermal expansion coefficient, i.e.,  $\beta = -\frac{1}{\rho} \frac{\partial \rho}{\partial T} \Big|_P$

$\rho$  = fluid density,

$\Delta T$  = appropriate temperature difference,

$L$  = appropriate macroscopic length scale,

$\nu$  = kinematic viscosity, and

$\alpha$  = thermal diffusivity.

The porous medium Rayleigh number is defined as the traditional Rayleigh number times the Darcy number [Da =  $k_{SAT}/L^2$ , (Bejan, 1984; among others)].

$$Ra \cdot Da = \frac{g \beta \Delta T k_{SAT} L}{\nu \alpha} \quad (2-5)$$

The stability criteria in a porous medium is consistent with the "Benard problem" which is a classic problem in natural convection books (Tritton, 1977; among others). The stability criterion is depicted in Figure 2-8 where, for a saturated porous medium, the critical Rayleigh number is shown to be a function of the Darcy number, Da. As the permeability of the medium increases, the Darcy number increases, and the porous medium approaches an open medium. The classical results are that for a porous

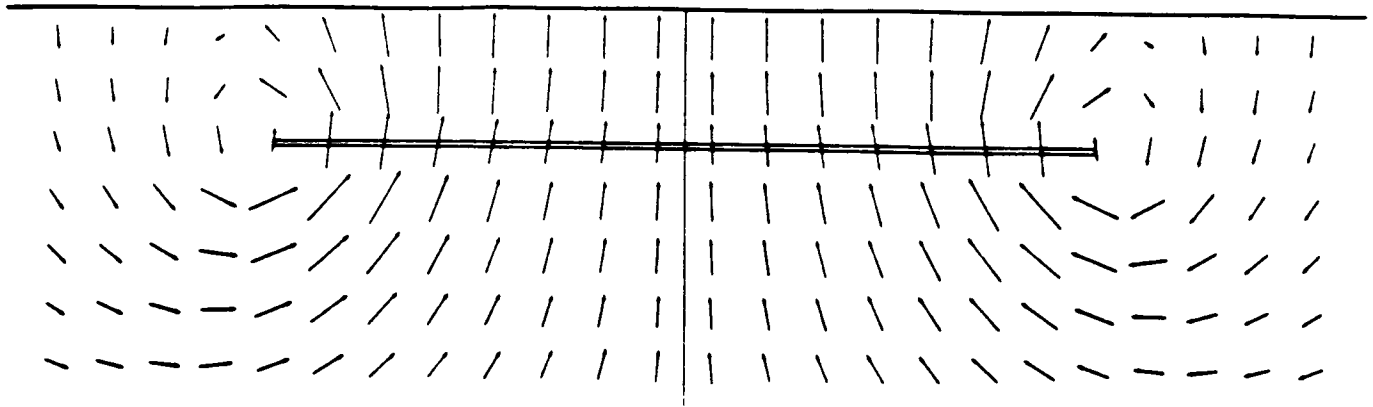


Figure 2-6. Buoyancy Driven Convection Patterns Around a Saturated Repository (Wang and Tsang, 1980)

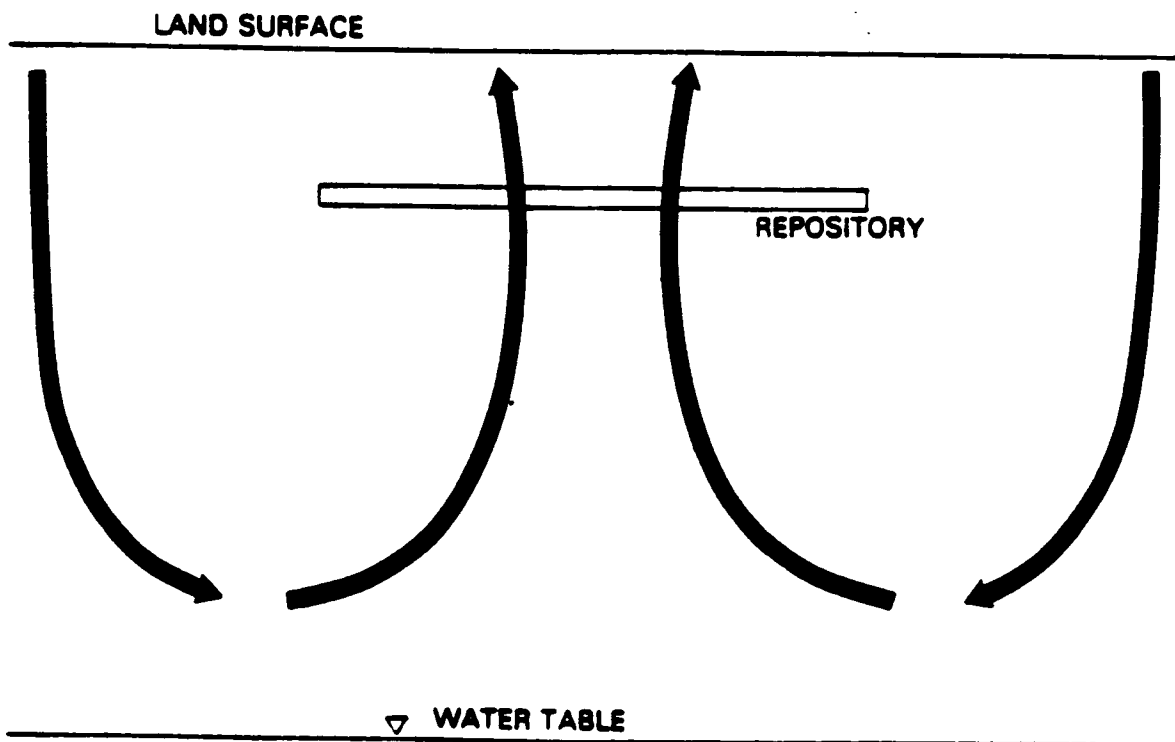


Figure 2-7. Illustration of Convective Circulation Pattern for the Gas Phase (Pollock, 1986)

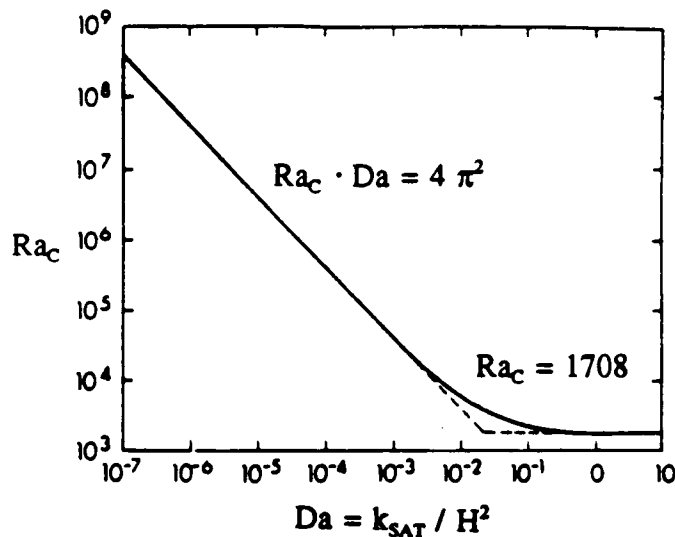


Figure 2-8. Critical Rayleigh Number (for the Benard Problem) Versus Dimensionless Permeability from Darcy's Limit to the Viscous Fluid Limit (Cheng, 1978; Among Others)

medium,  $Ra_c \cdot Da = 4 \pi^2$ , and for an open medium,  $Ra_c = 1708$  (Cheng, 1978; among others). Although not directly applicable to a partially saturated repository, these classical results provide a starting point with which to estimate the presence or absence of buoyancy driven flow. Assuming representative values for the proposed repository ( $L = 200$  m,  $\Delta T = 100$  °C), and gas properties for air ( $\beta = 1/(300$  K),  $\nu = 20 \times 10^{-6}$  m<sup>2</sup>/s,  $\alpha = 30 \times 10^{-6}$  m<sup>2</sup>/s), one can estimate that the gas phase permeability needs to be greater than  $10^{11}$  m<sup>2</sup> in order for buoyancy-driven flow to be important. This value for permeability is considered large and barely within the range of effective fracture permeability which is estimated to be from  $10^{16}$  to  $10^{11}$  m<sup>2</sup> (Pruess et al., 1990a; Peters et al., 1984; among others). From this simple analysis, the buoyancy-driven gas flow at Yucca Mountain is estimated to be negligible.

The relative importance of buoyancy-driven natural convection and molecular diffusion of water vapor were compared by Tsang and Pruess (1987), see Figures 2-9 and 2-10. Tsang and Pruess performed two calculations using an axisymmetric model of the repository (similar to Figure 2-1). Lengths and material properties are similar to those expected at Yucca Mountain. In Figure 2-9, molecular diffusion is considered. The gas flux near the repository (both above and below) is away from the repository. In Figure 2-10, molecular diffusion is neglected and the flow is much less and always directed above the repository. From these calculations, molecular diffusion is dominant near the repository. At distances further from the repository, the gas flow is much smaller, yet has a characteristic flow pattern of buoyancy-driven natural convection. Tsang and Pruess estimate the gas phase Darcy velocity to be about 4 cm/yr for a 95 °C repository temperature with effective fracture permeability of  $1.8 \times 10^{-14}$  m<sup>2</sup>. Tsang and Pruess consider this to be a "large" velocity, however, this appears to be quite small given that the repository is  $\sim 200$  m below ground surface. For "contaminant" transport, Tsang and Pruess note that the "pore" velocity is most appropriate. Using an effective fracture porosity of 0.0018, the gas pore velocity is 22 m/yr which is considerably larger than the Darcy velocity. Most radionuclides expected in HLW (and the molecular compounds they participate in) have very low vapor pressures, hence remain either in the solid or liquid phases with those exceptions noted earlier in this section.

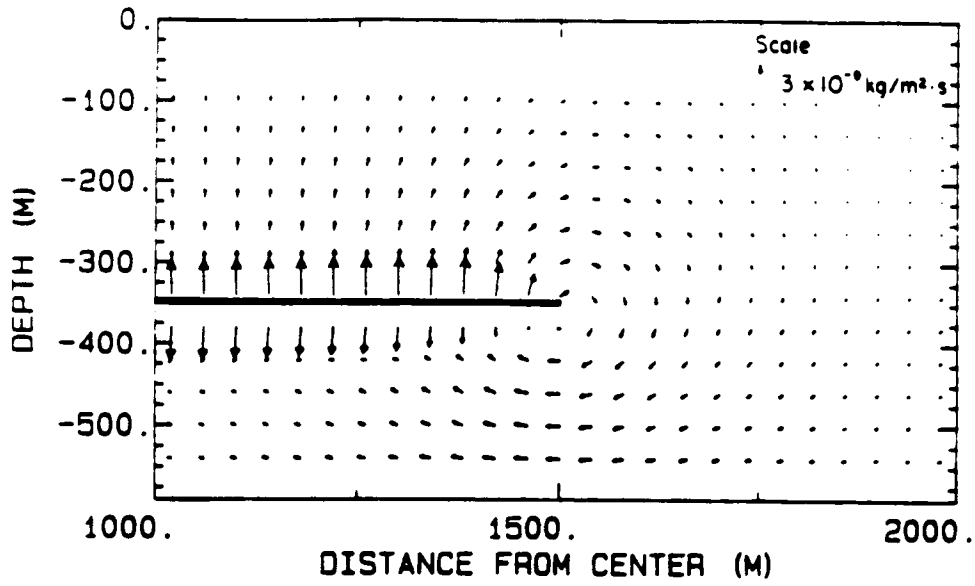


Figure 2-9. Gas Flux at 100 Years After Waste Emplacement Showing Flow Away from Repository Primarily Due to Diffusion of Water Vapor (Tsang and Pruess, 1987)

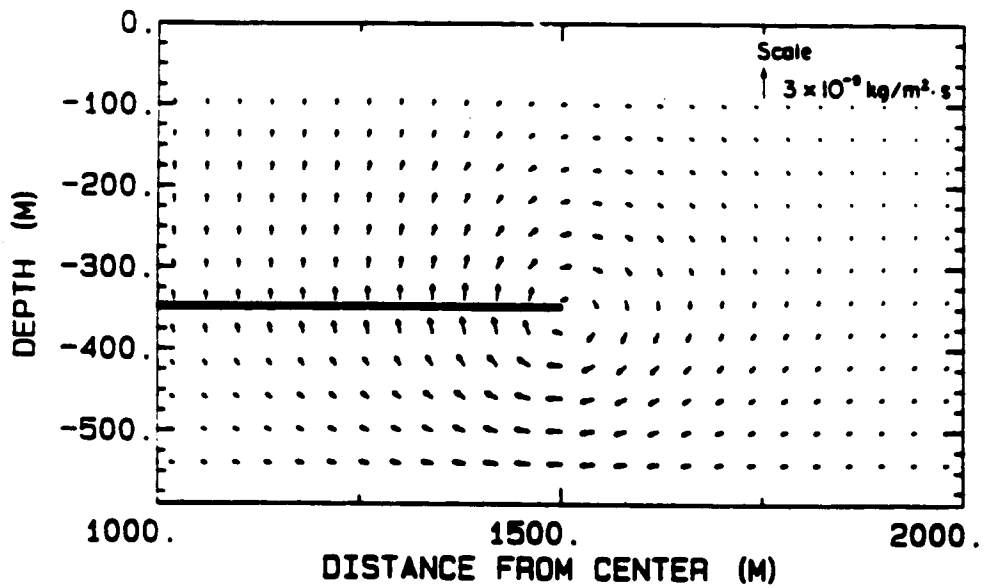


Figure 2-10. Gas Flux at 100 Years After Waste Emplacement Neglecting Molecular Diffusion of Water Vapor (Tsang and Pruess, 1987)

## **2.1.5 Computer Codes**

A number of computer programs have been written to predict thermal-hydrologic processes. Especially since 1985, there has been a dramatic increase in the numerical modeling of thermal-hydrologic processes in a partially saturated porous medium.

### **2.1.5.1 TOUGH**

Pruess (1987) has developed the TOUGH program which has received extensive usage (Pruess et al., 1990a,b; Doughty and Pruess, 1988; among others). TOUGH is derived from the MULKOM family of multiphase, multicomponent codes that were initially developed at Lawrence Berkeley Laboratory for geothermal reservoir applications. TOUGH was developed for application to the proposed geologic HLW repository located in partially saturated, fractured rock. TOUGH is capable of solving three-dimensional, two-phase (liquid and gas), two-component (water and air) fluid and heat transfer in a fractured, porous medium. The equations in TOUGH include gaseous diffusion, Darcy flow, capillary pressure, vaporization, and condensation. TOUGH is specifically designed for strongly heat-driven partially saturated flow, so that the heat of vaporization/condensation, conduction and convection are included in the energy equation. The conservation equations include air, water (combined liquid and gas phase), and energy. The water in the gas phase is assumed to be in local thermodynamic equilibrium so that the partial pressure of water in the gas equals the reduced vapor pressure through Kelvin's equation. TOUGH has been used at the CNWRA to simulate thermohydrologic laboratory experiments. Green et al. (1992) experienced numerical difficulties with TOUGH which limited the problems which could be simulated.

### **2.1.5.2 VTOUGH**

Nitao (1990) has developed VTOUGH at Lawrence Livermore National Laboratory for the U.S. Department of Energy. VTOUGH is a modification of TOUGH with improved numerical convergence and stability properties. Both TOUGH and VTOUGH have been used at the CNWRA where VTOUGH was found to be more robust (Green et al., 1992). The capabilities of TOUGH and VTOUGH are comparable.

### **2.1.5.3 PORFLOW**

Sagar and Runchal (1990) developed PORFLOW to model fluid flow, heat transfer, and mass transport in variably saturated geologic medium. PORFLOW was developed in support of environmental remediation activities being conducted at the Hanford Site for the U.S. DOE. A main feature is its ability to model three-dimensional geometries in both cartesian and cylindrical coordinate systems. The primary variables are hydraulic head (or pressure), temperature, and chemical species concentration. The gas phase is assumed to be stagnant and molecular diffusion is neglected. Runchal and Sagar (1992) have recently updated PORFLOW.

### **2.1.5.4 FEHMN**

Zyvoloski et al. (1991) have developed FEHMN to model heat and mass transfer using the finite element method. FEHMN was developed at Los Alamos National Laboratory and was designed for the partially saturated zone around the proposed Yucca Mountain repository. The code can solve nonisothermal, multiphase, multicomponent flow in a porous medium in cartesian two- and three-dimensional space, and in cylindrical coordinate systems.

#### **2.1.5.5 NORIA and PETROS**

Bixler (1985) developed NORIA, and Hadley (1985) developed PETROS, which are similar finite element codes for solving two-phase, two-component heat and mass transfer in porous media. Both codes were developed at Sandia National Laboratories in support of the Nevada Nuclear Waste Storage Investigations (NNWSI). The major distinction is that NORIA is only applicable for two-dimensional geometries, and PETROS is a one-dimensional code. Updegraff (1989) reported that NORIA was not able to simulate many test problems including a radial boiling front problem, a heat pipe problem, a two-dimensional infiltration problem, a convection cell problem, and a two-phase flow problem. Updegraff (1989) also reported that NORIA required significantly greater CPU time than TOUGH for a number of test problems.

#### **2.1.5.6 FRAC-UNIX**

Clemo et al. (1990) developed FRAC-UNIX at EG&G Idaho for the U.S. Department of Energy. FRAC-UNIX is a two-dimensional, saturated fluid and heat transport code for fractured porous media. FRAC-UNIX was originally designed to analyze fractured geothermal reservoirs, however it has been updated to be used in support of license applications for high-level waste disposal. FRAC-UNIX uses a dual-permeability model for the matrix and fracture hydrology, and uses a random-walk (marker particle transport) model for heat transfer. It is claimed that the random-walk model drastically reduces computer CPU requirements, however this claim does not appear to be substantiated. This issue can be related to the number of marker particles required to resolve the field. It is well documented that a Monte-Carlo algorithm has a slow rate of convergence (standard deviation inversely proportional to the square-root of the number of samples) hence the method may be efficient if approximate solutions are required. However, it may become prohibitively expensive if accurate solutions are required.

#### **2.1.5.7 GEOTHER**

Bian et al. (1987, 1988a,b) have developed GEOTHER (or GEO2) to model two-phase groundwater fluid flow and heat transport for high-level radioactive waste applications. GEOTHER evolved from a code developed by the U.S. Geological Survey. GEOTHER simulates multicomponent (water, noncondensable gases, rock/solid), porous and nonporous media (rock, waste container), two-phase (liquid, vapor) fluid and heat transfer using the finite volume method.

### **2.1.6 Summary and Conclusions**

In this section, the influence of the temperature field on hydrologic processes has been discussed. In particular, it has been noted that elevated temperatures will lead to vaporization of the groundwater. Temperature gradients will provide a driving force for water vapor flow into cooler regions. The water vapor will condense in cooler regions and potentially flow due to both gravity and gradients in capillary/adsorptive pressure. In a partially saturated repository, vaporization, gas flow and condensation are anticipated to be important processes in affecting the hydrologic flow field.

The importance of dripping in fracture networks was also discussed. Many of the hydrogeologic units at Yucca Mountain are known to be fractured with a low permeability matrix. Normally, fractures are expected to remain dry, however episodic rainfall and infiltration at the ground surface, and water vapor condensation are two mechanisms whereby the fractures may have a substantial amount of liquid flow. Given a sufficient amount of liquid in an initially dry fracture, the liquid is expected to drip

downward due to gravity forces. Thermal processes are expected to dry out the rock near the repository, and generate condensate dripping in fracture networks.

The influence of a temperature gradient on vapor diffusion in a partially saturated medium was discussed. In much of the earlier literature, differences were reported between experimental data and theoretical predictions based on a straightforward application of Fick's law. It has been hypothesized that water vapor and liquid in a nonisothermal porous medium interact to increase the effective vapor fluxes over theoretical predictions. The increase is most relevant in partially saturated medium, and diminishes for either saturated or dry medium. However, the available literature appears to be inconclusive as to how this nonisothermal enhancement should be modeled, and it has been neglected in many recent studies.

Computer programs that model coupled thermal-hydrologic processes were also discussed. One major difficulty in mathematical models and computer programs is the characterization of matrix-fracture interactions. A significant number of programs have been developed which indicate that there is considerable interest in the scientific community in modeling these processes.

## **2.2 HYDROLOGIC -> THERMAL**

Hydrologic processes (fluid flow) can influence thermal processes (temperature field). Coupled hydrologic-thermal processes are important because they may cause (i) the formation of a heat pipe, (ii) creation of a boiling zone, (iii) natural convection, or (iv) influence material properties of the medium. In this chapter, all four areas are discussed.

### **2.2.1 Heat Pipe**

A term "heat pipe" has been used in the engineering community to describe a situation where heat (thermal energy) is efficiently transferred with minimal temperature differences (Dunn and Reay, 1982). Heat pipes typically are engineered devices which consist of a sealed tube. The tube contains a two-phase fluid. The tube also has an internal wicking region and a hollow region for the counter flow of liquid and vapor from one end of the tube to the other end. One end is subjected to a high temperature and the other a lower temperature. Heat flows by vaporization of the fluid at one end, advection through the core to the other end, where it condenses and is wicked back to the hot end. Hence, the fluid flow is circular and continuous, with vapor flowing from high to low temperature and liquid flowing from low to high temperature.

In many industrial applications, heat pipes are designed to increase the efficiency of thermal processes. Although less common, natural systems can develop "heat pipe" types of flow which transfer large amounts of heat (Schubert and Straus, 1979; Pruess, 1985; Turcotte, 1989; among others). For the proposed HLW repository, the potential impact of a natural heat pipe has been theoretically investigated by Doughty and Pruess (1988, 1990, 1992). The heat-generating HLW creates a high temperature source and the surrounding rock provides the low temperature sink. The groundwater is vaporized near the HLW and flows through the medium to the lower temperature regions where it condenses. The condensed water may then flow back toward the HLW due to suction pressure gradients (frequently noted as capillary-driven flow).

Doughty and Pruess (1988) developed a model of the fluid and heat flow around a waste package as illustrated in Figure 2-11. After emplacement in the medium, the heat-generating waste is

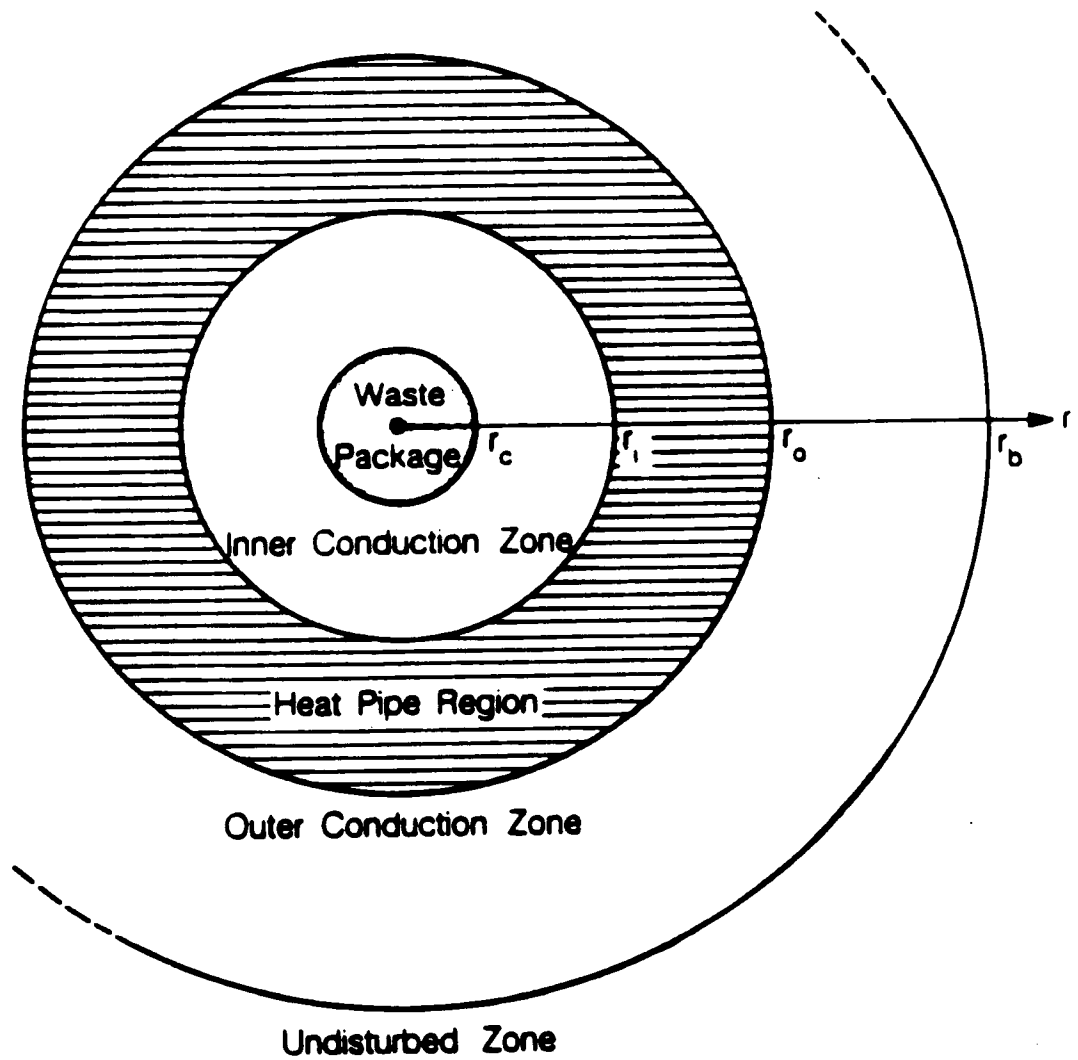


**Figure 2-11. Schematic of Heat-Transfer Regimes in a Plane Perpendicular to the Axis of the Waste Package (not to scale), (Doughty and Pruess, 1988)**

expected to dry a zone near the canister. The heat transfer mechanism in the dry zone is primarily conduction, as indicated in Figure 2-11. The next region is the heat pipe, and the outer region is the outer conduction zone. Only in the heat pipe region is the fluid flow expected to significantly influence the heat transfer.

The computed temperature (T), gas pressure (P), liquid saturation (S), and mole fraction of air in the gas phase (Y) are shown in Figure 2-12 for six different times as computed by Doughty and Pruess (1988). The heat pipe is distinguished by the region of near constant temperature of 100 °C (a "plateau" in temperature curves). The development of the heat pipe is especially evident after two months. The inner conduction zone is distinguished by the increase in temperature above 100 °C and can be seen after 1.3 years. The inner conduction zone continues to increase in size which indicates that the water is continuously driven from the medium adjacent to the HLW package.

Pruess et al. (1990b) report a comparison between an explicit fracture model and an effective continuum model for a heat pipe in a matrix whose permeability is representative of Topopah Spring densely welded tuff (2 microdarcy =  $2 \times 10^{-18}$  m<sup>2</sup> which is consistent with the values reported in Table B-1). The heat pipe is suppressed using the lower permeability matrix for either explicit or continuum model, as illustrated by the lack of a temperature plateau in Figure 2-13. The size of a heat pipe is strongly influenced by the matrix permeability, where high permeability encourages the development of a heat pipe (e.g., Figure 2-12 where  $k_{SAT} \sim 10^{-12}$  m<sup>2</sup>) and low permeability suppresses a heat pipe (e.g., Figure 2-13 where  $k_{SAT} \sim 10^{-18}$  m<sup>2</sup>). Because of the low matrix permeability at the proposed repository, a heat pipe is not anticipated to be important.

## 2.2.2 Condensate Dripping in Fractures, Boiling Zone

Condensate dripping in fractures has been experimentally observed at the DOE sponsored G-tunnel tests (Ramirez et al., 1991a,b; Lin et al., 1991). In the G-tunnel tests, heaters were installed in a partially saturated, fractured tuff which is similar to that at Yucca Mountain. The tests lasted on the order of months during which the rock near the heaters dried and a "saturation halo" developed (Buscheck and Nitao, 1992). It was observed that the *in situ* water vaporized near the heaters and flowed primarily in fractures towards cooler regions where it condensed on the fracture walls. During the early times in the tests, the condensate was imbibed in the surrounding matrix. At later times, the condensate flowed in fracture networks due to gravity. The flow of water vapor was not influenced by gravity while the condensate flow in the fractures was primarily gravity driven. The condensate above the heaters was observed to flow back towards the heaters. The condensate below the heaters flowed away from the heaters. The combined vaporization, vapor flow, condensation, and gravity-driven dripping in fractures tends to shed moisture away from waste canisters and down towards the water table. Because the densely welded tuff rock matrix has a low permeability, the condensate was found to drain great distances before imbibing into the matrix. The possibility of condensate dripping onto waste canisters for the proposed repository has been noted by Buscheck and Nitao (1992). Condensate dripping may be important in predicting waste canister corrosion processes and predicting canister integrity lifetimes.

In Section 2.1.2 of this report, thermal processes are shown to provide the impetus for condensate formation, which can lead to condensate drainage. In this section, the feedback of liquid dripping flow is discussed as it may influence thermal processes, that is, the temperature field. A strong hydrologic feedback to the temperature field may occur when condensate drains into a "boiling zone" thereby maintaining the temperature near 100 °C. The heat will be transferred by conduction into the

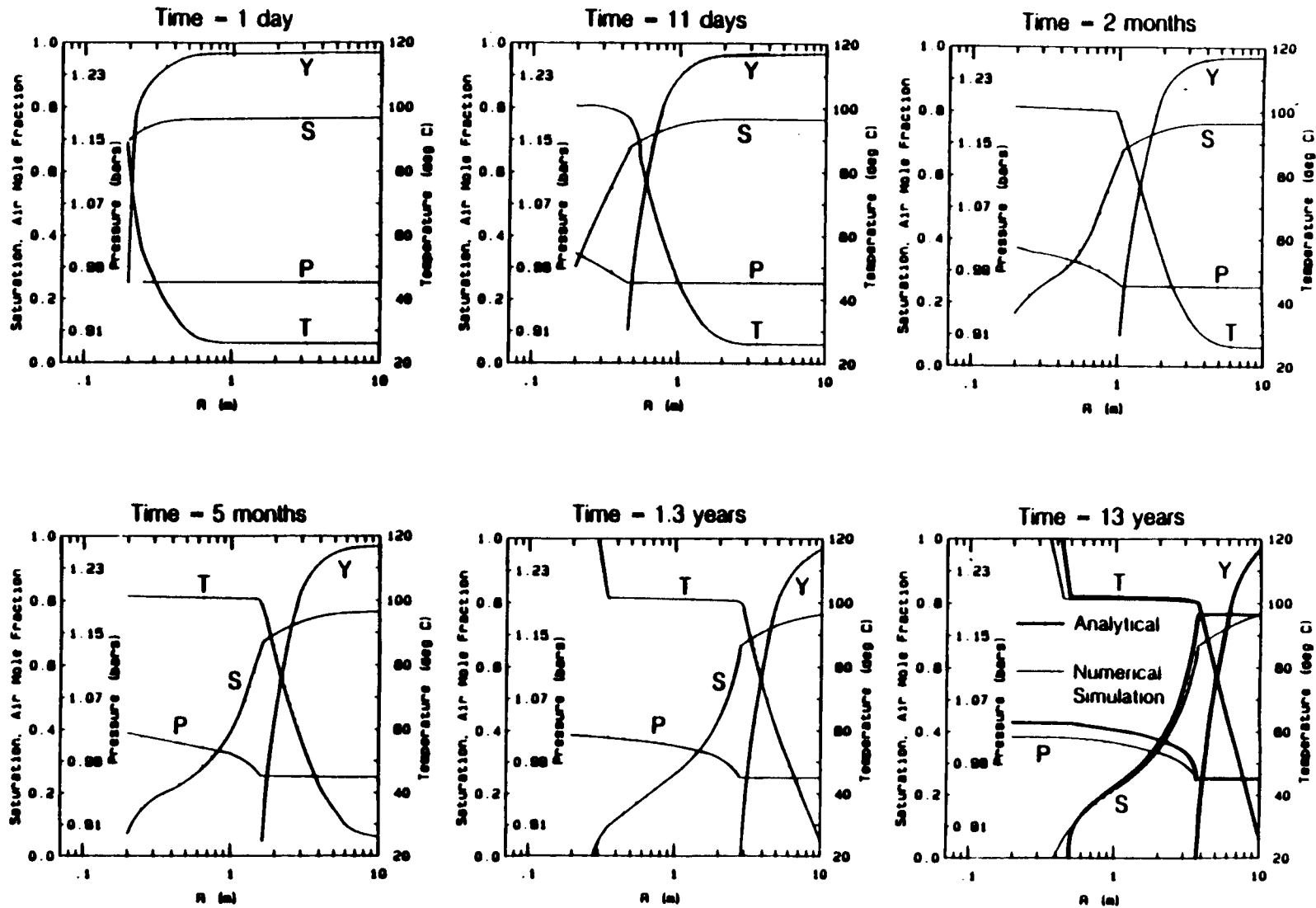
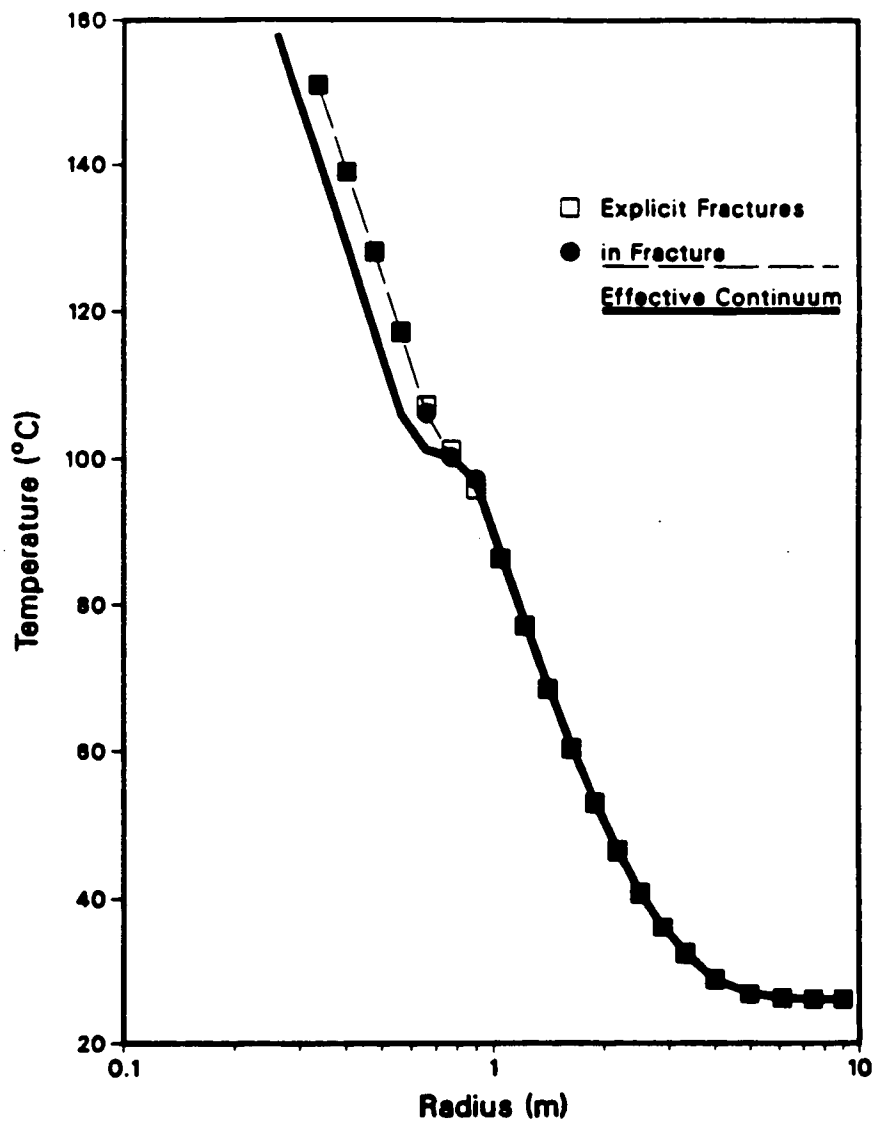


Figure 2-12. Numerically-Simulated Saturation, Pressure, Temperature, and Air-Mole-Fraction Profiles at Various Times (Doughty and Pruess, 1988). A Heat Pipe is Evident by a Temperature "Plateau."



**Figure 2-13. Temperature Profiles Showing a Lack of a Plateau Near 100 °C, Hence the Absence of a Heat Pipe. Calculations Based on an Explicit Fracture Model and an Effective Continuum Model Using Hydrologic Properties Representative of Topopah Spring Densely Welded Tuff (Pruess et al., 1990b).**

boiling region where it is removed by vaporization and vapor flow. In the G-tunnel tests, a region of constant temperature near 100 °C (i.e., a boiling zone) was observed.

The locations of temperature measurements and observed fractures for the G-tunnel tests are illustrated in Figure 2-14. A dry zone was observed around the heater using neutron logging measurements (Ramirez et al., 1991c). The fractures were experimentally observed to significantly affect the moisture redistribution and the temperature field. The fractures provided a preferential pathway for vapor flow and condensate drainage. The condensate drainage then influenced the temperature field. Temperature measurements were taken along a line both above (line P2 in Figure 2-14) and below (line P3 in Figure 2-14) the heater, and are plotted in Figures 2-15 and 2-16, respectively. A "plateau" was observed for some of the temperature measurements below the heater (see Figure 2-15, thermocouple numbers 88 and 89). These thermocouples were located to the lower left of the heater with 88 nearer the heater and adjacent to a vertically oriented fracture. It is noticeable that the plateau persisted for many days of the experiment. The value of the plateau is near 96 °C which corresponds to the boiling temperature of water for the elevation of the G-tunnel experiments. Hence, it is believed that draining condensate in the fracture acted to supply fluid to the region where boiling occurred. None of the thermocouples above the heater experience a plateau, hence gravity-driven condensate drainage is thought to be an important hydrologic process.

Zimmerman and Blanford (1986) also reported an experimentally observed dry zone, boiling region, and condensation region. The shape of the boiling region was governed by the presence (or absence) of fractures. Similarly, the boiling zone exhibited a temperature plateau of about 95 °C. "Water migrations" were noted to affect temperatures over localized regions of the rock, but these effects would disappear after the water was vaporized. Aside from localized regions in the rock, the hydrology did not significantly affect the temperature field. Zimmerman and Blanford (1986) attributed the observed temperature plateau to capillary-driven heat pipe phenomena. However, the localized nature of the plateau and the corroborating data from Lin et al. (1991) suggest that gravity-driven condensate drainage in fractures caused the temperature plateau (boiling region) as noted by Lin, et al.

### 2.2.3 Natural Convection

In Section 2.1.4 of this report, the temperature field is noted to influence the hydrologic flow field due to buoyancy-driven natural convection. In this section, the hydrologic flow field is noted to be able to affect the temperature field. Buoyancy-driven natural convection pertinent to a saturated geologic repository has been studied by Kulacki and Keyhani (1987) and Rajen and Kulacki (1987), among others. The repository was assumed to be in a saturated, homogeneous, isotropic medium and a repository-scale natural convection study was conducted. Rajen and Kulacki assumed the repository, as well as the side and top boundaries, to be impermeable. Although the boundary conditions and the assumption of a saturated homogeneous medium are not realistic for the present partially saturated repository, these early studies do contain basic information with which to gauge the importance of the thermal-hydrologic coupling.

The geometry used by Rajen and Kulacki (1987) is shown in Figure 2-17. The experimental results (from a scaled laboratory setup) and numerical results are shown in Figure 2-18. The Rayleigh number is a measure of the strength of the thermal driving force to induce fluid motion. The Nusselt number is defined as the ratio of conductive plus convective heat transfer, divided by the stagnant fluid

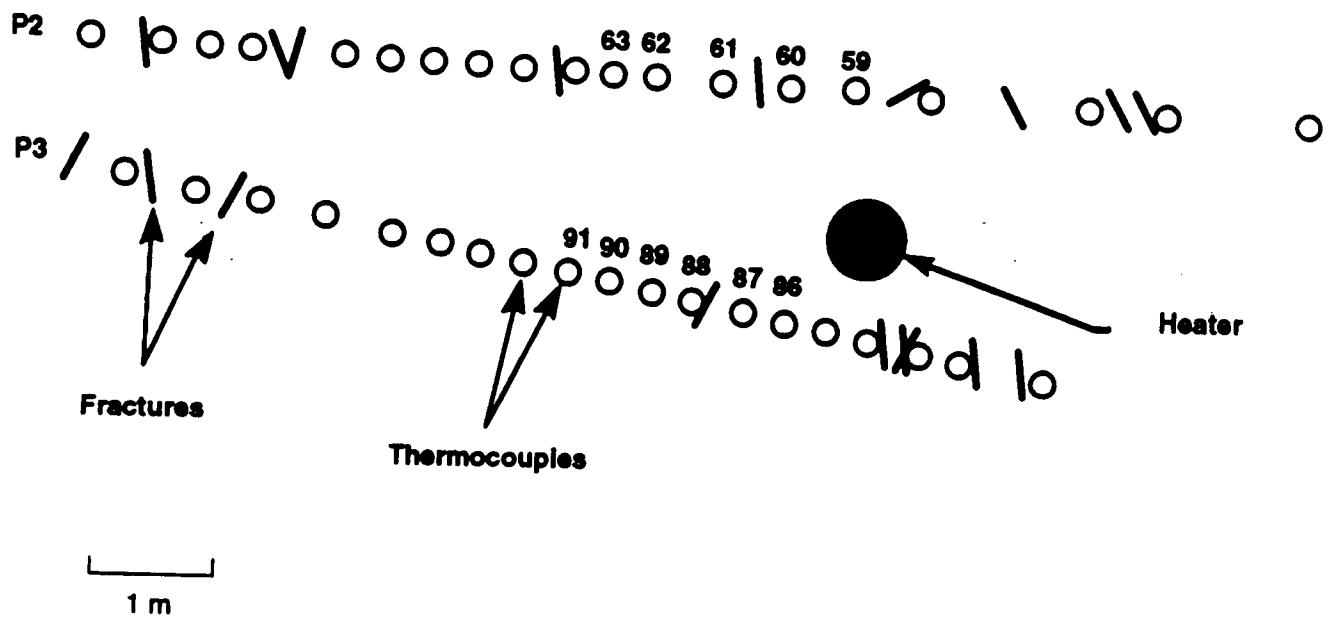


Figure 2-14. Location of Thermocouples, Major Fractures, and Heater in G-Tunnel Heater Tests (Adapted from Ramirez et al., 1991b)

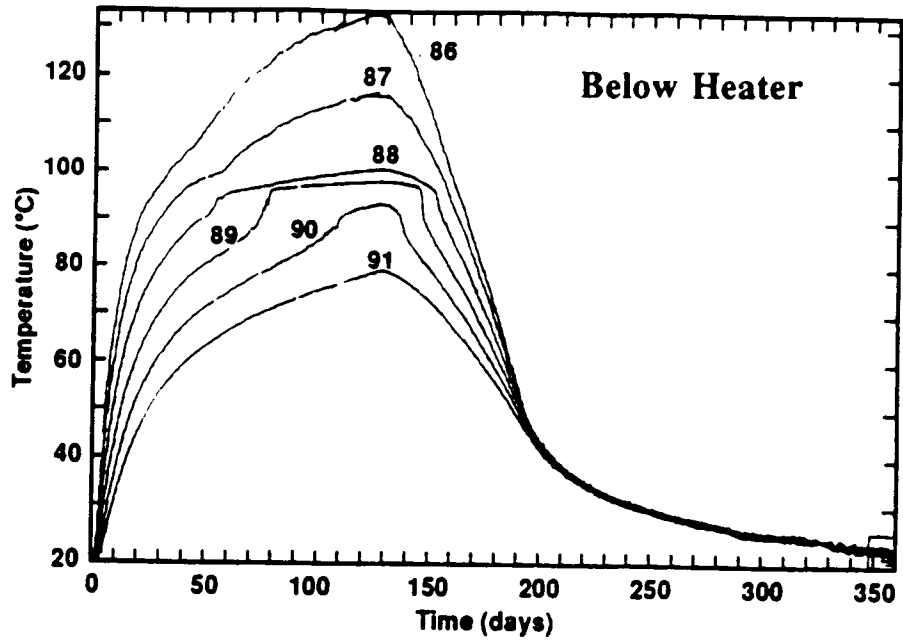


Figure 2-15. Temperature History of Selected Thermocouples Below the Heater, see Figure 2-14 for Thermocouple Locations (Lin et al., 1991)

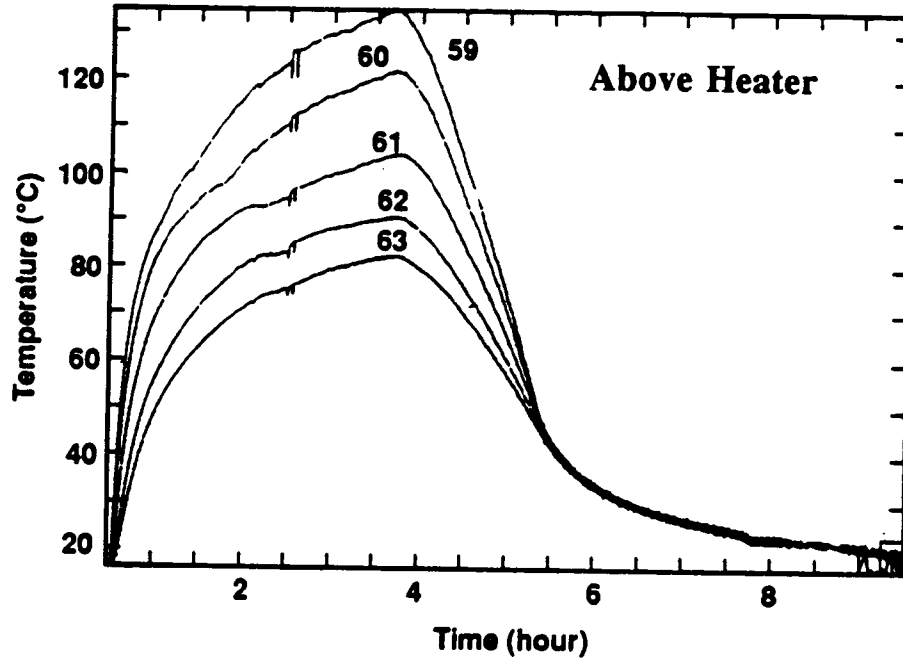


Figure 2-16. Temperature History of Selected Thermocouples Above the Heater, see Figure 2-14 for Thermocouple Locations (Lin et al., 1991)

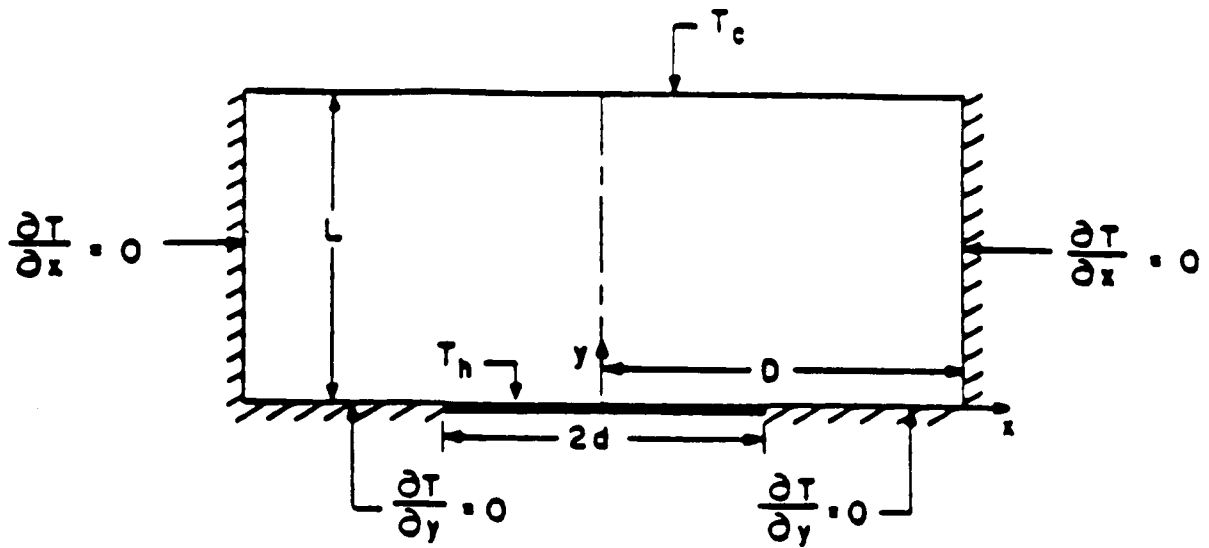


Figure 2-17. Two-Dimensional Model of the Overlying Medium at a Geologic Repository (Kulacki and Keyhani, 1987)

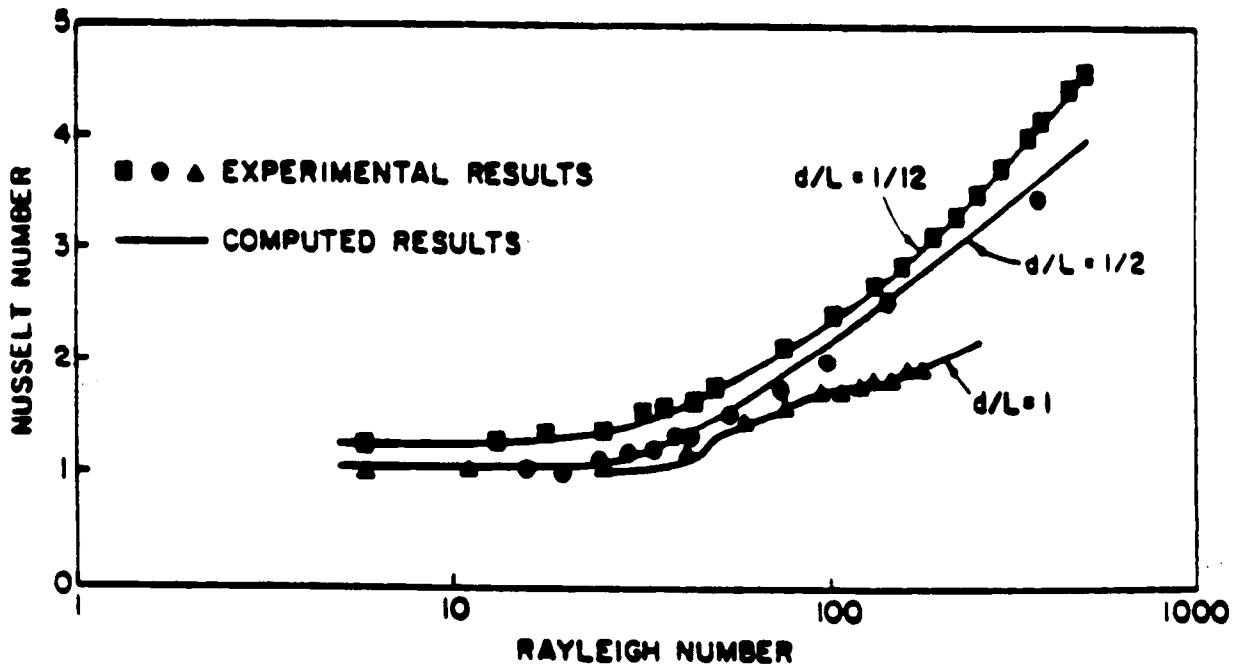


Figure 2-18. Experimental Results Which Reflect Repository Conditions for a Saturated, Homogeneous, Isotropic Medium, see Figure 2-17 (Rajen and Kulacki, 1987)

conductive heat transfer. As such, the Nusselt number is a measure of the strength of the convective fluid flow. For a stagnant fluid, the Nusselt number is unity and the heat transfer is due to conduction. As the Rayleigh number increases, the convective flows increasingly influence the heat transfer as seen by an increasing value for the Nusselt number.

The permeability of the medium used in Figure 2-18 was  $3.5 \times 10^9$  m<sup>2</sup> which is at least 2-4 orders of magnitude larger than that at Yucca Mountain (see Table B-1). The porous medium Rayleigh number is proportional to the saturated permeability (see Equation 2-5). Hence a typical repository scale Rayleigh number is expected to be 2-4 orders of magnitude smaller than those reported in Figure 2-18. From Figure 2-18, it is evident that at lower Rayleigh numbers, the Nusselt number is unity indicating negligible hydrologic effects on thermal processes. A unity Nusselt number also indicates an essentially stagnant fluid. Because of the partially saturated condition and low medium permeability, buoyancy-driven natural convection is anticipated to be negligible at Yucca Mountain.

#### **2.2.4 Material Properties**

The moisture content of a porous medium frequently has an influence on the effective material properties such as thermal conductivity and heat capacity. De Vries (1963, 1975) among others, has studied soils and reported semi-empirical correlations of the soil thermal conductivity and heat capacity as functions of mineral composition, porosity, and water content. Although theoretical models of effective properties are useful, direct experimental measurements are recommended.

Horton et al. (1983) and Horton and Wierenga (1984) have studied methods to measure the effective thermal conductivity of a porous media which include the cylindrical probe method and the microwave moisture-distribution method. These methods reflect continuing improvements in experimental techniques, especially in measuring partially saturated thermal conductivity as a function of moisture content. To date, much attention has focused on methods for soils and modified techniques are being adapted for low porosity tuffaceous rock.

Rasmussen et al. (1990) described a cylindrical probe method to measure thermal properties as functions of water content (see Figure 2-19). In this setup, a steady input is supplied to the heating unit and the temperature in the outer hole is measured and used to calculate the thermal conductivity. Rasmussen et al. (1990) reported that the thermal conductivity for Apache Leap tuff (similar to rock at Yucca Mountain) decreases by approximately 30 percent from fully saturated to oven dried conditions. The relationship between thermal conductivity and saturation was nonlinear and became more important for drier samples. The influence of saturation on thermal conductivity is substantially less than for hydraulic conductivity (where it decreases by many orders of magnitude), however the change can be important in determining the temperature field.

Radhakrishna et al. (1990) conducted thermal experiments simulating a backfilled disposal vault with a bentonite-sand buffer-backfill. The one-eighth scale model examined the thermal drying and rewetting of the medium. "Shrinkage cracks" in the buffer material occurred as a result of thermal drying. The rate of change in temperature increased as the drying zone increased, indicating a decrease in the thermal conductivity and thermal capacity of the buffer material. However, the drying zone and the formation of shrinkage cracks did not significantly decrease the efficiency of the buffer in its capacity to dissipate heat from the heater to the surrounding rock environment (Radhakrishna et al. 1990).

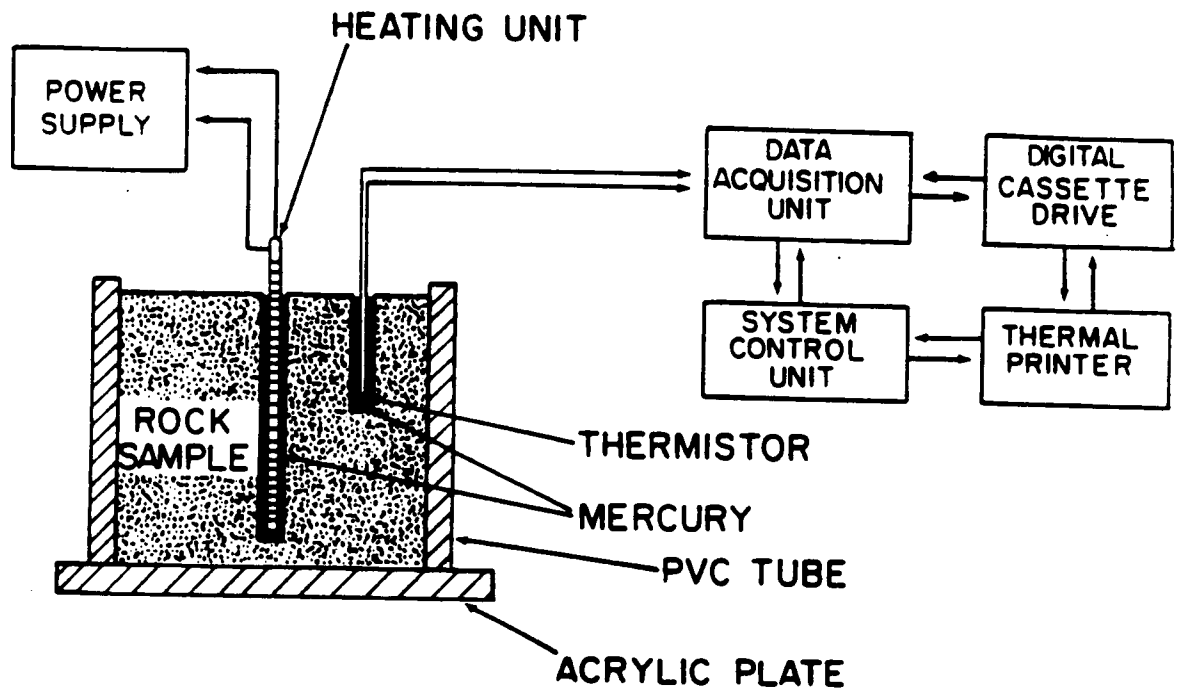


**Figure 2-19. Experimental Apparatus Used to Measure the Thermal Conductivity of Apache Leap Tuff as a Function of Water Content (Rasmussen et al., 1990)**

## 2.2.5 Summary and Conclusions

In this section, the influence of hydrologic processes on thermal processes (H -> T) was reviewed. Specifically four mechanisms of H -> T couplings were discussed in the areas of: (i) a heat pipe, (ii) boiling zone, (iii) buoyancy-driven natural convection, and (iv) thermal properties. Each coupling mechanism can be important, depending on specific conditions of the medium and processes.

The heat pipe is a coupling mechanism which efficiently transfers heat due to vaporization, pressure-driven vapor flow, condensation, and capillary-driven liquid flow. A distinguishing characteristic of a heat pipe is a plateau in the temperature profile (this is also a characteristic for gravity-driven condensate drainage into a boiling zone). The capillary-driven liquid flow in a heat pipe is expected to occur over a large area (Figure 2-11) as compared to localized areas for gravity-driven flow in fractures. For values of rock permeability relevant to Yucca Mountain, however, the heat pipe is not expected to be significant (Figure 2-13).

The gravity-driven condensate drainage in fractures into a boiling zone is another mechanism which can influence thermal processes. This coupling mechanism is very similar to the heat pipe, yet the difference is the dominant mechanism for liquid flow. In the heat pipe it is capillary-driven flow in the matrix, and here it is gravity-driven flow in the fractures. This mechanism may provide a sufficient flow of liquid into a boiling zone so that the temperature is maintained at 100 °C (i.e., a temperature plateau). The location and orientation of fractures is important in dictating where condensate flows. Hence, this mechanism is spatially localized, whereas the heat pipe mechanism is spatially distributed. This mechanism appears to be relevant to Yucca Mountain because the Topopah Spring unit is fractured and of low matrix permeability.

Buoyancy-driven natural convection is another mechanism for a H -> T coupling. However, the analyses in the literature suggest that natural convection at Yucca Mountain will have a negligible influence on thermal processes.

Thermal material properties (e.g., thermal conductivity) can also be influenced by hydrologic processes such as drying of the porous medium. There have been a number of studies which measure thermal properties of porous media such as tuffaceous rock. The effective thermal conductivity can be 30 percent lower for oven-dried tuff than for fully saturated tuff due to the lower conductivity of air compared with liquid water. Similarly, shrinkage cracks in drying buffer material have been experimentally reported. These changes, however, may be negligible because of the inherent uncertainty and spatial variability of thermal properties for the medium of interest at Yucca Mountain.

Overall, hydrologic processes may influence thermal processes through a number of coupling mechanisms. The couplings do appear plausible; however, most do not appear significant at Yucca Mountain. The most prominent coupling mechanism is gravity-driven condensate drainage in fractures which depends strongly on the temperature field and fracture locations. It is conceivable that liquid condensate will drain near a number of waste canisters, thereby maintaining the temperature near 100 °C (plateau). The other coupling mechanisms are possible, yet less likely or less significant.

## 2.3 THERMAL -> MECHANICAL

The emplacement of spent nuclear fuel underground has the effect of generating expansion of the rock mass, producing thermal stresses, and the potential for normal and shear displacements of the fractures. The extent of thermally induced stresses will depend on the thermal load which in turn depends on the age of the waste at the time of emplacement, canister spacing, etc. For high thermal loads, high temperature gradients are expected, hence high stress levels are expected near the waste emplacement canisters. The thermal stresses are expected to persist during the life of the repository.

### 2.3.1 Mechanical Properties and Material Strength

Preliminary testing of the thermal properties of the host rock in the Topopah Springs geologic unit at Yucca Mountain has shown low coefficients of thermal expansion and higher than expected thermal conductivity properties (Nimick, 1990). Such properties, if shown to be true based on further site characterization studies, would be considered favorable conditions in accommodating the induced thermal stresses developed by emplacement of the waste. However, the effect of temperature on the strength of rock in the potential repository horizon is not well determined at this time and needs further investigation. Rock strength generally decreases with increasing temperature. Price et al. (1987) reported that for samples from the potential repository horizon, Young's modulus shows an average decrease of 16 percent as the temperature is raised from 22 to 150 °C at both 0 and 5 MPa confining pressures.

Several preliminary analyses have also been conducted to determine the effect of thermal loading on the stability of underground excavations at Yucca Mountain. Arulmoli and St. John (1987), Christianson and Brady (1989), and Bauer and Costin (1990) have estimated temperature, stress, and deformation fields around emplacement holes in the potential repository. These studies conclude that spalling due to thermal stresses and fractures or slip along fractures are expected to be minor.

### 2.3.2 Thermally-Induced Stresses

Conductive heat transfer within a solid continuum was discussed briefly in Section A.1, with the three dimensional heat conduction equation given by Eq. A-8. This equation is given in its simplest form by assuming constant thermal conductivity and no energy source/sink terms present. In partially saturated rock with tightly packed joints and fractures, conduction through the medium, as governed by Eq. (A-8) would be the primary mode of heat transfer. Several *in situ* heated block tests completed to date suggest that conductive heat transfer is in fact dominant and sufficient to describe temperatures in jointed rock (Zimmerman et al., 1986 and Voegelé et al., 1981).

A change in the temperature of the medium results in a change in the state of stress and strain. In the case of linear elastic material behavior, the strain tensor can be assumed to consist of the sum of the components of strain due to an incremental change in temperature and those strain components due to mechanical deformation within the rock alone. This relation can be expressed as

$$e_{ij} = e_{ij}^{\circ} + e'_{ij} \quad (2-6)$$

where

- $e_{ij}^{\circ}$  = strain induced by an increment of temperature  
 $e'_{ij}$  = strain induced by mechanical deformation (Eq. C-5)

The temperature induced strain ( $e_{ij}^{\circ}$ ) can further be expressed as

$$e_{ij}^{\circ} = \alpha \Delta T \delta_{ij} \quad (2-7)$$

where

- $\alpha$  = linear thermal expansion coefficient ( $1/^{\circ}\text{C}$ )  
 $\Delta T$  = increment in temperature ( $^{\circ}\text{C}$ )  
 $\delta_{ij}$  = Kronecker delta function

The above relation represents a property of an isotropic body in which a change of temperature results in no change of shear, the only result being a change of volume of an elementary parallelepiped. Combining Eqs. (2-7) and (C-5) gives

$$e_{ij} = \alpha \Delta T \delta_{ij} + \frac{1}{2G} \left( \sigma_{ij} - \frac{\nu}{1+\nu} \sigma_{kk} \delta_{ij} \right) \quad (2-8)$$

where

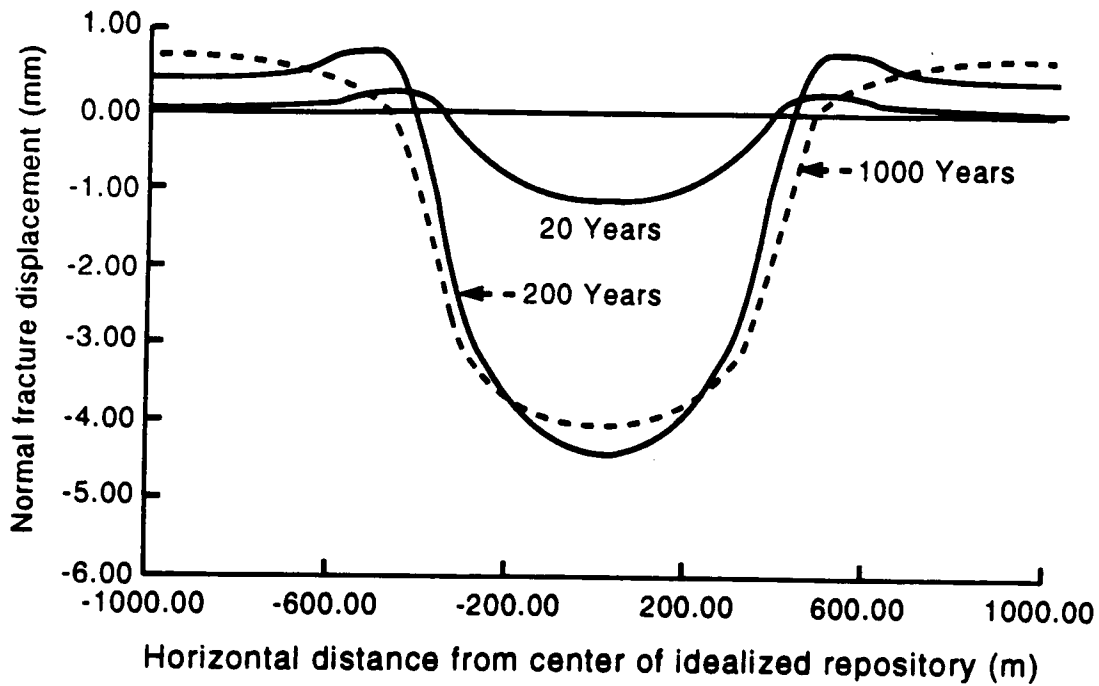
- $\sigma_{ij}$  = components of stress tensor

which are known as the Duhamel-Neumann relations (Nowacki, 1962). Solving this system of equations with respect to the stresses results in

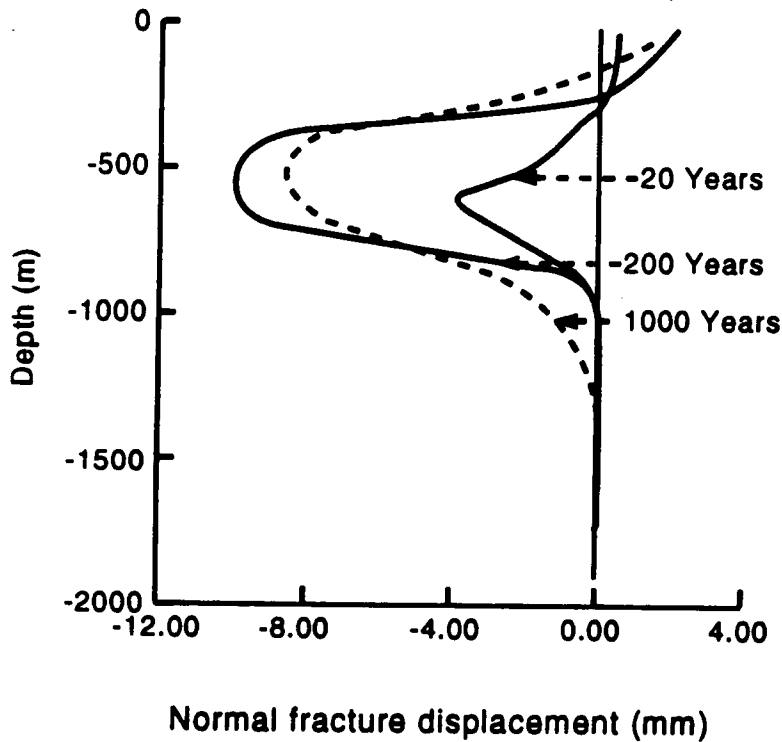
$$\sigma_{ij} = 2G \left[ e_{ij} + \frac{\nu}{1-2\nu} \left( e_{kk} - \frac{1+\nu}{\nu} \alpha \Delta T \right) \delta_{ij} \right] \quad (2-9)$$

which gives six stress equations for  $i$  and  $j$  equal to 1, 2, and 3. The second term within the parenthesis is responsible for the thermally induced portion of the stress.

Numerous studies have been conducted to determine the impact of thermal loading from an underground repository on the mechanical state. Shen and Stephansson (1990a) performed three-dimensional numerical simulations with the computer code 3DEC, in which they modeled an area  $2 \text{ km} \times 2 \text{ km} \times 2 \text{ km}$ . In this model, the repository heat loading was modeled with exponentially decaying heat sources, and excavations were left out. They found that the rock stresses varied proportionally with the change in rock temperature, and reached a maximum after 200 years (when the rock temperature in the repository region was at its maximum). Compared to the *in situ* stress, the stress level increased in the repository region, while a decrease was seen further away. No tensile stresses developed within the model. Figure 2-20 shows the normal displacement response of fractures in both the horizontal and vertical orientations intersecting the repository region. The 3DEC analysis shows that the normal displacement due to thermal loading results in both horizontal and vertical fractures closing in the region



(a)



(b)

**Figure 2-20. Thermally Induced Normal Fracture Displacement (a) for Horizontal Fracture Zone Just Beneath the Repository and (b) of Vertical Fracture Zone Intersecting Repository. A Positive Sign Indicates Opening Displacement. (From Shen and Stephansson, 1990a)**

around the repository. Outside this region, fractures were seen to open as much as 2 mm.

Shen and Stephansson (1990b) conducted a thermal-mechanical analysis at the tunnel scale using the 3DEC code. The dimensions for this model were 25 m × 25 m × 18 m, and the joint spacing was on the order of 1 m. Their results showed that the response of the rock mass to the thermal effect was most significant in the vicinity of the tunnel and deposition hole. Large compressive stresses and tensile stresses were shown to develop in the tunnel roof when the temperature reached its maximum after 200 years. The tensile stresses were of the order of the tensile strength, indicating the potential for local rock failure. All joints were seen to close during the thermal loading period.

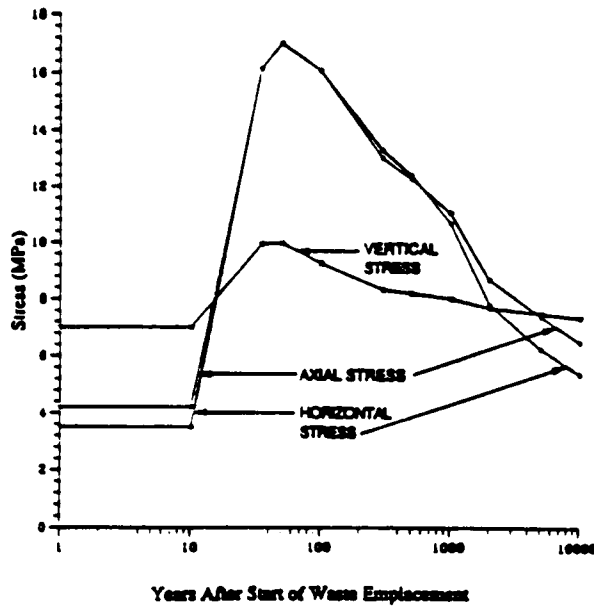
Costin and Chen (1991) performed a thermomechanical analysis of the G-tunnel heated block experiment using a two-dimensional finite element model incorporating a compliant-joint rock mass model. Their main goal of the work was in the verification and validation of numerical models for simulating the behavior of a jointed rock mass subjected to thermal and mechanical loads. They were able to obtain good quantitative agreement between the temperatures calculated from the model and the temperatures measured in the heated block experiment, when they took into account the convective loss of heat from the top surface of the heated block. Comparison of the thermally induced displacements between the finite element analysis and the heated block experiment provided much less quantitative agreement. The disagreement in the displacement results was considered to be due to uncertainties in the displacement measurements from some of the gauges, and the fact that a two-dimensional analysis was conducted of a truly three-dimensional experiment. In addition, the compliant-joint model assumes two sets of perpendicular joints and may not have been truly representative of the jointing in the actual block itself.

Bauer et al. (1991) performed two and three dimensional numerical analyses to predict thermal and stress environments in the vicinity of repository openings at Yucca Mountain. For the proposed power density and emplacement schedule for the waste, their results showed, in general, that openings close to heat sources would attain high temperatures and experience a significant stress increase. They considered stresses resulting from *in situ*, thermal, and seismic effects in designing the drifts, and found that for all drift types, the thermal stress is the greatest horizontal component included in the combination. Hardy and Bauer, 1991 report that the horizontal stress at the repository horizon can change from the initial conditions of 3 to 6 MPa up to 15 to 20 MPa, depending on the design assumptions and host rock properties. As a consequence, this thermal loading would require unique drift design considerations to reduce deterioration of the rock throughout the repository operational period. Figure 2-21 illustrates the stress history at the waste emplacement drift and tuff main drift for the Yucca Mountain repository, and shows that the thermal loading of a drift location around the repository is very location-dependent (Hardy and Bauer, 1992). The tuff main drift sees reduction in vertical stress but a significant increase in horizontal stress, even though its temperature rise is modest. This is due to thermal expansion of the rock mass in waste emplacement regions which surround the mains.

### 2.3.3 Computer Codes

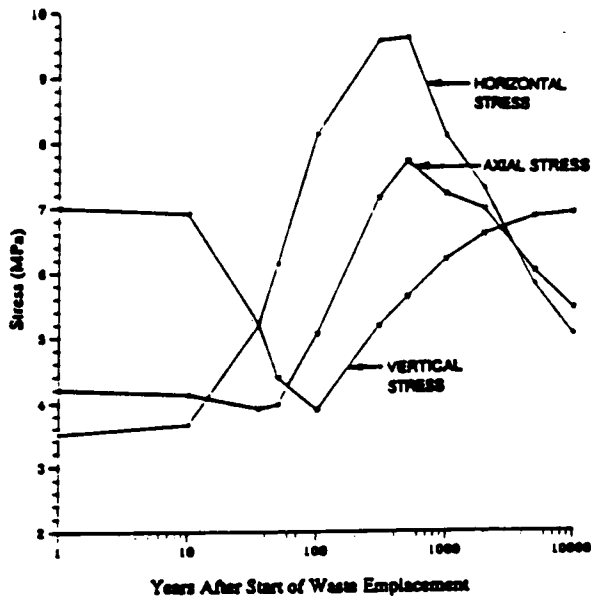
In most of the computer codes that perform coupled thermal-mechanical analysis, the coupling is assumed to be one-way (i.e., thermal affecting mechanical). This is primarily done because the thermal to mechanical coupling is dominant, causing changes not only in stresses and strains, but also in mechanical properties and material strength. The effect of mechanical changes on thermal properties is generally assumed to be negligible. Many computer codes perform thermal-mechanical analysis in a

### Emplacement Drift



(a)

### Tuff Main Access Drift



(b)

Figure 2-21. Thermomechanical Environment in the Vicinity of (a) Waste Emplacement Drift and (b) Tuff Main Access Drift at the Proposed Repository Beneath Yucca Mountain. (From Hardy and Bauer, 1992)

sequentially coupled manner. For instance, a heat transfer code is used to obtain the temperature distribution, which is then input into another mechanical code to calculate the temperature induced stresses. This approach is justifiable when performing linear elastic stress analysis, however, most rock joints behave nonlinearly. Thus, when explicitly modeling jointed rock mass behavior, one needs to apply the thermal loading in an incremental and realistic manner, while updating the mechanical state after each thermal loading increment. The following is a short list of some of the available computer codes applicable to the HLW program that can perform coupled thermal-mechanical analysis. The list includes only those codes that are considered most applicable to the high-level waste program, and can perform both thermal and thermomechanical analyses.

#### **2.3.3.1 UDEC, 3DEC**

Both the two-dimensional code UDEC (Board, 1989a) and three-dimensional code 3DEC (Cundall, 1988) have thermal-mechanical capabilities. Both codes are based on the discrete element method, which allows for explicit modeling of jointed rock mass behavior. The heat transfer in both codes is based on conductive transfer within the medium with the provision for temperature, flux, convective, or radiative boundaries. Only one-way coupling from thermal to mechanical is considered. Both codes use explicit and implicit finite difference schemes. The approach used in performing a coupled analysis with either code is to first run the problem out to some specified number of thermal time steps. At this point, the thermal or real time is held constant, while mechanical cycling is performed to reach a new equilibrium state. This process is then continued. The requirement in performing the simulation in this manner is that temperature increases between successive thermal time steps cause only "small" out-of-balance forces in blocks, especially for nonlinear problems.

#### **2.3.3.2 SPECTROM-32**

SPECTROM-32 is a finite element program for analyzing two-dimensional and axisymmetric inelastic thermomechanical problems related to the geologic disposal of nuclear waste (Callahan et al., 1989). The code is part of the SPECTROM (Special Purpose Engineering Codes for Thermal/Rock Mechanics) series of special-purpose computer programs developed by RE/SPEC, Inc., to address many unique rock mechanics problems encountered in analyzing radioactive wastes stored in geologic formations. The principal component models used in the SPECTROM-32 program involve thermoelastic, thermoviscoelastic, thermoelastic-plastic, and thermoviscoplastic types of material behavior. Special material considerations provide for the incorporation of limited tension material behavior and consideration of jointed material behavior. Numerous program options provide the capabilities for various boundary conditions, sliding interfaces, excavation, and backfill, which are important to the geologic disposal of radioactive wastes.

#### **2.3.3.3 STRES3D**

STRES3D is a semi-analytical computer model for infinite or semi-infinite regions, which makes use of solutions for constant and exponentially-decaying point heat sources. The rock mass is assumed to be intact and homogeneous and has properties that are stress-, temperature-, and time-dependent. For semi-infinite problems, the program models the earth surface as isothermal and stress free. The code has been shown to be efficient in modeling the temperatures and thermally-induced stresses generated from a typical repository layout containing a large number of waste emplacement panels (e.g., see Bauer et al., 1991).

#### 2.3.3.4 FLAC

FLAC (Fast Lagrangian Analysis of Continua) is a two-dimensional finite difference program for modeling soil and rock behavior (Board, 1989b). FLAC has features including: (i) models for large-strain plasticity, strain-softening, and volumetric yielding models, (ii) cable elements for modeling reinforcement, (iii) interfaces to represent joints, (iv) automated mesh generation, (v) groundwater flow and consolidation, and (vi) optional creep and thermomechanical modeling capabilities. The coupling capabilities within FLAC include  $T \rightarrow M$ ,  $H \rightarrow M$ , and  $M \rightarrow H$ . Thermal-hydrologic-mechanical coupled modeling can be accomplished within FLAC by first determining the thermomechanical response followed by cycling to hydrologic-mechanical equilibrium. In the case of nonlinear behavior, small thermal steps must be taken in order to obtain accurate results.

#### 2.3.4 Summary and Conclusions

In this section, the influence of the temperature field on mechanical processes has been discussed. In particular, in the near field the temperature rise in the rock adjacent to the borehole could approach 200 °C during the first 100 years (Figure A-2). The thermally-induced stresses will most likely be much larger than those due to the *in situ* stress field or induced by mechanical excavation and seismic events.

The computer codes listed have been widely used and give the analyst many options in modeling the long term mechanical behavior of a repository under thermal loading, assuming either continuum or discontinuum rock mass behavior. Numerous thermomechanical studies using these codes have been discussed in this section. These codes have many limitations and many options of these codes may need verification and validation against well-controlled laboratory or field experiments. Experimental and field studies on the impact of temperatures on mechanical properties and long term mechanical degradation will be needed.

### 2.4 MECHANICAL $\rightarrow$ THERMAL

Mechanical processes are characterized through the stress, strain and/or displacement fields, and thermal processes are characterized through the temperature field. The objective of this section is to review how mechanical processes may influence thermal processes ( $M \rightarrow T$ ) at Yucca Mountain. In the literature, the  $M \rightarrow T$  coupling has not been considered important, and is rarely mentioned in consideration of Yucca Mountain. The mechanical processes are thought to influence thermal processes by primarily changing fracture apertures, hence changing the effective thermal conductivity. Frictional dissipation of mechanical energy is another way which is analogous to viscous dissipation discussed in the subject of fluid mechanics (Bird et al., 1960). However, no literature considered frictional dissipation to be important, hence it is not considered here.

Lin et al. (1991) note that fractures were experimentally observed to affect the temperature field. Most notably, thermocouple readings indicated lower temperatures for locations behind fractures (i.e., fractures located between the thermocouple and the heat source). The fractures increased the effective thermal resistance to conductive heat transfer.

Mechanical processes may influence hydrologic and/or chemical processes which then influence thermal processes, yet this is considered a sequence of couplings and not a direct coupling (hence it is not considered in this section, but in other sections). For example, mechanical processes are expected to

change fracture apertures which may affect condensate drainage which then may affect the temperature field. As such, this would be a M -> H -> T sequence of couplings which would be discussed in this report as two one-way couplings, that is, M -> H, and H -> T. There is little to no discussion in the literature of direct M -> T couplings, primarily because there is no evidence that it is important.

## 2.5 THERMAL -> CHEMICAL

As suggested by the name thermodynamics, geochemical processes are strongly influenced by the temperature of the environment in which the process is operating. As discussed in Appendix B, most of the thermodynamic properties used in calculating geochemical equilibrium (equilibrium constants, free energies, activity coefficients) are nonlinear functions of temperature. Rates of reaction are also dependent on temperature through the Arrhenius rate equation. Most of these relationships are well defined by thermodynamic and kinetic theory, and are discussed only briefly below. The reader is referred to a variety of textbooks (e.g., Garrels and Christ, 1965; Moore, 1972; Alberty and Daniels, 1979; Lasaga and Kirkpatrick, 1981; Stumm and Morgan, 1981) for a more extensive and complete treatment of the effects of temperature.

### 2.5.1 Thermal Effects on Equilibrium Chemistry

#### 2.5.1.1 Equilibrium Constants (Log K)

For any chemical reaction at equilibrium, the thermodynamic relationships as described in Appendix B are applicable. As a function of temperature, the standard Gibbs free energy change  $\Delta G_R^\circ$  (J/mole) is defined by the relationship

$$\Delta G_R^\circ = \Delta H_R^\circ - T\Delta S_R^\circ \quad (2-10)$$

where

$\Delta H_R^\circ$  = enthalpy or heat content change of reaction (J/mole),  
 $\Delta S_R^\circ$  = entropy change of reaction (J/mole-K), and  
 T = temperature (K).

At a given temperature,  $\Delta H_R^\circ$  and  $\Delta S_R^\circ$  are determined by the relationships

$$\Delta H_R^\circ = \sum \Delta H_{F, \text{products}}^\circ - \sum \Delta H_{F, \text{reactants}}^\circ \quad (2-11)$$

$$\Delta S_R^\circ = \sum S_{F, \text{products}}^\circ - \sum S_{F, \text{reactants}}^\circ \quad (2-12)$$

where

$\Delta H_F^\circ$  = heat of formation of a compound from its elements in their standard state, and  
 $S_F^\circ$  = entropy of formation of a compound from its elements in their standard state.

Both  $\Delta H_R^\circ$  and  $\Delta S_R^\circ$  are also functions of temperature. The values of  $\Delta H_R^\circ$  and  $\Delta S_R^\circ$  necessary to calculate changes in enthalpy and entropy of reaction are available for a number of common minerals and species at a variety of temperatures (e.g., Robie et al., 1978), and can be simply looked up or interpolated for the temperature of interest. Alternatively, at constant pressure, the heat capacity  $c_p$  [J/(mole-K)] can be used to extrapolate to higher temperatures through the relationships

$$\Delta H_{R,T_2} - \Delta H_{R,T_1} = \int_{T_1}^{T_2} \Delta c_p \, dT \quad (2-13)$$

and

$$S_{T_2} - S_{T_1} = \int_{T_1}^{T_2} c_p \, d \ln T \quad (2-14)$$

where

$$\Delta C_p = \sum C_{p, \text{products}} - \sum C_{p, \text{reactants}}$$

Fit to experimental data,  $c_p$  is commonly reported for solids as an empirical power function of temperature with the general form  $a + bT + cT^{-2}$  ( $a, b, c$  = empirical constants), and is readily integrated (Garrels and Christ, 1965).

Once  $\Delta H_R^\circ$  and  $\Delta S_R^\circ$  are determined at the desired temperature, they can be substituted in Eq. (2-10) and the standard free energy of reaction can be calculated at the new temperature. Once  $\Delta G_R^\circ$  is obtained, the equilibrium constant ( $K$ ) for the reaction can then be calculated using the relationship

$$\Delta G_R^\circ = -RT \ln(K) \quad (2-15)$$

In practice, the rigorous thermodynamic approach outlined above is frequently simplified. The van't Hoff equation has been developed to calculate  $\log K$  values at a new temperature according to the relationship

$$\log K_{T_2} = \log K_{T_1} - \frac{\Delta H_R^\circ}{2.303R} \left( \frac{1}{T_2} - \frac{1}{T_1} \right) \quad (2-16)$$

This relationship assumes that the standard enthalpy of reaction remains constant over the temperature range of interest. According to this relationship,  $\log K$  plotted against  $1/T$  will yield a straight line with a slope of  $-\Delta H_R^\circ/2.303R$ . In practice,  $T_1 = 25^\circ\text{C}$  is commonly used as a reference temperature. Since  $\Delta H_R^\circ$  can only be safely assumed constant over a narrow temperature interval for many reactions, use of Eq. (2-17) is valid only over small temperature intervals. Allison et al. (1990) point out that the van't Hoff equation can lead to significant errors in extrapolating from a  $25^\circ\text{C}$  reference to temperatures on the order of  $100^\circ\text{C}$  or greater.

An alternative approach is used in several thermogeochemical models (Wolery, 1979; Morrey, 1988; Allison et al., 1990). This involves fitting the log K of a given reaction to a power function of temperature. This may be accomplished by tabulating data determined over a range in experimental temperatures and curve-fitting, or else by performing the analysis as outlined above and recasting the log K results in terms of an appropriate mathematical expression. Allison et al. (1990) proposed an expression of the form

$$\log K_T = A + B T + C/T + D \log(T) + E T^2 + F/T^2 + G T^{\frac{1}{2}} \quad (2-17)$$

where

A, B, C, D, E, F, and G = empirical coefficients determined for the reaction of interest.

### 2.5.1.2 Activity Coefficients

In electrolyte solutions, activity coefficient calculations are commonly expressed by an equation such as the Extended Debye-Hückel approximation (Stumm and Morgan, 1981)

$$\log \gamma_i = \frac{-A z_i^2 \sqrt{I}}{1 + B a_i \sqrt{I}} + b_i I \quad (2-18)$$

where

- A, B = constants characteristic of the solvent,
- $z_i$  = the charge on ion i,
- $a_i$  = ion size parameter (angstroms),
- $b_i$  = ion specific parameter that accounts for the decrease in solvent concentration, in concentrated solutions, and
- I = solution ionic strength (moles/kg H<sub>2</sub>O)

For water as a solvent, A and B depend on the dielectric constant  $\epsilon$  (dimensionless) and the absolute temperature T (Kelvin) of the solution (Stumm and Morgan, 1981)

$$A = 1.82 \times 10^6 (\epsilon T)^{-\frac{3}{2}} \quad (2-19)$$

and

$$B = 50.3 (\epsilon T)^{-\frac{1}{2}} \quad (2-20)$$

For dilute solutions, the effect of temperature on the activity coefficient is minor. At higher electrolyte concentrations, the effect of temperature is more pronounced, but the direction of the shift in the activity coefficient with temperature will depend on the species under consideration (Stumm and Morgan, 1981).

For many reactions,  $\Delta_c p$  is close to zero and  $\Delta H_R^\circ$  is essentially independent of temperature (Eq. 2-14). In these instances, the van't Hoff relationship (Eq. 2-17) is applicable and log K vs.  $1/T$  will result in a linear plot. Stumm and Morgan (1981) stress that the applicability of these assumptions and the magnitude and direction of the shift in thermodynamic equilibrium with temperature is dependent on

the thermodynamic properties of the species and phases involved in the reaction being considered. The solution composition, partial gas pressures, solid-solution, and pressure of the system will all help to condition the overall effect of temperature.

## 2.5.2 Temperature Effects on Nonequilibrium Chemistry

Lasaga (1981a) notes that reaction rate constants can increase by several orders of magnitude with temperature increases on the order of 100 °C. This is due to the higher potential energy of molecules and ions at higher temperatures. This additional energy increases the likelihood that molecules and ions involved in reaction will cross over potential barriers to reaction, leading to higher reaction rates. Experimental evidence suggests that the rate constant ( $k$ , in  $\text{sec}^{-1}$ ) for many reactions varies exponentially with increasing temperature. As described in Appendix B, this dependence is commonly expressed in terms of the Arrhenius equation such that

$$k = A_p \exp \left( -\frac{E_a}{RT} \right) \quad (2-21)$$

where

- $A_p$  = Pre-exponential factor,
- $E_a$  = Activation energy (J/mole),
- $R$  = Ideal Gas Constant [8.3147 J/(mole-K)], and
- $T$  = Absolute temperature (K)

Lasaga (1981a) notes that the pre-exponential factor  $A_p$  may vary weakly as a function of temperature. In general, however, it is difficult to separate the effects of a temperature dependent pre-exponential factor from the uncertainties inherent in the experimental data. If the activation energy  $E_a$  is assumed to be constant with respect to temperature, it can be seen from Eq. (2-22) that a plot of  $\ln k$  vs.  $1/T$  results in a straight line with a slope of  $E_a/R$  and an intercept of  $A$ . However, it is possible that  $E_a$  varies with temperature, in which case the  $\ln(k)-1/T$  plot would be curved. In addition, changes in reaction mechanisms may lead to a discontinuous variation of  $E_a$  with temperature.

For mineral dissolution at a constant pressure, Helgeson et al. (1984) proposed that the rate constant ( $k$ ) varies with temperature such that

$$k(T) = \frac{T}{T_0} k^0 \exp \left[ \frac{-\Delta H_m^\ddagger}{R} \left( \frac{1}{T} - \frac{1}{T_0} \right) \right] \quad (2-22)$$

where

- $T_0$  = original temperature (K),
- $k^0$  = rate constant at  $T_0$  ( $\text{moles-cm}^{-2}\text{-sec}^{-1}$ ), and
- $\Delta H_m^\ddagger$  = enthalpy of activation (J/mole)

## 2.5.3 Computer Codes

A number of computer codes have been developed to calculate geochemical equilibria and, to some extent, reaction kinetics. All of the codes rely on a large, appropriately formatted database containing the thermodynamic properties of a wide variety of minerals, gases, and aqueous species.

Particular emphasis will be placed on the abilities of the various codes to handle temperature variations. While the codes are generally not coupled to thermal processes to the extent that they are able to simulate the convective, conductive, and radiative heat transfer associated with a heat source, they are able to consider the effects of temperature on reaction thermodynamics. The codes have been summarized, compared and contrasted extensively for a variety of problem types (e.g., Nordstrom et al., 1979; Nordstrom and Ball, 1984; Kincaid et al., 1984a,b; Nordstrom and Munoz, 1985; Serne et al., 1990; Mangold and Tsang, 1991), and only a brief summary of the operational features of more commonly used and readily available codes will be given below.

Geochemical codes have generally followed one of two approaches to solving for chemical speciation (1) minimization of  $\Delta G_R^\circ$ , or (2) mass action/mass balance using equilibrium constants. Of the codes listed here, only SUPCRT uses the first approach; all other codes employ the second technique. Morrey et al. (1986) note that because the thermodynamic relationships are well established, different geochemical codes will tend to produce similar answers if the same thermodynamic data is used. Stated differently, the results of geochemical modeling are only as good as the data that are used. The codes listed below usually employ an individualized database, customized to meet the code's formatting requirements for looking up the appropriate values. Values in the database can be modified to incorporate newer, more reliable data or to include additional data not previously available. These data commonly come from a variety of sources that may or may not be referenced. Some of the more conventional sources of these data are listed in Table D-1.

#### 2.5.3.1 SUPCRT

The SUPCRT code (Helgeson et al., 1978; Johnson et al., 1991) was initially developed at the University of California, Berkeley, to calculate equilibrium geochemistry. The code has an extensive thermodynamic database that currently contains (Johnson et al., 1991) over 290 aqueous species, 175 minerals, and 16 gases. By calculating  $\Delta G_R^\circ$  for a reaction, temperature/pressure-independent coefficients and parameters are used to calculate the standard molal thermodynamic properties at elevated temperatures and pressures. The total P-T range available to the code is 0-1000 °C and 1-5000 bars. The data have been carefully screened and checked for internal consistency (Helgeson et al., 1978; Johnson et al., 1991). Since SUPCRT has been in the public domain since about 1978, extensive use in a variety of geochemical problems has resulted in an extremely robust and portable code. Written in FORTRAN 77, SUPCRT has been adapted to both UNIX- and DOS-based systems, and there is a new version available for the Apple MacIntosh (Johnson et al., 1991). Recent modifications to the code (Johnson et al., 1991) have resulted in a more streamlined code with user prompts to aid the user in constructing the input file for a given problem.

#### 2.5.3.2 PHREEQE

The PHREEQE (pH-REdox-EQuilibrium-Equations) equilibrium speciation code, based on the WATEQ and MIX2 codes, was developed in the 1970's by the U. S. Geological Survey (Parkhurst et al., 1980; Plummer et al., 1988). The code has been used extensively, and has been applied to a wide variety of geochemical problems. The code is able to model pH, redox potential, equilibrium speciation and mass transfer as a function of reaction progress. The code is also able to model the mixing of two aqueous solutions. The code has been modified by Brown et al. (1991) to allow mineral precipitation and dissolution, fixed pH, and electrostatic adsorption processes, and Pitzer's equations have been adapted to allow the calculation of activity coefficients in high ionic strength brines (Plummer et al., 1988). PHREEQE can also model the mixing of solutions of differing composition and the titration of one

solution against another. Input is formatted, although Fleming and Plummer (1983) developed an interactive program PHRQINPT for constructing the input files. Originally, the thermodynamic database had only a limited number of minerals available (approximately 40), but has since been enlarged to include up to 200 minerals (Parkhurst et al., 1990). In addition, Tweed (1988) developed the code PICKER to select an appropriately sized database from a larger database of the same format. The PHREEQE code uses conservation of charge, conservation of electrons, total alkalinity, mass-balance, mineral equilibrium, and mass-action expressions to calculate the chemical composition of a system at equilibrium. The code iterates towards a mass balance, using back substitution until the solution is within 20 percent of the convergence criteria, at which point a Newton-Raphson iteration scheme is used to calculate pH, Eh, and mineral saturations. PHREEQE uses the van't Hoff equation (Eq. 2-16) to correct equilibrium constants for temperature effects, and is therefore limited to fairly low temperatures. There is also an option for user-specified power function of the general form  $\log K = A + BT + C/T + D\log T + ET^2$  for mineral equilibrium constants as a function of temperature. The code is in FORTRAN, and has been adapted to VAX and IBM mainframe systems, as well as IBM personal computers.

### 2.5.3.3 WATEQ

The WATEQ and WATEQF series of codes were initially written in the early 1970's and have since been modified and updated (Truesdell and Jones, 1974; Plummer et al., 1976; Ball et al., 1979; Ball et al., 1987). Using tabulated equilibrium constants, the code calculates equilibrium distribution of elements in natural waters. Limited to 1 atmosphere, WATEQ uses the van't Hoff equation to model temperatures from 0-100 °C. The code can use either the Debye-Hückel or Davies equation to calculate activity coefficients. WATEQ has an extensive database that has been exhaustively documented and widely tested in a number of groundwater investigations. The code can only calculate chemical speciation for chemical equilibrium. WATEQ was originally written in PL/1 programming language. The code has been adapted to FORTRAN in the WATEQF series. Back substitution is used to solve for mass balance.

### 2.5.3.4 EQ3/EQ6

The EQ3/EQ6 code, developed at the University of California, Berkeley, in the late 1970's, is one of the more elaborate and complicated geochemical codes (Wolery, 1979; Wolery, 1983; Wolery et al., 1990). The EQ3/EQ6 package is composed of two programs; EQ3 calculates equilibrium aqueous speciation and determines the saturation indices (Q/K) for a wide variety of minerals, while EQ6 calculates mass transfer and reaction progress for heterogeneous precipitation/dissolution. The current database is extensive, and relies mainly on the internally consistent SUPCRT database for the more common species, minerals and gases. The database has recently been modified (Wolery et al., 1990) to include thermodynamic data for radionuclides, including uranium, plutonium, neptunium, thorium, and americium, although these data have not been checked for internal consistency. A limited number of solid-solution minerals are also available in the new database. EQ3/EQ6 has a wide variety of options allowing the user to tailor a simulation to a wide variety of applications. Although the code is largely restricted to dilute solutions by the activity/concentration models used, there is a limited amount of data available for using the Pitzer equations in high concentration brines (Jackson and Wolery, 1985; Jackson, 1988). There has also been some discussion on incorporating sorption models into EQ3/EQ6 (Viani, 1988).

The reaction path modeling available for EQ6 allows the code to consider reaction kinetics, and if the appropriate rate constants are available, reaction progress as a function of time is possible. The code extrapolates to higher temperatures by fitting a polynomial (up to 6th order) to temperature-log K

data. The code is restricted to 1 atmosphere at temperatures of 100 °C and lower. Up to 300 °C, pressure follows the steam saturation curve for pure water. Temperature can be varied as a user-assigned function of the reaction progress variable  $\xi$  (Eq. D-11). Input is formatted and very detailed, although the most recent version (Wolery et al., 1990) has a more user-friendly interface for creating input files. The code is in FORTRAN, and has been adapted to CDC and VAX mainframe and Cray supercomputer systems as well as Sun and Alliant workstations.

#### 2.5.3.5 MINTEQ

The MINTEQ family of codes (Felmy et al., 1983; Brown and Allison, 1987; Allison et al., 1990) is based on the earlier MINEQL code (Westall et al., 1976) and uses the WATEQ4 database. Also an equilibrium speciation code, MINTEQ allows modeling of mineral precipitation/dissolution, ion exchange, and redox processes. Nonequilibrium kinetics cannot be modeled, but seven adsorption models are currently available. The database from WATEQ4 is well documented and extensive (Ball et al., 1987). Additional modifications to the database (Turner, 1992) have included the radionuclide data for U, Pu, Am, Np, Th, Tc, Cs, Ra, Ru, Eu, Sn, and Zr from the EQ3/EQ6 database. By defining a limited number of basis species, MINTEQ is able to consider a large number of aqueous species, providing log K data is available. Much of the database is limited to calculations at 25 °C. Extrapolations to higher temperatures is accomplished through the van't Hoff equation if  $\Delta H_r^\circ$  data are available. An alternative approach is a database consisting of polynomial functions expressing log K as a function of temperature in a fashion similar to PHREEQE. Input is prepared using the preprocessor PRODEFA2 to define the problem of interest. Written in FORTRAN IV, and using a Newton-Raphson iteration scheme, the most recent version (MINTEQA2) is available through the U.S. Environmental Protection Agency for DEC VAX/VMS systems and for the IBM personal computer.

#### 2.5.3.6 GEOCHEM

Designed specifically for calculating equilibrium soil chemistry, the GEOCHEM code contains over 1800 equilibrium constant data for aqueous species involving over 80 elements and organic compounds (Sposito and Mattigod, 1980; Kincaid et al., 1984a,b; Sposito, 1986; Parker et al., 1987). The data is limited to 25 °C and 1 atm, with no options for extrapolation to higher temperatures and pressures. Elevated temperatures and pressures can only be modeled if the user modifies the log K values in the current database or creates a new database to reflect the higher temperatures. The code is written in FORTRAN IV and has been adapted to IBM and VAX mainframe systems as well as IBM personal computers. Input is either by formatted batch entry or through an interactive mode.

#### 2.5.3.7 ECHEM

ECHEM is a proprietary code developed by the Electric Power Research Institute (EPRI) as a part of the FASTCHEM hydrogeochemical transport code (Morrey, 1988). The approach used in ECHEM is similar to that used in the MINTEQ family of codes, using basis species and equilibrium constant data to model gas-mineral-aqueous speciation, redox, precipitation/dissolution, and adsorption processes. The database is based on a modified and extended version of the MINTEQ database (Krupka et al., 1988). Temperature effects are modeled either using the polynomial expression from MINTEQ or the van't Hoff relationship. Therefore, the code is limited to lower temperatures, probably below 100 °C. Pressure is restricted to 1 atmosphere. Eight sorption models are included, and activity coefficients are calculated using either the Davies or Debye-Hückel equations. Although the code is written in

FORTRAN, current applications are largely restricted to IBM mainframes with a networked IBM workstation configuration used by the FASTCHEM system.

### 2.5.3.8 HYDRAQL

HYDRAQL was developed at Stanford University (Papelis et al., 1988) as a refined and enhanced version of the MINEQL code (Westall et al., 1976). Particular attention was paid to improving the error messages associated with the code. A Newton-Raphson iteration method is used to solve the non-linear algebraic mass balance equations. Written in FORTRAN 77 for the IBM PC, the database formatting requirements of HYDRAQL are similar to MINEQL. The database is fairly complete, and can be modified and expanded to include additional data. Input is by a series of format-free batch files. A subroutine CHECK checks the input for self-consistency and calls up the error message subroutine if problems are encountered. Thermodynamic data ( $\log K$ ,  $\Delta H_R^\circ$ ) are stored relative to a restricted set of components which can be combined to form every species considered in the calculations. Data are retrieved from a formatted database according to the problem definition. Five surface complexation models are available to model sorption processes. Redox processes can also be modeled if the appropriate data are available. Temperature limits are 0 to 75 °C, and extrapolation beyond 25 °C is by the van't Hoff equation. The Davies equation is used to correct for ionic strength effects. The parameter A in the Davies equation (similar to Eq. 2-18 with  $B_a = 1.0$  and  $b_i = 0.3$ ) is corrected for temperature effects according to the parametric equation:

$$A = 0.50886 [ 8 \times 10^{-4} (T-25)] + 10^{-5}(T - 25)^2 \quad (2-23)$$

where

T = Temperature of interest (°C).

### 2.5.4 Summary and Conclusions

The equations outlining the effect of temperature on equilibrium and kinetic chemistry are presented. Geochemical codes that are commonly used to address thermochemical problems are described. These codes generally use either free energy minimization or mass action/mass balance considerations to solve for chemical equilibria. Code history, methods and limitations are also discussed. At present, only the EQ3/6 and PHREEQE codes are able to model reaction progress, and only EQ3/6 can model reaction kinetics as a function of time if appropriate rate constant data are available. Most of the codes use the van't Hoff equation (Eq. 2-16) relation to model  $\log K$ -temperature relationships, and are therefore limited to relatively low temperatures (< 100 °C). Some temperature predictions for the near-field exceed the likely limits of the van't Hoff equation (Appendix A), and curve-fitting of  $\log K$ -temperature data may be necessary to extrapolate. However, if a heat-pipe is established, temperature may be limited to the boiling temperature of the solution (Section 2.2). In addition, many of the thermodynamic data, especially for many of the key radionuclides, are only available for low temperatures. Most of the codes use either the Davies or Debye-Hückel relations to correct activity coefficients for ionic strength and are therefore limited to relatively dilute solutions. EQ3/6 and PHREEQE, however, have been modified to use the Pitzer equations to model high ionic strength brines. Although this may be necessary for localized areas of crevice corrosion, most water compositions reported for the Yucca Mountain vicinity are relatively low ionic strength solutions (e.g., Kerrisk, 1987). All of the codes are available in FORTRAN, and most are adapted for use on commonly available

mainframe and/or personal computers. It is clear that the coupled effects of temperature on system chemistry are significant and must be considered.

## **2.6 CHEMICAL -> THERMAL**

Chemical processes primarily affect the temperature field (and therefore thermal processes) through: (i) changes in material properties (e.g., thermal conductivity, heat capacity) and (ii) the production (or consumption) of heat through exothermic (or endothermic) chemical reactions.

### **2.6.1 Material Properties**

Chemical processes may change the heat capacity or the thermal conductivity of a porous medium through alterations or dissolution/precipitation. An example of an alteration is the hydrolysis of feldspars which can lead to the production of clays which have different thermal properties than the precursor minerals. An important effect would be on the thermal conductivity which would influence the conductive heat transfer.

However, the differences in conductivity of different minerals are generally small, and are treated as constant values in many analyses (Lewis, 1990). Under anticipated conditions at Yucca Mountain, variation in thermal properties due to chemical processes are likely to be of minimal importance relative to natural uncertainties.

### **2.6.2 Exothermic or Endothermic Reactions**

Dissolution/precipitation reactions during the hydrothermal alteration of rock may provide an additional source/sink to the overall heat balance for a given system. Norton and Cathles (1979) note that, except for quartz, the hydrolysis of most silicate and oxide minerals exhibits a negative enthalpy of reaction ( $\Delta H_R$ ), indicating a heat-producing exothermic reaction. This can be quite large, on the order of  $10^3$ - $10^4$  J/mol, and decreases with increasing temperature of reaction. Exothermic oxidation of sulfur and oxygen aqueous species are on the same order. In contrast, hydrolysis of quartz and sulfide minerals have positive enthalpies of reaction, which act as heat sinks of a similar magnitude. The mass balance analysis of Norton and Cathles (1979) examined the alteration of a quartz diorite to two separate mineral assemblages, quartz + sericite and K-feldspar + biotite at 300 °C, assuming that the heats of reaction for reversible and irreversible dissolution are equal and that the effects of aqueous dissociation reactions were minor. Total energy released due to exothermic hydrolysis reactions ranged from 185 to 285 J/g. Ellis and Mahon (1977) estimate that devitrification of volcanic glasses could release up to 335 J/g due to exothermic reactions. Norton and Cathles (1979) conclude that hydrolysis would extend the duration of a thermal perturbation, and that hydrolysis reactions can account for about 15 percent of the total heat content of an igneous pluton crystallizing from liquidus temperatures on the order of 700-800 °C. The degree to which this would perturb the temperature field would depend on the rate of reaction and the rate at which heat is transferred out of the altered rock.

Parry et al. (1980) also investigated the contribution of hydrothermal alteration on the heat flow in the geothermal system at Roosevelt Hot Springs, Utah. Exothermic alteration of feldspars to clays, and the oxidation of sulfur species were modeled as a function of alteration intensity. Exothermic reactions could have contributed as little as 30 J/cm<sup>3</sup> for fresh rock and as much as 7100 J/cm<sup>3</sup> for the most intensely altered rocks. However, measured and calculated temperatures profiles indicated that the

contribution of alteration reactions to the present-day (1980) heat flow was insignificant relative to the convective heat transport.

### 2.6.3 Summary and Conclusions

In this section, the coupling mechanisms by which chemical processes influence thermal processes were reviewed. Namely, (i) changes in material properties, and (ii) exothermic or endothermic chemical reactions were discussed. Although both coupling mechanisms are plausible, there appears to be little evidence to suggest they will be important at Yucca Mountain. Overall, the C->T coupling appears to be negligible in comparison with uncertainties in material properties and thermal loads of the emplaced HLW.

## 2.7 HYDROLOGIC -> MECHANICAL

The state of stress in a rock mass is coupled to groundwater flow. This coupling is present in both directions, as even small changes in the fracture openings cause large changes in permeability, and changes in permeability will in turn affect the groundwater flow and thereby the pressure acting on the rock. In applications where the fluid is pumped into the fractures or boreholes at high pressures, as in enhanced oil recovery and geothermal energy production, the hydrologic conditions strongly influence the mechanical state, as new fractures are created or existing fractures are propped open to enhance the permeability. However, in applications such as underground disposal of HLW, the fluid pressures in fractures are expected to be primarily a result of gravity. It is reasonable to assume that the majority of flow within the partially saturated geologic units at Yucca Mountain will be in fractures due to the low matrix permeabilities. If one assumes that these fractures would be fully saturated, the resulting fluid pressures would correspond to the height of the water column in the fracture. Since these pressures are small compared to the *in situ* state of stress within the rock, the H -> M coupling is expected to be much less important than the M -> H coupling.

### 2.7.1 Mechanical Properties

Due to the partially saturated nature of the tuff at the proposed repository site at Yucca Mountain, and that only periodic flow is likely to occur in the fractures, fluid induced changes in rock properties may not be important. Laboratory experiments have shown that rocks are generally weaker when saturated with water. Olsson and Jones (1980) show that for the Grouse Canyon Tuff, a volcanic rock unit located at the Nevada Test Site, saturated samples are approximately 24 percent weaker than dry samples in unconfined compression. No literature was found on the experimental testing of strength properties in partially saturated rocks more representative of conditions at Yucca Mountain, where one would expect the impact of hydrologic conditions on mechanical properties to be much less. Wada and Takahashi (1990), also obtained results that indicated a significant change in the Young's modulus of granitic rocks when subjected to a pressurized high temperature water environment up to 350 °C. Fluid within a fracture will also tend to act as a lubricant, and most likely cause a reduction in the shear strength of joints.

Unanticipated (i.e., low probability) processes and events such as large earthquakes, underground nuclear explosion testing, etc. could conceivably have a higher impact on the hydrologic to mechanical response of a fractured rock mass. For instance, such an event could suddenly cause an increase in the fluid pressure within a joint. If the joint or fault was under a shear stress, the fluid pressure could reduce

the effective stress across such a feature to such an extent that mechanical slip would occur, however, no literature was found concerning this phenomena.

### **2.7.2 Buffer Swelling**

It is expected that during closure of the repository, excavations (e.g., ramps and emplacement tunnels) will be backfilled. The backfill will most likely contain some proportion of bentonite which will create swelling pressure when saturated with water. Swelling pressures of 10 MPa were measured in the field for the Stripa Project for an almost completely saturated buffer material. However, the swelling depends on the final density of the buffer material and would be expected to vary from 3 to 15 MPa (Carlsson et al., 1989). Within an emplacement borehole, for instance, the swelling bentonite creates internal pressure in the filling which acts as a compressive stress in the normal direction towards the excavation walls. The swelling pressure, therefore, supports the excavation walls and relieves some of the compressive stresses in the circumferential direction to the excavation walls. However, if these circumferential stresses become tensile there is a risk of tensile failure and the creation of new fractures in the radial direction, occurring even many years after completion of the backfilling. The average uniaxial compressive and Brazilian tensile strengths of the Topopah Springs Tuff have been measured to be 95.9 MPa and 12.8 MPa, respectively, so that swelling induced cracking would be possible, depending on the magnitude of *in situ* and excavation induced compressive stresses around the openings. However, current design for the waste packages at Yucca Mountain calls for a small air gap between the waste canister and borehole wall.

### **2.7.3 Summary and Conclusions**

In this section, the impact of H-> M coupling has been discussed. It is expected that, for the Yucca Mountain repository site, pore pressures generated within the rock matrix as well as fluid pressures within fractures will have a negligible impact on the mechanical state of the rock. This is primarily due to the low matrix compressibility (i.e., matrix porosity is a weak function of stress) and the partially saturated nature of the site.

Swelling of buffer/backfill materials containing bentonite clay can create a H->M response depending on the percentage of bentonite and degree of saturation. Some swelling is beneficial in supporting the rock around the excavations and also in creating a good seal. However, too much swelling can generate large tensile stresses within the rock leading to fracturing.

Finally, it was emphasized that material properties can be influenced by the presence of moisture within the rock. Mechanical property testing conducted to date has dealt only with fully saturated rock specimens. For the Yucca Mountain welded tuff, these property tests would represent a lower bound on compressive strength.

## **2.8 MECHANICAL -> HYDROLOGICAL**

Mechanical processes can affect hydrologic processes primarily through fracture apertures which affect (i) effective hydraulic conductivity, and (ii) seismic pumping. For the tuffaceous rock at Yucca Mountain, the matrix is essentially incompressible for hydrologic considerations. Hence, in this section, only the changes in fracture aperture are considered as mechanisms for a M -> H coupling.

### 2.8.1 Effective Hydraulic Conductivity

The normal stresses across a fracture are expected to influence the fracture aperture. Increasing the compressive stress acts to close the fracture aperture while reducing the compressive stress acts to increase the fracture aperture. Also, natural rock joints or fractures exhibit some degree of roughness such that shearing of the joint causes dilation which increases the fracture hydraulic aperture. Shearing under low normal stresses causes the largest dilation as the joint rides up on the asperities.

It is theoretically convenient (for hydrologic purposes) to idealize fractures as being void regions between two parallel surfaces. For such an idealized fracture, it has been shown that small changes in the aperture can significantly change hydrologic flow rates and the flow field (Witherspoon et al., 1979). For a saturated fracture under a constant hydraulic head gradient, the total flow rate is proportional to the aperture cubed. Hence, in a fractured medium it may be important to understand mechanical processes to understand how fracture aperture changes, then to predict hydraulic behavior.

Rutqvist et al. (1991) analyzed the changes in hydraulic conductivity due to excavation induced stresses. Around a circular excavation, three orientations of fractures were considered: circumferential, radial and axial, as shown in Figure 2-22. For discussion purposes, radial fractures could act as a conduit for condensate drainage (see Sections 2.1.4 and 2.2.3) into or out of an excavation. Similarly, circumferential fractures can act to divert condensate drainage around an excavation. Rutqvist et al. (1991) note that excavation induced stresses will tend to (i) decrease the aperture for radial fractures, (ii) increase the aperture for circumferential fractures and (iii) increase the aperture for axial fractures. The first two results can be understood with the aid of Figure 2-23.

The circular excavation can be viewed as a two-dimensional, isotropic and homogeneous medium for which the conditions of plane strain can be applied. The normal stresses in the circumferential and radial orientations vary near the excavation as shown in Figure 2-23. The circumferential stress increases dramatically near the excavation surface, and this tends to close radial fractures. (For an isotropic, homogeneous rock mass medium in a hydrostatic stress field, the maximum circumferential compressive stress is two times greater at the surface of a circular excavation (see Brady and Brown, 1985). The radial compressive stress decreases near the excavation and is zero at the excavation surface. The decreased radial stress tends to open circumferential fractures near the excavation. Both of these effects decrease as the distance from the excavation into the medium is increased. These results have been deduced by Kelsall et al. (1984), Pusch (1989), Rutqvist et al. (1991), among others. The increase in axial hydraulic conductivity has been experimentally observed by Pusch (1989). However, this result is not obvious from the simple two-dimensional plane strain model.

The response of a rock mass to stress changes around an underground opening may result in the formation of an inelastic or "plastic" zone adjacent to the opening, depending on the properties of the rock mass and the magnitudes of the induced stresses. The distinction between the elastic and plastic zones around an underground opening is important with respect to stress distributions and the resultant effects on fracture permeability. As mentioned above in the elastic case, it is expected that the permeability of circumferential fractures should be increased, whereas the permeability of radial fractures should be reduced. However, in the case of plastic deformations adjacent to an opening, both the radial and circumferential stresses are reduced close to the wall in the plastic zone so that the permeability of both tangential and radial fractures should be increased in this localized area (Kelsall et al., 1984). The impact of this localized zone of increased permeability around the excavation is uncertain since the high stress concentrations would shift outward and consequently decrease joint apertures in this still elastic region. The whole plastic zone may be treated as part of the opening. The depth (stress level) at which inelastic or plastic behavior is first observed depends in general on the rock mass strength. Hoek and

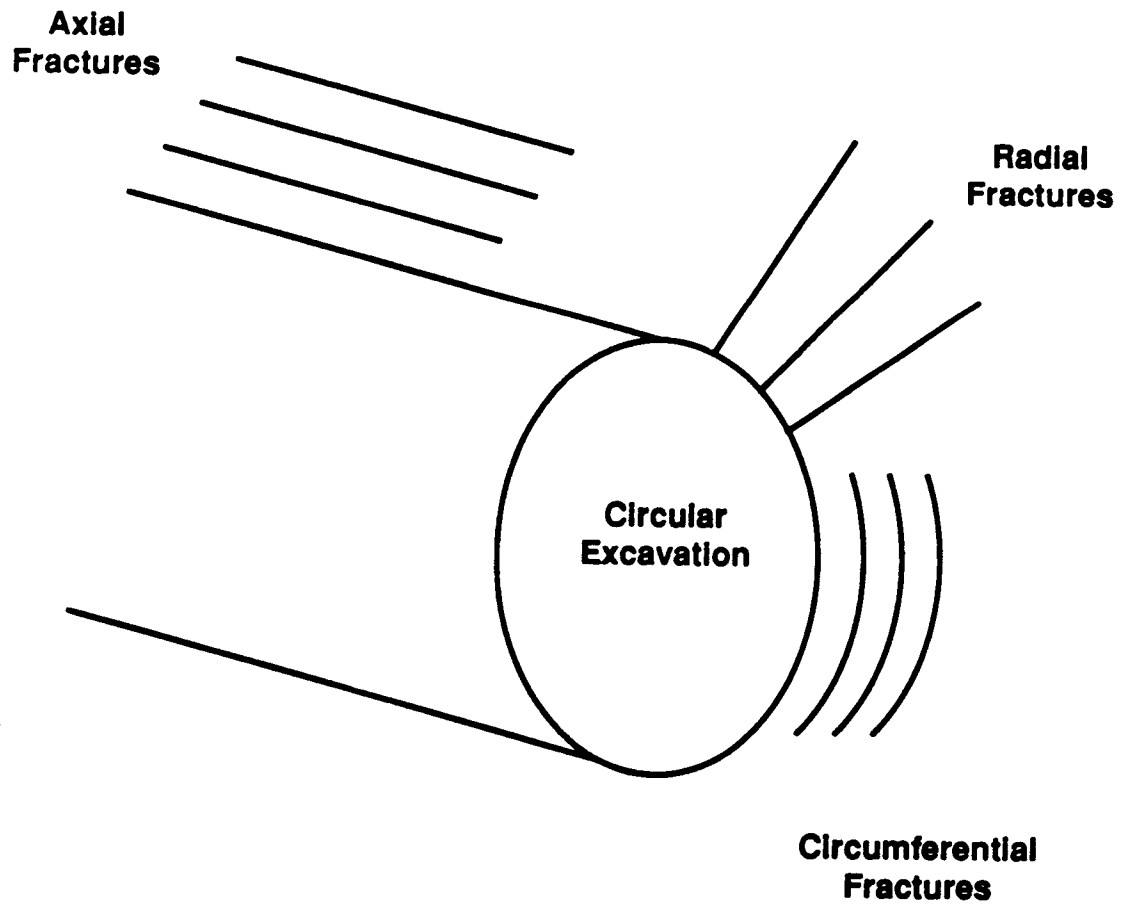


**Figure 2-22. Illustration of Axial, Radial, and Circumferential Fractures Around a Circular Excavation**

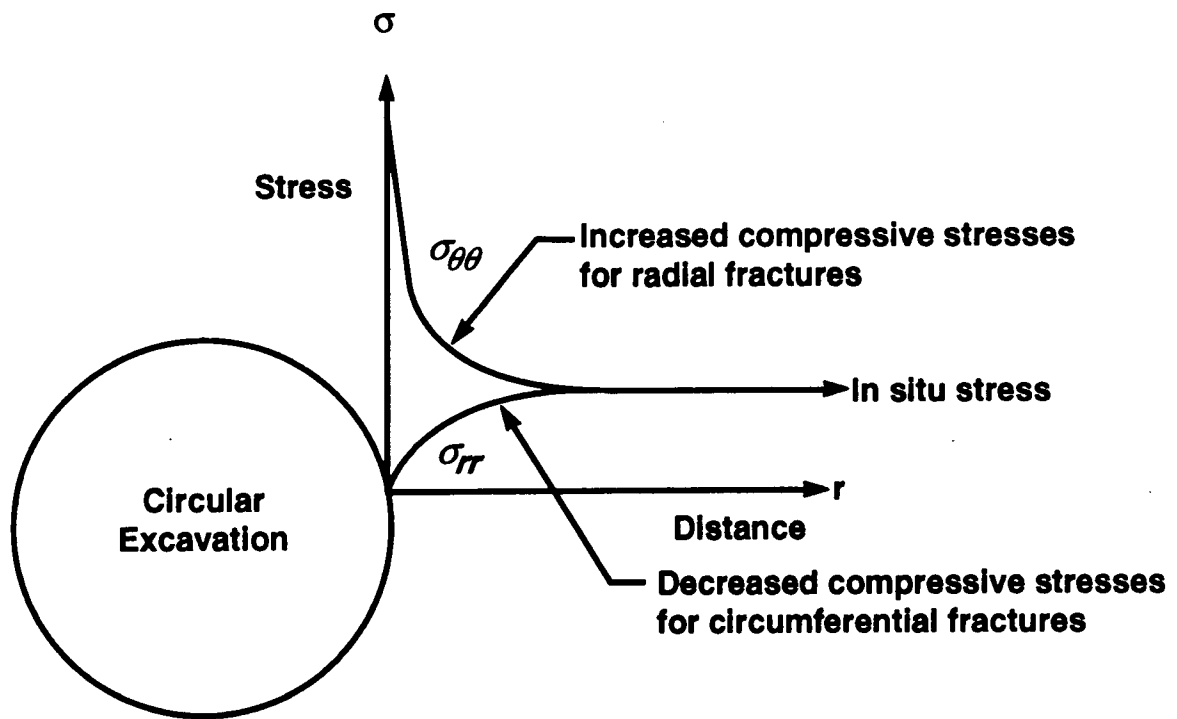


**Figure 2-23. Illustration of Normal Stresses in the Circumferential ( $\sigma_{\theta\theta}$ ) and Radial ( $\sigma_{rr}$ ) Orientation Around a Circular Excavation**

Brown (1980) provide an analytical solution to estimate the depths in a circular shaft at which the plastic and fracture zones will be first observed for given rock conditions. At the proposed repository horizon which is approximately 300 m below the surface, the inelastic zone around the excavations is expected to be small due to the strong nature of the Topopah Springs welded tuff and the relatively shallow depths. However, excavations into the weaker Calico Hills unit during site characterization studies may produce larger inelastic regions around the excavations, and consequently larger increases in permeability.

## 2.8.2 Seismic Pumping

The potential for large changes in the water table elevation as a result of seismic activity has been a consideration at Yucca Mountain (Szymanski, 1989; Archambeau and Price, 1991; Powers et al., 1991; Carrigan et al., 1991; National Research Council, 1992). Szymanski proposed that the water table at Yucca Mountain has periodically risen above the level proposed for a repository. The changes in water table elevation were proposed to be due to nearby earthquakes, hence a  $M \rightarrow H$  coupling known as "seismic pumping". In seismic pumping, seismic events compress the ground which result in reduced available storage volume for the liquid water. The liquid flows to increase the elevation of the water table. Szymanski proposed that tectonic cycles characterized by slow extensional deformation, and punctuated by seismic events induced large upwellings of the water table.

The scenario of seismic pumping at Yucca Mountain has been reviewed by Archambeau and Price (1991), Powers et al. (1991), Carrigan et al. (1991), the National Research Council (1992), among others. Probably the most extensive investigation of seismic pumping at Yucca Mountain has been conducted by the National Research Council (1992) in which they conclude that seismic pumping is inadequate to raise the water table significantly at Yucca Mountain.

Carrigan et al., (1991) conducted numerical analyses investigating the potential for water table excursions induced by seismic events at Yucca Mountain. The simulations employed a 2D elastic boundary element model of the Earth's crust to determine the pore pressure distribution following a seismic event. This pore pressure distribution was then used in an initial value hydrologic computational model that tracks the water table as a function of time in a two-dimensional hydrologic domain. The relation used between the pore pressure and volumetric strain may be derived as

$$P = \frac{-E}{3} \left[ \frac{1}{1 - 2\nu} \right] (e_{xx} + e_{yy}) \quad (2-24)$$

where

- P = pore pressure [N/m<sup>2</sup>],
- E = Young's modulus [N/m<sup>2</sup>],
- $\nu$  = Poisson's ratio [dimensionless], and
- $e_{ij}$  = components of strain [dimensionless]

Figure 2-24 shows the predicted maximum rise in the water table below Yucca Mountain (approximately 12 m) due to a 1 m slip on a vertical fault locked 750 m below the surface (250 m below the water table). This particular geometry in which the fault was locked some distance below the ground surface produced the largest strains and consequently largest pore pressures when slip was allowed to

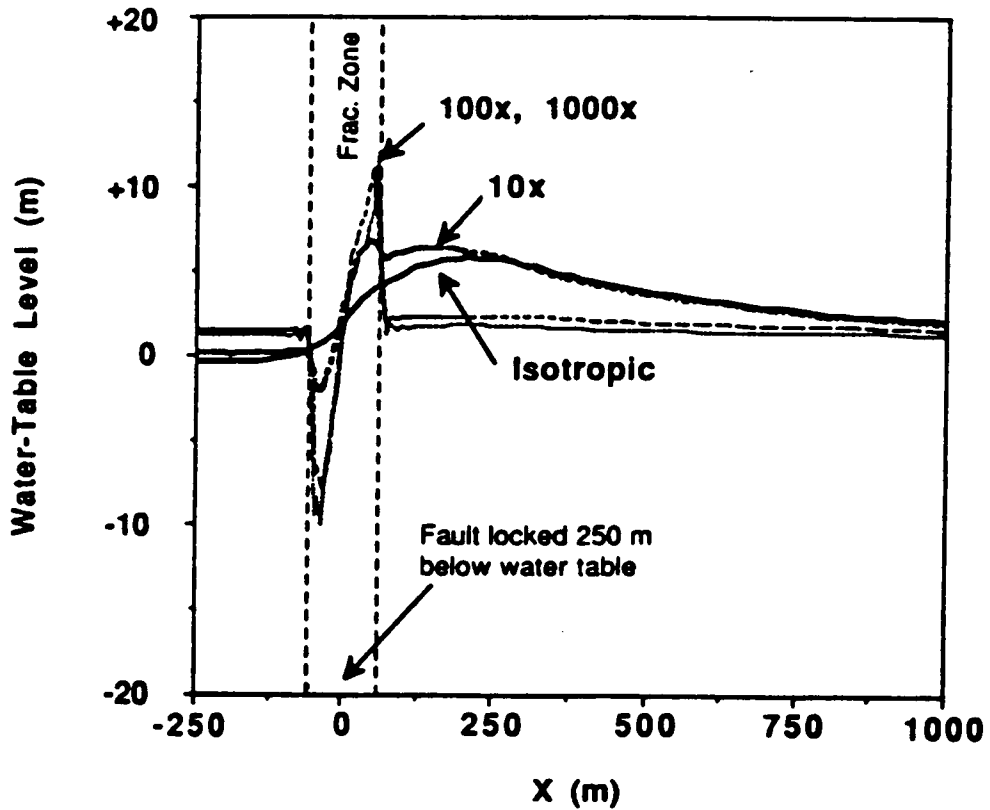


Figure 2-24. Water-Table Response for Isotropic Permeability and for Local Vertical Permeability Enhancement ( $10$  to  $10^3$ ) Within 100-m-Wide Anisotropic Region Centered on Normal Fault Simulating Zone of Vertical Fracturing (From Carrigan et al., 1991)

occur. The results in Figure 2-24 represent water table rises as a result of enhancing the vertical permeability with a 100 m wide region centered on the normal fault to simulate a zone of vertical fracturing. Much smaller water table rises occurred when no vertical fracturing was simulated. Since the current repository horizon at Yucca Mountain is 200-300 m above the water table, these results suggest that the impact of seismic pumping are negligible.

It is more conceivable for the Yucca Mountain area to experience more small scale repetitive seismic events. Such seismic events, if repeated over a long period of time (i.e., 10,000 years), could conceivably create preferential water pathways which would connect the emplacement area with a nearby perched water zone.

### **2.8.3 Summary and Conclusions**

In this section, mechanical to hydrologic (M -> H) coupling mechanisms have been reviewed. The primary coupling can be related to changes in fracture apertures since the rock matrix at Yucca Mountain is essentially incompressible for hydrologic considerations. Fracture apertures decrease for increased compressive stresses, and increase for decreased compressive stresses. The fracture apertures influence the effective hydraulic conductivity and storativity.

Around an excavation, the varying mechanical loads in the surrounding rock are expected to influence fracture apertures. In general, circular excavations pinch fractures directed into the excavation and open fractures circumferentially around an excavation. This tends to direct flow around an excavation versus into an excavation. The practical application of this coupling, however, may be insignificant due to large uncertainties in fracture apertures, locations, and conductivities.

A second M -> H coupling is described as seismic pumping which is related to gradual increases in liquid storativity, coupled with rapid decreases in storativity due to nearby seismic events. The storativity is closely related to the fracture apertures which decrease for increased compressive loads. The liquid is forced upwards, thereby raising the water table. Although seismic pumping has recently received much attention in the literature, it appears to be negligible at Yucca Mountain.

In summary, although plausible M -> H coupling mechanisms exist and have been discussed in the literature, the occurrence and significance of such couplings appears to be negligible at Yucca Mountain.

## **2.9 HYDROLOGIC -> CHEMICAL**

In the proposed repository environment, the potential for transport of radionuclides from the engineered barrier system through the geologic setting to the accessible environment is of chief concern in the performance of the proposed HLW repository. The chief method of radionuclide transport is anticipated to be as dissolved species in the liquid phase or, in the case of  $^{14}\text{C}$  and possibly  $^{129}\text{I}$ , as a gas in the vapor phase (DOE, 1988). Therefore, the coupling between the hydrologic system and the chemical system is of critical importance. The following is a summary of the various approaches used.

### 2.9.1 Equilibrium Solute Transport

In the absence of advective transport, chemical species are transported in the liquid phase in the direction of their concentration gradients (Freeze and Cherry, 1979). Referred to as molecular diffusion, this process is generally expressed (in one dimension) using Fick's first law

$$F = -D_m \frac{dC_w}{dx} \quad (2-25)$$

where

- F = mass flux (g solute/m<sup>2</sup> - s),
- D<sub>m</sub> = molecular diffusion coefficient (m<sup>2</sup>/s),
- C<sub>w</sub> = solute concentration (g/m<sup>3</sup>), and
- x = direction of transport

The concentration gradient dC<sub>w</sub>/dx is a negative quantity in the direction of transport, indicating that species migrate from areas of high to low concentration. The diffusion coefficient D<sub>m</sub> is determined experimentally for the individual ionic species under consideration. For major electrolytes in groundwater (e.g., Na<sup>+</sup>, Ca<sup>+</sup>, Cl<sup>-</sup>, HCO<sub>3</sub><sup>-</sup>), D<sub>m</sub> is in the range of 10<sup>-9</sup> m<sup>2</sup>/s at 25 °C, increasing with increasing temperature due to the higher kinetic activity of the electrolyte species. In porous media, the apparent diffusion coefficients (D<sub>m</sub><sup>\*</sup>) tend to be smaller (generally ranging from 1 to 50 percent of the diffusion coefficient) due to the more tortuous nature of the transport path. Fick's second law

$$\frac{\partial C_w}{\partial t} = D_m^* \frac{\partial^2 C_w}{\partial x^2} \quad (2-26)$$

can be used to describe molecular diffusion through porous media in space and time.

In practice, the contribution of molecular diffusion to solute transport is relatively insignificant compared to advective transport in the presence of groundwater movement and is not treated explicitly. Neglecting molecular diffusion and assuming that solute is only transported in the liquid phase, the classical deterministic convection-dispersion equation has been used in many studies to model nonreactive solute transport (e.g., Nielsen et al., 1986; Selim et al., 1990). For reactive solute transport in one dimension, the general equation is modified to account for the effects of water/rock interaction such that

$$\frac{\partial}{\partial t} \left( C_w + \frac{(1-\phi)}{\theta} \rho C_s \right) = \frac{\partial}{\partial x} \left( D \frac{\partial C_w}{\partial x} - v C_w \right) + \Phi \quad (2-27)$$

where

- C<sub>w</sub> = solute concentration in the liquid (kg/l),
- φ, θ = porosity and volumetric water content, respectively, of the medium (m<sup>3</sup>/m<sup>3</sup>)
- D = hydrodynamic dispersion coefficient (m<sup>2</sup>/s),
- v = mean pore velocity (m/s),
- C<sub>s</sub> = solute concentration (kg/kg) adsorbed on the solid phase,
- ρ = mean density of the medium (kg/m<sup>3</sup>), and
- Φ = solute sources and sinks in the system other than sorption, such as matrix diffusion, precipitation/dissolution, radioactive decay (Nielsen et al., 1986).

The hydrodynamic dispersion coefficient is similar in concept to the molecular diffusion coefficient ( $D_m$ ) of Eq. (2-25), and can be expressed for groundwater flow in terms of the effective molecular diffusion  $D_m^*$  coefficient, mean pore velocity  $v$ , and dispersivity  $\alpha$  (m) such that  $D = \alpha v + D_m^*$ . Equation (2-27) is frequently simplified by substituting the dry bulk density  $\rho_b = (1-\phi)\rho$  and fluid flux  $q = \theta v$  for  $\rho$  and  $v$ , respectively.

For steady-state flow conditions, assuming that the medium is homogeneous and incompressible with respect to material properties,  $\phi$ ,  $\rho$ ,  $v$ , and  $D$  can be treated as constants. If equilibrium sorption is the only attenuation mechanism other than dispersion considered,  $\Phi = 0$ , and Eq. (2-27) simplifies to

$$\frac{\partial}{\partial t}(C_w + \frac{(1-\phi)}{\theta}\rho C_s) = \left( D \frac{\partial^2 C_w}{\partial x^2} - v \frac{\partial C_w}{\partial x} \right) \quad (2-28)$$

$\partial C_s / \partial t$  is generally provided by a sorption model (Domenico and Schwarz, 1990). Using the simplest case of a linear sorption isotherm assuming instantaneous equilibrium,  $C_s = K_d C_w$ . Under these conditions, Eq. (2-28) simplifies further such that

$$\frac{\partial}{\partial t}[C_w(1 + \frac{(1-\phi)}{\theta}\rho K_d)] = \left( D \frac{\partial^2 C_w}{\partial x^2} - v \frac{\partial C_w}{\partial x} \right) \quad (2-29)$$

where

$K_d$  = sorption coefficient (l/kg).

Based on the assumption of the validity of the linear sorption isotherm, a retardation factor  $R_r$  can be defined to reflect the attenuation of solute transport relative to water velocity (or to the transport of a non-reactive solute), such that simplifying Eq. (2-29) to

$$R_r = \left( 1 + \frac{(1-\phi)}{\theta}\rho K_d \right) \quad (2-30)$$

$$\frac{\partial}{\partial t} R_r C_w = \left( D \frac{\partial^2 C_w}{\partial x^2} - v \frac{\partial C_w}{\partial x} \right) \quad (2-31)$$

It is stressed that the treatment of retardation ( $R_r$ ) developed in Eqs. (2-28) through (2-31) is subject to the validity of the linear isotherm and all of the assumptions and limitations inherent in the  $K_d$  approach (Davis and Kent, 1990; Turner, 1991). In addition to instantaneous sorption, however, several mechanisms can contribute to the retardation of solute transport, including precipitation/dissolution, matrix diffusion, fluid mixing, and radioactive decay. Under these conditions, the  $K_d$  approach is not valid,  $\Phi \neq 0$ , and retardation behaves in a much more complex manner than can be described using the simple  $R_r$  approach outlined above (McKinley and Alexander, 1992). A complex coupling of geochemical relations with transport equations is then required to account for the various mechanisms controlling contaminant transport (e.g., Krishnaswami et al., 1982; Miller and Benson, 1983; Leslie, 1991).

Returning to the case where a linear isotherm is valid and  $\Phi = 0$ , Eq. (2-27) can be adapted to two- and three-dimensional transport in the general form:

$$\frac{\partial}{\partial t} \left( C_w + \frac{(1-\phi)}{\theta} \rho C_s \right) = \nabla \cdot (\underline{D} \nabla C - \underline{v} C_w) \quad (2-32)$$

where

$\underline{D}$  = tensor hydrodynamic dispersion coefficient, and  
 $\underline{v}$  = vector mean pore velocity

which can be modified in a fashion similar to the development outlined above in Eqs. (2-27) through (2-31). From Eq. (2-30), if  $\theta$  does not vary with time,  $R_f$  can be considered constant. For a homogeneous, incompressible medium under hydrologically saturated conditions,  $\theta = \phi$ , and this may be a valid assumption. In a heterogeneous medium, however, volumetric moisture content varies as a complex function of both time and space, even under isothermal conditions, and  $\theta$  cannot generally be considered constant. As a result,  $R_f$  must also be evaluated as a function of time and space. Equation (2-32) also assumes that all available surfaces will be wetted, regardless of hydrologic saturation, and that there are no preferential zones of flow for mass transport through the volume (Clothier, 1984). Tritium experiments by Bond et al. (1982) suggested that piston displacement may be obtainable in partially saturated column experiments. In practice, however, most geological media are heterogeneous, and preferential flow and transport through permeable layers and fractures all serve to complicate the application of a simplified model (Ababou, 1991).

In general, the convection-dispersion equation requires numerical solution and simple analytical solutions are not readily derived. Bond and Phillips (1990) developed a one-dimensional analytical solution for cation transport. The solution assumes a general non-linear adsorption isotherm, although the exact approach depends on the shape of the isotherm. The model has been applied to column experiments in the Ca-Na-K system using isotherms determined by batch experiments with fairly good agreement, except at short times.

As discussed above, advective transport is assumed to be the principal mode of solute transport within permeable layers. Diffusion along chemical gradients is generally incorporated in the dispersion coefficient  $D$  in Eq. (2-32), and not considered explicitly. Modeling the spreading of a nonreactive solute plume by mechanical dispersion during advective transport through a heterogeneous, layered medium requires complex velocity distributions. Gillham et al. (1984) proposed an advection/diffusion model that minimizes this complexity by invoking molecular diffusion along chemical gradients between layers of contrasting hydraulic conductivities. In this fashion, less permeable layers tend to act as temporary storage cells; solutes are concentrated at the expense of the more permeable layers, and contaminant transport is attenuated. This molecular interpretation requires knowledge of the contrast in unit hydraulic conductivities of the layers, layer thickness, and the molecular diffusion coefficient for the solute. Unfortunately, these parameters are not always known with any degree of certainty, and Gillham et al. (1984) were required to use empirical estimation techniques. Travis and Nuttall (1987) also suggested that at the slow flow rates anticipated in the partially saturated zone at Yucca Mountain ( $< 1$  cm/yr), diffusion may become relatively more important as the magnitude of advective transport diminishes.

Fracturing of geologic media leads to heterogeneity at a variety of scales, greatly complicating the modeling of fluid flow and transport (Ababou, 1991). Deterministic modeling approaches have been modified for fracture flow in two basic ways. In the dual-porosity approach, the fracture network is treated as one effective porous medium, and the matrix as another. Effective values for hydraulic, transport, and sorptive properties are assigned to both fracture flow and matrix flow based on this assumption, and solute transport is described by a series of parallel equations similar to Eqs. (2-27 through 2-31). An additional term is required to consider cross-flow and transport between the fractures and the unfractured rock matrix (Dykhuizen, 1990). If coupling time scales are short relative to transport time scales, then fracture and matrix concentrations are comparable. Wilson and Dudley (1986) and Dykhuizen (1987) used this approach to describe one-dimensional transport in the partially saturated zone at Yucca Mountain. Neretnieks and Rasmuson (1984) also modified the approach to include radioactive decay during radionuclide transport in a fractured medium with varying velocity and block-size.

The second deterministic approach to modeling fracture flow is to use pipe or parallel plane flow to model transport in individual fractures separately from the rock matrix. This strategy is only practical if fracture flow is controlled by a relatively small number of dominant fractures. Huyakorn et al. (1983) proposed that this is perhaps a more computationally efficient approach than dual porosity, and modified the governing equations to incorporate radionuclide decay and diffusion into the matrix. The authors also note, however, that extension into three dimensions may prove problematic.

## **2.9.2 Nonequilibrium Solute Transport**

Reactive solute transport in the partially saturated zone is usually described using the convection-dispersion equation appropriate to the dimensionality of the problem (Eq. 2-32). For example, Nair et al. (1990) modified the convection-dispersion equation to develop a one-dimensional transport model for the three phase (gas-liquid-solid) system in the partially saturated zone. However, given the nonlinear nature of hysteretic effects, moisture content, hydraulic conductivity, and other hydraulic properties in the partially saturated zone, there is considerable uncertainty in the applicability of this equation to transport under variably saturated conditions and in the validity of the assumption of local equilibrium (Valocchi, 1985). If the assumption of equilibrium is valid, and if the convection-dispersion equation is adequate to describe solute transport in a partially saturated column experiment, it is expected that the eluted pulse of the solute will be roughly symmetrical in shape, increasing in concentration from zero to some maximum and decreasing back to zero. In practice, however, soils exhibit some structure, and elution curves from column experiments of both nonreactive and reactive solute transport are frequently asymmetrical (showing early breakthrough), and exhibit extensive tailing, asymptotically approaching some minimum, nonzero concentration. Van Genuchten and Wierenga (1976) also noted that tailing at larger pore volumes generally increases as porewater velocity decreases. Assuming that the convection-dispersion equation is appropriate, modeling kinetic solute transport in the partially saturated zone has followed two basic approaches. The first approach involves dividing the flow regime into two physically distinct domains. The second approach relies on chemical kinetics to reproduce observed profiles. Two reaction sites are proposed, one of which obeys chemical equilibrium, and the second of which follows nonequilibrium (usually first-order kinetic) processes.

### **2.9.2.1 Two-Region Transport**

Two-region (or two-component) transport models are based on the existence of two physically distinct regions in a porous medium (Coats and Smith, 1964; van Genuchten and Wierenga, 1976). In

one region, water is mobile and free to transport ions in solution. In the second region, water is considered immobile (or stagnant in some terminologies) in dead-end pore spaces. Mass transfer between the two regions is by diffusion alone. In one dimension, the two-region convection-dispersion transport equation becomes

$$\theta_{mo} \frac{\partial C_{w,mo}}{\partial t} + f \rho_b \frac{\partial C_{s,mo}}{\partial t} + \theta_{im} \frac{\partial C_{w,im}}{\partial t} + (1-f) \rho_b \frac{\partial C_{s,im}}{\partial t} = \theta_{mo} D_{mo} \frac{\partial^2 C_{w,mo}}{\partial x^2} - \theta_{mo} v \frac{\partial C_{w,mo}}{\partial x} \quad (2-33)$$

where

- mo, im = mobile and the immobile regions as subscripted,
- f = mass fraction of the solid phase that is in contact with the mobile fluid, and
- $\theta, \rho_b$  = volumetric water content and dry bulk density, respectively, as defined above.

Diffusion between the mobile and immobile regions is controlled by the relationship

$$\theta_{im} \frac{\partial C_{w,im}}{\partial t} + (1-f) \rho_b \frac{\partial C_{s,im}}{\partial t} = \alpha (C_{w,mo} - C_{w,im}) \quad (2-34)$$

where  $\alpha$  is an empirical mass transfer coefficient ( $s^{-1}$ ) between the stagnant and mobile waters. The degree of nonequilibrium represented in the system decreases as the rate of exchange between the two regions ( $\alpha$ ) increases relative to the rate of solute advection. It is important to note that local equilibrium is assumed to govern relationships in the mobile and immobile regions of the system. The two-region model as defined by Eqs. (2-33) and (2-34) is therefore not a model limited by reaction kinetics, but rather uses concentration differences at points along the direction of flow to simulate disequilibrium.

The two-region approach has been used in a number of studies (van Eijkeren and Loch, 1984; de Smedt and Wierenga, 1984; Jinzhong, 1988; Mansell et al., 1988; Selim et al., 1976, 1990). Bidner and Vampa (1989) modified the approach to include the effects of equilibrium sorption and nonequilibrium adsorption/desorption. Immobile water has been inferred from partially saturated column experiments that exhibit early breakthrough and asymmetric breakthrough curves (Bond and Wierenga, 1990). Skopp et al. (1981) noted that the fraction of stagnant water and the magnitude of the mass transfer coefficient are only defined by the results of experiments conducted under certain conditions; knowledge of the geometry and hydrologic properties of the medium is insufficient to predict the necessary parameters. De Smedt and Wierenga (1979) suggested that immobile water is indicated if fitting partially saturated transport data requires the use of a dispersion coefficient much larger than that predicted for saturated fluid flow. De Smedt and Wierenga (1984) noted a roughly linear increase in  $\alpha$  with increasing pore water velocity ( $v_m$ ) based on nonreactive transport column experiments. De Smedt and Wierenga (1984) also noted a positive linear correlation between mobile water ( $\theta_{mo}$ ) and total water content ( $\theta = \theta_{mo} + \theta_{im}$ ) of the medium. Bond and Wierenga (1990) conducted nonreactive solute transport experiments under both steady and unsteady partially saturated conditions to evaluate the two-region model. Under steady flow, early breakthrough and asymmetric breakthrough curves indicated the presence of small amounts of immobile water. Under unsteady flow conditions, however, the data were adequately described without invoking two regions. Bond and Wierenga (1990) attributed this to the differences in wetting patterns between the two cases. In the case of steady flow, water flow is already established and

biased towards preferential flow paths, resulting in dead-end pore space. In contrast, wetting of the soil during the unsteady experiments carried the tracer into the wetted pore space by advection alone, with little or no contribution from diffusive mass transfer between mobile and immobile water. Mansell et al. (1991) incorporated a mobile/immobile two-region approach to nonequilibrium transport into the direct-coupled model of Valocchi et al. (1981a,b). Selectivity coefficients, a measure of the preference of the adsorbent for one aqueous species over another, are allowed to vary in space and time as a function of changes in solution normality and composition. The authors reported that the model was successful in predicting  $\text{Na}^+$  and  $\text{Mg}^{2+}$  transport in laboratory experiments.

Skopp et al. (1981) further modified the two-region model to consider two homogeneous flow regions. One region consists of relatively rapid flow through macropores; the second region is governed by much slower matrix flow. Exchange between the two regions is modeled using a linear interaction coefficient. If the interaction coefficient is sufficiently large, the model reduces to the classical one-region convection dispersion equation (Eq. 2-32). In general, structured soils require small coefficient values, possibly due to flow channeling or clay dispersion. Reinterpreting the data of van Genuchten and Wierenga (1976) using this approach, Skopp et al. (1981) suggested that the mean diffusion path exceeds the average aggregate size, suggesting that the mobile/immobile assumption is inadequate.

### 2.9.2.2 Two-Site Transport

Many studies (Selim et al., 1976; Cameron and Klute, 1977; Jennings and Kirkner, 1984; Parker and Jardine, 1986; Kool et al., 1987) have proposed a two-site approach to modeling early breakthrough curves. One site is assumed to be governed by equilibrium sorption, and the second site assumes kinetic sorption reactions. As discussed by Nkedi-Kizza et al. (1984), adsorption on the equilibrium site (site 1) is governed by a linear sorption isotherm, while sorption at the nonequilibrium site (site 2) is governed by first-order, linear kinetics. The overall governing transport equation is

$$\left[1 + \frac{f\rho_b K_d}{\theta}\right] \frac{\partial C_w}{\partial t} + \frac{\rho_b \alpha_2}{\theta} [(1-f)K_d C_w - C_{s2}] = D \frac{\partial^2 C_w}{\partial x^2} - v \frac{\partial C_w}{\partial x} \quad (2-35)$$

where

- f = fraction of sites that are governed by equilibrium sorption,
- $K_d$  = linear sorption coefficient that is assumed valid for both sites, and
- $\alpha_2$  = a first-order kinetic rate coefficient for the nonequilibrium sorption sites.

Other variables ( $C_s$ ,  $C_w$ ,  $\rho_b$ ,  $D$ ,  $v$ ) are as defined previously.

Nkedi-Kizza et al. (1984) used a dimensionless parameterization of both the two-region and two-site models to demonstrate a mathematical equivalence of their dimensionless forms in terms of addressing nonequilibrium solute transport. Breakthrough curves (BTC) for  $^{45}\text{Ca}$ ,  $^3\text{H}$ , and  $^{36}\text{Cl}$  transport in water-saturated column experiments were fit reasonably well by the models, including the tailing observed for the different BTC's. The authors noted, however, that because only the forms of the dimensionless equations are directly comparable, this equivalence is only valid for simulations of the net effect of retardation at a macroscale. Since dependent dimensionless variables (e.g., one dimensionless variable,

$c_2$  measures either solution concentrations in the immobile water for the two-region model, or the sorbed concentration at the kinetic site in the two-site model) differ in the two models. microscopic measurements (unspecified by the authors) are necessary for discrimination between the conceptual models. It is also important to note that the authors use a linear sorption isotherm to describe the equilibrium sorption/concentration relationships in the transport models.

### 2.9.2.3 Stochastic Models

Recent studies suggest inadequacies in the deterministic, convection-dispersion approach to simulating solute transport in the partially saturated zone (e.g., Jury et al., 1983, 1986; Sposito et al., 1986; Roth et al., 1990a,b). Alemi et al. (1991) also indicated that retardation factors based on  $K_d$  values from batch equilibrium experiments were inadequate to fit the results of selenium transport through partially saturated soil columns. As a result, recent efforts to model fracture and permeability-induced heterogeneities and partially saturated transport have centered about the development of stochastic models. These models rely on performing large numbers of calculations to generate population statistics for hydraulic and transport properties. Statistical treatments of these probability distribution functions are then used to simulate heterogeneities at any scale. The specifics of the stochastic model techniques are beyond the scope of this text, and the reader is referred to other reviews (Dagan, 1986; van Genuchten and Jury, 1987; Ababou, 1991) for a more detailed discussion of stochastic models.

At present, stochastic approaches have been largely limited to nonreactive solute transport (e.g., Bresler and Dagan, 1981). Those studies that do deal with reactive transport have generally modeled retardation using a linear  $K_d$  approach (Jury et al., 1983). However, some studies have attempted to use more sophisticated sorption models (e.g., Yeh and Tripathi, 1991). Russo (1989a,b) developed a one-dimensional stochastic model using a mixed-ion diffuse double layer to simulate solid/solution interaction for a simplified Na-Ca-Cl system. Comparison of predicted results to field data from an arid soil site at Bet Dagan, Israel, suggested that interactions between soil and solutions may affect transport under transient conditions, and increase the hydrologic heterogeneity of the medium. Cvetkovic and Shapiro (1990) used a first-order kinetic approach to account for retardation in their stochastic models, although at equilibrium, the model reduces to a linear  $K_d$ . Van der Zee (1990) and van der Zee and Bolt (1991) attempted to address a maximum sorption limit using the Langmuir isotherm.

### 2.9.3 Computer Codes

Numerical codes that couple geochemical and transport models (hydrogeochemical models) have seen increasing use as tools for gaining insight into retardation processes and predicting the nature and extent of contaminant transport. Development of such comprehensive codes is being actively pursued by a number of research groups (LANL, LBL, PNL, SNL, ORNL, EPRI) using a variety of approaches. An evaluation of existing codes should consider accuracy, efficiency, flexibility, and computational requirements among other characteristics in an attempt to find the best balance between model completeness and applicability.

The efficiency of a given hydrogeochemical model is not only important for investigating the problem at hand, but it will also determine the ability of the program to be adapted to more complete (and complex) conceptual models. This efficiency in turn depends on both the approach taken toward coupling and the primary dependent variables (PDV's) that are chosen to represent the problem of interest (Kirkner and Reeves, 1988; Reeves and Kirkner, 1988; Yeh and Tripathi, 1989). Two approaches have been used

commonly to couple geochemical equilibria and transport models. Direct (one-step) coupling (Rubin and James, 1973; Valocchi et al., 1981a,b) involves insertion of the nonlinear, algebraic equations describing equilibrium geochemistry into the partial differential equations (PDE) that describe transport. This results in a set of nonlinear partial differential equations that are solved simultaneously for geochemistry and transport for a given set of PDV's. For the second method, geochemistry and mass transport equations are posed independently of one another, and solved sequentially rather than simultaneously. This two-step or "operator splitting" approach has been used successfully in several studies (Cederberg et al., 1985; Walsh et al., 1982).

While one-step coupling yields a more exact solution to the problem, the coefficient matrix must be reformulated for each iteration, leading to extensive computer calculation time and large memory requirements (Cederberg, 1985). Alternatively, two-step coupling requires the solution of only one set of equations in sequence, and uses computer resources much more effectively. Calculations (Cederberg, 1985; Yeh and Tripathi, 1989) indicate that a two-step coupling approach is more than 30 percent faster than direct coupling for a given problem. In addition, Yeh and Tripathi (1989) show that only a two-step approach will be able to model larger two- and three-dimensional problems, given likely limits on computational speed and memory storage in the foreseeable future. Numerical techniques employed in matrix formulation and solution and in iteration will also have an effect on run time and, therefore, run costs (Barry, 1990). Several studies (Yeh, 1985; Reeves and Kirkner, 1988; Yeh and Tripathi, 1989; Siegel et al., 1989) have evaluated a variety of solution strategies (e.g., successive overrelaxation, Gauss-Seidel) and iterative techniques (e.g., Picard, Newton-Raphson), and identified convergence problems. Even on a supercomputer, CPU times are large and run-time costs can amount to many thousands of dollars for a single 10,000-year simulation on a scale similar to Yucca Mountain (Siegel et al., 1989), and efficient numerical solutions are necessary to minimize run costs. In addition, because a transport code is envisioned as a part of an interactive approach to performance assessment, codes requiring extensive supercomputer time are at a distinct disadvantage. This disadvantage will become increasingly apparent in a stochastic approach that relies on performing a large number of calculations to develop adequate statistics. An elaborate, computationally slow code will become the limiting step in performing these calculations, making a stochastic modeling approach untenable without invoking significant (perhaps unrealistic) improvements in computer technology.

Thermodynamic data are of critical importance in modeling any geochemical system. A given hydrogeochemical code should use an established, current database that has been tested for accuracy and internal consistency, and is broad enough to include a relatively complete set of species, minerals, and complexes that are likely to be encountered in the geologic environment of interest (Kincaid et al., 1984a,b; Krupka et al., 1988). In addition, the necessary data for modeling important processes (sorption, precipitation/dissolution, ion exchange, activity, etc.) should be available. The database should be able to incorporate both updated information and additional data as needed for a given system. A readily available, public-domain database will have additional advantages of being tested through application to a wide variety of problems applications, and will also benefit from a general interest on the part of the research community in keeping the database consistent, accurate, and current. Finally, a relatively complete database should be readily accessible to the code in order to adapt the model to a variety of systems.

Although the degree of "user-friendliness" must not be developed at the expense of the accuracy or efficiency of a program, it should be considered in code selection (Siegel et al., 1989). The program should be accessible to a variety of users with varying levels of computer skills. Complicated or awkward formatting of input can make application of the model difficult, and limit its usefulness as a tool to study

a wide variety of systems or perform sensitivity analyses. Rigid input can also inhibit modification or correction of the input, perhaps leading to false starts and inaccurate data entry. Because these codes deal with potentially large numbers of chemical species and long time-intervals and distances, post-processing of the data is also important as an aid in interpreting the output from the hydrogeochemical model.

This section is not intended to be an exhaustive analysis of existing reactive transport codes, but is intended to focus the evaluation on flexible and efficient codes. Information about the code characteristics and the techniques was largely collected from user's manuals and key references listed in the table; additional information is available in Morrey et al. (1986), Siegel et al. (1989) and Mangold and Tsang (1991). In many instances, unnamed hydrogeochemical codes have been developed for a particular problem (Rubin and James, 1973; Valocchi et al., 1981a,b; Walsh et al., 1982; Codell and Murphy, 1992), and are not generally considered in this discussion. Two codes considered (NEFTRAN II and TRACR3D) are solute transport codes that do not explicitly account for the geochemistry of the water/rock system. The remainder of the codes are hydrogeochemical models. All codes are written in FORTRAN. With the exception of DYNAMIX and CHMTRNS, all of the codes are isothermal, equilibrium models, and do not currently incorporate reaction kinetics. It is also important to note that hydrogeochemical modeling is a dynamic area of research, and future developments may result in new, more powerful codes or in extensive modification to the existing models.

### 2.9.3.1 HYDROGEOCHEM

Developed for supercomputing facilities at Oak Ridge National Laboratory, the two-dimensional finite-element code HYDROGEOCHEM is able to model steady-state or transient flow conditions while considering a variety of chemical processes during reactive solute transport (Yeh and Tripathi, 1990, 1991). A two-step sequential approach is generally used to couple chemistry and transport, although a one-step coupling is available for comparison of run-time requirements. The transport module of HYDROGEOCHEM is based on the earlier fluid flow code FEMWATER (Yeh, 1987) and the transport code FEMWASTE (Yeh and Ward, 1981). Based on the approach used in the EQ3/EQ6 and PHREEQE geochemical codes, the newly developed geochemical module EQMOD, enables HYDROGEOCHEM to consider equilibrium aqueous complexation, ion exchange, surface complexation, precipitation/dissolution, redox and acid-base reactions. The code has been applied to several laboratory and field systems during development and testing, including radionuclide transport and leaching of uranium mill tailings.

### 2.9.3.2 DYNAMIX

The DYNAMIX code is based on the transport code TRUMP and the geochemical equilibrium code PHREEQE (Liu and Narasimhan, 1989a,b). Developed at the University of California, Berkeley, DYNAMIX is a three-dimensional code that employs a two-step coupling approach between chemistry and the fluid flow equation. The code is designed specifically to handle aqueous complexation, redox processes, ion exchange, and precipitation dissolution. The code is also being modified to use partial equilibrium to consider surface reaction-limited kinetic mineral dissolution. The code has been tested against two other reactive transport codes, PHASEQL/FLOW (Walsh et al., 1984) and THCC (Carnahan, 1987b) and found to be in reasonable agreement. For a 25 m × 1000 m two-dimensional simulation of leaching and transport of As and Se from fly ash over 30 years, DYNAMIX required approximately 3.4 CPU hours of CRAY supercomputer time (Liu and Narasimhan, 1989b).

### 2.9.3.3 CHEQMATE

Developed at Harwell Laboratory in the United Kingdom, the finite difference CHEQMATE (CHEMical EQUilibrium with Migration and Transport EQUations) code originally considered only molecular diffusion along concentration gradients and electromigration (Haworth et al., 1988a). The code has since been extended to consider advective transport of species through a series of heterogeneous media under constant flow conditions (Haworth et al., 1988b) and spherical geometries. The code is able to model one-dimensional transport using iterative two-step coupling and an assumption of local equilibrium. The chemical equilibrium is based on the PHREEQE geochemical code and relies on the PHREEQE thermodynamic database. Since the transport equations are only derived in terms of concentrations and thermodynamic activities are not considered, the code is limited to dilute aqueous solutions. Aqueous complexation, precipitation/dissolution, redox, and acid-base reactions are modeled, but adsorption/desorption, ion exchange, and reaction kinetics are not. The code is written in FORTRAN 77 and has been adapted to IBM Mainframe and CRAY2 computer systems. By scaling down the thermodynamic database to 10 elements, 50 species, and 20 minerals, a model has been adapted to IBM PC use (Haworth et al., 1988a).

### 2.9.3.4 TRANQL

The TRANQL code, developed at Stanford University, has been used to model multicomponent transport of Cd, Co, Br, and Cl (Cederberg, 1985; Cederberg et al., 1985). The code is based on the transport code ISOQUAD (Pinder, 1976; Pinder and Gray, 1977) and MICROQL (Westall, 1979), a scaled-down version of the MINEQL code. TRANQL has been evaluated by Siegel et al. (1989). The model is currently designed for one-dimensional simulation employing a mainframe computer system. The current system is able to model ion exchange and surface complexation sorption processes, but cannot handle precipitation/dissolution reactions. Pre- and post-processing routines have been developed to facilitate data entry and interpretation. The code is currently limited to a maximum of two mobile components and one sorbing substrate. Siegel et al. (1989) concluded that code flexibility is limited by its database, and for a simple system (14 complexes), reactive solute transport for a distance of 10 km over 10,000 years would require about 40 hours of CPU time on the Sandia National Laboratory CRAY-1.

### 2.9.3.5 FASTCHEM

The FASTCHEM system (Hostetler and Erikson, 1989; Hostetler et al., 1989) was developed by PNL for EPRI, and is based on the SATURN transport code and the MINTEQ geochemical code (Morrey et al., 1986). The program is modular in design, and incorporates a networked PC workstation for constructing input files to an online mainframe computer for transport and geochemical calculations. Post-processing of the output is performed on the mainframe for subsequent downloading and graphic display at the workstation. The code uses a modified version of the MINTEQ database and is valid for the temperature range 25 to 100 °C (Krupka et al., 1988; Criscenti et al., 1989). A Markov hydrological model is used to simulate solute movement through advection, diffusion, and hydrodynamic dispersion (Kincaid, 1988). This method involves discretizing a streamtube into a number of arbitrarily shaped bins. The total concentration of each solute in each bin is then expressed as an entry in a state vector, and the Markov transition matrix is used to predict the evolution of the state vector through time. Two-step coupling of geochemistry and transport is used for efficient computation. Only longitudinal dispersion is modeled; a series of parallel, one-dimensional, noninteracting streamtubes is used to model two-dimensional (and in theory three-dimensional) systems. Because of the streamtube construction,

FASTCHEM is somewhat limited in its ability to model transient conditions. The two-dimensional flow code EFLOW is run until steady-state is achieved. The steady-state flow field generated in this fashion is then processed into the necessary streamtubes by the code ETUBE. In order to simulate transient changes in hydraulic properties of the medium, it is necessary to redefine the boundary conditions at the appropriate timestep, and then run the EFLOW code again to achieve a steady-state flow field. ETUBE is executed again, and a new set of streamtubes is defined. Equilibrium geochemical processes include speciation, complexation, oxidation/reduction, and several different adsorption models ( $K_d$ , empirical isotherms, ion exchange, surface complexation). Activity relationships are modeled using the Davies or the extended Debye-Hückel equations.

#### 2.9.3.6 CTM

The CTM (Chemical Transport Model) code (Morrey and Hostetler, 1985; Erikson et al., 1990) is currently in development at PNL for the Low-Level Waste Management Division of the NRC, and incorporates many of the same methods and approaches as the proprietary FASTCHEM code. The database is the same as the FASTCHEM code, with further modifications to include the compilations of Wagman et al. (1982) and the uranium data of Tripathi (1984). The current version of the code has only been set up for one-dimensional, isothermal simulations assuming equilibrium. While the CTM code is currently designed to run on an IBM PS/2 Model 70, future developments for modeling two- and three-dimensional systems may require mainframe capabilities. Pre- and post-processing are available for data input and output through an interactive system. Output is designed to take advantage of several commercial graphics software packages currently available for the PS/2 system (SURFER/GRAPHER).

#### 2.9.3.7 CHEMTRN

The CHEMTRN code was developed at Lawrence Berkeley Laboratory (LBL), and has been applied to nuclear waste isolation and contaminant transport (Miller, 1983; Miller and Benson, 1983). The code uses the one-step direct coupling method, and is therefore more cumbersome than the two-step codes discussed above. CHEMTRN is an equilibrium code, and is similar to FASTCHEM/CTM in that it employs a one-dimensional streamtube to model fluid flow. Due to the one-step coupling, however, storage limitations will become a problem in extending the model to multiple dimensions. The code is able to model ion exchange, surface complexation (triple-layer model only), and precipitation/dissolution reactions as retardation mechanisms. No  $K_d$  or sorption isotherms are available for the code as it is currently configured. The model is limited to saturated flow through a homogeneous porous medium at constant temperature. In applications to date, the model has not employed an extensive, established thermodynamic database. The user is required to provide all of the reaction stoichiometries, equilibrium coefficients, CEC, sorption parameters, and other variables for each run using a formatted batch input. It does appear that data can be included from a variety of sources, but a database would have to be developed and modified for extensive use of this code.

#### 2.9.3.8 CHMTRNS

The CHMTRNS code was also developed at LBL (Noorishad et al., 1987), and represents a version of CHEMTRN that has been modified to include reaction kinetics, carbon isotope fractionation, and nonisothermal behavior. Multiple sorption models can be used in a given run. Formatted batch input is used for defining the problem and inputting the initial and boundary conditions. Each input deck consists of a minimum of twenty "cards," each card consisting of from one to seven parameters. Although the elaborate input makes the code flexible enough for application to a variety of systems and situations,

many of the parameters must be defined by the user, leading to complex data input. In addition, much of the thermodynamic, kinetic, and sorption data must be entered each time the model is run, limiting the ability of the code to perform multiple runs for sensitivity analysis. No pre- or post-processing of the data is currently available to help in data entry or interpretation. Data entry is similar to that for CHEMTRN.

#### **2.9.3.9 NEFTRAN and TRACR3D**

NEFTRAN II (Olague et al., 1991) and TRACR3D (Travis, 1984) are solute transport codes and do not explicitly consider the geochemical equilibria involved in contaminant migration. As such, they are not suitable for examining specific sorption processes. However, because the bulk of the calculation time involved in modeling reactive solute transport is spent calculating the geochemistry, solute transport codes are much quicker. They can therefore be adapted to model three-dimensional transport, radionuclide decay, and fractured media transport without overextending computer resources. In addition, they can be more finely discretized, and the physical aspect of solute transport can be examined in more detail.

### **2.9.4 Summary and Conclusions**

Coupling of chemical equilibria and mass transport may be accomplished using either a direct coupling approach or a two-step iterative approach (Yeh and Tripathi, 1989). Although a direct approach is more exact, a two-step approach is more efficient and offers the best hope for extending coupled reactive solute transport into two- and three-dimensional simulations. This efficiency also offers the most promise for the incorporation of more detailed and complex geochemical processes such as kinetics, colloidal transport, and microbial activity as data become available, without overtaxing available computer resources. An additional consideration is the use of stochastic models in probabilistic assessment of the role of partially saturated flow and geologic heterogeneities in solute transport. These models frequently rely on performing large numbers of calculations (e.g., Monte Carlo approach) to develop the necessary population statistics. Computer intensive geochemistry calculations may be inappropriate for this type of approach, and severely limit the application of currently available hydrogeochemical codes in stochastic modeling.

## **2.10 CHEMICAL -> HYDROLOGIC**

Chemical processes are expected to directly affect hydrologic processes through either (i) mineralogy of fracture surfaces, (ii) fracture healing, (iii) chemical osmosis, or (iv) fluid properties. Each is discussed further.

### **2.10.1 Mineralogy of Fracture Surfaces**

Gallegos et al. (1992) have studied the influence of fracture coating on the transfer of water between the fracture and the matrix in a partially saturated medium. It was determined that the mineralogy of the fracture surfaces may be important in restricting the imbibition of water into the matrix. This is considered theoretically important, especially for the validity of the equivalent continuum model (ECM) which was discussed in Appendix B of this report. The ECM assumes hydrologic equilibrium between the fractures and the matrix. If a fracture coating exists, then it may sufficiently reduce the rate of imbibition to cause the fracture and matrix to be out of hydrologic equilibrium. It was

found that the effect of the mineralized face ranged from negligible to strongly restricting water uptake into the matrix. The results are considered preliminary and future laboratory experiments are planned (Gallegos et al., 1992). The cause of chemical coating on fracture surfaces is closely related to the dissolution, movement, and precipitation of minerals associated with fracture healing which is discussed next.

### 2.10.2 Fracture Healing

Lin and Daily (1989), and Daily et al. (1987) conducted laboratory experiments to determine the hydrologic transport properties of Topopah Spring Tuff. One conclusion of this work is that the hydrologic permeability of intact rock is essentially independent of drying/wetting cycles at elevated temperatures for prolonged periods of time. Fractured rock, however, exhibited permeability decreases of more than 3 orders of magnitude during a 6 month experiment (Daily et al., 1987). The decrease of permeability was attributed to "fracture healing" which consists of dissolution and precipitation of minerals such as silica. Hence, the permeability of fractured tuff was found to be strongly dependent on temperature and time.

The implication of fracture healing on the near field hydrology has been studied by Lin and Daily (1989). Here, it is hypothesized that a heat-generating waste package will sufficiently elevate the near-field temperatures and induce fracture healing so that an envelope of low permeability rock will surround the waste packages. The envelope of low permeability rock would diminish possible infiltration of water into the vicinity of the waste packages, hence help keep the packages dry for extended periods of time. Numerical simulations of Travis and Nutall (1987) predicted similar results modeling two-dimensional transport in Yucca Mountain.

### 2.10.3 Chemical Osmosis

Chemical osmosis describes a condition where a gradient of solute concentration causes a flux of solvent (i.e., liquid fluid). The process of osmosis is frequently discussed in textbooks in the context of "reverse osmosis" which is applied to desalinization and ultrafiltration of water. In textbook discussions, osmosis is described as occurring through a semipermeable membrane which preferentially passes water molecules but does not permit the passage of solutes. In the broader sense, osmosis has been applied to diffusional processes through a porous medium which provide a driving potential for the flux of water.

Carnahan (1984) describes thermodynamically coupled mass transport processes in a saturated clay, in which chemical osmosis is described. Here chemical osmosis describes the flux of solvent driven by a gradient in solute concentration

$$\bar{v}_L = \nabla C_1 \quad (2-36)$$

where

- $\bar{v}_L$  = solvent (liquid) velocity
- $\nabla$  = gradient operator, and
- $C_1$  = concentration of species I (solute) in the liquid

Carnahan (1984b) notes that there is a lack of experimental data on chemical osmosis and other thermodynamically coupled constitutive properties (e.g., thermal osmosis, the Soret effect). By estimating coefficients from the literature, Carnahan conducted numerical simulations. The simulations indicated that chemical osmosis can cause a significant flux of water, up to 3 or 4 orders of magnitude greater than Darcy's flux in a saturated clay.

Jamet et al. (1990) expanded on the concept of constitutively coupled processes based on the ideas from nonequilibrium thermodynamics. Again, chemical osmosis was considered with a host of other couplings. One conclusion is that under very idealized situations, the secondary couplings (e.g., chemical osmosis) may be more important than the primary couplings (Darcy's law, Fick's law, Fourier's law). The relative importance of the couplings depends on the values of the phenomenological coefficients which unfortunately are typically not available in the literature.

#### **2.10.4 Fluid Properties**

Chemical processes are expected to influence fluid properties such as density, viscosity and vapor pressure. It is established that the density of water is affected by the introduction of dissolved species into solution (e.g., Sourirajan and Kennedy, 1962; Potter and Brown, 1977; Bischoff, 1991). In general, the density of saline water (liquid) is greater at a given temperature and pressure than that of pure water (Figure 2-25). In hydrothermal environments, hydrohaline convection has been proposed where salinity dependent density gradients add to thermally driven convection and enhance and focus fluid flow and heat transfer (Forster and Smith, 1990).

The presence of dissolved gases such as CO<sub>2</sub> can also change fluid density (Takenouchi and Kennedy, 1965; Bowers and Helgeson, 1983; Sterner and Bodnar, 1991). At low pressures and temperatures, however, the solubility of CO<sub>2</sub> in pure water is small. As a result of this low solubility, the fluid will separate into a low density, high CO<sub>2</sub> phase (vapor) and a second high density, H<sub>2</sub>O rich liquid phase. At temperatures and pressures on the order of those anticipated at Yucca Mountain, CO<sub>2</sub> is almost completely insoluble in pure H<sub>2</sub>O, and the effect of dissolved CO<sub>2</sub> on water density is negligible. The addition of NaCl to the system further decreases the CO<sub>2</sub> solubility (Takenouchi and Kennedy, 1965; Bowers and Helgeson, 1983).

As shown in Figure 2-26, fluid viscosity also increases with increasing salinity at constant temperature and pressure (Forster and Smith, 1990). Increasing viscosity tends to reduce advective hydrologic transport.

Under certain conditions, the direct effects of salinity on water density and viscosity may be overshadowed by the indirect effects of shifting the liquid-vapor curve and the critical point to higher pressures and temperatures with increased salinity (Figure 2-27) (Bischoff, 1991). The shift in the critical point with salinity can be quite pronounced, from 374 °C and 220 bars for pure water to 500 °C and 582 bars for 13.6 wt % NaCl. This shifts the position of the near-critical region to a different pressure-temperature region. Dissolved CO<sub>2</sub> also shifts the critical point of water to higher pressures and lower temperatures (Figure 2-28). At low temperatures and pressures, however, the effect of CO<sub>2</sub> is negligible except at very high mole percent CO<sub>2</sub>, and the shift in the P-T trajectory of the liquid-vapor curve is not appreciable. Assuming behavior analogous to the pure water system, fluid properties in the near-critical region such as density, heat capacity, and enthalpy can vary widely over narrow ranges in temperature and pressure (Johnson and Norton, 1991). However, at low pressures on the order of 1 atmosphere, the

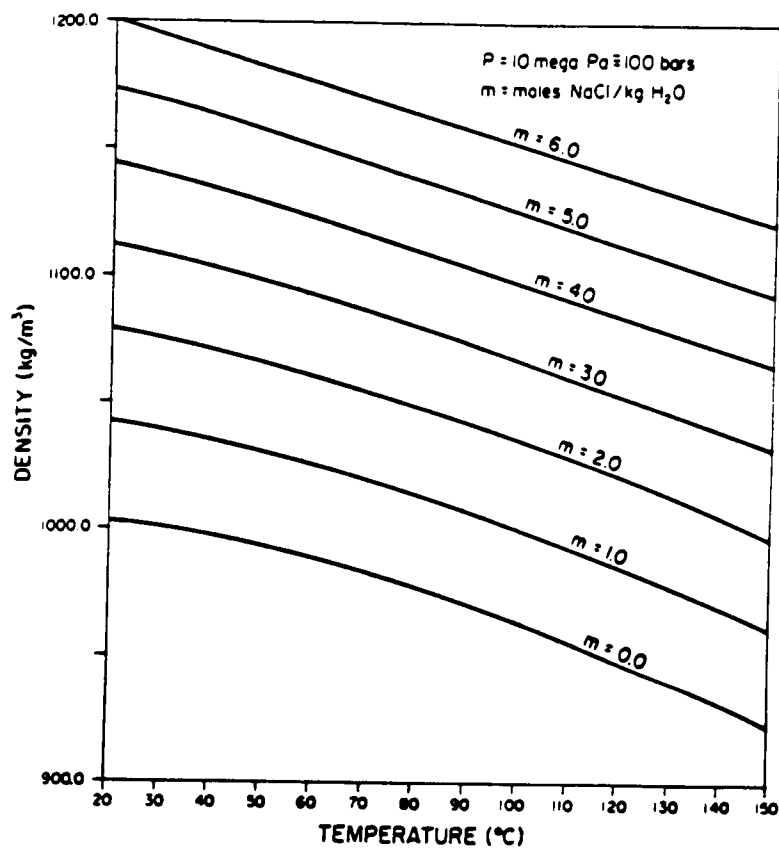


Figure 2-25. Water Density as a Function of Temperature for Different Salinities ( $m = \text{moles NaCl/kg H}_2\text{O}$ ) at a Constant Pressure of 10 MPa  $\approx$  100 atm (After Forster and Smith, 1990)

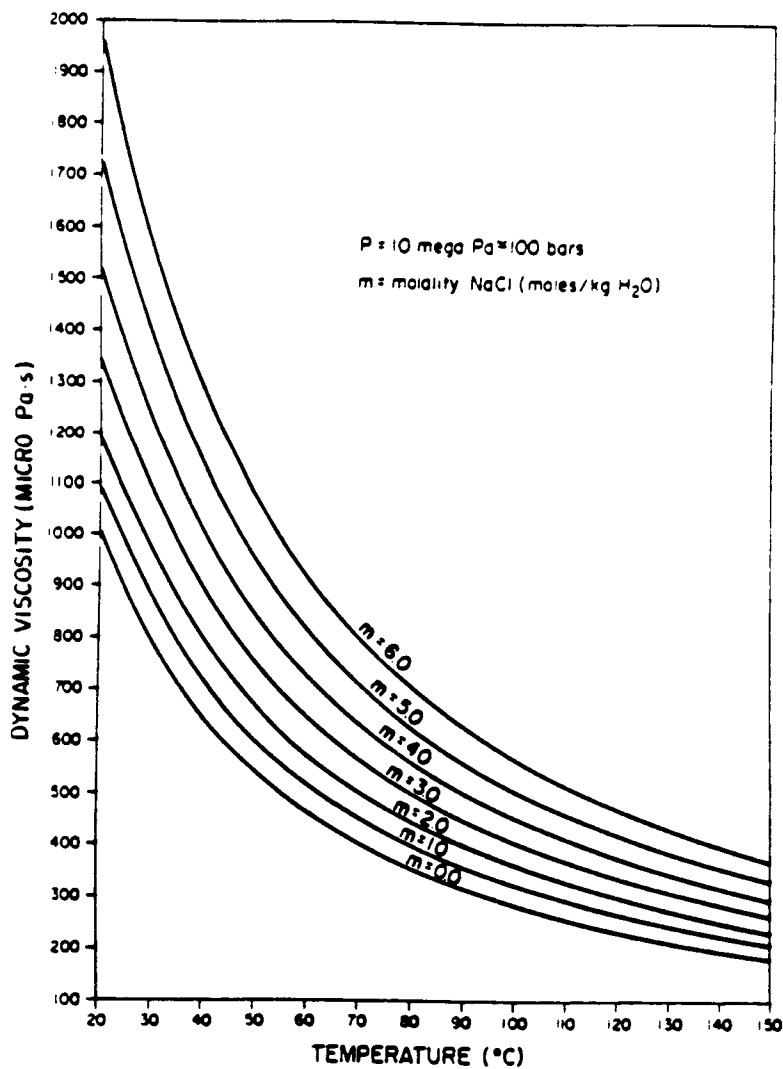


Figure 2-26. Dynamic Viscosity of Water as a Function of Salinity for Constant  $P = 10 \text{ MPa} \approx 100 \text{ atm}$  (After Forster and Smith, 1990)

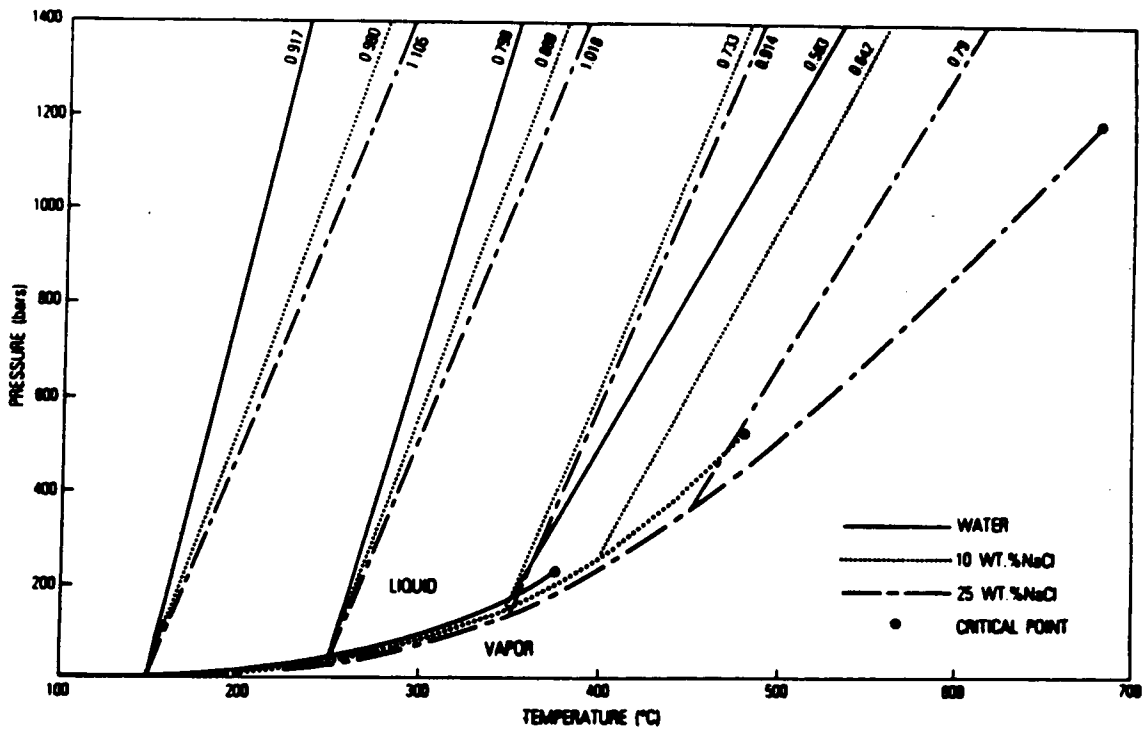


Figure 2-27. Shifting of the Vapor-Liquid Line for Pure Water (Solid Line) With the Addition of 10 wt% NaCl (Dotted Line) and 25 wt% NaCl (Dashed Line). The Critical Points are also Shown. The Straight Lines are Isochores Representing Constant Density Fluids with P-T. The Numbers Represent the Density in  $\text{g/cm}^3$ . After Roedder (1984)

boiling point of water is not affected greatly by increased salinity (DOE, 1988). At the low temperatures and pressures anticipated in the geologic repository, these variations are likely to be small and of minimal significance relative to other uncertainties.

Like liquids, the physiochemical properties of gases are controlled at a basic level through varying gas composition as a function of chemistry. Largely controlled by contact with the atmosphere, water vapor, carbon dioxide and oxygen are the most critical gases in most hydrologically partially saturated natural systems. The presence of buffers in groundwaters, such as the  $\text{Fe}^{2+}/\text{Fe}^{3+}$  redox couple and solution alkalinity, also serves to control gas partial pressures. The  $\text{CO}_2$  content of gases in the partially saturated zone at Yucca Mountain exhibits considerable variation with respect to both time and space (Murphy, 1989), ranging up to about 1.6 percent  $\text{CO}_2$  by volume. Gas in equilibrium with J-13 water from hydrologically saturated Topopah Spring Tuff is approximately 1.5 percent  $\text{CO}_2$  by volume, and the  $\text{CO}_2$  content of air is about 0.03 percent. Several studies (Takenouchi and Kennedy, 1964, 1965; Bowers and Helgeson, 1983) indicate the importance of  $\text{CO}_2$  in the  $\text{H}_2\text{O}-\text{CO}_2-\text{NaCl}$  system (Figure 2-28). At low pressures, however, the shift in the liquid-vapor curve is negligible. Because of the relatively large amount of water present in the Yucca Mountain system (40-70 percent saturated), gas composition is likely to be chemically saturated with water (Murphy, 1989). As a result of the low  $\text{CO}_2$  gas concentrations and low gas pressures anticipated at Yucca Mountain, the effect of variations in  $\text{CO}_2$  on gas thermal properties is likely to be negligible.

The effects of mineral redistribution on fractured tuff permeability has been discussed in Section 2.10.2 with respect to fracture healing. An additional potential effect is on medium porosity and permeability due to electrically charged swelling clays (also see Section 2.7.2). In the presence of poorly hydrolyzed cations such as  $\text{Na}^+$ , the electrical double layer (EDL) around charged particles can cause the expansion of swelling clays such as smectite, and also tends to promote clay dispersion. This in turn clogs pores with fine particles, shifting the pore-size distribution to smaller diameter pores, and reduces the permeability, hydraulic conductivity (K), and water diffusivity (D) (Siyag et al., 1983; Nielsen et al., 1986) of the medium (Figure 2-29). Called the salinity effect by Nielsen et al. (1986), this phenomenon has been documented in numerous studies of partially saturated soils under arid and semi-arid conditions (Suarez et al., 1984; Russo, 1989b; Goldberg et al., 1991). Even under saturated conditions, K can be reduced by an order of magnitude or more (Laryea et al., 1982; Nielsen et al., 1986). Brandl (1981) observed that with the addition of portlandite [ $\text{Ca}(\text{OH})_2$ ] to soil aggregates, permeabilities initially increased, before decreasing with curing age. It seems that poorly hydrolyzed  $\text{Ca}^{++}$  initially reduces swelling of clays, "unclogging" pores. As time passes, however, the cement begins to harden, filling voids and reducing permeability once again.

Variations in overall solution chemistry and moisture content also influence the magnitude of the salinity effect. Suarez et al. (1984) noted decreasing hydraulic conductivities with increasing pH. This is likely due to the fact that at low pH, the surface charge is high, and edge-surface bonding of clays, as well as bonding of positively charged oxides to negatively charged clay surfaces, occurs. Under these conditions, clay dispersion is low, and the adverse effect on hydraulic conductivity is minimal. As the pH increases, the surface charge decreases, clay dispersion is enhanced, and the salinity effect is amplified (Suarez et al., 1984). In a similar manner, at low ionic strengths or with predominantly monovalent cations, the EDL expands outward from particle surfaces into the pores, leading to a more pronounced salinity effect with decreasing electrolyte concentration (Nielsen et al., 1986). Finally, as the moisture content decreases, the water film becomes thinner, and the thickness of the EDL becomes relatively more important. Under drying conditions, reductions in D and K due to the salinity effect become more pronounced, with decreases of as much as 3 orders of magnitude, as the moisture content declines from  $0.5 \text{ cm}^3/\text{cm}^3$  to  $0.3 \text{ cm}^3/\text{cm}^3$  (Siyag et al., 1983).

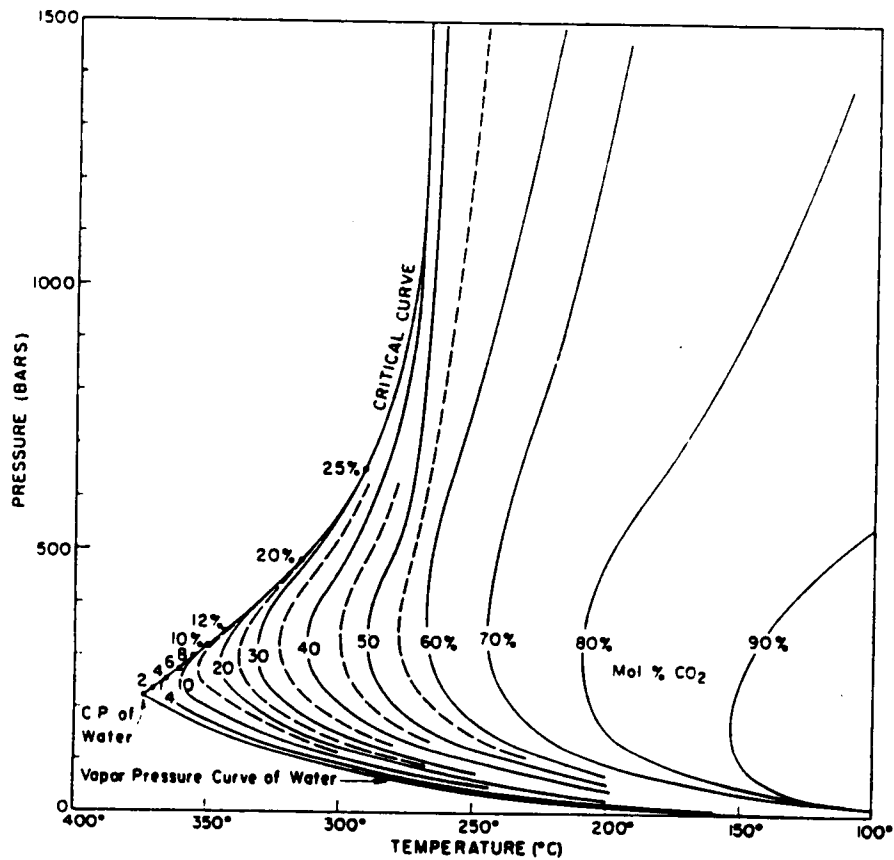
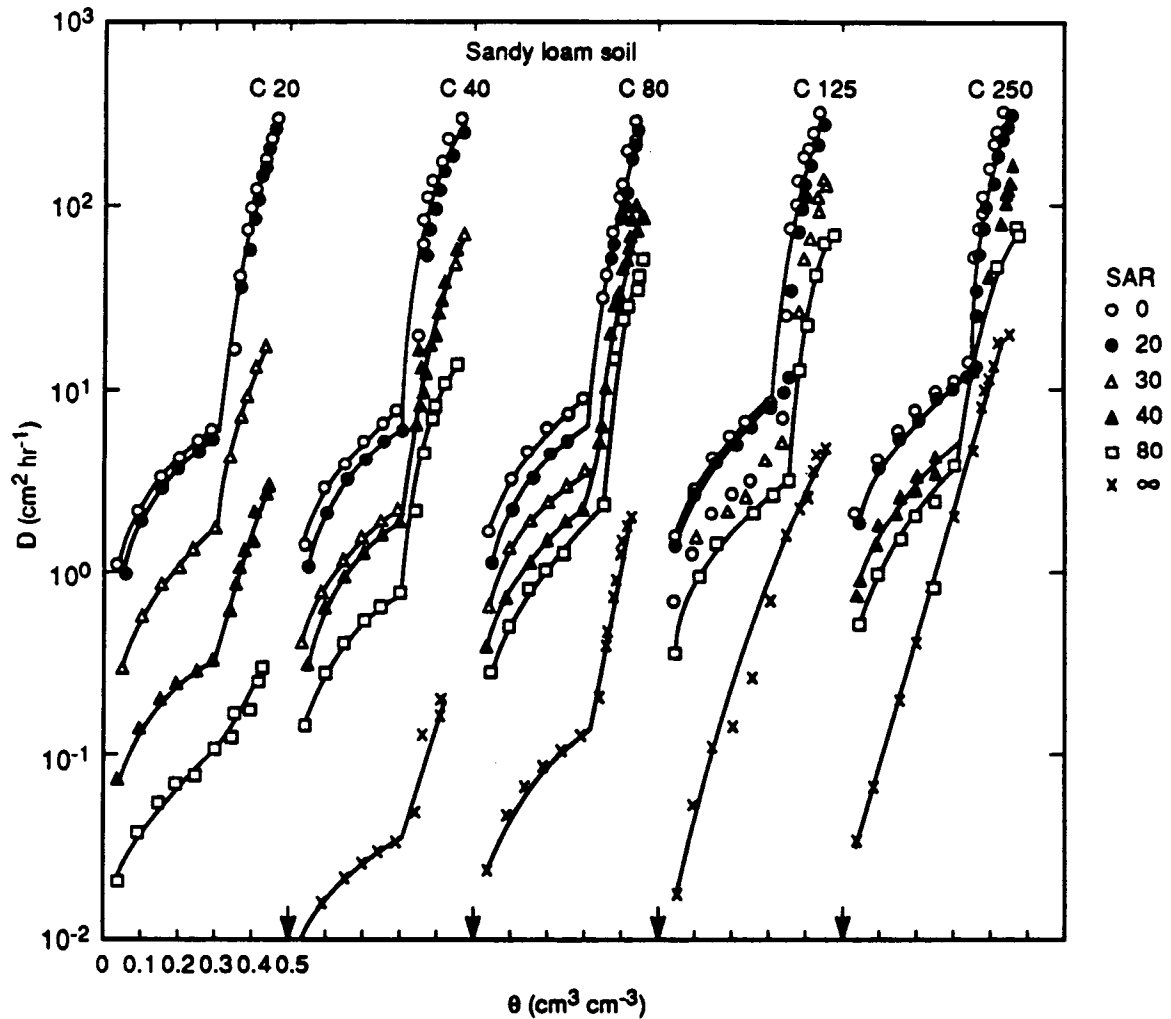


Figure 2-28. P-T Plot of Isocompositional Curves for the Gas Phase in Equilibrium with the Liquid Phase for the System H<sub>2</sub>O-CO<sub>2</sub>. The Critical Curve for the System Extends from the Critical Point for Water (374°C and 220 bars) to Lower Temperatures and Higher Pressures. The Minimum Critical Temperature Occurs at Approximately 266°C and about 2150 bars. After Takenouchi and Kennedy (1964)



**Figure 2-29. Soil Water Diffusivity as a Function of Water Content and Sodium Adsorption Ratio (SAR) at Different Electrolyte Concentrations (C = 20 to 250 meq/l). SAR is a Measure of Total Solution Na<sup>+</sup> Concentration Relative to Ca<sup>++</sup> + Mg<sup>++</sup> (i.e. SAR = C<sub>Na</sub>/[C<sub>Mg</sub> + C<sub>Ca</sub>]<sup>1/2</sup>). The Salinity Effect Increases with Increasing SAR. (After Siyag et al., 1983)**

Most of these studies have been conducted in soils, and the extent to which the treatment is applicable to intact rock, such as the volcanic tuffs at Yucca Mountain, is very uncertain. However, expandable smectitic clays are present as alteration products of the various tuff units (Broxton et al., 1987), and possibly as colloidal particles as well (Means et al., 1983). Water chemistries in the vicinity of Yucca Mountain indicate a sodium bicarbonate solution at low ionic strengths (Kerrisk, 1987). Given the arid climate of southern Nevada, it is possible that a correlation between solution chemistry and hydraulic properties of the geologic media, similar to that outlined above for soils, may exist at Yucca Mountain.

### **2.10.5 Summary and Conclusions**

The coupling mechanisms for chemical to hydrologic (C -> H) processes have been reviewed in this section. In total, four mechanisms were discussed: mineralogy of fracture surfaces, fracture healing, chemical osmosis, and fluid properties. The mineralogy of the fracture surfaces can be important in the imbibition of liquid into the matrix, hence influences the applicability of the effective continuum model. Fracture healing has been experimentally observed where minerals precipitate in fractures thereby influencing fracture apertures and hydraulic conductivity. Chemical osmosis is a mechanism where liquid flows due to a dissolved species concentration gradient. Chemical composition can also influence fluid properties such as density, viscosity, and vapor pressure.

Each of these coupling mechanisms appears relevant to Yucca Mountain, however none appears significant. Probably the most important coupling mechanism is the mineralogy of fracture surfaces because this influences the distance liquid drains in a fracture before being imbibed into the matrix. Fracture healing may also be important in the near field as "healing" fractures may shield waste canisters from fracture flow, however this influence may be negligible in comparison with uncertainties associated with the surrounding rock (hydrologic conductivity, heterogeneities, fracture locations, etc). In summary, C -> H couplings appear to be negligible in comparison with inherent uncertainties associated with hydrologic processes at Yucca Mountain.

### **2.11 MECHANICAL -> CHEMICAL**

Mechanical stresses in the repository environment will affect the chemistry of the system mostly through pressure changes in the system. The effects of pressure on chemical equilibrium are well established and can be calculated through thermodynamics. The effects of pressure on nonequilibrium processes are less well understood, but an assumption of partial equilibrium can allow for modeling reaction progress as a function of pressure. Because the repository will be constructed in the partially saturated zone at Yucca Mountain, gas pressure at the repository is expected to be close to 1 atmosphere, and pressure effects are likely to be overshadowed by temperature effects as discussed in Sections 2.5 and 2.6.

It is also possible that the chemistry will be perturbed by the construction of the repository itself. Fracturing of the rock can expose fresh, reactive surfaces to the fluids, enhancing reaction rates. Opening of new pathways can alter gas flow, potentially leading to large changes in the partial pressures of critical gas such as CO<sub>2</sub> and O<sub>2</sub> (Murphy, 1990).

### 2.11.1 Pressure Effects on Chemical Equilibrium

At constant temperature, the key relationship between the free energy of reaction and pressure is

$$\left(\frac{\partial \Delta G_R}{\partial P}\right)_T = \Delta V_R = \sum V_{\text{products}} - \sum V_{\text{reactants}} \quad (2-37)$$

where

- P = pressure (atmospheres, bars or Pascals)  
 V = molal volume (m<sup>3</sup>) of the products and reactants as subscripted, and  
 ΔV<sub>R</sub> = volume changes of reaction

For a given temperature T, and assuming a reference pressure of 1 atmosphere, integration of Eq. 2-37 results in

$$\Delta G_{R,T,P} = \Delta G_{R,T,1}^\circ + \int_1^P \Delta V_R dP \quad (2-38)$$

As written in Eq. 2-38, ΔV<sub>R</sub> is dependent on pressure. For solids and liquids, molal volume as a function of pressure is represented by the coefficient of isothermal compressibility, β (atm<sup>-1</sup>) such that

$$\beta = -\frac{1}{V} \left(\frac{\partial V}{\partial P}\right)_T \quad (2-39)$$

Molal volumes can also be expressed as a polynomial function of pressure (Richardson and McSween, 1989), which can be readily integrated.

If ΔV<sub>R</sub> is independent of pressure, it is treated as a constant and the integration of Eqs. 2-37 and 2-38 is greatly simplified. Solids are relatively incompressible (i.e., β is very small), and volume changes with pressure are slight. At relatively low pressures (tens of atmospheres) in the absence of a gas phase, liquids are also generally assumed to be incompressible. For this reason, ΔV<sub>R</sub> is commonly assumed to be constant for chemical reactions only involving solids and liquids. For a constant ΔV<sub>R</sub>, combining Eq. 2-38 with the equilibrium relationship (Eq. D-6) ΔG<sub>R</sub><sup>°</sup> = -RT[ln(K)] yields the relationship

$$\ln \frac{K_{P_2}}{K_1} = -\frac{\Delta V_R (P_2 - 1)}{RT} \quad (2-40)$$

At constant temperature and electrolyte concentration (m<sub>i</sub>), activity coefficients (γ<sub>i</sub>) vary as a function of pressure according to the relationship

$$\left(\frac{\partial \ln \gamma_i}{\partial P}\right)_{T,m} = \frac{V_i - V_i^\circ}{RT} \quad (2-41)$$

where

$V_i$  = partial molar volume of species  $i$  under actual conditions, and  
 $V_i^\circ$  = partial molar volume under defined standard-state conditions.

Because partial molar volumes of dissolved species are a function of ionic strength, Stumm and Morgan (1981) point out that pressure effects on equilibrium constants will differ for aqueous solutions as compared to high ionic strength solutions.

In contrast to solids and liquids, changes in total pressure can result in significant changes in gas molar volumes and partial pressures, and therefore in chemical reactions involving gas phases. According to the Ideal Gas Law, pressure ( $P$ ) and volume ( $V$ ) are related such that

$$PV = nRT \quad (2-42)$$

where

$R$  = ideal gas constant,  
 $T$  = absolute temperature (K), and  
 $n$  = number of moles.

For one mole of gas,  $PV/RT = 1$  indicates that the gas behaves ideally. At temperatures of interest and at pressures up to 1 atmosphere, most gases behave ideally and no additional corrections are necessary. For pressures between one and several hundred atmospheres,  $PV/RT < 1$  for many gases, indicating the gas is more compressible than would be expected. This is likely to be due to attractive forces between the molecules which reduce the effective volume of the gas mixture. An empirical relationship called the van der Waals equation (e.g., Richardson and McSween, 1989) has been developed to account for this deviation from ideality such that

$$\left[ P + \left( \frac{a}{V^2} \right) \right] (V - b) = RT \quad (2-43)$$

where

$a, b$  = empirical factors determined for each gas.

In an ideal gas mixture, the partial pressure of an ideal gas is defined as the pressure that the gas would exert if it occupied the same volume alone (e.g., Freeze and Cherry, 1979). The total pressure of the ideal gas mixture is therefore equal to the sum of the component partial pressures. For gases B, C, and D interacting according to the reaction  $bB + cC = dD$ , the equilibrium constant  $K$  is defined such that

$$K = \frac{(f_D)^d}{(f_B)^b (f_C)^c} \quad (2-44)$$

where

$f_i^i$  = fugacity of the gas  $i$  raised to the reaction coefficient  $i$ .

Fugacity is related to the partial pressure of the gas by assuming a standard state fugacity, and through the use of a fugacity coefficient  $\gamma$  such that  $f_i = \gamma_{f,i}P(i)$ . A standard-state pressure of 1 atmosphere is commonly chosen. As the gas mixture approaches ideal behavior,  $\gamma_{f,i} \rightarrow 1$ . Over a wide range in temperature  $\gamma_{f,i} \approx 1$  for most real gases at pressures near 1 atmosphere. In a similar fashion, most real gas mixtures exhibit ideal behavior for pressures between 0 and 1 atmospheres and the fugacity of each gas in the mixture is approximately equal to its partial pressure. In the partially saturated zone at Yucca Mountain, total gas pressures of 1 atmosphere are anticipated, and an assumption of ideal behavior is reasonable.

### 2.11.2 Pressure Effects on Nonequilibrium Chemistry

As mentioned in the introduction, the pressure effects on reaction rates are less clearly understood. If a reaction progress approach assuming local equilibrium (see Appendix D) is used, the development outlined above is appropriate. Transition-state theory (Stumm and Morgan, 1981; Lasaga, 1981b) uses a modified form of Eq. 2-40 to express the effect of pressure on the rate constant for the formation of an activated complex (e.g.,  $X^\ddagger$ ) such that

$$\left( \frac{\partial \ln(k)}{\partial P} \right)_{T, m} = - \frac{\Delta V^\ddagger}{RT} \quad (2-45)$$

where the volume of activation  $\Delta V^\ddagger = V^\ddagger - (V_A + V_B)$ , for  $A + B \rightarrow X^\ddagger$ . Assuming a standard state of 1 atm and that  $\Delta V^\ddagger$  is constant with pressure, integrating Eq. 2-45 yields a form similar to Eq. 2-40 such that:

$$\frac{\ln \frac{k_{P_2}}{k_1}}{RT} = - \Delta V^\ddagger (P_2 - 1) \quad (2-46)$$

From Eq. 2-46, a plot of  $\ln k_{P_2}$  versus  $P$  yields  $\Delta V^\ddagger$ . If  $\Delta V^\ddagger < 0$ , then the rate constant increases with pressure.

### 2.11.3 Pressure Solution

Mineral dissolution in response to stresses at grain-grain contacts, and the mobilization and reprecipitation of chemical species in response to the resultant chemical gradients is observed in many types of diagenetic and metamorphic environments. Dewers and Ortoleva (1990a) noted that this type of "stress-driven water-rock interaction" is divided into two distinct classes: (i) pervasive intergranular pressure solution (IPS) and (ii) the development of localized textures called stylolites. Two types of mechanisms are discussed by Dewers and Ortoleva (1990a). Water-Film Diffusion (WFD) involves dissolution in response to variations in normal stress across contacts; chemicals diffuse down the chemical potential gradients along the contact in a thin water film adsorbed to the grain surface. Free-Face Pressure Solution (FFPS) includes dissolution stimulated by elastic strain energy at contact asperities and possible increases in surface area resulting from crushing at the microscale.

Pervasive intergranular pressure solution tends to remove textural heterogeneities through time. As the dissolution reaction proceeds under stress, the grain-grain contact increases in area. Small area

point contacts tend to redistribute faster and larger areas tend to react slower, resulting in a relatively narrow spatial average. Water-Film Diffusion tends to favor this process. Conversely, Free-Face Pressure Solution tends to favor the preservation of small area asperities, maintaining and enhancing existing textural heterogeneities in the medium, and promoting the development of stylolites. Rates of FFPS are limited by diffusion at grain contacts. Faster rates of reaction tend to minimize stylolite development.

In a series of recent papers (Ortoleva et al., 1987; Dewers and Ortoleva, 1990a,b), a coupled mechanical-chemical model was developed to simulate the growth of stylolites during the burial and compaction of sandstones. A representative element volume was assumed to be made up of a large number of identical grains (truncated spheres) arranged in a regular array. The model used three types of contact surfaces and a free face area, and considered WDS and FFPS to be the only mechanisms contributing to pressure solution. Pressure normal to the contact is different for the four different surface types. Solute transport is only by diffusion. The pressures and times considered are generally greater (0-3 km depth of burial, and 0 to 550 million years) than those of interest in a HLW repository.

#### **2.11.4 Computer Codes**

As is the case with temperature effects, geochemical codes are not generally coupled to mechanical processes in the sense of directly simulating the effects of stress on chemistry. Pressure effects can be simulated, however, though the number of geochemical codes which can extrapolate beyond 1 atmosphere is much more limited than those that can consider thermochemical processes. Below is a brief listing of those codes that can take into account pressure variations. The codes are discussed in more detail in Section 2.6. More complete listings are available in other studies (Nordstrom and Ball, 1984; Nordstrom and Munoz, 1985; Morrey et al., 1986; Serne et al., 1990; Mangold and Tsang, 1991).

##### **2.11.4.1 SUPCRT**

SUPCRT is perhaps the most flexible geochemical code that deals with pressure variations. The thermodynamic data are internally consistent (Helgeson et al., 1978) and extrapolation to 5000 bars and 1000 °C is possible in the most recent version (Johnson et al., 1991).

##### **2.11.4.2 EQ3/EQ6**

The EQ3/EQ6 code is able to model pressure variations in a somewhat limited fashion. Below 100 °C, the code is limited to 1 atmosphere. Above 100 °C, the pressure variation with temperature is constrained to follow the liquid-vapor saturation curve for the pure-H<sub>2</sub>O system. For this reason, the code is limited to a single, fixed pressure for a given temperature, and a maximum pressure of 220 bars at the critical point of 374 °C (Roedder, 1984).

#### **2.11.5 Summary and Conclusions**

The equations governing the effect of pressure on chemical processes are presented and discussed. Liquids and solids are generally considered incompressible (no volume change) except at very high pressures. Gases are strongly affected by pressure, and the ideal gas law is used to describe gas behavior. An assumption of ideality is typically adequate at low pressures on the order of 1 atmosphere or less. Deviations from ideality are described using the empirical van der Waals equation. Pressure also influences reaction rate constants. At the gas pressures anticipated in the proposed repository, however,

these effects are minimal and an assumption of ideality is probably adequate. Pressure solution is discussed, but times and pressures of interest in the repository environment are significantly less than those for which pressure solution has been modeled.

## 2.12 CHEMICAL -> MECHANICAL

The chemical effects of water and other aqueous environments can play an important role in the deformation and strength of rocks. Certain chemical environments have long been known to enhance the propagation of fractures in rock. For example, Dunning et al. (1980), and Westwood (1974) have shown that the presence of aqueous chemical environments results in a measurable and sometimes substantial weakening in single crystals of quartz and other geological materials. Atkinson (1979a), Boozer et al. (1963), and Vutukuri (1974) have demonstrated that aqueous chemical environments also have a weakening effect on polycrystalline geologic materials. This weakening effect has been observed to be a result of the reduction in the surface free energy of the materials due to absorption of species from the chemical environments (Dunning et al., 1980). It has also been thought that the zeta potential (surface electrostatic potential) also plays a role in chemomechanical weakening.

### 2.12.1 Chemical Effects on Rock Fracture Propagation

The potential role of surface free energy in chemomechanical weakening can be observed from the Griffith energy balance theory of crack propagation, as shown below (Griffith, 1920).

$$U = (W_L + U_e) + U_s \quad (2-47)$$

where

- $W_L$  = work done to displace the outer boundary of the material (J),
- $U_e$  = stored elastic strain energy (J),
- $U_s$  = surface free energy (J), and
- $U$  = total energy of the system (J).

The crack system is said to be in equilibrium (i.e., neither being extended or closed) when  $dU/dc = 0$ , where  $c$  is the crack length. Lawn and Wilshaw (1975) showed that the critical stress ( $\sigma_c$ ) required to propagate the crack or flow is

$$\sigma_c = \left[ \frac{2E U_s}{(1 - \nu^2) \pi c} \right]^{1/2} \quad (2-48)$$

where

- $\nu$  = Poisson's ratio,
- $E$  = Young's modulus (N/m<sup>2</sup>), and
- $U_s$  = Surface free energy (J).

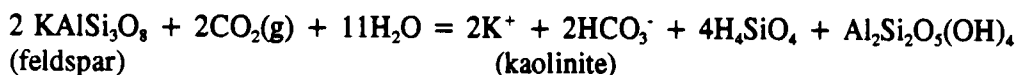
Equation (2-48) shows the dependency of the critical stress to the surface free energy. In other words, a reduction in the surface free energy would result in a reduction in the critical stress required to

propagate the crack. The role of the zeta potential has been found to be more complex in its impact on crack propagation.

Dunning et al. (1984) conducted laboratory experiments on the effects of various aqueous chemical environments on crack propagation in quartz. Figure 2-30 shows the results of their experiments. The figure shows that the crack propagation stresses for the natural quartz decrease sharply from an ambient atmospheric environment to one containing water (H<sub>2</sub>O). As the chemical environment becomes progressively more cationic, the crack propagation stresses are seen to further decrease as a result of adsorption of the chemical species into the rock. They also found that the surface free energy more closely correlated with crack propagation stress than the square of the crack propagation stress as indicated by Eq. 2-48. This apparent disparity with the Griffith energy balance concept could be due to the possibility that surface energy reduction is only one of several operating mechanisms of weakening.

### 2.12.2 Degradation of Mechanical Properties Due to Chemical Action

Mechanical properties of rock may be altered by chemical processes at the most basic level through dissolution/precipitation of minerals from solution or the replacement of one mineral by another during alteration (Helgeson, 1979; Stumm and Morgan, 1981; Henley et al., 1985; Murphy and Helgeson, 1987). An example of such a transformation is the hydrolysis of feldspars (minerals which make up 50 percent or more of the Topopah Spring tuff) to micas and clays such as muscovite and kaolinite. Although the dissolution of feldspar is incongruent, the overall alteration of feldspar to kaolinite in the presence of CO<sub>2</sub> can be written in the general form:



Mineral reactions of this type are commonly observed in geothermal systems and in hydrothermally altered rock associated with ore deposits, and as secondary products of surface weathering (Rose and Burt, 1979; Henley et al., 1985). Broxton et al. (1987) identified clay alteration assemblages of illite, smectite, and/or chlorite below Yucca Mountain in the Crater Flat Tuff. Bish (1986) used the illite/smectite transition to identify a greater than 10 million year paleohydrothermal system associated with the Timber Mountain Caldera. Based on illite/smectite chemistry, alteration temperatures were as low as 100 °C at the southern end of Yucca Mountain.

Alteration minerals such as clays and micas have different physical properties from the minerals in fresh rock. Alteration minerals like clays, especially swelling clays such as smectite, are weaker than feldspars and can have a pronounced effect in decreasing the strength of the rock. For tuffs in the Yucca Mountain vicinity, a general decrease in Young's Modulus is observed for rocks containing a significant clay (smectite) component (DOE, 1988). Friction coefficients for clay lined fractures are also generally less than those for fresh rock (DOE, 1988). Conversely, precipitation of silica (Rimstidt et al., 1989) can indurate rocks and increase rock strength.

Temperatures anticipated in association with the emplacement of high-level waste (Appendix A) are high enough for significant alteration (200 - 250 °C, see Figure A-2). In the absence of water, however, hydrolysis reactions will not occur. The drying out of the near-field due to waste emplacement can serve to reduce the extent of alteration. As discussed in Section 2.1, flow through fractures is possible, and clay alteration may occur along fracture surfaces.

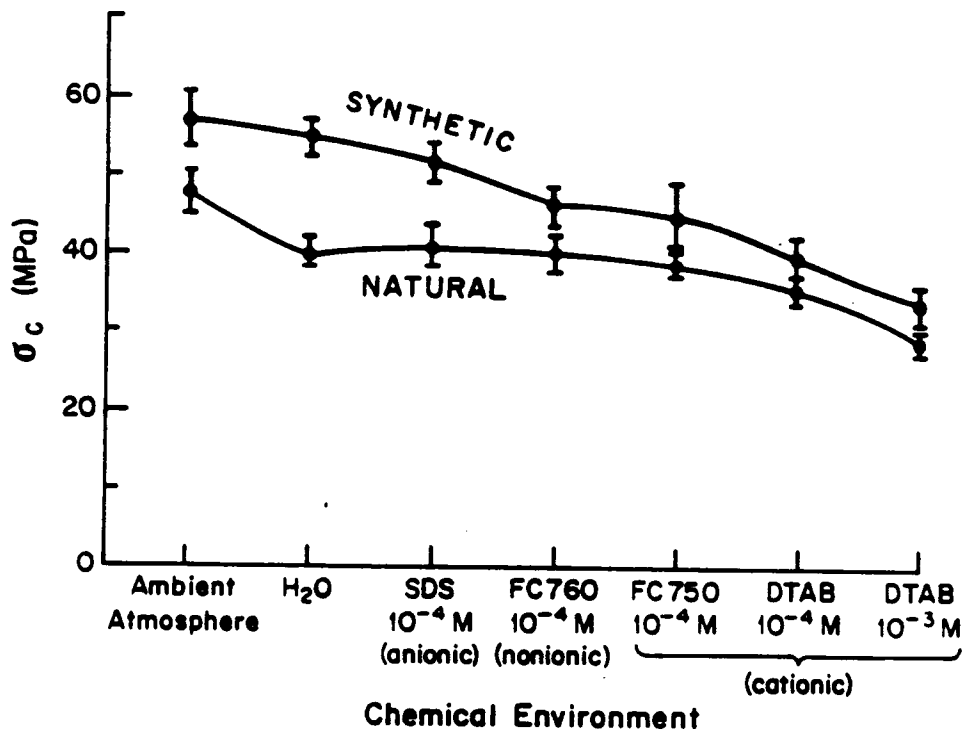


Figure 2-30. Crack Propagation Stress of Synthetic and Natural Quartz Samples Plotted Versus Chemical Environment (From Dunning et al., 1984)

### 2.12.3 Stress Corrosion Cracking

Stress corrosion cracking (SCC) has been discussed by Atkinson and Meredith (1987) for minerals and rocks as well as by others for glass, ceramics, and metals. The significance of SCC in geologic materials appears uncertain because of the wide range of variables encountered. For the engineered barrier system of a repository, however, SCC has been identified as a potentially important failure mechanism for waste packages (DOE, 1988).

Metals exposed to certain aqueous solutions while under a tensile stress may be subject to crack initiation and propagation leading to premature failure through a process called stress corrosion cracking. Once initiated, SCC can occur fairly quickly, with crack velocities ranging from  $10^{-12}$  to  $10^{-3}$  m/s (Macdonald and Cragolino, 1989). Two different modes of cracking occur; transgranular cracks run across the grain, and intergranular cracks propagate along grain boundaries. As discussed by Jones and Ricker (1987), SCC mechanisms include, among others: (i) pre-existing active-path mechanisms, (ii) absorption-related mechanisms, and (iii) strain-assisted active-path mechanisms. Intergranular SCC along reactive grain boundaries is an example of the first type. Reduction of  $H^+$  ions to adsorbed hydrogen atoms, followed by incorporation of atomic hydrogen into the metal lattice and the resultant embrittlement of the metal, is an example of type (ii). As an example of strain-assisted, active-path SCC, transgranular SCC proceeds as a series of steps that involve the rupture of a protective passive film by straining, anodic localized dissolution of the metal at the crack tip, and repassivation of the crack walls.

The rate and extent of SCC depends on the alloy being considered, the amount of stress involved, and the chemical environment in which the metal is placed. Stresses can be provided either through external means such as bending, or be due to residual internal stresses resulting from manufacture, forming, and machining of the metal. As in many alloy/environment systems, the time to failure for several stainless steels in boiling concentrated  $MgCl_2$  brines (42 percent  $MgCl_2$  at  $154^\circ C$ ) increases with decreasing applied stress (Figure 2-31). For each steel there exists a threshold value, ranging from 10 to 100 percent of the 0.2 percent yield strength, below which SCC does not occur. Crack growth rates can be expressed in terms of a stress intensity factor,  $K_I$ , which is proportional to the applied stress and to the square root of the crack length (Figure 2-32). For low values, crack growth rate is dependent on  $K_I$ . At high values, crack propagation rate is independent of  $K_I$ . The upper limit is the critical value,  $K_{IC}$ , where crack growth due to mechanical overloading is observed in inert environments (Macdonald and Cragolino, 1989). Below  $K_{IC}$  is considered to be the region of stress corrosion cracking or subcritical crack growth. For stainless steels exposed at  $250^\circ C$  to a simulated boiling water reactor (BWR) environment (Figure 2-32), as well as for many other alloy/environment systems, a threshold stress intensity factor ( $K_{ISCC}$ ) exists, below which crack growth is exceedingly slow ( $< 10^{-11}$  m/s).

As can be seen from Figure 2-31, the resistance to SCC in a given environment is dependent on the specific alloy being considered. Figure 2-33 shows the effect of nickel content on the susceptibility to SCC of Fe-Cr-Ni alloys exposed to a boiling  $MgCl_2$  solution. For a constant applied stress, there is a significant decrease in failure time due to SCC for Ni-contents between about 5 and 30 percent. Above about 40 percent nickel, failure did not occur in 30 days. Farmer et al. (1988a,b) provided extensive surveys of SCC in steels and copper-based alloys. As pointed out by Macdonald and Cragolino (1989), even small amounts of impurities or variations in alloy composition may result in significant differences in SCC susceptibility. Segregation of impurities, such as tin, phosphorous, and arsenic, during heat treatment may serve to enhance intergranular SCC of low-alloy steels. Surface condition also affects a

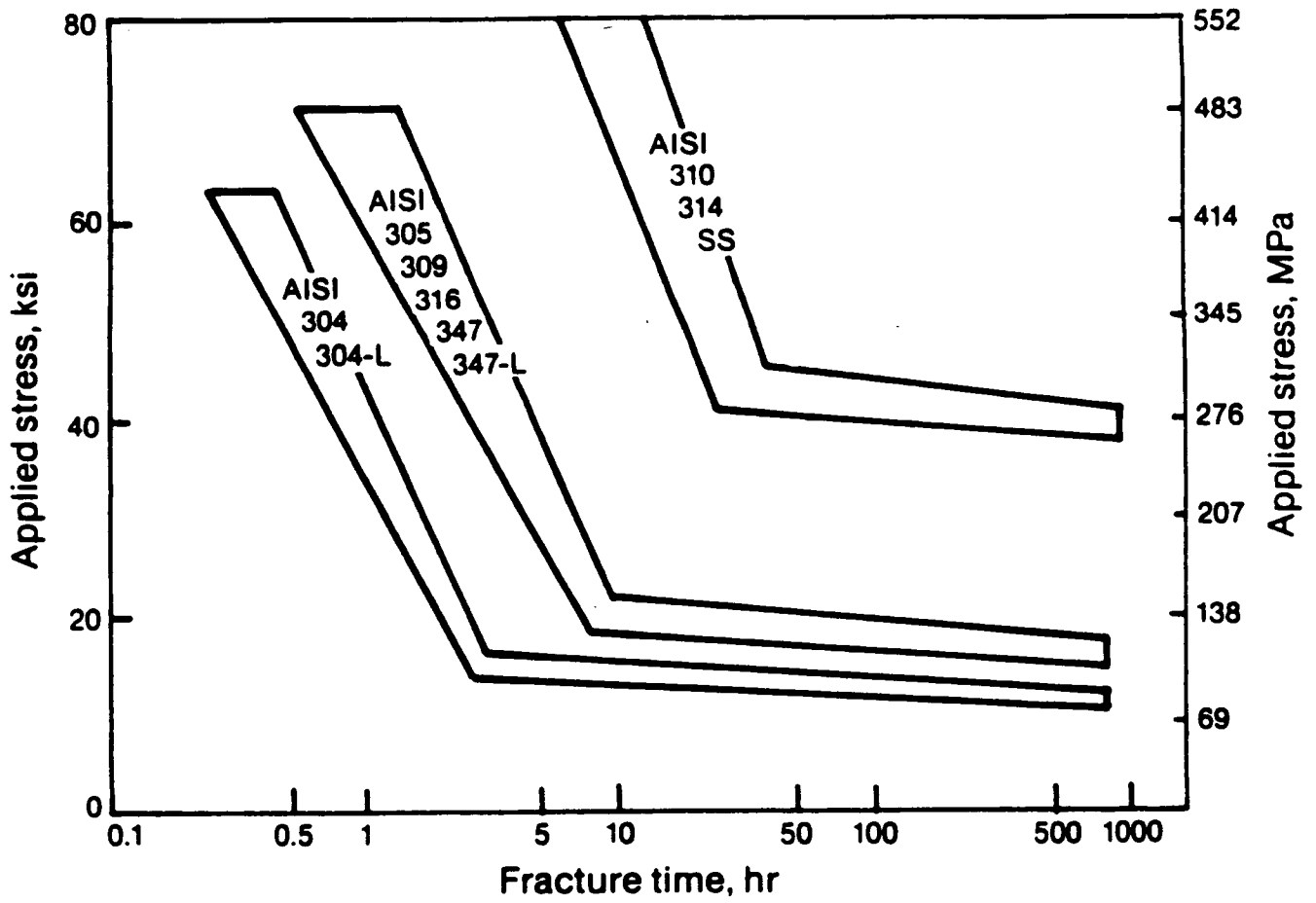


Figure 2-31. Resistance to SCC as a Function of Applied Stress. Metals are Commercial Stainless Steel in Boiling 42% MgCL<sub>2</sub> at 154 °C (after Fontana and Greene, 1978)

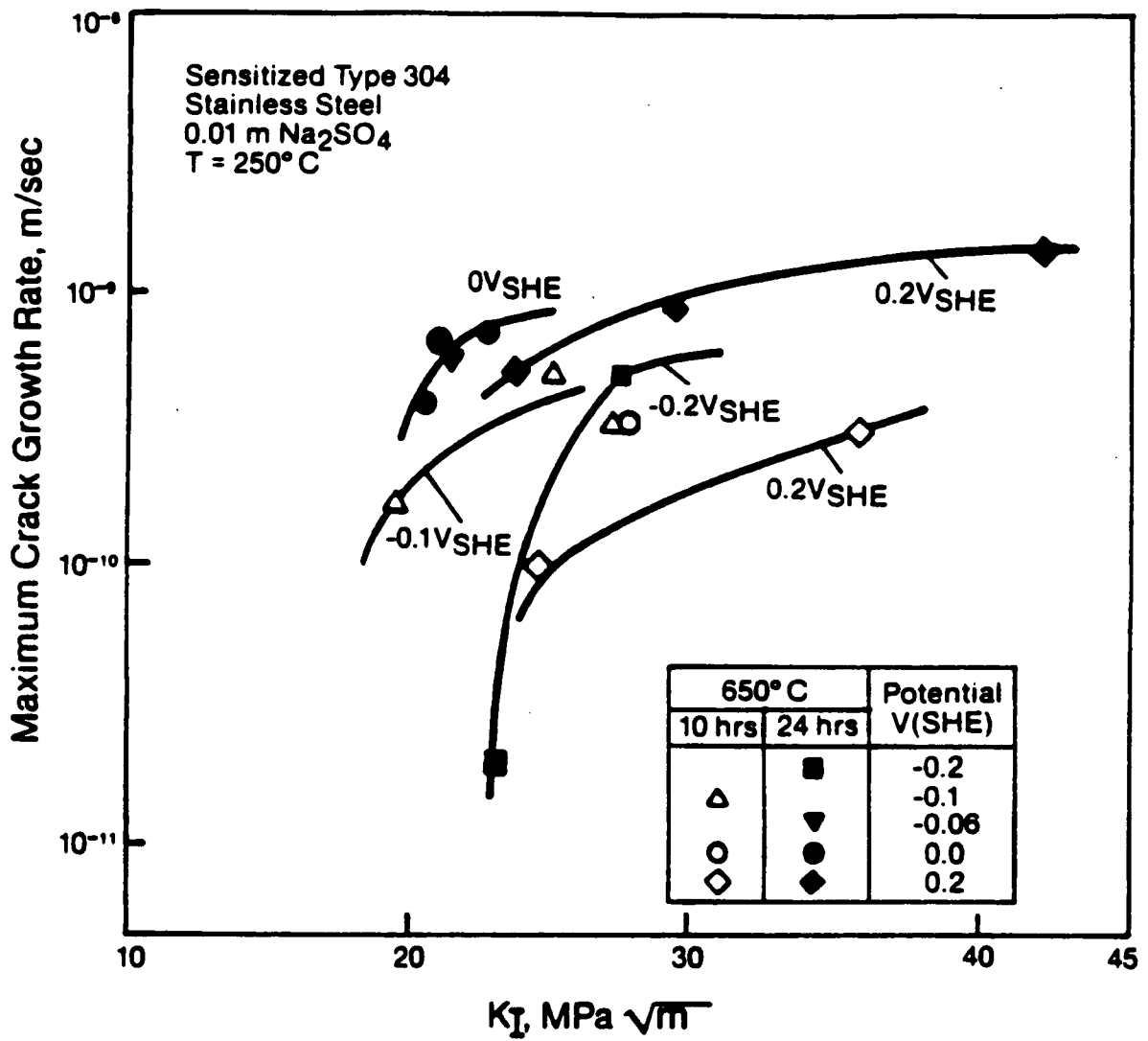


Figure 2-32. Crack Growth Rate (m/s) as a Function of Stress Intensity (MPa m<sup>1/2</sup>) for Type 304 Stainless Steel (after Chung et al., 1985)

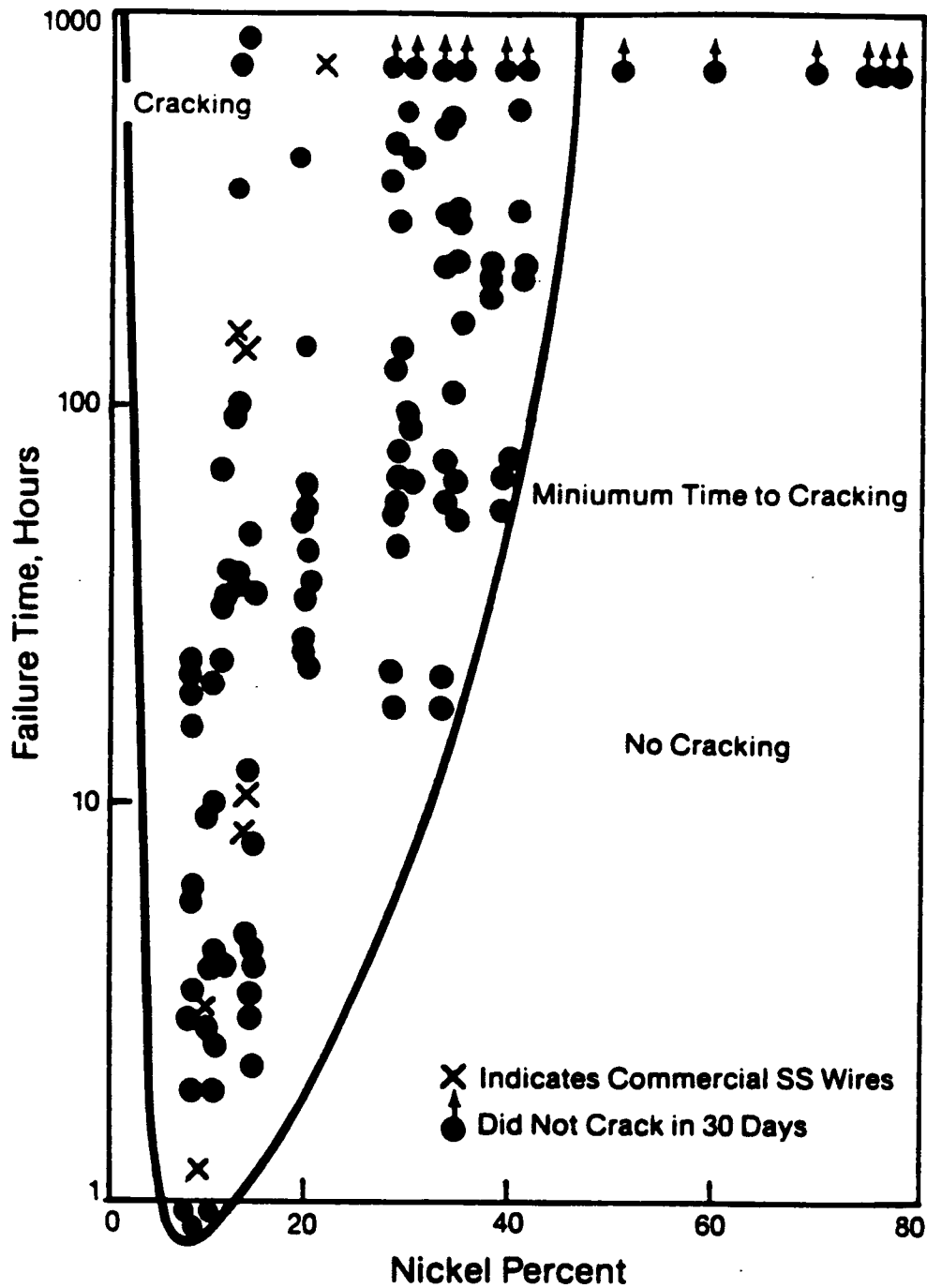


Figure 2-33. Susceptibility of Fe-18Cr-xNi Alloys to SCC in Boiling 42% MgCl<sub>2</sub> as a Function of Nickel Content (after Copson, 1959)

metal's resistance to SCC. Scoring and grooves provide focus points for local enhanced stress, facilitating the initiation of SCC.

The chemical environment also controls susceptibility to SCC. Anodic dissolution at the crack tip is enhanced by the anion content of the solution. Cracking rates for stainless steel tend to increase with increasing chloride and oxygen contents of water (Farmer et al., 1988a). For SCC mechanisms (i) and (iii), crack growth rates are proportional to the anodic current density on a strained metal surface. In some cases, the metallic cation in solution is an indirect factor influencing cracking. Farmer et al. (1988a) noted that  $Mg^{2+}$  is most aggressive in attacking Type 304 stainless steel in water containing 100 ppm  $Cl^-$  at 100 °C, while  $Na^+$  is the least aggressive. This is probably due to the fact that readily hydrolyzable cations such as  $Mg^{2+}$  produce greater amounts of  $H^+$  (and lower pH) through hydrolysis than poorly hydrolyzed cations such as  $Na^+$ . The presence of species such as  $H_2S$  in the solution enhances cracking due to hydrogen embrittlement [mechanism (ii)]. Macdonald and Cragolino (1989) noted that the electric potential difference established at the metal/water interface is the critical electrochemical factor controlling SCC. Below and above a certain potential range, which varies with metal/solution system type, repassivation of the metal occurs so rapidly that cracks growth through dissolution is inhibited in the case of mechanisms (i) and (iii).

Stress corrosion cracking is dependent on a tensile stress being applied to the metal. In the repository environment, it seems likely that most of the macroscopic stress applied to waste canisters and metal components in the repository will be compressive. However, residual stresses from metal forming and tempering may provide the necessary tensile stress. Bending of metal components in response to compression produces tension on the outside of the bend.

#### **2.12.4 Summary and Conclusions**

The effect of chemical processes on mechanical processes has been discussed in this section. It has been noted that the crack propagation stress for a fracture under either shear or tensile stresses can be substantially reduced depending on the chemical environment under which it exists. The section also discussed chemical processes in which certain minerals within the rock will be altered (e.g., alteration of feldspar to kaolinite). Such alteration of minerals can significantly lower the strength of the rock. However, due to the partially saturated nature of the Yucca Mountain site and the drying out of the rock in the near-field due to waste emplacement, chemical processes may not likely become important on the mechanical state of the rock mass until well into the containment and isolation periods. Stress corrosion cracking is also discussed. Because stress corrosion cracking (SCC) is difficult to predict, and because the exact conditions anticipated at Yucca Mountain are imperfectly understood, much effort is currently under way to study SCC under likely repository conditions (DOE, 1988).

### 3 THREE-WAY COUPLED PROCESSES

In this section, three-way couplings are considered. In total, four three-way couplings can be considered: {TMH, THC, TMC, MHC}. In Section 2, one-way coupling mechanisms have been discussed, hence this chapter primarily synthesizes the results of Section 2. As a matter of presentation, the discussion in Section 2 has concentrated on possible coupling mechanisms while this chapter concentrates on probable (or important) couplings. In addition, computer programs are emphasized in this chapter primarily out of necessity because the problems are complicated.

Because the material in this section is a synthesis of material in Section 2, and because certain couplings are more important than others, only two three-way couplings are explicitly discussed in this section: {THM, THC}. The TMC and HMC couplings have not received as much discussion in the literature. An assessment of the importance of different couplings is included in Section 4 of this report.

#### 3.1 THERMAL-HYDROLOGIC-MECHANICAL COUPLING

The one-way couplings (i.e.,  $T \rightarrow M$ ,  $H \rightarrow M$ ) discussed in Section 2.0 become further complicated when one considers the coupling between any three processes. Modeling these three-way couplings is made difficult by the fact that there is inexact knowledge of the couplings and governing equations. During radioactive decay of the high-level waste, the resulting temperature field will generate thermal stresses which produce normal and shear displacements of the fractures and compression or tension within the matrix. Heating of the groundwater in the vicinity of the repository produces vaporization, vapor flow, condensation, or condensate flow, and hence the coupled system becomes one involving thermal, hydrological, and mechanical interactions (THM). An example of THM coupling is the effect of changing temperature and pore fluid pressure on mechanical changes of the rock fractures, such as those observed in hot dry rock experiments (Tsang, 1991).

The fundamental laws governing static equilibrium, fluid flow, and heat flow are coupled through the dependent variables of the solid displacement vector, fluid pressure, and medium temperature (Biot, 1941). These laws, in conjunction with constitutive equations, provide the approximate mathematical model of the coupled quasilinear, thermal-hydraulic-mechanical phenomena in saturated porous elastic media. Additional extensions to the theory are necessary to simulate phenomena in porous fractured rocks, and partially saturated rock.

The complexity of the thermal-hydrologic-mechanical equations is such that an analytic (mathematical) solution for even simple initial- and boundary-value problems is not likely to be found. However, numerical solutions can be sought, if the mathematical model is good. Various numerical schemes using well-known numerical techniques such as finite-element and finite-difference have been developed for THM modeling, and are discussed later in this section. Most of the computer codes for modeling coupled THM processes are only partially verified against existing analytical solutions for two-way couplings such as hydromechanical, thermomechanical, and hydrothermal problems. Also, in some computer codes the coupled equations are directly solved, whereas in other programs the THM coupling occurs in the solution process. For example, the solution process may involve running the thermal analysis out to some period of time, and then feeding the resulting temperatures into the mechanical routine to update the thermally induced stresses. Finally, the changes in the mechanical state will be used to update the hydrologic state.

### 3.1.1 DECOVALEX International Project

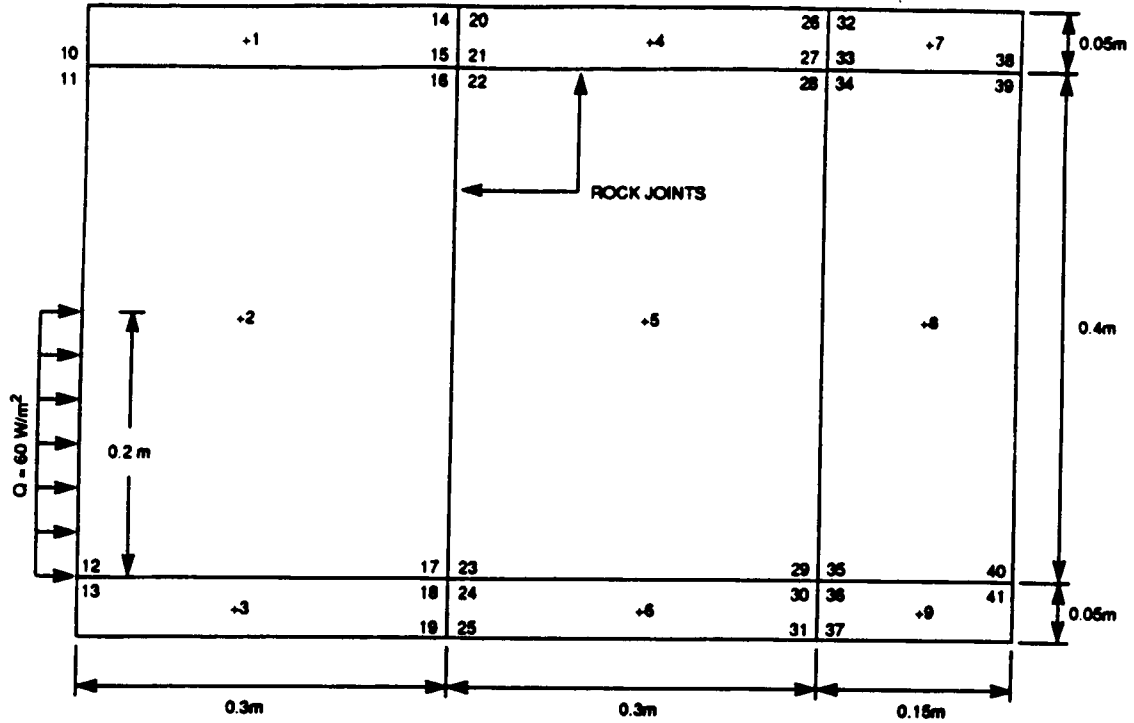
An international project titled DECOVALEX (DEvelopment of COupled models and their VALidation against EXperiments in nuclear waste isolation) was begun in 1990 to increase the understanding of various thermal-hydrological-mechanical processes of importance for radionuclide release and transport from a repository to the biosphere and how they can be described by mathematical models. The main objectives of DECOVALEX are:

- to support the development of codes for thermohydrromechanical (THM) modeling for jointed rocks;
- to investigate and to apply suitable algorithms for THM modeling;
- to investigate the capabilities of different codes to describe laboratory experiments and to perform verification of codes;
- to compare theory and model calculations with experiments;
- to design validation experiments by means of THM model studies.

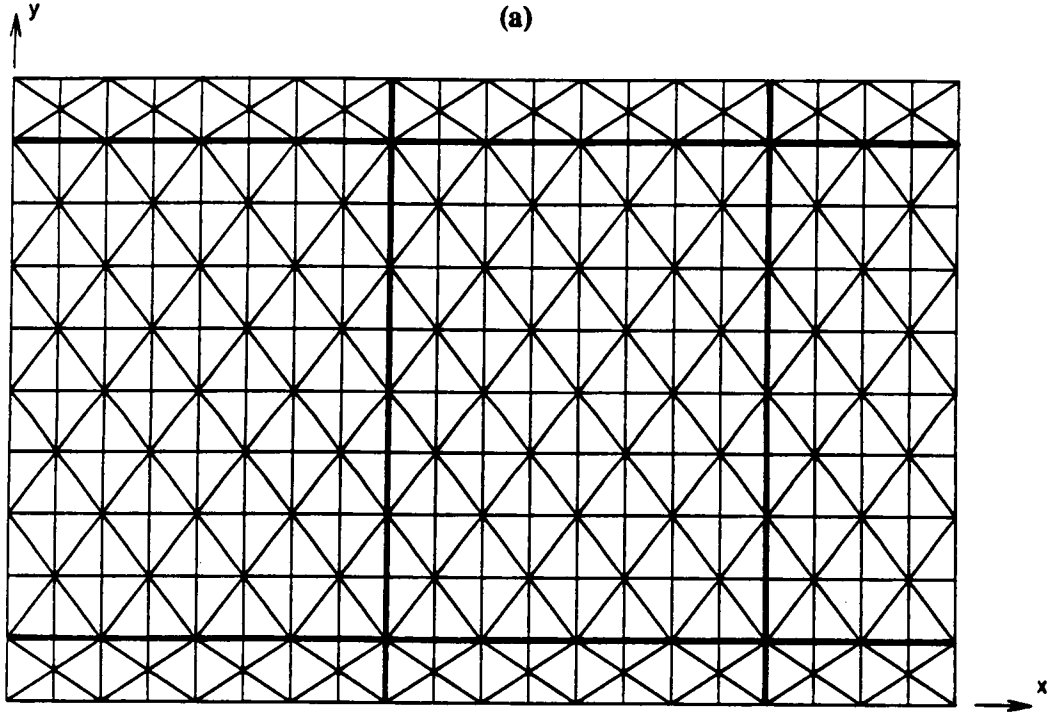
During the first phase of DECOVALEX, a series of bench-mark and test case problems have been designed to validate computer codes against each other as well as experimental data. One problem that has been used as a bench-mark problem for DECOVALEX is shown in Figure 3-1(a). This bench-mark test consisted of an assemblage of nine blocks, separated by two sets of planar fractures, one set being horizontal and the other vertical. The dimensions and locations of monitoring points are shown in Figure 3-1(a). The rock was subjected to *in situ* compressive stresses of 4.0 MPa in both the horizontal and vertical directions. The mechanical boundary conditions consisted of zero normal displacements around the four edges of the model (i.e., boundaries were rollered). The rock matrix was assumed to be linear elastic, while the joint constitutive relations followed the Coulomb-Friction model.

The hydraulic boundary conditions consisted of a fixed pressure of 10.0 kPa on the left model boundary and a fixed pressure of 11.0 kPa along the right model boundary. Both the top and bottom boundaries were assumed to be impermeable. The initial fluid pressure through the model was specified to be 10.0 kPa, and initial aperture for the joints under the *in situ* conditions was specified as 300 microns. For the thermal analyses, an initial temperature distribution of 15 °C was assumed. A constant flux of 60 W/m<sup>2</sup> was applied to the lower left model boundary over a length of 0.2 m as shown in Figure 3-1(a). All other portions of the model boundary were assumed to be adiabatic.

Figure 3-1(b) shows the blocks discretized into finite difference triangles for use by the computer code UDEC for this bench-mark problem. Since UDEC is based on the discrete element method, the fractures as shown in Figure 3-1(a) are explicitly incorporated in the analysis. Thus, the blocks are allowed to slide relative to one another, rotate, as well as deform elastically. Figure 3-2(a) shows the temperature contours obtained from UDEC after steady-state conditions have been achieved. For this particular problem, the specified heat flux resulted in a maximum temperature rise of approximately 6.2 °C as seen along the left edge of the model as shown in Figure 3-2(a) (Ahola et al., 1992). The thermal expansion accompanying this temperature rise resulted in a slight increase in the mechanical stress state as well as a decrease in apertures up to 18 microns along portions of the vertical

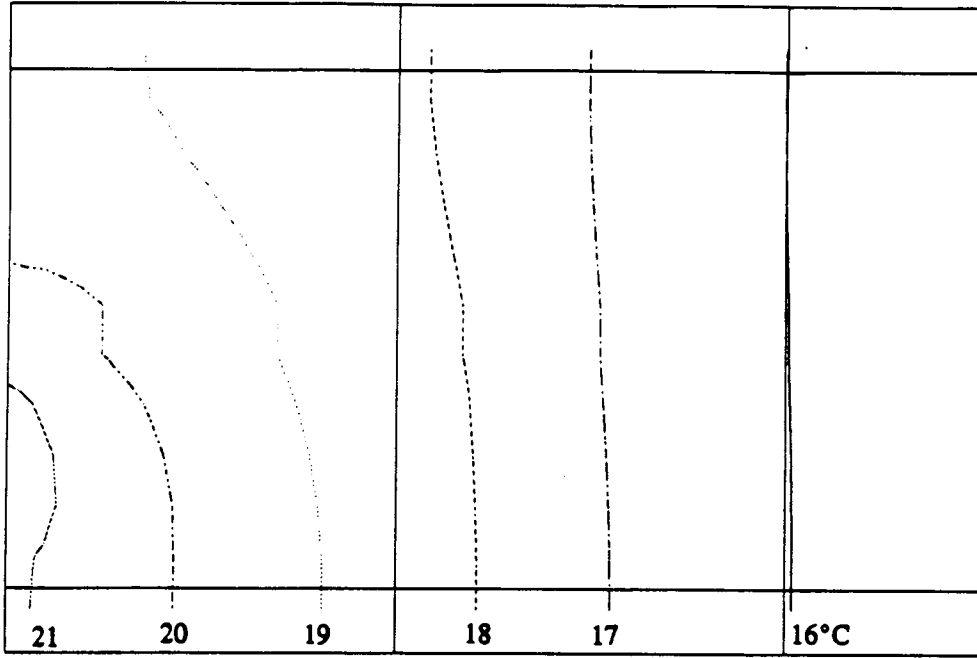


(a)

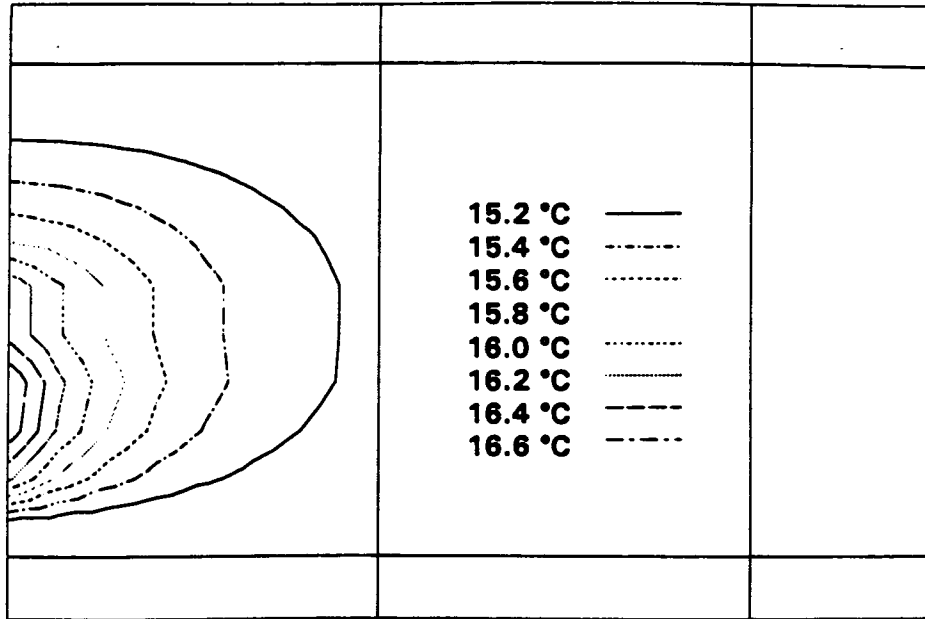


(b)

Figure 3-1. Coupled Thermal-Hydrologic-Mechanical (THM) Bench-Mark Problem for DECOVALEX. (a) Block Geometry Showing Location of Monitoring Points and Applied Heat Flux. (b) Zone Discretization for Discrete Element Code UDEC.



(a)



(b)

**Figure 3-2. Coupled THM Bench-Mark Problem for DECOVALEX. (a) Temperature Contours Assuming Only Conduction Heat Transfer through the Rock Medium. (b) Temperature Contours Taking into Account Conduction as well as the Effect of Forced Convection through the Horizontal Fractures.**

and horizontal joints. Even so, fluid flow still remained primarily in the horizontal fractures as a result of the large initial hydraulic aperture and negligible buoyancy effects. The UDEC code does not have the capability to model flow within the matrix, nor thermal-hydrologic coupling. Thus, the impact of forced convection within the fractures was neglected in Figure 3-2(a). Based on engineering estimates of the effect of forced convection within the fractures, a case was run in which the gridpoints along horizontal fractures were fixed at 15 °C. Figure 3-2(b) shows the resulting temperature contours which represent more closely the true solution with only a maximum temperature rise of approximately 2 °C. For this particular problem, it was found that the effect of the H -> T coupling was of importance mainly due to the large aperture and flow rates. Had the aperture been smaller or the rock matrix and fractures partially saturated as at Yucca Mountain, the hydrologic impact on the temperature field would have been negligible. A maximum temperature rise of approximately 2 °C was also obtained with the finite-element computer code MOTIF. The MOTIF code simulated flow within the fractures and matrix as well as conductive and convective heat transfer.

### 3.1.2 Computer Codes for THM Modeling

#### 3.1.2.1 ROCMAS

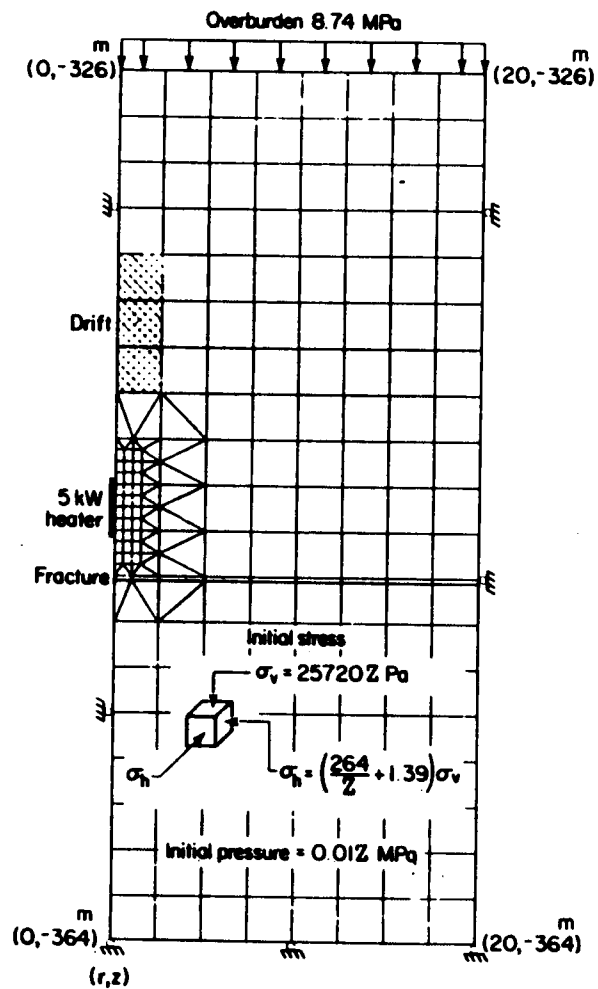
ROCMAS (ROC Mass Analysis Scheme) is a finite element code which is used to investigate coupled thermal-hydraulic-mechanical behavior of liquid-saturated, fractured porous rocks (Noorishad et al., 1984; Noorishad and Tsang, 1989). The time integration is performed by a predictor-corrector method and the final coupled matrix formulation is solved implicitly. A tri-linear law defines the closure behavior of the fractures and an ideal elastic-plastic law models its shear behavior. Peak shear strength is obtained from a Coulomb criterion.

The ROCMAS code has been used to simulate the thermohydrromechanical environment around a waste canister, or heater (Noorishad et al., 1984). The objective was to study the changes of fluid inflow to a heater borehole induced by the temperature rise. Figure 3-3(a) shows the 2D axisymmetric finite element mesh which includes a horizontal fracture intersecting the bottom of the emplacement borehole. The fracture is assumed fully saturated, and extends out to a hydrostatic boundary at the edge of the mesh.

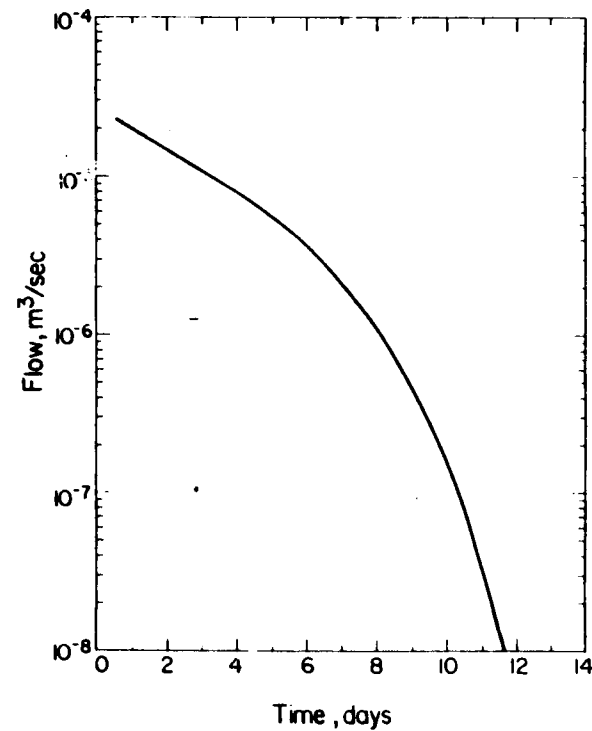
Figure 3-3(b) shows the variation of fluid inflow to the heater borehole as a function of time. Before the heater raises the temperature of a large volume of the rock, the flow from the hydrostatic outer boundary to the borehole at atmospheric pressure is high. Later in time, with the heated rock above the fracture expanding and the fracture aperture near the heater borehole closing, the flow decreases sharply. Figure 3-4 shows the evolution of the fracture aperture profile, together with the variations of the pressure and temperature distributions. The pressure at 0 days represents the full hydrostatic pressure in the fracture before excavating the emplacement hole. The pressure diminishes rapidly after excavation and before major development of the thermal front. As thermal stresses are generated causing closure of the fracture, the pressure again rises. After approximately 14 days, the pressure in the fracture again reaches its full hydrostatic value.

#### 3.1.2.2 GENASYS

GENASYS (Geotechnical Engineering Analysis System) is a two- and three-dimensional hybrid boundary-element finite-element code for computing the coupled fracture flow, heat flow, and



(a)



(b)

Figure 3-3. Coupled Thermal-Hydrologic-Mechanical Analyses Using ROCMAS Showing (a) Finite Element Model of the Source Environment and (b) Variation of Fluid Inflow to the Heater Borehole as a Function of Time after Heater is Turned on. (From Noorishad et al., 1984)

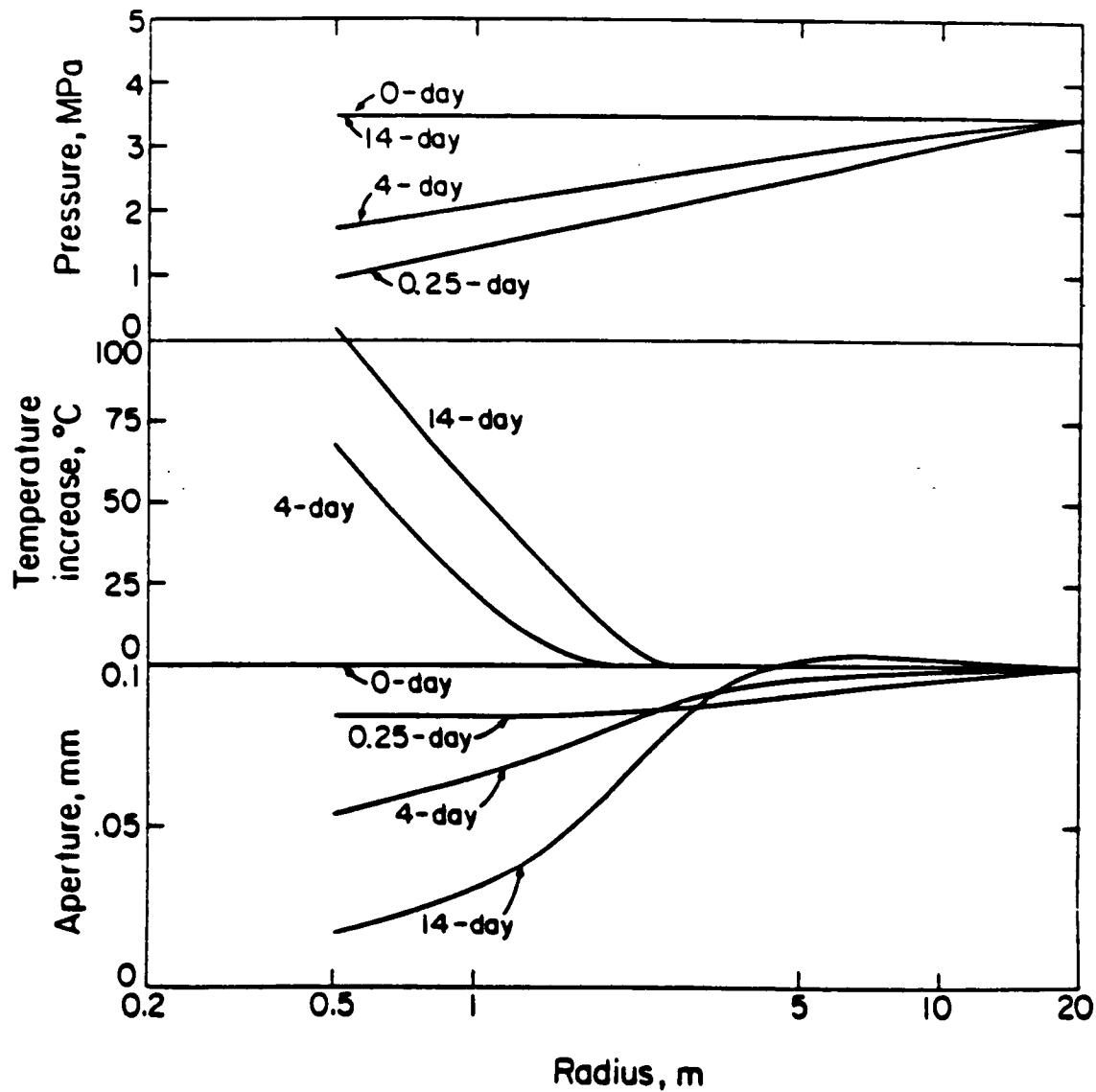


Figure 3-4. Pressure and Aperture Profiles in the Fracture Generated by ROCMAS for Various Durations, and Temperature Profiles along Heater Midplane (from Noorishad et al. 1984)

deformation response of fractured rock masses (Wijesinghe, 1989). In GENASYS the fractures in the rock mass are represented as one or more discrete curved surfaces. The fracture surfaces can have any arbitrary shape and orientation, and can intersect to form a fracture network. The far-field response is treated primarily linearly and nonlinearities are concentrated along fracture surfaces. The hybrid boundary-element finite-element approach keeps the computational problem at the manageable level.

### 3.1.2.3 THAMES

THAMES 2D and 3D (Thermal, Hydraulic And MEchanical System analysis), (Ohnishi et al., 1990) is a three dimensional finite element code developed to perform analysis of fully coupled thermal, hydraulic and mechanical behavior of saturated and partially saturated geologic media. The mathematical formulation of the model utilizes the Biot's theory of consolidation, with the Duhamel-Neuman form of Hook's law and the energy balance equation. Fully coupled thermal, hydraulic, and mechanical processes are analyzed and the coupled equations are solved simultaneously. Nonlinear heat conductivity, specific heat, and thermal expansion may be used in the computation. Stress dependent fracture permeability of rocks and permeability as a function of void ratio of soils may also be incorporated into the analysis. THAMES 3D models an elastic medium and is unable to simulate phase change of water. A one dimensional consolidation test has been used to verify the hydromechanical behavior of the code. Thermal stresses induced in a thick walled cylinder with a constant temperature gradient have been used to test the mechanical-thermal behavior. Heat transfer in moving groundwater has been the third problem for THAMES 3D verification. This is the only method for verification since fully coupled THM processes are not solved analytically at present. Calculations of a synthetic deep nuclear waste repository have been performed using the two-, and three-dimensional versions of THAMES (Ohnishi et al., 1990).

### 3.1.2.4 FEHMS

FEHMS (Finite Element Heat Mass Stress) was developed for solving coupled, and nonlinear, fluid flow-heat transfer-solid deformation problems in porous, fractured, geological media (Kelkar and Zvyoloski, 1991). The code uses an implicit time-differencing scheme, which allows for larger time steps several orders of magnitude larger than those expected for explicit schemes. The code is capable of fully three-dimensional simulations.

## 3.1.3 Summary and Conclusions

In this section, the three-way coupling between thermal, hydrologic, and mechanical processes has been discussed. Much of the literature related to these three processes has been primarily numerical studies, with the computer codes being verified against available analytic solutions for the various possible two-way couplings. Due to the lack of analytic solutions for three-way couplings, laboratory and field studies are recommended for validating computer codes. Cooperative international projects, such as DECOVALEX, are important in providing the necessary database of experimental studies.

## 3.2 THERMAL-HYDROLOGIC-CHEMICAL COUPLING

As discussed in Section 2, each of the four processes being considered (thermal, hydrologic, mechanical and chemical), are involved in a series of two-way couplings. The relative importance of each of these couplings varies, as does the degree to which the effects involved are understood.

Many of the equations necessary for the modeling of the various two-way couplings have been presented in Section 2. However, three-way coupling between these processes is much less well-understood. As a result, there is relatively little available in the way of computer codes for modeling the interaction between more than two processes. With respect to nonlinear chemical processes, an iterative approach to coupling offers the best chance of success for numerical predictions in the proposed repository system (Yeh and Tripathi, 1989). The discussion presented in this section is limited to presenting phenomena either postulated or observed. The occurrence of many of these in a natural environment awaits confirmation in many cases.

In a discussion of the effect of coupled processes on solute transport in the near-field, Jamet et al. (1990) characterized coupling as being of two types. The first type involves those phenomena that result from the effects of coupling on material properties for the solid, fluid, and gas phases (e.g., density, viscosity, vapor pressure). This can also include those couplings that can affect properties of the medium of interest (e.g., permeability, porosity). The second type includes those effects that appear in the relevant equations, which have been referred to as *Onsager's coupled processes* (Carnahan, 1984a,b; 1987a). While Onsager's processes include many possible effects, Jamet et al. (1990) indicated that only a few have a nonnegligible effect on solute transport. Those that involve coupling between thermal, hydrologic, and chemical processes are discussed in this section.

### 3.2.1 Effects of Coupling on Material Properties and Media Characteristics

The porosity and permeability of a given medium may be enhanced by the dissolution of the minerals that make up the matrix of the medium. An extreme example of this type of porosity enhancement is the dissolution of limestones in karst terrain to produce sinkholes and caves. Conversely, precipitation may serve to plug available porosity, reducing permeability (Section 2.10). As discussed in Section 2.5, mineral solubility is strongly dependent on the pressure and temperature of the system of interest. Many common minerals such as quartz, fluorite, anhydrite, and metal sulfides exhibit a prograde solubility such that precipitation (i.e., decreasing solubility) is favored with decreasing temperature (Holland and Malinin, 1979; Cathles, 1983). Silica scale in geothermal wells is due in large part to the cooling and/or boiling of silica supersaturated fluids as they rise to the surface (Cline et al., 1992). In contrast, at a given constant pH and  $p(\text{CO}_2)$ , carbonates such as calcite and dolomite tend to precipitate from solution with increasing temperature. This is known as retrograde solubility, and is in evidence as the carbonate scaling in hot water heaters. Precipitation and dissolution may also be controlled by kinetic processes. For example, while calcite precipitates readily, silica precipitation is kinetically controlled in geothermal systems and may not occur for some time after saturation has been reached (Cathles, 1983; Thomas and Gudmundsson, 1989).

The effect of temperature is only one control on mineral solubility; other critical parameters include solution pH,  $p(\text{CO}_2)$ ,  $p(\text{O}_2)$ , and salinity (Thomas and Gudmundsson, 1989; Murphy, 1990). For example, boiling of a solution through pressure release will preferentially fractionate dissolved  $\text{CO}_2$  from the liquid ( $\text{CO}_{2(\text{aq})}$ ) to the vapor phase ( $\text{CO}_{2(\text{g})}$ ) and calcite will precipitate (Thomas and Gudmundsson, 1989). The amount of calcite deposited will vary depending on the composition and temperature of the solution. More calcite will be deposited in response to  $\text{CO}_{2(\text{g})}$  release at lower temperature. In addition, more calcite will precipitate with increasing ionic strength (Holland and Malinin, 1979). In geothermal systems, boiling can also oxidize sulfide minerals and  $\text{H}_2\text{S}$  in solution, leading to the formation of acid-sulfate waters. Waters under these conditions exhibit low pH (< 1 to 3), which leads to the hydrolysis and dissolution of common rock-forming minerals such as feldspars, and the formation of clay minerals

such as kaolinite (Rose and Burt, 1979; Henley et al., 1985). Boiling of the fluid associated with the emplacement of HLW can result in fractionation of CO<sub>2</sub> to the gas phase, leading to significant variations in pH for the coexisting groundwater, affecting aqueous speciation and mineral solubility (Murphy, 1990).

Given the temperature dependent solubility of different minerals, it is possible that solutions (both liquid and gas phase) moving by thermally-driven convection will redistribute chemical components such as silica and calcite. This type of redistribution has been observed in laboratory heater experiments with Yucca Mountain tuff under partially saturated conditions (Rimstidt et al., 1989). Silica and iron dissolved near the heater, were transported in solution and precipitated as amorphous silica, iron hydroxides, clay, and zeolite at the cooled end of the system. In the nonisothermal transient experiments of Lin and Daily (1990) on samples of the Topopah Spring tuff, permeability was progressively reduced by three orders of magnitude from  $1.3 \times 10^{-14}$  m<sup>2</sup> to about  $10^{-17}$  m<sup>2</sup> due to narrowing of fracture aperture by silica deposition. Experiments of Vaughan (1987) using granite cores indicated that although porosity was reduced by a relatively small amount, permeability was reduced by over 95 percent.

Numerical simulations have also been used to predict the redistribution of silica and calcite. Using a modified version of the TRACR3D code (Section 2.9), Travis and Nuttall (1987) suggested that reduced permeability due to quartz reprecipitation may enhance waste isolation. In contrast, Verma and Pruess (1988) used the code MULKOM (Pruess, 1983) to model equilibrium silica precipitation and dissolution, and determined that the amount of silica redistribution in a hydrologically saturated fractured medium did not have a significant effect on near-field temperatures, pore pressures or fluid flow. Simulations of <sup>14</sup>C transport in partially saturated rock (Codell and Murphy, 1992) indicate that after an early initial release of <sup>14</sup>C to the gas phase, calcite will precipitate and will serve to sequester <sup>14</sup>C at longer times.

Mineral precipitation and dissolution can also affect the retardation of radionuclide migration due to introduction and/or removal of sorptive minerals (Turner, 1991). Minerals such as zeolites, clays, and oxides can be dissolved and reprecipitated, depending on temperature and fluid chemistry. In addition, removal of radionuclides from solution, either due to the precipitation of stoichiometric radioelement compounds or coprecipitation as an impurity in other minerals, is also affected by the temperature (and chemistry) of the solution. By machining circular flow channels into granite blocks, Walton et al. (1985) constructed thermal-convection loops to study the effects of heat and mass transport on radionuclide migration. A 40 °C temperature gradient was applied across the system. Several radionuclides (<sup>125</sup>Sb, <sup>60</sup>Co, and <sup>54</sup>Mn) were concentrated at the hot side of the experiment, probably by sorption on iron oxyhydroxides. <sup>144</sup>Ce and <sup>99</sup>Tc were present in elevated concentrations on the cold side of the apparatus.

Because many common minerals exhibit prograde solubility, higher temperatures, particularly in the near-field environment, allow kinetic barriers to be overcome and result in a greater ionic strength for the groundwater. This tends to collapse the electrostatic double layer formed around electrically charged particles such as colloids (McDowell-Boyer et al., 1986). This reduces electrostatic repulsion, and promotes particle attachment and aggregation. This in turn will reduce colloid transport of radionuclides.

### 3.2.2 Onsager's Coupled Processes

Carnahan (1984a, 1987a) identified six possible components of solute flux due to temperature, pressure, and chemical gradients (Table 3-1). With regard to coupling thermal, hydrologic, and chemical processes, these can be divided into two major categories; solute transport associated with volume flux (advection) and solute movement relative to fluid motion (diffusion). Transport associated with volume flux is divided into three fluxes: thermal osmosis (temperature gradient), advection according to Darcy's Law (pressure gradient), and chemical osmosis (chemical gradient). Three additional fluxes of the second type include thermal or Soret diffusion in response to the temperature gradient, ultrafiltration or reverse osmosis in response to pressure gradients, and mass diffusion according to Fick's Law in response to concentration gradients.

In one-dimensional simulations of transport a single ideal solute across a one-meter column of saturated clay, Carnahan (1984a) has reported that when processes are coupled, the water flux due to thermal osmosis can exceed the Darcy flux by as much as three orders of magnitude when subjected to a temperature gradient of 2 °C/m. For compacted clays and a temperature gradient of about 20 °C/m, water flux due to thermal osmosis can reach 10<sup>-8</sup> m/s (Jamet et al., 1990).

The equations describing advection, the movement of fluid in response to pressure gradients, have been presented in Appendix B. Chemical osmosis, the movement of water in response to concentration gradients, has also been suggested by Carnahan (1984a) as a major factor in fluid flux. Numerical simulations indicate that water flux in clays from less to more concentrated zones can be as much as 3 to 4 orders of magnitude greater than Darcy's flux. This is counterbalanced by the flux of solute back across the membrane by pressure gradients (ultrafiltration/reverse osmosis). In coupled systems, Carnahan indicates that reverse osmosis is of minor significance compared to chemical osmosis.

Once the fluid has moved in response to the system gradients, solute can also move in and out of the fluid parcel. Thermal or Soret diffusion involves the movement of solute in response to the temperature gradient. In an isothermal, isobaric system (solution, solid, or gas) initially at chemical equilibrium, the imposition of a thermal gradient leads to a redistribution of chemical species as the solution seeks to reattain chemical equilibrium. These processes may become more important for increasing temperature gradients (Jamet et al., 1990; Guy and Schott, 1992). Jamet et al. (1990) note that Soret diffusion can act as an ore deposition mechanism in geothermal environments. The effect tends to be more pronounced for lighter elements; less volatile species tend to concentrate near the cold parts of the system. The sensitivity of a given element to Soret diffusion is measured by the Soret coefficient,  $S_T$ :

$$S_T = \frac{D'}{D_m} = \frac{\nabla c}{c(1 - c) \nabla T} \quad (3-1)$$

where:

- $D'$  = thermal diffusion coefficient (m<sup>2</sup>/s-K),
- $D_m$  = molecular diffusion coefficient (m<sup>2</sup>/s),
- $c$  = solute mass fraction (dimensionless), and
- $T$  = temperature (K).

**Table 3-1. Summary of Driving Potentials, Fluid Pressure, Temperature, and Species Concentration, and How They are Expected to Generate a Flux of Fluid, Heat or Species (Modified from Carnahan, 1987a)**

Flux	Driving Potential		
	Fluid Pressure Gradient	Temperature Gradient	Species Concentration Gradient
Fluid (Gas or Liquid)	Darcy's Law	Thermal Osmosis	Chemical Osmosis
Heat	Thermal Filtration	Fourier's Law	DuFour Effect
Species	Reverse Osmosis or Ultrafiltration	Soret Effect	Fick's Law

$S_T$  values are generally positive as opposed to the temperature gradient. Values range from about  $10^2$  to  $10^3$  °C<sup>-1</sup> for glasses and aqueous solutions (Jamet et al., 1990; Guy and Schott, 1992). Studying Soret element migration in radioactive glassforms, Guy and Schott (1992) report that relatively light element compounds such as Na<sub>2</sub>O, B<sub>2</sub>O<sub>3</sub>, Li<sub>2</sub>O, and H<sub>2</sub>O are susceptible to migration by Soret diffusion, while predicting weak diffusion for heavier radioelements such as Sr, Cs, Pu, Am, and Np. Thermal diffusion is relatively minor in the simulations of Carnahan (1984). Molecular diffusion according to Fick's Law in response to chemical gradients tends to work to balance the effects of Soret diffusion.

In fluids (liquid or gas), an additional coupling is found between the Soret effect and thermally driven water convection and is called the thermogravitational effect (TGE) (Jamet et al., 1990; Guy and Schott, 1992). Because convection and Soret diffusion operate in the same direction, this coupling can greatly magnify the effects due to Soret diffusion alone, with concentration gradients up to 5 orders of magnitude larger than nonconvective values. If the velocity due to convection is too large, the fluid will tend to homogenize, and concentration gradients are diminished. If velocity is too slow, the coupling will be weak and the concentration gradient will be dominated by Soret diffusion.

### 3.2.3 Computer Codes

Because of the inherent complexities, there are few codes at present that attempt to simulate the effects of the coupling between these three processes. As mentioned previously most of the thermal-chemical codes do not consider fluid flow. Coupled hydrogeochemical codes are limited to isothermal conditions, and most of the thermal-fluid flow codes do not explicitly consider chemistry. The codes discussed below (and also in Section 2.9) can handle variable temperature. Generally, however, the temperature gradient is specified for the problem; heat transfer is decoupled from fluid flow and chemistry, and its effects are not considered explicitly.

### 3.2.3.1 CHMTRNS

As discussed in Section 2.9, CHMTRNS (Noorishad et al., 1987) is a one-step coupled program that has been used to model  $^{14}\text{C}$  age-dating and silica reaction kinetics. The code is able to consider nonisothermal conditions. There is no accompanying thermodynamic database, and the data must be input specifically for each problem. The code has been limited to one-dimensional systems. The more exact but less efficient one-step coupling used by CHMTRNS will probably limit the future application of the code to more complex problems because of excessive computer requirements (Yeh and Tripathi, 1989).

### 3.2.3.2 THCC

THCC (Thermo-Hydro-Chemical Coupling) begun as an extension of the CHEMTRN code (see Section 2.9), was developed at Lawrence Berkeley Laboratory (Carnahan, 1987b,c, 1988, 1990) to model isothermal and nonisothermal hydrochemical transport. The code can model both homogeneous and heterogeneous chemical reactions of aqueous speciation, precipitation/dissolution, redox, and ionic strength/activity effects. Ion exchange can also be modeled to a limited extent. Temperature dependent chemistry is modeled by using equilibrium constant data fit to a log (K)-temperature relationship similar (but not identical to) the form presented in Eq. 2-17. For a constant flow velocity under hydrologically saturated conditions, chemistry and hydrology equations are directly coupled (one-step). Heat transfer, however, is decoupled and solved iteratively. It is assumed that heat transport has no effect on fluid flow, and that the heats of reaction do not affect the temperature distribution. The necessary equilibrium constant data and the constants for the log (K)-temperature relationship are provided as input for each run. It is currently limited to one-dimensional simulations, or radial flow, and has been used to model uranium oxidation/reduction and migration in a simplified Si-Ca-CO<sub>2</sub>-H<sub>2</sub>O environment.

### 3.2.3.3 Codell and Murphy (1992)

For a limited representation of the Ca-CO<sub>2</sub>-H<sub>2</sub>O system, Codell and Murphy (1992) have iteratively coupled nonisothermal equilibrium chemistry with the two-phase flow code described by Ampter and Ross (1990) to model  $^{14}\text{C}$  transport and retardation through partially saturated rock. Applied specifically to Yucca Mountain, a vertical one-dimensional column was constructed with dimensions and boundary conditions appropriate to the proposed repository. Liquid saturation was approximated with an empirical model based on numerical simulations of Nitao (1988) with a maximum saturation of 80 percent. Gas was assumed to migrate upwards only and  $^{14}\text{C}$  transport was assumed only to occur by advection in the gas phase. Carbon-14 is removed from solution by calcite precipitation and by radioactive decay. Within the constraints of the assumptions made, the model results indicate that the aqueous solution remains the largest reservoir of  $^{14}\text{C}$ . Immobilization in the aqueous phase results in a retardation by a factor of 30 to 40 relative to gas transport. Calcite precipitation also acts as a significant long-term sink for  $^{14}\text{C}$ .

### 3.2.3.4 HYDROGEOCHEM

As discussed in Section 2.9, HYDROGEOCHEM (Yeh and Tripathi, 1990, 1991) was developed at Oak Ridge National Laboratory. The code is very elaborate and able to accommodate a wide variety of conditions and processes. The code is able to account for changes in chemical equilibrium due to the effects of temperature, pressure and ionic strength. It does not appear at present, however, that the effects of heat on fluid flow are explicitly incorporated in the model. The code has been used to simulate

several different types of problems in an effort to evaluate the effects of different processes on contaminant transport.

### 3.2.3.5 Cline et al. (1992)

Cline et al. (1992) have modified the earlier one-dimensional model of Donaldson (1968) to simulate two-phase flow and quartz precipitation in geothermal systems. The conceptual model is one of a single phase fluid entering the base of the system at a constant temperature and mass flux. Temperature at the surface is fixed at 100 °C and 1 bar. As the fluid rises due to buoyancy effects, temperature decreases as a function of pressure decreases along the pure H<sub>2</sub>O liquid/vapor curve. If the mass flux of the fluid exceeds a threshold value of about 10<sup>-6</sup> kg/m<sup>2</sup> s, the saturation pressure fixed by the liquid/vapor curve will exceed the confining pressure of the system and the fluid will boil. Permeability is allowed to vary vertically, and relative permeability of liquid and vapor phases are modeled as a function of temperature for the one-component H<sub>2</sub>O system. Silica chemistry is controlled by fluid/quartz equilibria, and it is assumed that the fluid is saturated with quartz when it is input at the base of the system. Vein walls are assumed to be quartz, and the fluid maintains equilibrium with quartz as it rises to the surface. Quartz precipitates as the fluid cools and as a result of decreased solubility with the formation of a vapor phase. The effect of quartz precipitation on permeability is not specifically considered. Cline et al. (1992) examined variations in the height of the boiling column, amount of vapor generated, and the intensity of quartz precipitation for ranges in temperature, mass flux, and permeability reasonable for geothermal systems.

### 3.2.4 Summary and Conclusions

In this section, coupled THC processes were discussed. Two types of couplings were discussed: material property couplings and phenomenological couplings (Onsanger's coupled processes). Material properties and media characteristics can be influenced especially by temperature-dependent chemical processes. Dissolution, alteration, and/or precipitation may be important in the near-field where temperature variations are largest. Onsanger's coupled processes represent fluxes of either fluid, heat, or species due to gradients in either pressure, temperature, or species concentration. The primary couplings are known as Fourier's, Darcy's, and Fick's laws; however, secondary couplings (thermal osmosis, chemical osmosis, the DuFour effect, etc.) may need to be considered in special cases. The literature was reviewed where the importance of the secondary couplings appears to be either negligible or uncertain in cases of practical interest. Computer codes were also summarized where it was found that coupled THC codes typically considered the temperature and fluid flow fields as input into geochemical codes.

## 4 FOUR-WAY COUPLED PROCESSES

In this section, the four processes (thermal, hydrologic, mechanical, and chemical) are considered for the four-way coupled behavior. The individual one-way couplings were discussed in Section 2, and three-way couplings were discussed in Section 3. Hence, this section synthesizes and analyzes the previous discussions without introducing new coupling mechanisms. The purpose for studying a process is reviewed, and the importance of the couplings are compared so that the most important couplings can be identified.

### 4.1 PERFORMANCE OBJECTIVES

The performance objectives of a geologic repository dictate the type of studies that need to be performed. The processes of interest in this work are THMC. There are numerous citations in the regulations which require the study of coupled processes. These regulations are summarized in 10 CFR Part 60, and especially in Sections 60.111, 60.112, and 60.113. In these regulations, the motivation for studying processes is presented as well as specific processes and couplings being identified as evidently being important [10 CFR 60.133(i)].

In the regulations, the performance objectives are discussed in three distinct time periods in the life of a geologic repository: operation, containment, and isolation [especially see 10 CFR 60.102(d) and (e)]. The operation period is the time until permanent closure of the repository. The containment period is from closing to 300-1000 years. The isolation period is from the end of containment until ~ 10,000 years. An alternative interpretation is to view the operation period from 0 - closure, the containment period for 0 - 1000, and the isolation period from 0 - 10,000 years. In light of the present discussion, the difference between these interpretations is considered insignificant.

The regulatory requirements are distinct for each of the three time periods. The operation period is especially concerned with stability of mined excavations, the containment period is especially concerned with radionuclide containment by the engineered barrier system, and the isolation period is especially concerned with radionuclide containment by the geologic setting. Hence, there are three distinct time periods (operation, containment, isolation) which have distinct regulatory concerns.

The performance objectives for each time period are most logically described as requiring specific studies pertinent to specific processes. Hence, the performance objectives dictate which processes must be studied and sufficiently understood. The processes most closely related to the performance objectives depend on the time period of the repository. For example, during the operation time period, performance objectives are most closely related to mechanical processes because mechanical processes and loads dictate the stability of underground excavations. Likewise, during the containment and isolation time periods, the performance objectives are most closely related to chemical processes. A study of chemical processes leads to an assessment of the corrosion of the waste containers, and the radionuclide migration through the geologic setting. Hence, an understanding of the repository performance objectives is necessary to assess the importance of processes and couplings.

### 4.2 IMPORTANCE OF COUPLINGS

An assessment of the importance of coupled THMC processes are summarized in Tables 4-1, 4-2, and 4-3. Each table is specific for:

**Table 4-1. Assessment of the Importance of Coupled THMC Processes for Anticipated Processes and Events, for Performance Objectives Associated with the Operations Time Period of the Proposed HLW Repository. (10 CFR 60.111)**

	<b>Thermal</b>	<b>Hydrologic</b>	<b><u>MECHANICAL</u></b>	<b>Chemical</b>
Thermal ->	N/A	1	1	3
Hydrologic ->	2	N/A	3	3
Mechanical ->	3	3	N/A	3
Chemical ->	3	3	2	N/A

**Table 4-2. Assessment of the Importance of Coupled THMC Processes for Anticipated Processes and Events, for Performance Objectives Associated with the Containment Time Period at the Proposed HLW Repository. (10 CFR 60.113)**

	<b>Thermal</b>	<b>Hydrologic</b>	<b>Mechanical</b>	<b><u>CHEMICAL</u></b>
Thermal ->	N/A	1	1	1
Hydrologic ->	2	N/A	2	1
Mechanical ->	3	2	N/A	2
Chemical ->	3	3	2	N/A

**Table 4-3. Assessment of the Importance of Coupled THMC Processes for Anticipated Processes and Events, for Performance Objectives Associated with the Isolation Time Period at the Proposed HLW Repository. (10 CFR 60.112)**

	<b>Thermal</b>	<b>Hydrologic</b>	<b>Mechanical</b>	<b><u>CHEMICAL</u></b>
Thermal ->	N/A	1	2	1
Hydrologic ->	2	N/A	3	1
Mechanical ->	3	3	N/A	3
Chemical ->	3	2	2	N/A

Key: 1 - Primary  
 2 - Secondary  
 3 - Tertiary

Note: The affected process of primary regulatory interest is highlighted in all capital letters and underlined in the tables.

- a time period (operation, containment, or isolation),
- anticipated processes and events,
- performance objectives, and
- the proposed geologic repository at Yucca Mountain.

Each of these specifications narrows the scope of the tables and hopefully increases the usefulness of this summary. It is easiest to state that all processes and couplings need to be considered, and there would be no errors in such a statement. However, such a broad statement is not considered useful in identifying the important couplings as well as the negligible couplings. It is expected that many calculations will be performed, hence it is prudent that resources be directed to the most important processes and couplings. Through a review of process couplings (as summarized in Section 2), and comparison of processes, the most important processes can be identified.

The description of "time period", "anticipated processes and events", "performance objectives", and "proposed repository" are used in the tables and are considered important in narrowing the scope of the tables. The "time periods" and "performance objectives" have been discussed in Section 4.1, and are not discussed further. The other descriptions are discussed here.

In the tables, the term "anticipated processes and events" is used to narrow the scope and is defined in the regulations (10 CFR 60.2): "Anticipated processes and events means those natural processes and events that are reasonably likely to occur during the period the intended performance objective must be achieved." The term "reasonably likely" implies a probability of occurrence which is unspecified in the regulations. Although unspecified, the probability is on the order of one occurrence during the time period of interest. Hence, the couplings assessed in the tables are only applied to those processes and events which are reasonably likely to occur.

In the tables, the term "proposed repository" is used to narrow the scope of the tables to concentrate on the couplings pertinent at Yucca Mountain. Hence the tables are not for a generic repository. Previously, other geologic locations were considered as possible repository locations. These included salt, granite, basalt, and shale (Wang et al., 1983). These locations have different mechanical, thermal, hydrologic and chemical properties, hence different processes and couplings would be expected.

A spatial designation of container, near-field, and far-field was also considered to help clarify where coupled processes may need to be considered. The spatial description would have been in parallel with the temporal description (operation, containment, and isolation). However, the spatial description is closely related to the performance objective which is related to the principle process. Hence after consideration, the spatial description was not adopted for this work and is considered an implicit part of the performance objective.

The tables summarize an "assessment of the importance of coupled THMC processes." The term assessment is used to emphasize that this is a summary of the state-of-the-art. Although a large amount of effort was expended in reviewing the literature, it is probable that portions of the literature have not been reviewed. Also, because the scientific knowledge of the processes is continually improving, it is probable that future assessments will be more definitive. Hence, the reader is cautioned that these assessments are likely to be updated. Nonetheless, the authors believe it is important to summarize this review of the literature as best as currently possible in order to guide future work.

Having discussed the scope and caveats of the tables, the information content of the tables will be discussed next.

The tables summarize 12 one-way couplings in parallel with Section 2 of this report (e.g., T->H, T->M). The motivating processes are in the left column and the influenced processes are in the upper row. The self couplings (i.e., T->T, H->H, M->M, C->C) are not logically discussed in this context, and are noted to be nonapplicable (N/A).

Within each box in the tables are subjective numerical ratings for the assessed importance of each one-way coupling. The ratings are 1=primary, 2=secondary, and 3=tertiary. The definition of ratings are as follows: primary = confidently expected to be important; secondary = potentially important, however coupling may be neglected without significant errors; tertiary = confidently expected to be negligible. Hence in Table 4-1, the T->H coupling is considered a "primary" coupling so that if hydrologic processes are to be studied then thermal processes should also be considered. Similarly, in Table 4-1, the M->C coupling is considered "tertiary" and is expected to have negligible influence on chemical processes.

Although these ratings are subjective, the justification for each of the ratings is provided in Section 2 of this report. For example, the T->H coupling is considered important because of: (i) vaporization and condensation of water, (ii) condensate dripping in fractures, and (iii) vapor diffusion. These coupling mechanisms are expected to affect the hydrologic processes.

Figure 4-1 summarizes the assessments presented in the tables, however the information is presented in a hopefully more illuminating way. Again, the three time periods are considered (operation, containment, isolation). The four processes are shown (T, H, M, C), with the processes most closely related to the regulatory performance objectives inside a highlighted circle. The primary couplings are indicated with solid lines, the secondary with dashed lines, and the tertiary are not drawn. In the left column, all four processes are shown with all primary and secondary couplings. As a subset, only the primary couplings with processes influencing the process of regulatory performance interest are shown in the right column. From Figure 4-1, the importance of mechanical processes during operation is highlighted and the necessity for considering thermal processes is highlighted. However after operation, chemical processes are most closely related to performance objectives. Also, thermal and hydrologic processes are shown to be significantly influencing chemical processes.

It is interesting that mechanical processes are crucial during operation, however are relatively unimportant during containment and isolation. Conversely, chemical processes are important during containment and isolation, but not during operation. Thermal processes are important to consider throughout the life of the repository, however, thermal processes are only important as they affect other processes. Similarly, hydrologic processes are not directly important in the performance objectives, but are important in influencing chemical processes during the containment and isolation time periods.

From Figure 4-1, one may conclude that the primary couplings as indicated in the right column should confidently be considered in assessing performance objectives. In light of the best currently available information, the secondary couplings may be neglected. However, the possibility exists that future studies and improved understanding may show them to be non-negligible.

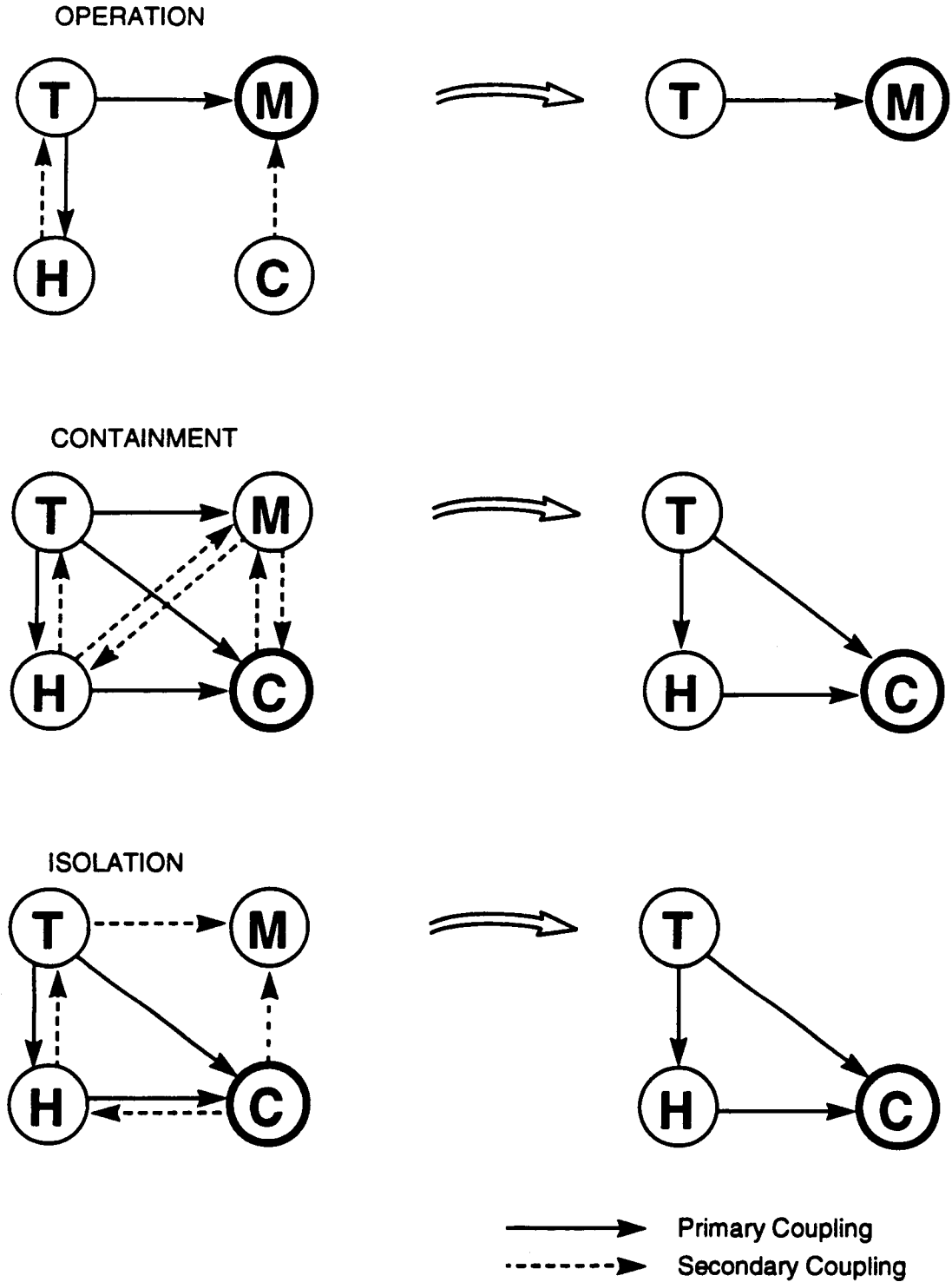


**Figure 4-1. Illustration of the Important Processes and Couplings During the Operation, Containment, and Isolation Periods for Anticipated Processes and Events at the Proposed Repository. The Right Column is a Subset of the Left Where Only Primary Couplings Which Feed into the Processes of Primary Regulatory Interest are Shown.**

### 4.3 SUMMARY AND CONCLUSIONS

In this section, fully coupled THMC processes are considered. The importance of studying processes is related to the regulatory performance objectives (10 CFR Part 60, especially Sections 60.111, 60.112, and 60.113). The current understanding of processes and couplings which was present in Section 2, is synthesized into an overall assessment of the importance of the different couplings. Each coupling is considered for three time periods (operation, containment, isolation), for anticipated processes and events, for the regulatory performance objectives, and for the proposed repository at Yucca Mountain. Based on the performance objectives outlined in the regulations, mechanical processes are especially important during the operation time period because it is most closely related to stability of mined excavations and retrievability. Similarly, chemical processes are especially important during the containment and isolation time periods because it is most closely related to corrosion and release of radionuclides, and then migration of radionuclides through the geologic setting. This assessment is based on the current understanding of interactions and couplings, and is useful in guiding future work.

## 5 SUMMARY AND RECOMMENDATIONS

A comprehensive literature review has been conducted to establish the state of knowledge relevant to modeling coupled thermal-hydrologic-mechanical-chemical processes as it is pertinent to the proposed HLW repository at Yucca Mountain, Nevada. This assessment attempts to identify potential technical deficiencies in the subject with regard to coupling mechanisms between processes.

This section describes those topics which are of major concern and should be considered in planning future work:

- the adequacy of current mathematical models;
- the lack of well documented coupled-effects experiments;
- the need for validation of mathematical models.

The following material is a concise summary of the key findings of this literature search, with particular attention to the issues of concern noted above.

### 5.1 TWO-WAY COUPLED PROCESSES

Coupled analyses among pairs of processes provide a fundamental basis for multiple couplings involving three or more processes. Considering the four kinds of processes (T, H, M, C) the number of possible one-way couplings is twelve. Each one-way coupling was discussed in Section 2. The importance of each one-way coupling within three different time periods of the proposed HLW repository was discussed in Section 4. This assessment is subjective and based on our current knowledge and may have to be modified as new data and information emerge. Pairs of one-way couplings can be combined into a two-way coupling (e.g., T <-> H) which are summarized here.

The potential influence of the temperature field on hydrologic processes was assessed to be strong. The elevated temperatures in a repository will lead to vaporization of the groundwater. Temperature gradients will provide a driving force for the water vapor to flow into cooler regions. The water vapor has the potential to condense in cooler regions and flow due to both gravity and pressure gradients. Thus vaporization, gas flow, condensation, and liquid flow are anticipated to be important processes in affecting the near-field hydrology in the proposed repository at Yucca Mountain. Many of the hydrogeologic units at Yucca Mountain are fractured with a low permeability matrix. Episodic rainfall and infiltration at the ground surface, and water vapor condensation are two mechanisms whereby the fractures may transmit a substantial amount of liquid. More work, however, needs to be done on the study of such effects in fractured porous systems which should include characterization of matrix-fracture interactions. Hydrologic processes may also affect thermal processes through a number of coupling mechanisms, the most important one being the gravity-driven condensate drainage in fractures towards the heat source. Mechanical processes can affect hydrologic processes primary through fracture apertures which in turn affect hydrologic conductivity and fluid storativity.

The potential influence of the temperature field on mechanical response was also assessed to be strong and represents the well-known thermomechanical effects. More work should be done in this area to evaluate the impact of existing fractures and joints, and the impact of temperature on mechanical properties and long term mechanical degradation.

The thermal effects on chemical behavior include chemical thermodynamics as well as all temperature effects on the equilibrium constants and kinetics of chemical reactions. At present, only a few codes such as EQ3/6 and PHREEQE are able to fully model reaction processes, and even fewer codes (e.g., EQ3/6) can model reaction kinetics as a function of time if appropriate rate constant data are available. Much of the thermodynamic data, especially for many of the key radionuclides, are only available for low temperatures. The coupled effects of temperature on system chemistry can be significant and further study should be done.

The hydrologic-chemical coupling includes chemical equilibria and mass transport in fractured porous rocks. Interaction between fluids, the rock matrix, and fracture-lining materials should be taken into account. Currently available computational methods have many limitations and need additional work.

## **5.2 THREE-WAY COUPLED PROCESSES**

Among the four processes, there can only be four possible three-way couplings: THM, THC, MHC, and TMC. The thermal-hydrologic-mechanical coupling describes the thermally induced hydromechanical behavior of fractured rocks, where both heat and fluid pressure may change the fracture apertures with the result that buoyant flow may be strongly affected. Most of the computer codes available for modeling coupled THM processes have many limitations and are only partially verified against analytical solutions for two-way couplings such as hydromechanical, thermomechanical, and hydrothermal problems. Studies related to partially saturated media are almost nonexistent and are recommended.

The thermal-hydrologic-chemical coupling includes chemical reactions and heat and mass transport in rock masses. A chemical reaction could be mineral precipitation (or dissolution), which changes the rock permeabilities to fluid flow. Such a process has been studied in hydrothermal systems. For problems related to nuclear waste repositories, further quantitative studies are recommended.

## **5.3 FOUR-WAY COUPLED PROCESSES**

In a situation where all four processes are interrelated, the coupling is the four-way coupling, THMC. As discussed in Section 4, this coupling is most important during the containment period (i.e., closure until 300-1000 years). This coupling includes the chemical reaction and mass transport under both thermal and hydraulic loading. The thermal effects may cause mechanical changes in fracture apertures, hence fracture permeability. Chemical precipitation and dissolution may also change the permeability of the rock mass. These two effects join together to influence the fluid flow and chemical transport.

It is generally assumed that numerical methods will be used extensively for coupled analyses for design and performance assessment of the proposed HLW geological repository. The numerical methods should take into account the coupled behavior considering both time and geometric scales. Essential features of a selected computer code are that it can model the processes and the non-negligible coupling mechanisms, and that the partially saturated, discontinuous nature of the rock mass be simulated.

Perhaps the most critical aspect of the application of a computational method is validation of the mathematical models. Development of well-controlled laboratory or field experiments appears to be the most feasible approach for validation of mathematical models, hence are recommended.

## 6 REFERENCES

- Ababou, R. 1991. *Approaches to Large Scale Unsaturated Flow in Heterogeneous, Stratified, and Fractured Geologic Media*. NUREG/CR-5743. Washington, D.C.: U. S. Nuclear Regulatory Commission (NRC).
- Ahola, M.P., S. Hsiung, L. Lorig, and A.H. Chowdhury. 1992. *Thermo-Hydro-Mechanical Coupled Modeling: Multiple Fracture Model, BMT2; Coupled Stress-Flow Model, TCI. DECOVALEX-Phase I*. CNWRA 92-005. San Antonio, TX: Center for Nuclear Waste Regulatory Analyses (CNWRA).
- Alberty, R.A., and F. Daniels. 1979. *Physical Chemistry*. New York, NY: Wiley.
- Alemi, M.H., D.A. Goldhamer, and D.R. Nielsen. 1991. Modeling selenium transport in steady-state, unsaturated soil columns. *Journal of Environmental Quality* 20: 89-95.
- Allison, J.D., D.S. Brown, and K.J. Novo-Gradac. 1990. *MINTEQA2/PRODEFA2, A Geochemical Assessment Model for Environmental Systems: Version 3.0 User's Manual*. Athens, GA: U.S. Environmental Protection Agency (EPA).
- Amadei, B., and R.E. Goodman. 1981. A 3-D constitutive relation for fractured rock masses. *Proceedings International Symposium on the Mechanical Behavior of Structured Media*. Ottawa, Canada.
- Ampter, S., and B. Ross. 1990. Simulation of gas flow beneath Yucca Mountain, Nevada with a model based on freshwater head. R.G. Post ed. *Proceedings of the Symposium on Waste Management*. Tucson, AZ: University of Arizona: 915-925.
- Archambeau, C.B., and N.J. Price. 1991. *An Assessment of J.S. Szymanski's Conceptual Hydrotectonic Model. Minority Report of the Special DOE Review Panel*. Washington, D.C.: U.S. Department of Energy (DOE).
- Arulmoli, K., and C.M. St. John. 1987. *Analysis of Horizontal Waste Emplacement Boreholes of a Nuclear Waste Repository in Tuff*. SAND86-7133. Albuquerque, NM: Sandia National Laboratories (SNL).
- Atkinson, B.K. 1979. Fracture toughness of Tennessee sandstone and Carrea marble using the double beam torsion testing method. *International Journal of Rock Mechanics and Mineral Science and Geomechanical Abstracts* 16: 49-53.
- Atkinson, B.K., and P.G. Meredith. 1987. The theory of subcritical crack growth with applications to minerals and rocks. B.K. Atkinson, ed. *Fracture Mechanics of Rock*. New York, NY: Academic Press
- Baes, C.F., and R.E. Mesmer. 1976. *The Hydrolysis of Cations*. New York, NY: Wiley.

- Ball, J.W., E.A. Jenne, and D.K. Nordstrom. 1979. *Chemical Modeling in Aqueous Systems. Speciation, Sorption, Solubility, and Kinetics*. E.A. Jenne, ed. American Chemical Society (ACS) Symposium Series 93. Washington, D.C.: ACS: 815-835.
- Ball, J.W., D.K. Nordstrom, and D.W. Zachmann. 1987. *WATEQ4F - A Personal Computer FORTRAN Translation of the Geochemical Model WATEQ2 with Revised Database*. USGS-OFR-87-50. Reston, VA: U.S. Geological Survey (USGS).
- Bandis, S.C., A.C. Lumsden, and N.R. Barton. 1983. Fundamentals of rock joint deformation. *International Journal of Rock Mechanics and Mineral Science and Geomechanical Abstracts* 20: 249-268.
- Banerjee, P.K., and S. Ahmad. 1985. Advanced three-dimensional dynamic analysis by boundary element methods. T.A. Cruse, et al., eds. *Advanced Topics in Boundary Element Analysis*. New York, NY: American Society of Mechanical Engineers (ASME) 72: 65-81.
- Bard, A.J., R. Parsons, and J. Jordan eds. 1985. *Standard Potentials in Aqueous Solutions. International Union of Pure and Applied Chemistry Series*. New York, NY: Marcel Dekker.
- Barry, D.A. 1990. Supercomputers and their use in modeling subsurface solute transport. *Reviews of Geophysics* 28(3): 277-295.
- Barton, N.R., S.C. Bandis, and K. Bakhtar. 1985. Strength, deformation and conductivity coupling of rock joints. *International Journal of Rock Mechanics and Mineral Science and Geomechanical Abstracts* 22(3): 121-140.
- Barton, N.R., and S.C. Bandis. 1982. Effects of block size on the shear behavior of jointed rock. *23rd U.S. Symposium on Rock Mechanics*. Rotterdam, Netherlands: A.A. Balkema.
- Bauer, S.J., and L.S. Costin. 1990. *Thermal and Mechanical Codes First Benchmark Exercise Part II: Elastic Analysis*. SAND89-0757. Albuquerque, NM: SNL.
- Bauer, S.J., M.P. Hardy, and M. Lin. 1991. Predicted thermal and stress environments in the vicinity of repository openings. *Proceedings of the High-Level Radioactive Waste Management Conference*. La Grange Park, IL: American Nuclear Society (ANS): 564-571.
- Bear, J. 1972. *Dynamics of Fluids in Porous Media*. New York, NY: Dover.
- Bear, J., and Y. Bachmat. 1991. *Introduction to Modeling of Transport Phenomena in Porous Media*. Norwell, MI: Kluwer Academic Publishers Group.
- Bejan, A. 1984. *Convection Heat Transfer*. New York, NY: Wiley.
- Benson, L.V., and L.S. Teague. 1980. *A Tabulation of Thermodynamic Data for Chemical Reactions Involving 58 Elements Common to Radioactive Waste Package Systems*. LBL-11448. Berkeley, CA: Lawrence Berkeley Laboratory (LBL).

- Bettess, P., and O.C. Zienkiewicz. 1977. Diffraction and refraction and surface waves using finite and infinite elements. *International Journal for Numerical Methods in Engineering* 11: 1271-1290.
- Bian, S.H., M.J. Budden, and S.C. Yung. 1987. *Application of GEOTHER/VT4 to Assess Groundwater Transients in a High-Level Radioactive Waste Repository*. PNL-SA-14502. Richland, WA: Pacific Northwest Laboratory (PNL).
- Bian, S.H., M.J. Budden, C.L. Bartley, and S.C. Yung. 1988a. *GEOTHER Evaluation and Improvement: A Progress Report Including Test Cases for Two-Dimensional BWIP Analysis*. PNL-6245. Richland, WA: PNL.
- Bian, S.H., M.J. Budden, C.L. Bartley, and S.C. Yung. 1988b. *GEOTHER/VT4: A Two-Phase Groundwater Fluid Flow and Heat Transport Code for High-Level Radioactive Waste Applications*. PNL-6517. Richland, WA: PNL.
- Bidner, M.S., and V.C. Vampa. 1989. A general model for convection-dispersion-dynamic adsorption in porous media with stagnant volume. *Journal of Petroleum Science and Engineering* 3: 267-281.
- Biot, M.A. 1941. General theory of three-dimensional consolidation. *Journal of Applied Physics* 12: 144-164.
- Bird, R.B., W.E. Stewart, and E.N. Lightfoot. 1960. *Transport Phenomena*. New York, NY: Wiley.
- Bischoff, J.L. 1991. Densities of liquids and vapors in boiling NaCl-H<sub>2</sub>O solutions: A PVTX summary from 300° to 500 °C. *American Journal of Science* 291: 309-338.
- Bish, D.L. 1986. *Evaluation of Past and Future Alterations in Tuff at Yucca Mountain, Nevada, Based on the Clay Mineralogy of Drill Cores USW G-1, G-2, & G-3*. LA-10667-MS. Los Alamos, NM: Los Alamos National Laboratory (LANL).
- Bixler, N.E. 1985. *NORIA—A Finite Element Computer Program for Analyzing Water, Vapor, Air, and Energy Transport in Porous Media*. SAND84-2057. Albuquerque, NM: SNL.
- Board, M. 1989a. *UDEC (Universal Distinct Element Code) Version ICG1.5*. NUREG/CR-5429. Volume 2. Washington D.C.: NRC.
- Board, M. 1989b. *FLAC (Fast Lagrangian Analysis of Continua) Version 2.20*. NUREG/CR-5430. Washington D.C.: NRC.
- Bond, W.J., B.N. Gardiner, and D.E. Smiles. 1982. Constant-flux adsorption of a tritiated calcium chloride solution by a clay soil with anion exclusion. *Soil Science Society of America Journal* 46: 1133-1137.

- Bond, W.J., and I.R. Phillips. 1990. Approximate solutions for cation transport during unsteady, unsaturated soil water flow. *Water Resources Research* 26(9): 2195-2205.
- Bond, W.J., and P.J. Wierenga. 1990. Immobile water during solute transport in unsaturated sand column. *Water Resources Research* 26(10): 2475-2481.
- Boozer, G., K. Killer, and S. Serdengecti. 1963. Effects of pore fluid on the deformational behavior of rocks subject to triaxial compression. *Proceedings 5th Rock Mechanics Symposium*. 579-625.
- Bowers, T.S., and H.C. Helgeson. 1983. Calculation of the thermodynamic and geochemical consequences of nonideal mixing in the system  $H_2O-CO_2-NaCl$  on phase relations in geologic systems: equations of state for  $H_2O-CO_2-NaCl$  fluids at high pressures and temperatures. *Geochimica et Cosmochimica Acta* 47: 1247-1275.
- Brady, B.H.G., and E.T. Brown. 1985. *Rock Mechanics for Underground Mining*. London: George Allen & Unwin.
- Brandl, H. 1981. Alteration of soil parameters by stabilization with lime. *Proceedings of the Eleventh International Conference of Soil Mechanics and Foundation Engineering*. Stockholm, Sweden: SKI: 587-595.
- Brebbia, C.A. 1978. *The Boundary Element Method for Engineers*. New York, NY: Wiley.
- Bresler, E., and G. Dagan. 1981. Convective and pore scale dispersive solute transport in unsaturated heterogeneous fields. *Water Resources Research* 17(6): 1683-1693.
- Brown, D.S., and J.D. Allison. 1987. *MINTEQA1, An Equilibrium Metal Speciation Model: User's Manual*. EPA/600/3-87/012. Athens, GA: EPA.
- Brown, P.L., A. Haworth, S.M. Sharland, and C.J. Tweed. 1991. *HARPHRO: A Geochemical Speciation Program Based on PHREEQE*. NSS-R.188. Oxon, United Kingdom: Harwell Laboratory.
- Broxton, D.E., D.L. Bish, and R.G. Warren. 1987. Distribution and chemistry of diagenetic minerals at Yucca Mountain, Nye County, NV. *Clays Clay Mineral* 35: 89-110.
- Buscheck, T.A., and J.J. Nitao. 1988. *Preliminary Scoping Calculations of Hydrothermal Flow in Variably Saturated, Fractured, Welded Tuff during the Engineered Barrier Design Test at the Yucca Mountain Exploratory Shaft Test Site*. UCID-21571. Livermore, CA: Lawrence Livermore National Laboratory (LLNL).
- Buscheck, T.A., and J.J. Nitao. 1992. The impact of thermal loading on repository performance at Yucca Mountain. *Proceedings of the High-Level Radioactive Waste Management Conference*. La Grange Park, IL: ANS: 1003-1017.

- Callahan, G.D., A.F. Fossum, and D.K. Svalstad. 1989. *Documentation of Spectrom-32: A Finite Element Thermomechanical Stress Analysis Program*. Volume 1. DOE/CH/10378-2. Washington D.C.: DOE.
- Cameron, D.R., and A. Klute. 1977. Convective-dispersive solute transport with a combined equilibrium and kinetic adsorption model. *Water Resources Research* 13(1): 183-188.
- Carlsson, H., L. Carlsson, and R. Pusch. 1989. *Rock Quality Designation of the Hydraulic Properties in the Near Field of a Final Repository for Spent Fuel*. SKB Technical Report 89-21. Stockholm, Sweden: SKB.
- Carnahan, C.L. 1984a. Thermodynamically coupled mass transport processes in a saturated clay. C.M. Jantzen, J.A. Stone, and R.C. Ewing, eds. *Scientific Basis for Nuclear Waste Management — VIII*. Pittsburgh, PA: Materials Research Society (MRS): 491-498.
- Carnahan, C.L. 1984b. Thermodynamic coupling of heat and matter flows in near-field regions of waste repositories. G.L. McVay, ed. *Scientific Basis for Nuclear Waste Management — VII*: Pittsburgh, PA: MRS: 1023-1030.
- Carnahan, C.L. 1987a. Effects of coupled thermal, hydrological and chemical processes on nuclide transport. *Proceedings of the GEOVAL 1987 Symposium in Stockholm, Volume 2*. Stockholm, Sweden: Swedish Nuclear Power Inspectorate (SKI): 493-506.
- Carnahan, C.L. 1987b. Simulation of chemically reactive solute transport under conditions of changing temperature. *Coupled Processes Associated with Nuclear Waste Repositories*. C.F. Tsang, ed. San Diego, CA: Academic Press: 249-257.
- Carnahan, C.L. 1987c. Simulation of uranium transport with variable temperature and oxidation potential: The computer program THCC. J.K. Bates and W.B. Seefeldt, eds. *Scientific Basis for Nuclear Waste Management — X*. MRS: Pittsburgh, PA: 713-721.
- Carnahan, C.L. 1988. Some effects of data base variations on numerical simulations of uranium migration. *Radiochimica Acta* 44/45: 349-354.
- Carnahan, C.L. 1990. Coupling of precipitation/dissolution reactions to mass diffusion via porosity changes. D.C. Melchior and R.L. Bassett, eds. *Chemical Modeling of Aqueous Systems II*. American Chemical Society Series 416. Washington, D.C.:ACS: 234-242.
- Carrigan, C.R., G.C.P. King, G.E. Barr, and N.E. Bixler. 1991. Potential for water-table excursions induced by seismic events at Yucca Mountain, NV. *Geology* 19: 1157-1160.
- Cathles, L.M. 1983. An analysis of the hydrothermal system responsible for massive sulfide deposition in the Hokuroku Basin of Japan. *Economic Geology, Mono.* 5: 439-487.
- Cederberg, G.A. 1985. *TRANQL: A Ground-Water Mass-Transport and Equilibrium Chemistry Model for Multicomponent Systems*. Ph.D. Dissertation. Stanford, CA: Stanford University.

- Cederberg, G.A., R.L. Street, and J.O. Leckie. 1985. A groundwater mass transport and equilibrium chemistry model for multicomponent systems. *Water Resources Research* 21(8): 1095-1104.
- Center for Nuclear Waste Regulatory Analyses. 1990 *Report on Research Activities for Calendar Year*. W.C. Patrick, ed. CNWRA 90-01A or NUREG/CR-5817. San Antonio, TX: CNWRA. Washington D.C.: NRC.
- Charlez, P.A. 1991. *Rock Mechanics—Theoretical Fundamentals Volume 1*. Paris, France: Editions Technip.
- Chase, M.W., Jr., C.A. Davies, J.R. Downey, Jr., D.J. Frurip, R.A. McDonald, and A.N. Syverud. 1985a. JANAF thermochemical tables. 3rd Ed. Part I (Al-Co). *Journal of Physical and Chemical Reference Data* 14(1): 1-926.
- Chase, M.W., Jr., C.A. Davies, J.R. Downey, Jr., D.J. Frurip, R.A. McDonald, and A.N. Syverud. 1985b. JANAF thermochemical tables. 3rd Ed. Part II (Cr-Zr). *Journal of Physical and Chemical Reference Data* 14(1): 927-1856.
- Chen, E.P. 1986. Two-dimensional continuum model for jointed media with orthogonal sets of joints. *Symposium on Rock Mechanics Proceedings*. University of Alabama. SME/AIME: 862-867.
- Chen, E.P. 1990. A constitutive model for jointed rock mass with two intersecting sets of Joints. *Proceedings, International Conference on Jointed and Faulted Rock*. Vienna, Austria: A.A. Balkema.
- Cheng, P. 1978. Heat transfer in geothermal systems. *Advances in Heat Transfer* 14: 1-105.
- Christianson, M.C., and B. Brady. 1989. *Analysis of Alternative Waste Isolation Concepts*. NUREG/CR-5389. Washington, D.C.: NRC.
- Chung, P.A. Yoshitake, G. Cragolino, and D.D. Macdonald. 1985. Environmentally controlled crack growth rate of type 304 stainless steel in high temperature sulfate solutions. *Corrosion* 41: 159-168.
- Clemo, T.M., J.D. Miller, L.C. Hull, and S.O. Magnuson. 1990. *FRAUC-UNIX Theory and User's Manual*. EGG-EP-9029. Idaho Falls, ID: EG&G Idaho.
- Cline, J.S., R.J. Bodnar, and J.D. Rimstidt. 1992. Numerical simulation of fluid flow and silicate transport and deposition in boiling hydrothermal solutions: Applications to epithermal gold deposits. *Journal of Geophysical Research* 97(B6): 9085-9103.
- Clothier, B.E. 1984. Solute travel times during trickle irrigation. *Water Resources Research* 20(12): 1848-1852.

- Coats, K.H., and B.D. Smith. 1964. Dead-end pore volume and dispersion in porous media. *Society of Petroleum Engineering Journal* 4: 073-84.
- Codell, R.B., and W.M. Murphy. 1992. Geochemical model for  $^{14}\text{C}$  transport in unsaturated rock. *Proceedings of the High-Level Radioactive Waste Management*. La Grange Park, IL: ANS: 1959-1965.
- Cook, R.D. 1981. *Concepts and Applications of Finite Element Analysis*. New York, NY: Wiley.
- Copson, H.R. 1959. Effect of composition on stress corrosion cracking of some alloys containing nickel. T.N. Rhodin, ed. *Physical Metallurgy of Stress Corrosion Fracture*. New York, NY: Interscience.
- Cordfunke, E.H.P., and P.A.G. O'Hare. 1978. *The Chemical Thermodynamics of Actinide Elements and Compounds. Part 3. Miscellaneous Actinide Compounds*. Vienna, Austria: International Atomic Energy Agency (IAEA).
- Costin, L.S., and E.P. Chen. 1991. A thermomechanical analysis of the G-tunnel heated block experiment using a compliant-joint rock-mass model. *International Journal for Numerical and Analytical Methods in Geomechanics* 15: 379-398.
- Cox, J.D., D.D. Wagman, and V.A. Medvedev, ed. 1989. *CODATA Key Values for Thermodynamics*. New York, NY: Hemisphere.
- Criscenti, L.J., M.L. Kemner, R.L. Erikson, C.J. Hostetler, J.R. Morrey, and J.S. Fruchter. 1989. *The FASTCHEM™ Workstation for Integrating Pre- and Postprocessing Functions*. EPRI-EA-5871. Palo Alto, CA: Electric Power Research Institute (EPRI).
- Cundall, P.A. 1971. A computer model for simulating progressive, large-scale movement in blocky rock systems. *Proceedings of the International Symposium on Rock Fracture II*. Nancy, France: II-8.
- Cundall, P.A. 1988. Formulation of a three-dimensional distinct element model Part I. A scheme to detect and represent contacts in a system composed of many polyhedral blocks. *International Journal of Rock Mechanics and Mineral Science and Geomechanical Abstracts* 25(3): 106-107.
- Cundall, P.A., and J.V. Lemos. 1988. Numerical simulation of fault instabilities with the continuously-yielding joint model. *Proceedings of the Symposium on Rockbursts and Seismicity in Mines*. Charles Fairhurst, ed. University of Minnesota. Rotterdam, Netherlands: A.A. Balkema: 147-152.
- Cundall, P.A., and R.D. Hart 1989. Numerical modeling of discontinua. *1st U.S. Conference on Discrete Element Methods*. G.G.W. Mustoe, et al., eds. Golden, CO: Colorado School of Mines Press.

- Cvetkovic, V.D., and A.M. Shapiro. 1990. Mass arrival of sorptive solute in heterogeneous porous media. *Water Resources Research* 26(9): 2057-2067.
- Dagan, G. 1986. Statistical theory of groundwater flow and transport: pore to laboratory, laboratory to formation, and formation to regional scale. *Water Resources Research* 22(9): 120S-134S.
- Daily, W., W. Lin, and T. Buscheck. 1987. Hydrological properties of Topopah Spring tuff: Laboratory measurements. *Journal of Geophysical Research* 92: 7854-7864.
- Davis, J.A., and D.B. Kent. 1990. Surface complexation modeling in aqueous geochemistry. *Reviews in Mineralogy, Volume 23: Mineral-Water Interface Geochemistry*. M.F. Hochella, Jr., and A.F. White, eds. Mineralogical Society of America: Washington, D.C.: 177-260.
- de Donder, T., and P. van Rysselberghe. 1936. *Thermodynamic Theory of Affinity: A Book of Principles*. Stanford, CA: Stanford University Press.
- de Marsily, G. 1986. *Quantitative Hydrogeology, Groundwater Hydrology for Engineers*. New York, NY: Academic.
- de Smedt, F., and P.J. Wierenga. 1979. Mass transfer in porous media with immobile water. *Journal of Hydrology* 41: 59-67.
- de Smedt, F., and P.J. Wierenga. 1984. Solute transfer through columns of glass beads. *Water Resources Research* 20(2): 225-232.
- de Vries, D.A. 1963. Thermal properties of soils. *Physics of Plant Environment*. W.R. Van Wijk, ed. Amsterdam: North-Holland Publishing Company.
- de Vries, D.A. 1975. Heat transfer in soils. *Heat and Mass Transfer in the Biosphere*. D.A. de Vries and N.N. Afgan, eds. Washington, D.C.: Scripta Book Co.: 5-28.
- Dewers, T., and P. Ortoleva. 1990a. A coupled reaction/transport/mechanical model for intergranular pressure solution, stylolites, and differential compaction and cementation in clean sandstones. *Geochimica et Cosmochimica Acta* 54: 1609-1625.
- Dewers, T., and P. Ortoleva. 1990b. Geochemical self-organization III: A mean field, pressure solution model of metamorphic differentiation. *American Journal of Science* 290: 473-521.
- DOE (U.S. Department of Energy). 1988. *Site Characterization Plan: Yucca Mountain Site, Nevada Research and Development Area, Nevada*. DOE/RW-0199. Washington, D.C.: Office of Civilian Radioactive Waste Management (OCRWM).
- DOE (U.S. Department of Energy). 1990. *Yucca Mountain Project Reference Information Base*. YMP/CC-0002 (Version 04.002). Las Vegas, NV: DOE.

- Domenico, P.A., and F.W. Schwarz. 1990. *Physical and Chemical Hydrogeology*. New York, NY: Wiley.
- Donaldson, I.G. 1968. The flow of steam water mixtures through permeable beds: a simple simulation of a natural undisturbed hydrothermal region. *New Zealand Journal of Science* 11: 3-23.
- Doughty, C., and K. Pruess. 1988. A semianalytical solution for heat-pipe effects near high-level nuclear waste packages buried in partially saturated geological media. *International Journal of Heat and Mass Transfer* 31(1): 79-90.
- Doughty, C., and K. Pruess. 1990. A similarity solution for two-phase fluid and heat flow near high-level nuclear waste packages emplaced in porous media. *International Journal of Heat and Mass Transfer* 33(6): 1205-1222.
- Doughty, C., and K. Pruess. 1991. *A Mathematical Model for Two-Phase Water, Air, and Heat Flow around a Linear Heat Source Emplaced in a Permeable Medium*. LBL-30050. Berkeley, CA: LBL.
- Doughty, C., and K. Pruess. 1992. A similarity solution for two-phase water, air, and heat flow near a linear heat source in a porous medium. *Journal of Geophysical Research* 97(B2): 1821-1838.
- Drever, J.I. 1982. *The Geochemistry of Natural Waters*. Englewood Cliffs, NJ: Prentice-Hall.
- Duncan, J.M., and R.E. Goodman. 1968. *Finite Element Analysis of Slopes in Jointed Rocks*. U.S. Army Corps of Engineers Report TR 1-68.
- Dunn, P.D., and D.A. Reay. 1982. *Heat Pipes*. New York, NY: Pergamon Press.
- Dunning, J.D., W.L. Lewis, and D.E. Dunn. 1980. Chemo-mechanical weakening in the presence of surfactants. *Journal of Geophysical Research* 85(B10): 5344-5354.
- Dunning, J.D., D. Petroviski, J. Schuyler, and A. Owens. 1984. The effects of aqueous chemical environments on crack propagation in quartz. *Journal of Geophysical Research* 89(B6): 4115-4123.
- Dykhuisen, R.C. 1987. Transport of solutes through unsaturated fractured media. *Water Research* 21(12): 1531-1539.
- Dykhuisen, R.C. 1990. A new coupling term for dual-porosity models. *Water Resources Research* 26(2): 351-356.
- Eckert, E.R.G., and R.M. Drake, Jr. 1987. *Analysis of Heat and Mass Transfer*. New York, NY: Hemisphere.

- Edlefsen, N.E., and A.B.C. Anderson. 1943. Thermodynamics of soil moisture. *Hilgardia* 15(2): 31-298.
- Ellis, A.J., and W.A.J. Mahon. 1977. *Chemistry and Geothermal System*. New York, NY: Academic Press.
- Elrashidi, M.A., and W.L. Lindsay. 1984. *Fluorine Supplement to Technical Bulletin 134: Selection of Standard Free Energies of Formation for Use in Soil Chemistry*. Technical Bulletin 134 (supplement). Fort Collins, CO: Colorado State University, Experiment Station (CSUES).
- Erikson, R.L., C.J. Hostetler, and M.L. Kemner. 1990. *Mobilization and Transport of Uranium at Uranium Mill Tailings Disposal Sites*. NUREG/CR-5169. Washington, D.C.: NRC.
- Farmer, J.C., R.A. van Konynenburg, R.D. McCright, and D.B. Bullen. 1988a. *Survey of Degradation Modes of Candidate Materials for High-Level Radioactive-Waste Disposal Canisters. Volume 3: Localized Corrosion and Stress Corrosion Cracking of Austenitic Alloys*. UCID-21362. Livermore, CA: LLNL.
- Farmer, J.C., R.A. van Konynenburg, R.D. McCright, and G.E. Gdowski. 1988b. *Survey of Degradation Modes of Candidate Materials for High-Level Radioactive-Waste Disposal Canisters. Volume 4: Stress Corrosion Cracking of Copper-Based Alloys*. UCID-21362. Livermore, CA: LLNL.
- Felmy, A.R., D. Girvin, and E.A. Jenne. 1983. *MINTEQ: A Computer Program for Calculating Aqueous Geochemical Equilibria*. Washington, D.C.: EPA.
- Fleming, G.W., and L.N. Plummer. 1983. *PHRQINPT—An Interactive Computer Program for Constructing Input Data Sets to the Geochemical Simulation Program PHREEQE*. Water Resources Investigations Report 83-4236. Reston, VA: USGS.
- Fontana, M.G., and N.D. Greene. 1978. *Corrosion Engineering*. New York, NY: McGraw-Hill.
- Forster, C., and L. Smith. 1990. Fluid flow in tectonic regimes. B.E. Nesbitt, ed. *Short Course on Fluids in Tectonically Active Regimes of the Continental Crust*. Nepean, Ontario, Canada: Mineralogical Association of Canada: 1-47.
- Forsythe, G.E., and W.R. Warsow. 1960. *Finite Difference Methods for Partial Differential Equations*. New York, NY: Wiley.
- Forsyth, P.A. 1990. Radioactive waste disposal heating effects in unsaturated fractured rock. *Numerical Heat Transfer*. 17: 29-51.
- Forsyth, P.A., and R.B. Simpson. 1989. *A Two Phase, Two Component Model for Natural Convection in a Porous Medium*. CS-89-55. Waterloo, Ontario, Canada: Department of Computer Science, University of Waterloo.

- Forsyth, P.A., and R.B. Simpson. 1991. A two-phase, two-component model for natural convection in a porous medium. *International Journal for Numerical Methods in Fluids* 12: 655-682.
- Fossum, A.F. 1985. Effective elastic properties for a randomly jointed rock mass. *International Journal of Rock Mechanics and Mineral Science and Geomechanical Abstracts* 22(6): 467-470.
- Fox, R.W., and A.T. McDonald. 1978. *Introduction to Fluid Mechanics*. New York, NY: McGraw-Hill.
- Freeze, R.A., and J.A. Cherry. 1979. *Groundwater*. Englewood Cliffs, NJ: Prentice-Hall.
- Fuger, J., and F.L. Oetting. 1976. *The Chemical Thermodynamics of Actinide Elements and Compounds. Part 2. The Actinide Aqueous Ions*. Vienna, Austria: IAEA.
- Gallegos, D.P., S.G. Thoma, and D.M. Smith. 1992. Impact of fracture coating on the transfer of water across fracture faces in unsaturated media. *Proceedings of the High-Level Radioactive Waste Management Conference*. La Grange Park, IL: ANS: 728-745.
- Garrels, R.M., and C.L. Christ. 1965. *Solutions, Minerals, and Equilibria*. San Francisco, CA: Freeman, Cooper and Company.
- Gerrard, C.M. 1982. Elastic models of rock masses naming one, two and three sets of joints. *International Journal of Rock Mechanics and Mineral Science and Geomechanical Abstracts* 19: 15-23.
- Gillham, R.W., E.A. Sudicky, J.A. Cherry, and E.O. Frind. 1984. An advection-diffusion concept for solute transport in heterogeneous unconsolidated geological deposits. *Water Resources Research* 20(3): 369-378.
- Goldberg, S., H.S. Forster, and E.L. Heick. 1991. Flocculation of illite/kaolinite and illite/montmorillonite mixtures as affected by sodium adsorption ratio and pH. *Clays Clay Minerals* 39: 375-380.
- Green, R., R. Manteufel, F. Dodge, and S. Svedeman. 1992. *Theoretical and Experimental Investigation of Thermohydrologic Processes in a Partially Saturated, Fractured Porous Medium: A Summary of Work Through December 1991*. CNWRA 92-006. San Antonio, TX: CNWRA.
- Grenthe, I., J. Fuger, R.J. Lemire, A.B. Muller, C. Nguyen-Trung, and H. Wanner. 1992. *Chemical Thermodynamics Series, Volume 1: Chemical Thermodynamics of Uranium*. New York, NY: Elsevier.
- Griffith, A. 1920. The phenomena of rupture and flow in solids. *Philosophical Transactions. Royal Society of London. Series A. Mathematical and Physical Sciences* 221: 163-197.

- Gureghian, A.B., and B. Sagar. 1991. Evaluation of DCM3D—a dual continuum, 3-D groundwater flow code for unsaturated, fractured, porous media. *Report on Research Activities for Calendar Year 1990*. W.C. Patrick, ed. NUREG/CR-5817. Washington, D.C.: NRC.
- Guy, C., and J. Schott. 1992. Modeling of sorption diffusion in radioactive waste glass. *Applied Geochemistry Suppl. Issue No. 1*: 33-40.
- Haas, J.L., Jr. 1974. *PHAS20, A Program for the Simultaneous Multiple Regression of a Mathematical Model to Thermochemical Data*. AD-780301. Springfield, VA: National Technical Information Service (NTIS).
- Hadley, G.R. 1985. *PETROS—A Program for Calculating Transport of Heat, Water, Vapor and Air Through a Porous Material*. AD-780301. Springfield, VA: NTIS.
- Hahn, J.K. 1988. Realistic animation of rigid bodies. *Computer Graphics* 22 (4): 299-308.
- Hallquist, J.O. 1988. *User's Manual for DYNA2D—An Explicit Two-Dimensional Hydrodynamic Finite Element Code with Interactive Rezoning and Graphical Display*, UCID-18756, Rev. 3. Livermore, CA: LLNL.
- Hardy, M.P., and S.J. Bauer. 1991. *Drift Design Methodology and Preliminary for the Yucca Mountain Site Characterization Project*. SAND89-0837. Albuquerque, NM: SNL.
- Hardy, M.P., and S.J. Bauer. 1992. Invited paper: Rock mechanics considerations in designing a nuclear waste repository in hard rock. *Proceedings of the 33rd U.S. Symposium on Rock Mechanics*. J.R. Tillerson and W.R. Wawersik, eds. Rotterdam, Netherlands: A.A. Balkema: 1041-1050.
- Harvie, C.E., N. Moller, and J.H. Weare. 1984. The prediction of mineral solubilities in natural waters: the Na-K-Mg-Ca-Cl-SO<sub>4</sub>-OH-HCO<sub>3</sub>-CO<sub>3</sub>-CO<sub>2</sub>-H<sub>2</sub>O system to high ionic strengths at 25 C. *Geochimica et Cosmochimica Acta* 48: 723-751.
- Haworth, A., S.M. Sharland, P.W. Tasker, and C.J. Tweed. 1988a. *A Guide to the Coupled Chemical Equilibria and Migration Code CHEQMATE*. NSS-R.113. Oxon, United Kingdom: Harwell Laboratory.
- Haworth, A., S.M. Sharland, P.W. Tasker, and C.J. Tweed. 1988b. *Extensions to the Coupled Chemical Equilibria and Migration Code CHEQMATE*. NSS-R.115. Oxon, United Kingdom: Harwell Laboratory.
- Helgeson, H.C. 1970. A chemical and thermodynamic model of ore deposition in hydrothermal systems. *Fiftieth Anniversary Symposia*. B.A. Morgan, ed. Washington, D.C.: Mineralogical Society of America Special. 3: 155-186.
- Helgeson, H.C. 1979. *Mass Transfer Among Minerals and Hydrothermal Solutions*. H.L. Barnes, ed. New York, NY: Wiley.

- Helgeson, H.C., J.M. Delany, H.W. Nesbitt, and D.K. Bird. 1978. Summary and critique of the thermodynamic properties of rock-forming minerals. *American Journal of Science* 278A: 1-229.
- Helgeson, H.C., W.M. Murphy, and P. Aagaard. 1984. Thermodynamic and kinetic constraints on reaction rates among minerals and aqueous solutions. II. Rate constants, effective surface area, and the hydrolysis of feldspar. *Geochimica et Cosmochimica Acta* 48: 2405-2432.
- Hem, J.D. 1985. *Study and Interpretation of the Chemical Characteristics of Natural Water*. Water-Supply Paper 2254. Alexandria, VA: USGS.
- Henley, R.W., A.H. Truescell, P.B. Barton, Jr., and J.A. Whitney. 1985. *Fluid—Mineral Equilibria in Hydrothermal Systems: Reviews in Economic Geology, Volume 1*. J.M. Robertson, ed. El Paso, TX: Society of Economic Geologists.
- Hillel, D. 1980a. *Fundamentals of Soil Physics*. New York, NY: Academic Press.
- Hillel, D. 1980b. *Applications of Soil Physics*. New York, NY: Academic Press.
- Hodgkinson, D.P., and P.J. Bourke. 1980. Initial assessment of the thermal stresses around a radioactive waste depository in hard rock. *Annals of Nuclear Energy* 7: 541-552.
- Hoek E., and Brown E.T. 1980. *Underground Excavations in Rock*. London, UK: Institute of Mining and Metallurgy (IMM).
- Hoffman, R.. 1981. *STEALTH—A Lagrangian Explicit Finite Difference Code for Solids, Structural, and Thermohydraulic Analysis, Introduction and Guide*. EPRI NP-2080-CCM-SY. Palo Alto, CA: EPRI.
- Hohorst, J.K., A. Buccafurni, E.R. Carlson, R. Chambers, S.V. Chmielewski, D.L. Hagrman, N.L. Hampton, J.K. Hohorst, E.T. Laats, R.E. Mason, M.L. McComas, K.A. McNeil, R.L. Miller, M.A. Morgan, C.S. Olsen, and G.A. Reymann. 1990. *SCDAP/RELAP5/MOD2 Code Manual, Volume 4: MATPRO-A Library of Materials Properties for Light-Water-Reactor Accident Analysis*. NUREG/CR-5273. Washington, D.C.: NRC.
- Holland, H.D., and S.D. Malinin. 1979. The solubility and occurrence of non-ore minerals. *Geochemistry and Hydrothermal Ore Deposits*. H.L. Barnes, ed. New York, NY: Wiley: 461-508.
- Horton, R., P.J. Wierenga, and D.R. Nielsen. 1983. Evaluation of methods for determining the apparent thermal diffusivity of soil near the surface. *Soil Science Society of America Journal* 47(1): 25-32.
- Horton, R., and P.J. Wierenga. 1984. The effect of column wetting on soil thermal conductivity. *Soil Science* 138(2): 101-108.

- Hostetler, C.J., and R.L. Erikson. 1989a. *FASTCHEM™ Package, Vol. 5: User's Guide to the EICM Coupled Geohydrochemical Transport Code*. EPRI-EA-5870-CCM. Palo Alto, CA: EPRI.
- Hostetler, C.J., R.L. Erikson, J.S. Fruchter, and C.T. Kincaid. 1989b. *FASTCHEM™ Package, Vol. 1: Overview and Application to a Chemical Transport Problem*. EPRI-EA-5870. Palo Alto, CA: EPRI.
- Huyakorn, P.S., B.H. Lester, and J.W. Mercer. 1983. An efficient finite element technique for modeling transport in fractured porous media 2. Nuclide decay chain transport. *Water Resources Research* 19(5): 1286-1296.
- Incropera, F.P., and D.P. Dewitt. 1981. *Fundamentals of Heat Transfer*. New York, NY: Wiley.
- Jackson, K.J. 1988. *Verification and Validation Studies of the Addition of Pitzer's Equations to the EQ3/6 Brine Model*. UCRL-53841. Livermore, CA: LLNL.
- Jackson, K.J., and T.J. Wolery. 1985. Extension of the EQ3/6 Computer Codes to Geochemical Modeling of Brines. C.M. Janzten, J.A. Stone, and R.C. Ewing, eds. *Scientific Basis for Nuclear Waste Management — VIII*. Pittsburgh, PA: Materials Research Society: 507-514.
- Jamet, P., D. Fargue, and G. de Marsily. 1990. Coupled processes in the near-field. P. Sellin, M. Apted, and J. Gago, eds. *Proceedings From the Technical Workshop on Near-Field Performance Assessment for High-Level Waste Held in Madris, October 15-17, 1990*. Stockholm, Sweden: Swedish Nuclear Fuel and Waste Management Company (SKB): 91-110.
- Jennings, A.A., and D.J. Kirkner. 1984. Instantaneous equilibrium approximation analysis. *Journal of the Hydraulic Division of the American Society of Civil Engineers* 110: 1700-1717.
- Jinzhong, Y. 1988. Experimental and numerical studies of solute transport in two-dimensional saturated-unsaturated soil. *Journal of Hydrology* 97: 303-322.
- Johnson, J.W., and D. Norton. 1991. Critical phenomena in hydrothermal systems: State, thermodynamic, electrostatic, and transport properties of H<sub>2</sub>O in the critical region. *American Journal of Science* 291: 541-648.
- Johnson, J.W., E.H. Oelkers, and H.C. Helgeson. 1991. *SUPCRT92: A Software Package for Calculating the Standard Molal Thermodynamic Properties of Minerals, Gases, Aqueous Species, and Reactions from 1 to 5000 bars and 0° to 1000°C*. Livermore, CA: LLNL.
- Jones, R.H., and R.E. Ricker. 1987. *Stress corrosion cracking. Metal Handbook, 9th Edition, Volume 13. Corrosion*. Metals Park, OH: American Society of Metallurgy, Inc. (ASMI).
- Jury, W.A., G. Sposito, and R.E. White. 1986. A transfer function model of solute transport through soil. 1. Fundamental concepts. *Water Resources Research* 22(2): 243-247.

- Jury, W.A., H. El Abd, and T. Collins. 1983. Field scale transport of nonadsorbing and adsorbing chemicals applied to the soil surface. D.M. Nielsen and M. Curl, eds. *Proceedings of the National Water Well Association/U.S. Environmental Protection Agency Conference on Characterization and Monitoring of the Vadose (Unsaturated) Zone*. Dublin, OH: National Water Well Association.
- Kelkar, S., and G.A. Zyvoloski. 1991. An efficient, three dimensional, fully-coupled hydro-thermo-mechanical simulation: FEHMS. *11th SPE Symposium on Reservoir Simulation, Anaheim, CA*.
- Kelsall, P.C., J.B. Case, and C.R. Chabannes. 1984. Evaluation of excavation-induced changes in rock permeability. *International Journal of Rock Mechanics and Mineral Science and Geomechanical Abstracts* 21(3): 123-135.
- Kerrisk, J.F. 1987. *Groundwater Chemistry at Yucca Mountain, Nevada, and Vicinity*. LA-10929-MS. Los Alamos, NM, Los Alamos National Laboratory (LANL).
- Key, S.W. 1987. *SPECTROM-331. A Finite Element Computer Program for the Large Deformation Elastic and Inelastic, Transient Dynamic Response of Three-Dimensional Solids and Structures*. RE/SPEC Topical Report RSI-0299. Rapid City, SD: RE/SPEC.
- Kincaid, C.T. 1988. *FASTCHEM™ Package, Vol. 3: User's Guide to the ETUBE Pathline and Streamtube Database Code*. EPRI-EA-5870-CCM. Palo Alto, CA: EPRI.
- Kincaid, C.T., J.R. Morrey, and J.E. Rogers. 1984a. *Geohydrochemical Models for Solute Migration, Vol 1: Process Description and Computer Code Selection*. EPRI-EA-3417. Palo Alto, CA: EPRI.
- Kincaid, C.T., J.R. Morrey, S.B. Yabusaki, A.R. Felmy, and J.E. Rogers. 1984b. *Geohydrochemical Models for Solute Migration, Vol. 2: Preliminary Evaluation of Selected Computer Codes*. EPRI-EA-3417. Palo Alto, CA: EPRI.
- Kirkner, D.J., and H. Reeves. 1988. Multicomponent mass transport with homogeneous and heterogeneous chemical reactions: Effect of the chemistry on the choice of numerical algorithm. 1. Theory. *Water Resources Research* 24(10): 1719-1729.
- Klavetter, E.A., and R.R. Peters. 1985. *Development of Flow Models for Fractured, Porous Media Based on Two Different Conceptual Models*. SAND85-0855C. Albuquerque, NM: SNL.
- Klavetter, E.A., and R.R. Peters. 1986. *Estimation of Hydrologic Properties of an Unsaturated, Fractured Rock Mass*. SAND84-2642. Albuquerque, NM: SNL.
- Kool, J.B., J.C. Parker, and M.T. Van Genuchten. 1987. Parameter estimation for unsaturated flow and transport models: A review. *Journal of Hydrology* 91: 255-293.

- Krishnaswami, S., W.C. Graustein, K.K. Turekian, and J.F. Dowd. 1982. Radium, thorium and radioactive lead isotopes in groundwaters: application to the in situ determination of adsorption-desorption rate constants and retardation factors. *Water Resources Research* 18(6): 1633-1675.
- Krupka, K.M., R.L. Erikson, S.V. Mattigod, J.A. Schramke, C.E. Cowan, L.E. Eary, J.R. Morrey, R.L. Schmidt, and J.M. Zachara. 1988. *Thermochemical Data Used by the FASTCHEM™ Package*. EPRI-EA-5872. Palo Alto, CA: EPRI.
- Kulacki, F.A., and M. Keyhani. 1987. Heat transfer aspects of nuclear waste disposal. *Heat Transfer Problems in Nuclear Waste Management*. E.V. McAssey, Jr., and V.E. Schrock, eds. HTD-67. New York, NY: ASME: 1-17.
- Laryea, D.B., D.E. Elrick, and M.J.L. Robin. 1982. Hydrodynamic dispersion involving cationic adsorption during unsaturated transient water flow in soil. *Soil Science of America Journal* 46: 667-671.
- Lasaga, A.C. 1981a. Rate laws of chemical reactions. *Reviews in Mineralogy, Volume 8: Kinetics of Geochemical Processes*. A.C. Lasaga, and R.J. Kirkpatrick, eds. Washington, D.C.: Mineralogical Society of America: 1-68.
- Lasaga, A.C. 1981b. Transition State Theory. *Reviews in Mineralogy, Volume 8: Kinetics of Geochemical Processes*. A.C. Lasaga, and R.J. Kirkpatrick, eds. Washington, D.C.: Mineralogical Society of America: 135-170.
- Lasaga, A.C., and R.J. Kirkpatrick, eds. 1981. *Reviews in Mineralogy, Volume 8: Kinetics of Geochemical Processes*. Washington, D.C.: Mineralogical Society of America.
- Lawn, B., and T. Wilshaw. 1975. *Fracture of Brittle Solids*. New York, NY: Cambridge University Press.
- Leslie, B.W. 1991. *Decay Series Disequilibrium Applied to the Study of Rock-Water Interaction in the Coso and the Salton Sea Geothermal Systems*. Ph.D. Dissertation. Los Angeles, CA: University of Southern California.
- Lewis, T. 1990. Fluid flow in tectonic regimes. B.E. Nesbitt, ed. *Short Course on Fluids in Tectonically Active Regimes of the Continental Crust*. Mineralogical Association of Canada: 49-74.
- Lienhard, J.H. 1987. *A Heat Transfer Textbook*. Englewood Cliffs, NJ: Prentice-Hall.
- Lin, W., and W.D. Daily. 1989. Laboratory study of fracture healing in Topopah Spring Tuff-implications for near field hydrology. *Nuclear Waste Isolation in the Unsaturated Zone Focus '89 Proceedings*. La Grange Park, IL: ANS: 443-449.

- Lin, W., and W. Daily. 1990. Hydrological properties of Topopah Spring Tuff under a thermal gradient: laboratory results. *International Journal of Rock Mechanics and Mineral Science and Geomechanical Abstracts* 27: 373-385.
- Lin, W., A. Ramirez, and D. Watwood. 1991. *Temperature-Measurements from a Horizontal Heater Test in G-Tunnel*. UCRL-JC-106693. Livermore, CA: LLNL.
- Liu, C.W., and T.N. Narasimhan. 1989a. Redox-controlled multiple-species reactive chemical transport 1. Model development. *Water Resources Research* 25(5): 869-882.
- Liu, C.W., and T.N. Narasimhan. 1989b. Redox-controlled multiple-species reactive chemical transport 2. Verification and application. *Water Resources Research* 25(5): 883-910.
- Love, A.E.H. 1944. *A Treatise on the Mathematical Theory of Elasticity, 4th Edition*. New York, NY: Dover.
- Macdonald, D.D., and G.A. Cragolino. 1989. Corrosion of steam cycle materials. P. Cohen, ed. *The ASME Handbook on Water Technology for Thermal Power Systems*. New York, NY: ASME.
- Mangold, D.C., and C. Tsang. 1991. A summary of subsurface hydrological and hydrochemical models. *Reviews of Geophysics* 29(1): 51-79.
- Mansell, R.S., S.A. Bloom, H.M. Selim, and R.D. Rhue. 1988. Simulated transport of multiple cations in soil using variable selectivity coefficients. *Soil Science Society of America Journal* 52: 1533-1540.
- Mansell, R.S., S.A. Bloom, and L.A.G. Aylmore. 1990. Simulating cation transport during unsteady, unsaturated water flow in sandy soil. *Soil Science* 150: 730-744.
- Manteufel, R.D. 1991. *Heat Transfer in an Enclosed Rod Array*. Ph.D. Thesis. Cambridge, MA: Massachusetts Institute of Technology, Department of Mechanical Engineering.
- McDowell-Boyer, L.M., J.R. Hunt, and N. Sitar. 1986. Particle transport through porous media. *Water Resources Research* 22(13): 1901-1921.
- McKinley, I.G., and W.R. Alexander. 1992. Constraints on the applicability of in situ distribution coefficient values. *Journal of Environmental Radiochemistry*. In press.
- Means, J.L., A.S. Maest, and D.A. Crerar. 1983. *Organic Geochemistry of Deep Ground Waters and Radionuclide Partitioning Experiments Under Hydrothermal Conditions*. ONWI-448. Columbus, OH: Office of Nuclear Waste Isolation (ONWRI).
- Miller, C.W. 1983. *CHEMTRN User's Manual*. LBL-16152. Berkeley, CA: Earth Sciences Division, LBL.

- Miller, C.W., and L.V. Benson. 1983. Simulation of solute transport in a chemically reactive heterogeneous system: Model development and application. *Water Resources Research* 19(2): 381-391.
- Montazer, P., and W.E. Wilson. 1984. *Conceptual Hydrologic Model of Flow in the Unsaturated Zone, Yucca Mountain, Nevada*. Water Resources Investigations Report 84-4345 Denver, CO: USGS.
- Moore, W.J. 1972. *Physical Chemistry, 4th ed.* Englewood Cliffs, NJ: Prentice-Hall.
- Morland, L.W. 1974. Elastic response of regulatory jointed media. *Geophysical Journal. Royal Astronomical Society* 37: 435-446.
- Morrey, J.R. 1988. *FASTCHEM™ Package. Volume 4: User's Guide to the ECHM Equilibrium Geochemistry Code*. EA-5870-CCM. Palo Alto, CA: EPRI.
- Morrey, J.R., and C.J. Hostetler. 1985. Coupled geochemical and solute transport code development. Jacobs, G.K., and S.K. Whatley, eds. *Proceedings of the Conference on the Application of Geochemical Models to High-Level Nuclear Waste Repository Assessment, Oak Ridge, Tennessee, October 2-5, 1984*. NUREG/CP-0062. Washington, D.C.: NRC.
- Morrey, J.R., C.T. Kincaid, C.J. Hostetler, S.B. Yabusaki, and L.W. Vail. 1986. *Geohydrochemical Models for Solute Migration. Volume 3: Evaluation of Selected Computer Codes*. EA-3417. Palo Alto, CA: EPRI.
- Mulay, S.P. 1988. *Diffusion of Heat and Mass Transfer in Partially Saturated Porous Media*. Ph.D. Thesis. Chicago, IL: Illinois Institute of Technology.
- Murphy, W.M. 1989. *Constraints on the Chemistry of Groundwater in the Unsaturated Zone at Yucca Mountain, Nevada, and in the Proposed Repository at That Site*. San Antonio, TX: CNWRA.
- Murphy, W.M. 1990. Performance assessment perspectives with reference to the proposed repository at Yucca Mountain, Nevada. P. Sellin, M. Apted, and J. Gago, eds. *Proceedings From the Technical Workshop on Near-Field Performance Assessment for High-Level Waste Held in Madrid, October 15-17, 1990*. Stockholm, Sweden: SKB:11-24.
- Murphy, W.M., and H.C. Helgeson. 1987. Thermodynamic & kinetic constraints on reaction rates among minerals and aqueous solutions. III. Activated complexes & pH-dependence of the rates of feldspar, pyronene, wollastonite, and alivine hydrolysis. *Geochimica et Cosmochimica Acta* 51:3137-3154.
- Nair, S., D. Longwell, and C. Seigneur. 1990. Simulation of chemical transport in unsaturated soil. *Journal of Environmental Engineering* 116: 214-235.
- National Research Council. 1992. *Ground Water at Yucca Mountain: How High Can it Rise?* Washington, D.C.: National Academy Press.

- Naumov, G.B., B.N. Ryzhenko, and I.L. Khodakovsky. 1974. *Handbook of Thermodynamic Data*. U.S. Geological Survey WRD-74-001. Springfield, VA: NTIS.
- Neretnieks, I., and A. Rasmuson. 1984. An approach to modeling radionuclide migration in a medium with strongly varying velocity and block sizes along the flow path. *Water Resources Research* 20(12): 1823-1836.
- Nielsen, D.R., M.T. Van Genuchten, and J.W. Biggar. 1986. Water flow and solute transport processes in the unsaturated zone. *Water Resources Research* 22(9): 89s-108s.
- Nimick, F.B. 1990. *The Thermal Conductivity of Seven Thermal/Mechanical Units at Yucca Mountain, Nevada*. SAND88-1387. Albuquerque, NM: SNL.
- Nitao, J.J. 1988. *Numerical Modeling of the Thermal and Hydrological Environment Around a Nuclear Waste Package Using the Equivalent Continuum Approximation: Horizontal Emplacement*. UCID-21444. Livermore, CA: LLNL.
- Nitao, J.J. 1991. Theory of matrix and fracture flow regimes in unsaturated, fractured porous media. *Proceedings of the High-Level Radioactive Waste Management Conference*. La Grange Park, IL: ANS: 845-852.
- Nitao, J.J., T.A. Buscheck, and D.A. Chesnut. 1992. The implications of episodic nonequilibrium fracture-matrix flow on site suitability and total system performance. *Proceedings of the High-Level Radioactive Waste Management Conference*. La Grange Park, IL: ANS: 279-296.
- Nkedi-Kizza, P., J.W. Biggar, H.M. Selim, M.T. van Genuchten, P.J. Wierenga, and J.M. Davidson. 1984. On the equivalence of two conceptual models for describing ion exchange during transport through an aggregated oxisol. *Water Resources Research* 20(8): 1123-1130.
- Noorishad, J., C.F. Tsang, and P.A. Witherspoon. 1984. Coupled thermal-hydraulic-mechanical phenomena in saturated fractured porous rocks: numerical approach. *Journal Geophysical Research* 89(B12): 10365-10374.
- Noorishad, J., C.L. Carnahan, and L.V. Benson. 1987. *Development of the Non-Equilibrium Reactive Chemical Transport Code CHMTRNS*. LBL-22361. Berkeley, CA: LBL.
- Noorishad, J., and C.F. Tsang. 1989. *Recent Enhancement of the Coupled Hydro-Mechanical Code: ROCMAS II*. Technical Report 89: 4. Stockholm, Sweden: SKI.
- Nordstrom, D.K., and J.W. Ball. 1984. Chemical models, computer programs and metal complexation in natural waters. *Complexation of Trace Metals in Natural Waters*. C.J.M. Kramer and J.C. Duinker, ed. Netherlands: Martinus Nijhoff/Dr. J.W. Junk Publishing Co.: 149-169.

- Nordstrom, D.K., and J.L. Munoz. 1985. *Geochemical Thermodynamics*. Menlo Park, CA: The Benjamin/Cummings Publishing Co.
- Nordstrom, D.K., L.N. Plummer, T.M.L. Wigley, T.J. Wolery, J.W. Ball, E.A. Jenne, R.L. Bassett, D.A. Crerar, T.M. Florence, B. Fritz, M. Hoffman, G.R. Holdren, G.M. Lafon, S.V. Mattigod, R.E. McDuff, F.M.M. Morel, M.M. Reddy, G. Sposito, and J. Thrailkill. 1979. Comparison of computerized chemical models for equilibrium calculations in aqueous systems. *Chemical Modeling in Aqueous Systems. Speciation, Sorption, Solubility, and Kinetics*. E.A. Jenne, ed. Washington, D.C.: ACS: 857-892.
- Nordstrom, D.K., L.N. Plummer, D. Langmuir, E. Busenberg, H.M. May, B.F. Jones, and D.L. Parkhurst. 1990. Revised chemical equilibrium data for major water-mineral reactions and their limitations. *Chemical Modeling of Aqueous Systems II*. D.C. Melchior, and R.L. Bassett, eds. Washington, D.C.: ACS: 398-413.
- Norton, D., and L.M. Cathles. 1979. Thermal Aspects of Ore Deposition. H.L. Barnes, ed. *Geochemistry of Hydrothermal Ore Deposits*. New York, NY: Wiley: 611-631.
- Nowacki, W. 1962. *Thermoelasticity*. Oxford, England: Pergamon Press.
- Oetting, F.L., M.H. Rand, and R.J. Ackerman. 1976. *The Chemical Thermodynamics of Actinide Elements and Compounds. Part 1. The Actinide Elements*. Vienna, Austria: IAEA.
- Ohnishi, Y., M. Nishigaki, A. Kobayashi, and S. Akiyama. 1990. Three dimensional coupled thermo-hydraulic mechanical analysis code with PCG method. *Proceedings International Symposium. GEOVAL-90*. Stockholm Sweden:SKI 14-17.
- Olague, N.E., D.E. Longsine, J.E. Campbell, and C.D. Leigh. 1991. *User's Manual for the NEFTRAN II Computer Code*. NUREG/CR-5618. Washington, D.C.: NRC.
- Olsson, W.A., and A.K. Jones. 1980. *Rock Mechanics Properties of Volcanic Tuffs from the Nevada Test Site*. SAND80-1453. Albuquerque, NM: SNL.
- O'Neal, W.C., D.W. Gregg, J.N. Hockman, E.W. Russell, and W. Stein. 1984. *Preclosure Analysis of Conceptual Waste Package Designs for a Nuclear Waste Repository in Tuff*. UCRL 53595. Livermore, CA: LLNL.
- Ortoleva, P., E. Merino, J. Chadam, and C.H. Moore. 1987. Geochemical self-organization. I: Feedback mechanisms and modeling approach. *American Journal of Science* 287: 979-1002.
- Pabalan, R.T., and K.S. Pitzer. 1990. Chemical Modeling of Aqueous Systems II. ACS Symposium Series II. *Models for aqueous electrolyte mixtures for systems extending from dilute solutions to fused salts*. D. Melchior, and R.L. Bassett, eds. Washington, D.C.: ACS: 44-57.

- Papelis, C., K.F. Hayes, and J.O. Leckie. 1988. *Hydraql: A Program for the Computation of Chemical Equilibrium Composition of Aqueous Batch Systems Including Surface-Complexation Modeling of Ion Adsorption at the Oxide/Solution Interface*. Technical Report No. 306. Stanford, CA: Department of Civil Engineering, Stanford Univ.
- Park, U-Sun. 1991. *Gaseous and semi-volatile radionuclides*. Presentation to the Nuclear Waste Technical Review Board, June 25-27. Washington, D.C.: DOE.
- Parker, D.R., L.W. Zelazny, and T.B. Kinraide. 1987. Improvements to the program GEOCHEM. *Soil Science Society of America Journal* 51: 488-491.
- Parker, J.C., and P.M. Jardine. 1986. Effects of heterogeneous adsorption behavior on ion transport. *Water Resources Research* 22(8): 1334-1340.
- Parkhurst, D.L., D.C. Thorstenson, and L.N. Plummer. 1980. *PHREEQE—A Computer Program for Geochemical Calculations*. USGS Water Research Investigations 80-96. Reston, VA: USGS.
- Parkhurst, D.L., D.C. Thorstenson, and L.N. Plummer. 1990. *PHREEQE: A Computer Program for Geochemical Calculations: Revised and Reprinted August, 1990*. USGS Water Research Investigations 80-96. Reston, VA: USGS.
- Parry, W.T., J.M. Ballantyne, and N.L. Bryant. 1980. Hydrothermal alteration enthalpy and heat flow in the Roosevelt Hot Springs Thermal Area, UT. *Journal of Geophysical Research* 85: 2559-2566.
- Peters, R.R., and E.A. Klavetter. 1988. A continuum model for water movement in an unsaturated fractured rock mass. *Water Resources Research* 24(3): 416-430.
- Peters, R.R., E.A. Klavetter, I.J. Hall, S.C. Blair, P.R. Heller, and G.W. Gee. 1984. *Fracture and Matrix Hydrologic Characteristics of Tuffaceous Materials from Yucca Mountain, Nye County, Nevada*. SAND84-1471. Albuquerque, NM: SNL.
- Philip, J.R., and D.A. de Vries. 1957. Moisture movement in porous materials under temperature gradients. *Transactions, American Geophysical Union* 38(2): 222-232.
- Phillips, S.L., F.V. Hale, L.F. Silvester, and M.D. Siegel. 1988. *Thermodynamic Tables for Nuclear Waste Isolation: Aqueous Solutions Database*. NUREG/CR-4864. Washington, D.C.: NRC.
- Pinder, G.F. 1976. *Galerkin Finite Element Models for Aquifer Simulation*. Princeton Univ. Unpublished report.
- Pinder, G.F., and W.G. Gray. 1977. *Finite Element Simulation in Surface and Subsurface Hydrology*. New York, NY: Academic Press.

- Pitzer, K.S. 1973. Thermodynamics of electrolytes, 1. Theoretical basis and general equations. *Journal of Physical Chemistry* 77: 268-277.
- Pitzer, K.S. 1979. Theory: ion interaction approach. *Activity Coefficients in Electrolyte Solutions*. M. Pytkowicz, ed. Boca Raton, FL: CRC Press: 157-208.
- Plummer, L.N., B.F. Jones, and A.H. Truesdell. 1976. *WATEQF - A FORTRAN IV Version of WATEQ, a Computer Program for Calculating Chemical Equilibrium of Natural Waters*. USGS-WRI-76-13. Denver, CO: USGS.
- Plummer, L.N., D.L. Parkhurst, G.W. Fleming, and S.A. Dunkle. 1988. *A Computer Program Incorporating Pitzer's Equations for Calculation of Geochemical Reactions in Brines*. USGS-WR-88-4153. Washington, D.C.: USGS.
- Pollock, D.W. 1982. *Fluid Flow and Energy Transport in a High-Level Radioactive Waste Repository in Unsaturated Alluvium*. Ph.D. Thesis. Urbana, IL: University of Illinois at Urbana-Champaign.
- Pollock, D.W. 1986. Simulation of fluid flow and energy transport processes associated with high-level radioactive waste disposal in unsaturated alluvium. *Water Resources Research*. 22(5): 765-775.
- Potter, M.C., and J.F. Foss. 1982. *Fluid Mechanics*. Okemos, MI: Great Lakes Press.
- Potter, R.W., and D.L. Brown. 1977. *The Volumetric Properties of Aqueous Sodium Chloride Solutions From 0° to 500° C and Pressures Up to 2000 bars Based on a Regression of Available Data in the Literature*. USGS Bull: 1421-C: Reston, VA: USGS.
- Powers, D.W., J.W. Rudnicki, and L. Smith. 1991. *External Peer Review Panel Majority Report*. Washington, D.C.: DOE.
- Price, J.G., S.T. Conlon, and C.D. Henry. 1987. Tectonic controls on orientation and size of epithermal veins. *North American conference on Tectonic Control of Ore Deposits*. Rolla, MO.
- Prigogine, I. 1955. *Introduction to Thermodynamics of Irreversible Processes*. New York, NY: Wiley.
- Pruess, K. 1983. *Development of the General Purpose Simulator MULKOM*. Annual Report 1982. Berkeley, CA: LBL.
- Pruess, K. 1985. A quantitative model of vapor dominated geothermal reservoirs as heat pipes in fractured porous rock. *Transactions. Geothermal Resources Council* 9(ii): 353-361.
- Pruess, K. 1987. *TOUGH User's Guide*. NUREG/CR-4645. Washington, D.C.: NRC.

- Pruess, K., and J.S.Y. Wang. 1987. Numerical modeling of isothermal and nonisothermal flow in unsaturated fractured rock: A review. D.D. Evans and T.J. Nicholson, eds. *Geophysical Monograph 42: Flow and Transport Through Unsaturated Fractured Rock*. Washington, D.C.: American Geophysical Union: 11-21.
- Pruess, K., J.S.Y. Wang, and Y.W. Tsang. 1987. *Effective continuum approximation for modeling fluid and heat flow in fractured porous tuff*. SAND 86-7000. Albuquerque, NM: SNL.
- Pruess, K., J.S.Y. Wang, and Y.W. Tsang. 1990a. On thermohydrologic conditions near high-level nuclear wastes emplaced in partially saturated fractured tuff 1. Simulation studies with explicit consideration of fracture effects. *Water Resources Research* 26(6): 1235-1248.
- Pruess, K., J.S.Y. Wang, and Y.W. Tsang. 1990b. On thermohydrologic conditions near high-level nuclear wastes emplaced in partially saturated fractured tuff 2. Effective continuum approximation. *Water Resources Research* 26(6): 1249-1261.
- Pusch, T. 1989. Alteration of the hydraulic conductivity of rock by tunnel excavation. *International Journal of Rock Mechanics and Mineral Science and Geomechanical Abstracts* 26(1): 79-83.
- Radhakrishna, H.S., K.C. Lau, and A.M. Crawford. 1990. Experimental modeling of the near-field thermal regime in a nuclear-fuel waste disposal vault. *Engineering Geology* 28: 337-351.
- Rajen, G., and F.A. Kulacki. 1987. Experimental and numerical study of natural convection in a porous layer locally heated from below — A regional laboratory model for a nuclear waste repository. HTD-67. E.V. McAssey, Jr., and V.E. Schrock, eds. *Heat Transfer Problems in Nuclear Waste Management*. New York, NY: ASME: 19-26.
- Ramirez, A.L., et al. 1991a. *Prototype Engineered Barrier System Field Tests (PEBSFT) Progress Report through November 1, 1988*. UCID-106159. Livermore, CA: LLNL.
- Ramirez, A.L. et al. 1991b. *Prototype Engineered Barrier Systems Field Test (PEBSFT) Final Report*. UCID-106159. Livermore, CA: LLNL.
- Ramirez, A.L., R.C. Carlson, and T.A. Buscheck. 1991c. *In Situ Changes in the Moisture Content of Heated, Welded Tuff Based on Thermal Neutron Measurements*. UCRL-ID-104715. Livermore, CA: LLNL.
- Rard, J.A. 1989. *Chemical Thermodynamics of Technetium*. UCRL-100554. Livermore, CA: LLNL.
- Rasmussen, T.C., and D.D. Evans. 1987. *Unsaturated Flow and Transport Through Fractured Rock Related to High-Level Waste Repositories*. NUREG/CR-4655. Washington, D.C.: NRC.

- Rasmussen, T.C., and D.D. Evans. 1989. *Fluid Flow and Solute Transport Modeling Through Three-Dimensional Networks of Variably Saturated Discrete Fractures*. NUREG/CR-5239. Washington, D.C.: NRC.
- Rasmussen, T.C., D.D. Evans, P.J. Sheets, and J.H. Blanford. 1990. *Unsaturated Fractured Rock Characterization Methods and Data Sets at the Apache Leap Tuff Site*. NUREG/CR-5596. Washington, D.C.: NRC.
- Read, D., and T.W. Broyd. 1989. *The CHEMVAL Project: Status Report, March 1989*. Richland, WA: PNL.
- Reeves, H., and D.J. Kirkner. 1988. Multicomponent mass transport with homogeneous and heterogeneous chemical reactions: Effect of the chemistry on the choice of numerical algorithm. 2. Numerical results. *Water Resources Research* 24(10): 1730-1739.
- Richardson, S.M., and H.Y. McSween. 1989. *Geochemistry: Pathways and Processes*. Englewood Cliffs, NJ: Prentice Hall.
- Rimstidt, J.D., W.D. Newcomb, and D.L. Shettel, Jr. 1989. A vertical thermal gradient experiment to simulate conditions in vapor dominated geothermal systems, epithermal gold deposits, and high-level radioactive repositories in unsaturated media. *Proceedings of the 4th International Symposium on Water-Rock Interaction*. A.A. Balkema, in Rotterdam, Netherlands: 585-588.
- Robie, R.A., B.S. Hemingway, and J.R. Fisher. 1978. *Thermodynamic Properties of Minerals and Related Substances at 298.15 K and 1 Bar (10<sup>5</sup> Pascals) 2 Pressure and at Higher Temperatures*. USGS Bull. 1452, reprinted with corrections 1979. Washington, D.C.: USGS.
- Rockhold, M.L., B. Sagar, and M.P. Connelly. 1992. *Three-Dimensional Modeling of Unsaturated Flow in the Vicinity of Proposed Exploratory Shaft Facilities at Yucca Mountain, Nevada*. PNL-7474. Richland, WA: PNL.
- Roedder, E. 1984. *Reviews in Mineralogy, Volume 12: Fluid Inclusions*. Washington, D.C.: Mineralogical Society of America.
- Roglans-Ribas, J., and B.I. Spinrad. 1989. A simplified thermal analysis of a nuclear waste repository. *Annals of Nuclear Energy* 16(8): 371-382.
- Rose, A.W., and D.M. Burt. 1979. Hydrothermal alteration. H.L. Barnes, ed. *Geochemistry of Hydrothermal Ore Deposits*. New York, NY: Wiley: 173-235.
- Roth, K., W.A. Jury, and H.A. Fluhler. 1990a. Solute transport through unsaturated soil: the field evidence. *Agronomy Abstracts, Soil Science Society of America 82nd Annual Meeting*. San Antonio, TX: Soil Science Society of America: 218.

- Roth, K., H. Fluhler, W.A. Jury, and J.C. Parker. 1990b. Prediction of cation transport in soils using cation exchange reactions. *Field-Scale Solute and Water Transport Through Soil*. H.M. Selim, R.S. Mansell, L.A. Gaston, H. Fluhler, and R. Schulin, eds. Basel, Switzerland: Birkhauser Verlag: 223-238.
- Rubin, J. 1983. Transport of reacting solutes in porous media: relation between mathematical nature of problem formulation and chemical nature of reactions. *Water Resources Research* 19(5): 1231-1252.
- Rubin, J., and R.V. James. 1973. Dispersion affected transport of reacting solutes in saturated porous media: Galerkin method applied to equilibrium-controlled exchange in unidirectional steady water flow. *Water Resources Research* 9(5): 1332-1356.
- Runchal, A.K., and B. Sagar. 1992. *PORFLOW: A Multifluid Multiphase Model for Simulating Flow, Heat Transfer and Mass Transport in Fractured Porous Media, User's Manual — Version 2.40*. CNWRA 92-003. San Antonio, TX: CNWRA.
- Russo, D. 1989a. Field-scale transport of interacting solutes through the unsaturated zone: 1. Analysis of the spatial variability of the transport properties. *Water Resources Research* 25(12): 2475-2485.
- Russo, D. 1989b. Field scale transport of interacting solutes through the unsaturated zone: 2. Analysis of the spatial variability of the field response. *Water Resources Research* 25(12): 2487-2495.
- Rutqvist, J.O. Stephansson, J. Noorishad, and C.F. Tsang. 1991. Modeling of hydro-thermo-mechanical effects in a fracture intersecting a nuclear waste deposition hole. *Proceedings of High-Level Radioactive Waste Management Conference*. La Grange Park, IL: ANS: 547-554.
- Sadiq, M., and W.L. Lindsay. 1979. *Selection of Standard Free Energies of Formation for Use in Soil Chemistry*. Technical Bulletin 134. Fort Collins, CO: CSUES.
- Sadiq, M., and W.L. Lindsay. 1981. *Arsenic Supplement to Technical Bulletin 134: Selection of Standard Free Energies of Formation for Use in Soil Chemistry*. Technical Bulletin 134 (supplement). Fort Collins, CO: CSUES.
- Sagar, B., and A.K. Runchal. 1990. *PORFLO-3: A Mathematical Model for Fluid Flow, Heat, and Mass Transport in Variably Saturated Geologic Media, Theory and Numerical Methods, Version 1.0*. WHC-EP-0042. Richland, WA: Westinghouse Hanford Company.
- Sagar, B., and A.B. Gureghian. 1991. Performance Assessment Research. *Report on Research Activities for Calendar Year 1991*. W.C. Patrick. CNWRA 90-01A. San Antonio, TX: CNWRA.
- Schubert, G., and J.M. Straus. 1979. Steam-water counterflow in porous media. *Journal of Geophysical Research* 84(B4): 1621-1628.

- Scott, R.B., R.W. Spengler, S. Diehl, A.R. Lappin, and M.P. Chornack. 1982. Geologic character of tuffs in the unsaturated zone at Yucca Mountain, southern Nevada. *Role of the Unsaturated Zone in Radionuclide and Hazardous Waste Disposal*. J. Mercer, P.S. Rao, and I.W. Marine, eds. Ann Arbor, MI: Ann Arbor Science: 289-335.
- Selim, H.M., J.M. Davidson, and R.S. Mansell. 1976. Evaluation of a 2-site adsorption-desorption model for describing solute transport in soils. *1976 Summer Computer Simulation Conference*. La Jolla, CA: Simulation Councils, Inc.: 444-448.
- Selim, H.M., R.S. Mansell, L.A. Gaston, H. Fluhler, and R. Schulin. 1990. *Field-Scale Solute and Water Transport Through Soil*. K. Roth, H. Fluhler, W.A. Jury, and J.C. Parker, eds. Prediction of cation transport in soils using cation exchange reactions. Basel, Switzerland: Birkhauser Verlag: 223-238.
- Serne, R.J., R.C. Arthur, and K.M. Krupka. 1990. *Review of Geochemical Processes and Codes for Assessment of Radionuclide Migration Potential at Commercial LLW Sites*. PNL-7285. Richland, WA: PNL.
- Shen, B., and O. Stephansson. 1990a. *3DEC: Mechanical and Thermomechanical Analysis of Glaciation and Thermal Loading of a Waste Repository*. SKITR90: 3. Stockholm, Sweden: SKI.
- Shen, B., and O. Stephansson 1990b. *Modeling of Rock Mass Response to Repository Excavations, Thermal Loading from Radioactive Waste and Welling Pressure of Buffer Material*. SKITR90: 12. Stockholm, Sweden: SKI.
- Shi, G.H., and R.E. Goodman 1988. Discontinuous Deformation Analysis — A New Method for Computing Stress, Strain and Sliding of Block Systems. *Key Questions in Rock Mechanics*. Rotterdam, Netherlands: A.A. Balkema, 381-393.
- Shock, E.L., and H.C. Helgeson. 1988. Calculation of the thermodynamic and transport properties of aqueous species at high pressures and temperatures: Correlation algorithms for ionic species and equation of state predictions to 5 kb and 1000 °C. *Geochimica et Cosmochimica Acta* 52: 2009-2036.
- Shock, E.L., and H.C. Helgeson. 1990. Calculation of the thermodynamic and transport properties of aqueous species at high pressures and temperatures: Standard partial molal properties of organic species. *Geochimica et Cosmochimica Acta* 54: 915-945.
- Siegel, M.D., R. Rechard, K.L. Erickson, J.O. Leckie, D.B. Kent, D.A. Grover, S.J. Phillips, R.V. Guzowski, and S. Faith. 1989. *Progress in Development of a Methodology for Geochemical Sensitivity Analysis for Performance Assessment. Volume 2: Speciation, Sorption, and Transport in Fractured Media*. NUREG/CR-5085. Washington, D.C.: NRC.
- Siegel, R., and J.R. Howell. 1981. *Thermal Radiation Heat Transfer*. New York, NY: McGraw-Hill.

- Siyag, R.S., R. Pal, and S.R. Poonia. 1983. Water transmission of unsaturated soil samples in relation to mixed Na-(Ca + Mg) solutions. *Geoderma* 31: 107-116.
- Skopp, J., W.R. Gardner, and E.J. Tyler. 1981. Solute movement in structured soils: two-region model with small interaction. *Soil Science Society of America Journal* 45: 837-842.
- Smith, R.M., and A.E. Martell. 1976. *Critical Stability Constants. Volume 4: Inorganic Complexes*. New York, NY: Plenum Press.
- Sokolnikoff, I.S. 1956. *Mathematical Theory of Elasticity*. New York, NY: McGraw-Hill.
- Sourirajan, S., and G.C. Kennedy. 1962. The system NaCl-H<sub>2</sub>O at elevated temperatures and pressures. *American Journal of Science* 260: 114-141.
- Sposito, G. 1986. Corrections to the program GEOCHEM. *Soil Science Society of America Journal* 50: 270.
- Sposito, G., and S.V. Mattigod. 1980. *GEOCHEM: A Computer Program for the Calculation of Chemical Equilibria in Soil Solutions and Other Natural Water Systems*. Riverside, CA: Report from University of California, Riverside.
- Sposito, G., R.E. White, P.R. Darrah, and W.A. Jury. 1986. A transfer function model of solute transport through soil. 3. The convection-dispersion equation. *Water Resources Research* 22(2): 255-262.
- Sterner, S.M., and R.J. Bodnar. 1991. Synthetic fluid inclusions. X: Experimental determination of P-V-T-X properties in the CO<sub>2</sub>-H<sub>2</sub>O system to 6 Kb and 700 °C. *American Journal of Science* 291: 1-54.
- Stumm, W., and J.J. Morgan. 1981. *Aquatic Chemistry. An Introduction Emphasizing Chemical Equilibria in Natural Waters*. New York, NY: Wiley.
- Suarez, D.L., J.D. Rhoades, R. Lavado, and C.M. Grieve. 1984. Effect of pH on saturated hydraulic conductivity and soil dispersion. *Soil Science Society of America Journal*. 48: 50-55.
- Sverjensky, D.A., E.L. Shock, and H.C. Helgeson. 1991. Prediction of the thermodynamic properties of inorganic aqueous metal complexes to 1000 °C and 5 kb. *Geochimica et Cosmochimica Acta* 55. Submitted for publication.
- Szymanski, J.S. 1989. *Conceptual Considerations of the Yucca Mountain Ground Water System with Special Emphasis on the Adequacy of This System to Accommodate a High-Level Nuclear Waste Repository*. Unpublished report. Washington, D.C.: DOE.
- Takenouchi, S., and G.C. Kennedy. 1964. The binary system H<sub>2</sub>O-CO<sub>2</sub> at high temperatures and pressures. *American Journal of Science* 262: 1055-1074.

- Takenouchi, S., and G.C. Kennedy. 1965. The solubility of carbon dioxide in NaCl solutions at high temperatures and pressures. *American Journal of Science* 263: 445-454.
- Tanger, J.C. IV, and H.C. Helgeson. 1988. Calculation of the thermodynamic and transport properties of aqueous species at high pressures and temperatures: revised equations of state for the standard partial molal properties of ions and electrolytes. *American Journal of Science* 288: 19-98.
- Thomas, D.M., and Gudmundsson. 1989. Advances in the study of solids deposition in geothermal systems. *Geothermics* 18: 5-15.
- Thomson, W. 1871. On the equilibrium of vapor at a curved surface of liquid. *Philosophical Magazine* 42: 448-452.
- Timoshenko, S.P., and J.N. Goodier. 1970. *Theory of Elasticity*. New York, NY: McGraw-Hill.
- Todreas, N.E., and M.S. Kazimi. 1990. *Nuclear Systems I, Thermal Hydraulic Fundamentals*. New York, NY: Hemisphere.
- Travis, B.J. 1984. *TRACR3D: A Model of Flow and Transport in Porous/Fractured Media*. LA-9667-MS. Los Alamos, NM: LANL.
- Travis, B.J., and H.E. Nuttall. 1987. *Two-Dimensional Numerical Simulation of Geochemical Transport in Yucca Mountain*. LA-10532-MS. Los Alamos, NM: LANL.
- Tripathi, V.S. 1984. *Uranium(VI) Transport Modeling: Geochemical Data and Submodels*. Ph.D. Dissertation. Stanford, CA: University of Stanford.
- Tritton, D.J. 1977. *Physical Fluid Dynamics*. Berkshire, England, United Kingdom: Von Nostrand Reinhold.
- Truesdell, A.H., and B.F. Jones. 1974. WATEQ—A computer program for calculating chemical equilibria of natural water. *Journal of Research U.S. Geological Survey* 2: 233-248.
- Tsang, C.F. 1987. Introduction to coupled processes. *Coupled Processes Associated with a Nuclear Waste Repositories*. C.F. Tsang, ed. San Diego, CA: Academic Press: 1-6.
- Tsang, C.F. 1991. Coupled hydromechanical—thermochemical processes in rock fractures. *Reviews of Geophysics* 29(4): 537-551.
- Tsang, Y.W., and K. Pruess. 1987. A study of thermally induced convection near a high-level waste repository in partially saturated fractured tuff. *Water Resources Research* 23(10): 1958-1966.
- Turcott, D.L. 1989. A heat pipe mechanism for volcanism and tectonics on Venus. *Journal of Geophysical Research* 94(B3): 2779-2785.

- Turner, D.R. 1991. *Sorption Modeling for High-Level Waste Performance Assessment: A Literature Review*. CNWRA 91-011. San Antonio, TX: CNWRA.
- Turner, D.R. 1992. Radionuclide sorption modeling using the MINTEQA2 speciation code. *Science Basis for Nuclear Waste Management—XVI*. Abstract. (to be published).
- Tweed, C.J. 1988. *A Guide to PICKER—A Data-Selection Tool for the Program PHREEQE*. AERE-R.12515. Oxon, United Kingdom: Harwell Laboratory.
- U.S. Code of Federal Regulations. 1992. *Disposal of High-Level Radioactive Wastes in Geologic Repositories*. Part 60 Chapter I, Title 10, Energy. Washington, D.C.: Office of the Federal Register.
- Updegraff, C.D. 1989. *Comparison of Strongly Heat-Driven Flow Codes for Unsaturated Media*. NUREG/CR-5367. Washington, D.C.: U.S. Nuclear Regulatory Commission.
- Valocchi, A.J. 1985. Validity of the local equilibrium assumption for modeling sorbing solute transport through homogeneous soils. *Water Resources Research* 21(6): 808-820.
- Valocchi, A.J., P.V. Roberts, G.A. Parks, and R.L. Street. 1981a. Simulation of the transport of ion-exchanging solutes using laboratory-determined chemical parameter values. *Ground Water* 19(6): 600-607.
- Valocchi, A.J., R.L. Street, and P.V. Roberts. 1981b. Transport of ion-exchanging solutes in groundwater: Chromatographic theory and field simulation. *Water Resources Research* 17(5): 1517-1527.
- van der Zee, S.E.A.T.M. 1990. Analysis of solute redistribution in a heterogeneous field. *Water Resources Research* 26(2): 273-278.
- van der Zee, S.E.A.T.M., and G.H. Bolt. 1991. Deterministic and stochastic modeling of reactive solute transport. *Journal of Contaminant Hydrology* 7: 75-93.
- van Eijkeren, J.C.H., and J.P.G. Loch. 1984. Transport of cationic solutes in sorbing porous media. *Water Resources Research* 20(6): 714-718.
- van Genuchten, R. 1978. *Calculating the Unsaturated Hydraulic Conductivity with a New, Closed-Form Analytical Model*. Research Report 78-WR-08. Princeton, NJ: Department of Civil Engineering, Princeton University.
- van Genuchten, M.T. 1980. A closed-form equation for predicting the hydraulic conductivity of unsaturated soils. *Soil Science Society of America Journal* 44: 892-898.
- van Genuchten, M.T., and P.J. Wierenga. 1976. Mass transfer studies in sorbing porous media, 1. Analytical solutions. *Soil Science Society of America Journal* 40: 473-480.

- van Genuchten, M.T., and W.A. Jury. 1987. Progress in unsaturated flow and transport modeling. *Reviews of Geophysics* 25(2): 135-140.
- van Konynenburg, R.A. 1991. Gaseous release of carbon-14: why the high-level waste regulations should be changed. *Proceedings of the High-Level Radioactive Waste Management Conference*. La Grange Park, IL: ANS: 313-319.
- Vaughan, P.J. 1987. Analysis of permeability reduction during flow of heated, aqueous fluid through Westerly Granite. C. Tsang, ed. *Coupled Processes Associated with Nuclear Waste Repositories*. Orlando, FL: Academic Press: 529-539.
- Verma, K., and K. Pruess. 1988. Thermohydrological conditions and silica redistribution near high-level nuclear waste emplaced in saturated geological formations. *Journal of Geophysical Research* 93(B2): 1159-1173.
- Viani, B. 1988. *Interim Report on Modeling Sorption with EQ3/6*. UCID-21308. Livermore, CA: LLNL.
- Voegele, M., E. Gardin, D. Lingle, M. Board, and N. Barton. 1981. Site characterization of joint permeability using the heated block test. *Proceedings of the 22nd U.S. Symposium on Rock Mechanics*. Rotterdam, Netherlands: A.A. Balkema: 120-127.
- Vutkuri, V. 1974. The effect of liquids on the tensile strength of limestone. *International Journal of Rock Mechanics* 11: 27-29.
- Wada, C., and H. Takahashi. 1990. Prediction of changes in elastic moduli due to water-rock interaction during operation of granitic HDR geothermal system. *Geothermics* 19(N1): 61-75.
- Wagman, D.D., W.H. Evans, V.B. Parker, R.H. Shumm, I. Halow, S.M. Bailey, K.L. Churney, and R.L. Nuttall. 1982. *The NBS Tables of Chemical Thermodynamic Properties. Selected Values for Inorganic and C1 and C2 Organic Substances in SI Units*. New York, NY: ACS.
- Walsh, M.P., L.W. Lake, and R.S. Schechter. 1982. A description of chemical precipitation mechanisms and their role in formation damage during stimulation by hydrofluoric acid. *Journal of Petroleum Technology* 34: 2097-2112.
- Walton, F.B., J.P.M. Ross, and D.G. Juhnke. 1985. The effects of simultaneous heat and mass transport on radionuclide migration. C.M. Jantzen, J.A. Stone, and R.C. Ewing, eds. *Scientific Basis for Nuclear Waste Management — VIII*. Pittsburgh, PA: MRS: 663-672.
- Wang, J.S.Y. 1992. Variations of hydrological parameter of tuff and soil. *Proceedings of the High-Level Radioactive Waste Management Conference*. La Grange Park, IL: ANS: 727-736.

- Wang, J.S.Y., and C.F. Tsang. 1980. Buoyancy flow in fractures intersecting a nuclear waste repository. F.A. Kulacki, and R.W. Lyczkowski, eds. *Heat Transfer in Nuclear Waste Disposal: Winter Annual Meeting of ASME*. HTD-16. Chicago, ILL: ASME: 105-112.
- Wang, J.S.Y., D.C. Mangold, R.K. Spencer, and C.F. Tsang. 1983. *Thermal Impact of Waste Emplacement and Surface Cooling Associated with Geologic Disposal of Nuclear Waste*. NUREG/CR-2910. Washington, D.C.: NRC.
- Wang, J.S.Y., and T.N. Narasimhan. 1985. Hydrologic mechanisms governing fluid flow in a partially saturated, fractured, porous medium. *Water Resources Research* 21(12): 1861-1874.
- Wang, J.S.Y., and T.N. Narasimhan. 1986. *Hydrologic Mechanisms Governing Partially Saturated Fluid Flow in Fractured Welded Units and Porous Nonwelded Units at Yucca Mountain*. LBL-21022. Berkeley, CA: LBL.
- Wang, H.F., B.P. Bonner, S.R. Carlson, B.J. Kowallis, and H.C. Heard. 1989. Thermal stress cracking in granite. *Journal of Geophysical Research* 94(B2): 1745-1758.
- Wark, K. 1983. *Thermodynamics*. New York, NY: McGraw-Hill.
- Westall, J. 1979. *MICROQL: I. A Chemical Equilibrium Program in BASIC*. Zurich, Switzerland: Swiss Federal Institute of Technology.
- Westall, J.C., J.L. Zachary, and F.M.M. Morel. 1976. *MINEQL, A Computer Program for the Calculation of Chemical Equilibrium Composition of Aqueous Systems*. Tech. Note 18. Cambridge, MA: MIT.
- Westwood, A. 1974. Control and application of environment sensitive fracture processes. *Journal of Material Science* 9: 1871-1895.
- Whirley, R.G. 1991. *DYNA3D—A Nonlinear, Explicit, Three-Dimensional Finite Element Code for Solid and Structural Mechanics—User Manual*, UCRL-MA107254. Livermore, CA: LLNL.
- Whitaker, S. 1977. Simultaneous heat, mass, and momentum transfer in porous media: Theory of drying. *Advances in Heat Transfer* 13: 119-203.
- Wijesinghe, A.M. 1989. Hydrothermomechanical simulator development task. J. Yow, Jr. et al., eds. *Repository Technology Program Activities: FY 1988*. UCID-21600. Berkeley, CA: LLNL: 3-14.
- Williams, J.R., G. Hocking, and G.G.W. Mustoe 1985. The theoretical basis of the discrete element method. *Proceedings of the NUMETA '85 Conference*. Swansea, UK: A. A. Balkema: 897-906.

- Wilson, M.L., and A.L. Dudley. 1986. *Radionuclide Transport in an Unsaturated, Fractured Medium*. SAND-86-7017C. Albuquerque, NM: SNL.
- Witherspoon, P.A., J.S.Y. Wang, K. Iwai, and J.E. Gale. 1979. Validity of cubic law for fluid flow in a deformable rock fracture. *Water Resource Research* 16(6): 1016-1024.
- Wolery, T.J. 1979. *Calculation of Chemical Equilibrium Between Aqueous Solution and Minerals. The EQ3/6 Software Package*. UCRL-52658. Berkeley, CA: LLNL.
- Wolery, T.J. 1983. *EQ3NR. A Computer Program for Geochemical Aqueous Speciation-Solubility Calculations: User's Guide and Documentation*. UCRL-53414. Livermore, CA: LLNL.
- Wolery, T.J., K.J. Jackson, W.L. Bourcier, B.E. Bruton, K.G. Knauss, and J.M. Delany. 1990. Current status of the EQ3/6 software package for geochemical modeling. *Chemical Modeling of Aqueous Systems II*. D. Melchior and R. L. Bassett, eds. ACS Symposium Series 416. Washington, D.C.: SCS: 104-116.
- Wollenberg, H.A., J.S.Y. Yang, and G. Korbin. 1983. *An Appraisal of Nuclear Waste Isolation in the Vadose Zone in Arid and Semi-Arid Regions*. NUREG/CR 3158. Washington, D.C.: NRC.
- Woods, T.L., and R.M. Garrels. 1987. *Thermodynamic Values at Low Temperature for Natural Inorganic Materials: An Uncritical Summary*. New York, NY: Oxford University Press.
- Yeh, G.T. 1985. Comparisons of successive iteration and direct methods to solve finite element equations of aquifer contaminant transport. *Water Resources Research* 21(3): 272-280.
- Yeh, G.T. 1987. *FEMWATER: A Finite Element Model of Water Flow Through Saturated-Unsaturated Porous Media, 1st Revision*. ORNL-5567/R1. Oak Ridge, TN: Oak Ridge National Laboratory (ORNL)
- Yeh, G.T., and V.S. Tripathi. 1989. A critical evaluation of recent developments in hydrogeochemical transport models of reactive multichemical components. *Water Resources Research* 25(1): 93-108.
- Yeh, G.T., and V.S. Tripathi. 1990. *HYDROGEOCHEM: A Coupled Model of Hydrological and Geochemical Equilibrium of Multi-Component Systems*. ORNL-6371. Oak Ridge, TN: ORNL.
- Yeh, G.T., and V.S. Tripathi. 1991. A model for simulating transport of reactive multispecies components: Model development and demonstration. *Water Resources Research* 27(12): 3075-3094.
- Yeh, G.T., and D.S. Ward. 1981. *FEMWASTE: A Finite Element Model of WASTE Transport Through Saturated-Unsaturated Porous Media*. ORNL-5522. Oak Ridge, TN: ORNL.

- Yunker, J.L. et al. 1992. *Report of Early Site Suitability Evaluation of the Potential Repository Site at Yucca Mountain, Nevada*. SAIC-91/8000, Washington, D. C.: Science Applications International Corp.
- Zienkiewicz, O.C. 1979. *The Finite Element Method*. New York, NY: McGraw-Hill.
- Zienkiewicz, O.C., and K. Morgan 1983. *Finite Element and Approximations*. New York, NY: Wiley.
- Zimmerman, R.M., R.L. Schuch, D.S. Mason, M.L. Wilson, M.E. Hall, M.P. Board, R.P. Bellman, and M.L. Banford. 1986. *Final Report: G-Tunnel Heated Block Experiment*. SAND84-2620. Albuquerque, NM: SNL.
- Zimmerman, R.W., and M.K. Blanford. 1986. Expected thermal and hydrothermal environments for waste emplacement holes based on G-Tunnel heater experiments. *27th U.S. Symposium on Rock Mechanics*. H. Hartman, ed. Littleton, CO: Society of Mining Engineers: 874-882.
- Zyvoloski, G., Z. Dash, and S. Kelkar. 1991. *FEHMN 1.0: Finite Element Heat and Mass Transfer Code*. LA-12062-MS. Los Alamos, NM: LANL.

**APPENDIX A**  
**THERMAL PROCESSES**

## THERMAL PROCESSES

The thermal processes are controlled by the temperature field which is needed to (i) calculate the thermal-mechanical environment to predict preclosure underground opening stability and postclosure stability of emplacement boreholes, (ii) model the thermal-hydrologic environment during operation and after closure of the repository to predict performance of the engineered barrier systems, and (iii) predict the thermal-hydrologic-chemical environment for radionuclide transport to the accessible environment through the geologic setting.

The thermal loading and the resulting temperature field are expected to have a significant influence on hydrologic, mechanical, and chemical processes, which then influence the underground opening stability and the performance objectives of the repository. It is expected that the placement of heat-generating HLW will elevate the temperature field, cause a redistribution of the *in situ* water, create thermal-mechanical stresses in the rock, affect canister corrosion processes, and affect the geochemical transport of radionuclides. Likewise, the hydrologic, mechanical, and chemical processes have the possibility of influencing the temperature distribution.

For the effects of thermal processes to be predicted, mathematical models need to be established and accepted as accurately representing the thermal physics. In this section, the development of a general mathematical model for heat transfer at the proposed HLW repository is presented. The common assumptions and approximations are discussed as they lead to special cases of the mathematical models. This section is completed by briefly describing how the thermal processes may be influenced by hydrologic, mechanical, or chemical processes.

### A.1 MATHEMATICAL MODELS

A traditional approach has been adopted for presenting the mathematical model in a conservation equation for energy followed by constitutive equations.

#### A.1.1 Conservation Equation

The conservation of energy equation is the basis for the mathematical model, which is used to predict the temperature distribution. The conservation of energy equation can be written in either the differential (Pollock, 1982, 1986; Whitaker, 1977; Forsyth 1990; Forsyth and Simpson, 1991; Todreas and Kazimi, 1990) or integral (Pruess, 1987; Runchal and Sagar, 1992) form using a variety of defined variables from the literature. The choice of either differential or integral equations is considered to be based on convenience, and both can be shown to be equivalent. Similarly, the choice of variable names and definitions is frequently based on convenience. In this work, the conservation of energy equation is presented in differential form

$$\frac{\partial e_{SLG}}{\partial t} = - \nabla \cdot ( \bar{q}_B + \bar{j}_B ) + Q_B \quad (A-1)$$

where

$e_{sLG}$	= stored energy in solid, liquid, and gas phases [J/m <sup>3</sup> ]
$\vec{q}_B$	= advective flux of energy [W/m <sup>2</sup> ]
$\vec{j}_E$	= diffusive flux of energy [W/m <sup>2</sup> ]
$Q_E$	= volumetric source/sink of energy [W/m <sup>3</sup> ]

In Eq. A-1, the term on the left-hand side is the local rate of change of stored (or accumulated) energy. The first term on the right-hand side is the divergence of the advective and diffusive fluxes. The last term on the right-hand side is an energy source/sink which may be due to radioactive decay heat, exothermic/endothermic chemical reactions, and/or viscous dissipation of mechanical energy.

In the next section, the constitutive equations for the stored energy and energy fluxes are introduced. By introducing mathematical models for these terms, assumptions and approximations are introduced. It is convenient to discuss one assumption that is routinely accepted in thermal analyses. In many discussions (and in this work), the "thermodynamic" internal energy is of primary interest, because it is directly related to temperature. Therefore, the energy equation (Eq. A-1) is assumed to be valid for thermodynamic energy, which results from the subtraction of the mechanical energy equation from the total energy equation (Todreas and Kazimi, 1990). The changes in kinetic and gravitational-potential energy are assumed to be negligible in comparison to changes in internal energy. In addition, the viscous dissipation is considered negligible.

### A.1.2 Constitutive Equations

In this section, the constitutive equations for the energy equation are presented. The first constitutive equation is for the stored energy, which is expressed as the summation of solid, liquid, and gas phase contributions.

$$e_{sLG} = (1 - \phi) \rho_s h_s + \phi S_L \rho_L h_L + \phi S_G \rho_G h_G \quad (A-2)$$

where

$\rho$	= density [kg/m <sup>3</sup> ]
$h$	= enthalpy [J/kg]
$\phi$	= porosity (m <sup>3</sup> void/ m <sup>3</sup> medium) [dimensionless]
$S$	= saturation (m <sup>3</sup> phase/ m <sup>3</sup> void) [dimensionless]
$s$	= solid phase [subscript]
$L$	= liquid phase [subscript]
$G$	= gas phase [subscript]

In Eq. A-2, the enthalpy,  $h$ , is used instead of the internal energy,  $u$ , (Pollock, 1982, 1986). The solid and liquid phase enthalpies and internal energies are approximately equal ( $h_s \approx u_s$ ,  $h_L \approx u_L$ ), because the solid and liquid are approximately incompressible. As such, they are used interchangeably in the literature. For nearly constant gas pressures, the energy associated with volumetric changes is negligible in comparison with the energy associated to temperature changes. The gas phase enthalpy is then approximately equal to the gas phase internal energy and the distinction between  $h_G$  and  $u_G$  is frequently neglected.

The liquid and gas saturations are equal to the fractions of the pore volume occupied by the liquid and gas, respectively. By definition, the saturations sum to unity

$$S_L + S_G = 1 \quad (\text{A-3})$$

The advective flux of energy,  $\bar{q}_B$ , is distinguished from the diffusive flux where advection is attributed to the bulk movement of fluid (either liquid or gas phase) and diffusion is attributed to molecular mixing. The advective energy flux consists of liquid and the gas phases contributions

$$\bar{q}_B = h_L \rho_L \bar{v}_L + h_G \rho_G \bar{v}_G \quad (\text{A-4})$$

where

$$\bar{v} = \text{area-averaged velocity [m/s]}$$

The area-averaged fluid velocities are considered parts of the hydrologic process and are discussed in Appendix B, hence a mathematical model for these fluxes is not presented here.

The diffusive energy flux,  $\bar{j}_B$ , consists of a conductive component and a gas phase mass diffusion component which is neglected here because it has a minor contribution relative to conductive heat transfer (Pollock, 1986). The conductive heat flux is given by Fourier's Law

$$\bar{j}_B = -k_T \nabla T \quad (\text{A-5})$$

where

$$\begin{aligned} k_T &= \text{thermal conductivity of the medium [W/(m-K)], and} \\ T &= \text{temperature [K].} \end{aligned}$$

The energy source/sink term,  $Q_B$ , in Eq. (A-1) is intended to be very general and may include radioactive decay heat and exothermic/endothermic chemical reactions. The radioactive decay heat associated with high-level radioactive waste can be distinguished between actinide decay reactions and fission product decay reactions (see Figure A-1).

At short times after discharge from a nuclear reactor ( $t < 100$  years), the heat generation is due primarily to fission product decay. At longer times, the heat generation is due primarily to actinide decay reactions. In Figure A-1, the thermal power is noted to decrease approximately linearly with time, especially for the larger times. In earlier studies of the geologic disposal of HLW, a nominal case for freshly emplaced fuel was assumed to be 10 years discharged from the reactor (O'Neal et al., 1984). In more recent studies (Buscheck and Nitao, 1992), fuels have been assumed with longer decay times (30 and 60 years). With "cooler" fuels, a larger number of spent fuel assemblies may be placed in a single disposal canister, and/or the disposal canisters may be placed closer together to change the repository areal power density (APD). The potential benefits of high APDs is currently being studied by Buscheck and Nitao (1992), among others.

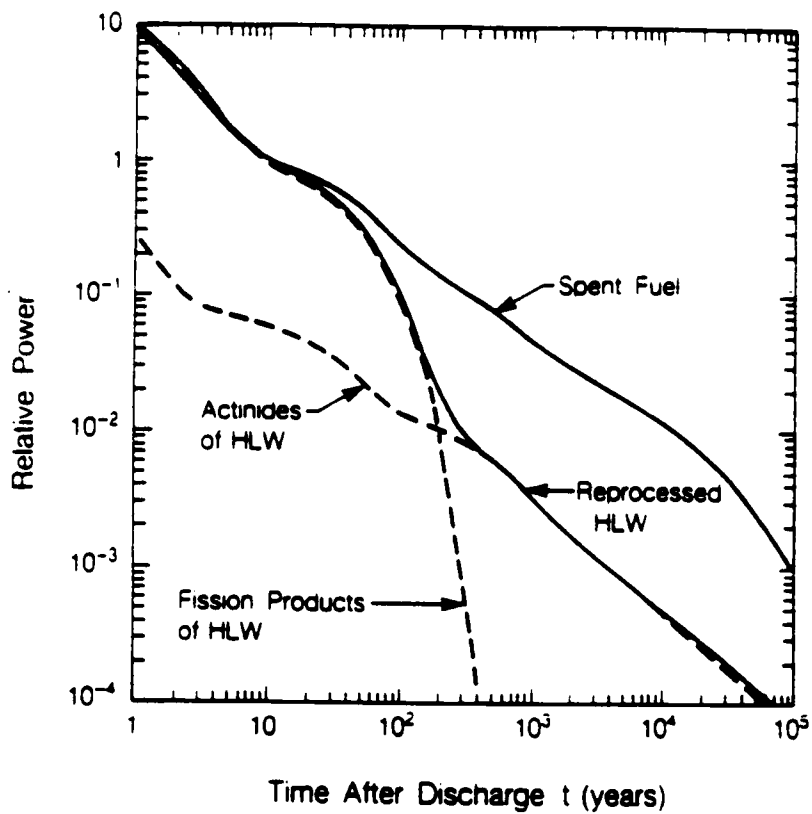


**Figure A-1. Relative Thermal Power of HLW Showing the Importance of Fission Products at Short Times and Actinides at Long Times (Verma and Pruess, 1988; among others)**

This summarizes a mathematical model that describes the conservation of energy and related constitutive equations. The mathematical models for the material properties ( $\rho_L$ ,  $\rho_G$ ,  $h_L$ , and  $h_G$ ) are not presented here, because they are considered straightforward (Pollock, 1986; Green et al., 1992; among others). At this point, it is assumed that the material properties can be calculated. Two simplifications and special cases are presented.

## A.2 SPECIAL CASES FOR THE MATHEMATICAL MODEL

In the literature, it is common to find studies which are based on subsets of the mathematical model presented in Section A.1. Descriptions, such as "conduction dominated" and "heat pipe," have been used in the literature and represent subsets of the complete model.

### A.2.1 Conduction Dominated

The description, "conduction dominated," is used to indicate that the advective heat transfer is negligible in comparison with the conductive heat transfer

$$|\vec{j}_E| \gg |\vec{q}_E| \quad (A-6)$$

Similarly, changes in the stored energy are assumed to be dominated by the energy stored in the solid phase

$$|\Delta((1 - \phi) \rho_s h_s)| \gg |\Delta(\phi S_L \rho_L h_L)| + |\Delta(\phi S_G \rho_G h_G)| \quad (A-7)$$

It is commonly assumed that the internal energy of the solid is linearly related to the temperature,  $h_s = c_s T$ , through the heat capacity,  $c_s$ . The thermal conductivity is assumed to be constant, so that the energy equation can be simplified to the heat conduction equation (where, for additional simplicity, the energy source/sink term is neglected,  $Q_E = 0$ )

$$\frac{\partial T}{\partial t} = \alpha \nabla^2 T \quad (A-8)$$

where

$$\alpha = \text{thermal diffusivity } [\alpha = k_T / (\rho_s c_s)]$$

The heat conduction equation is considered to be a simpler mathematical model of the energy equation and is frequently used to predict the temperature distribution at the proposed HLW repository (Roglan-Ribas and Spinrad, 1989; among others). The application of the heat conduction equation is justified when heat conduction is the dominant heat transfer mechanism and the energy storage in the solid phase is the dominant energy accumulation mechanism. For many far-field (tens to hundreds of meters from waste packages) temperature predictions, these assumptions are expected to be valid, especially when liquid flow is negligible (Buscheck and Nitao, 1992).

O'Neal et al. (1984) have calculated the temperature field in waste packages and in the surrounding host rock (see Figure A-2). It was assumed that conduction was the dominant heat transfer mechanism in the host rock, while conduction, natural convection, and thermal radiation were modeled

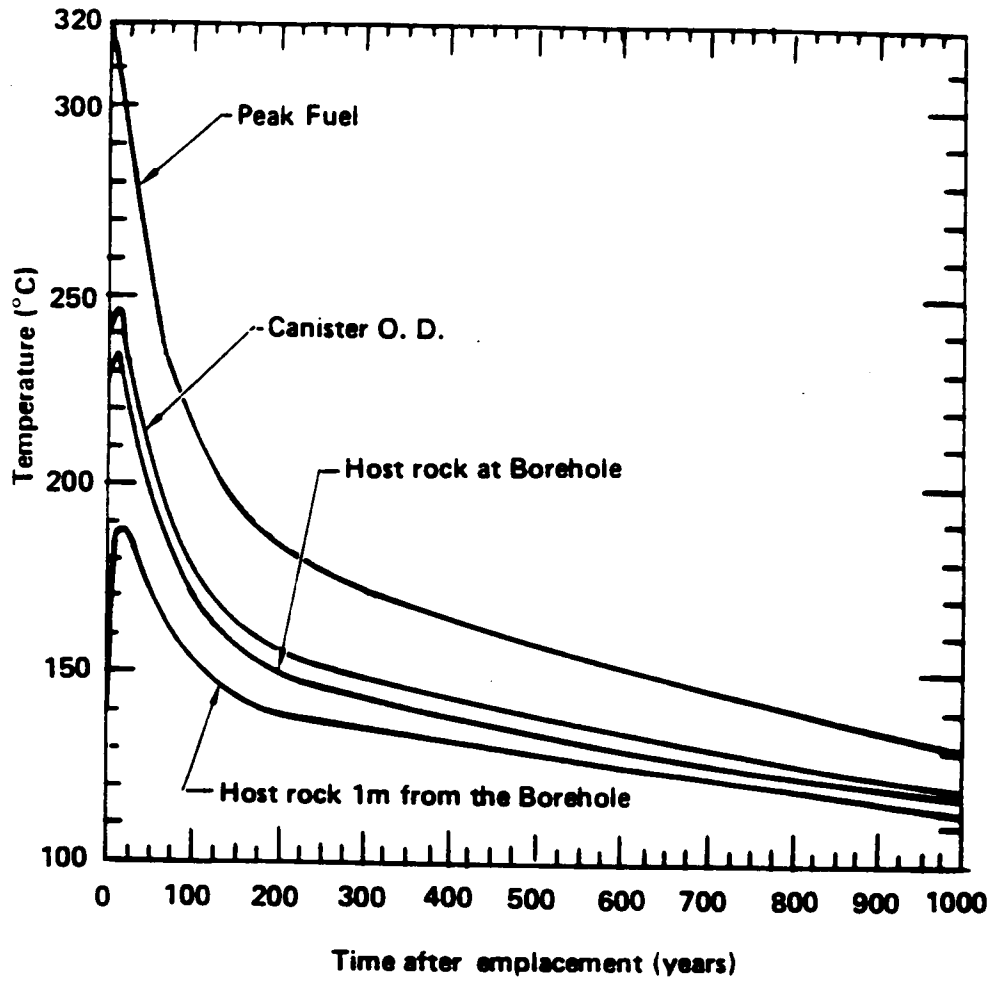


Figure A-2. Typical Temperature Histories of Waste Package Components and Host Rock near Emplaced Spent Fuel Canister (O'Neal et al., 1984)

in the spent fuel assemblies, fuel to canister gaps, and canister to host rock gaps. Although the work of O'Neal et al. is dated, it remains useful in ascertaining the expected temperature profiles near waste packages. Currently, the DOE is exploring repository design options, hence more exact information is necessary for more exact analyses. The work of O'Neal et al. highlights that a significant volume of the surrounding host rock may reach high temperatures ( $> 100\text{ }^{\circ}\text{C}$ ), which will enhance rock dry-out.

### A.2.2 Heat Pipe

The term, "heat pipe," has been used in the literature to describe a condition where the dominant heat transfer mechanism is due to vapor and liquid counterflow (Doughty and Pruess, 1992; among others). The liquid water is vaporized at one location and moves by advection to a second location where it condenses. Liquid water is drawn from the region where condensation occurs to where vaporization occurs, hence there is liquid flow and vapor flow in opposite directions (counterflow). The heat of vaporization required to change phase from liquid to gas creates a net heat flow from the location of vaporization to condensation. It is important to note that the heat pipe effect does not require a temperature gradient, and, therefore, can be isothermal. Also, the traditional heat pipe contains a single species of fluid, hence, in this discussion only, water vapor is considered, and air is assumed not to be present.

In the mathematical model for the conservation of energy (Eq. A-1), the heat pipe is typically described as being a steady-state phenomenon

$$\frac{\partial e_{sLG}}{\partial t} = 0 \quad (\text{A-9})$$

in a region which has no heat sources

$$Q_B = 0 \quad (\text{A-10})$$

and occurs when advective heat transfer is dominant

$$|\bar{q}_B| \gg |\bar{j}_B| \quad (\text{A-11})$$

The advective fluxes of mass in the liquid and gas phases are equal in magnitude and opposite in direction

$$\bar{q}_{w,G} = -\bar{q}_{w,L} \quad (\text{A-12})$$

However, due to differences in enthalpy, the advective energy flux is nonzero and can be quite large, based on the magnitude of the mass fluxes

$$\bar{q}_B = h_G \bar{q}_G + h_L \bar{q}_L = h_{LG} \bar{q}_G \quad (\text{A-13})$$

where

$$h_{LG} = \text{enthalpy of vaporization for water } (h_{LG} = h_G - h_L) \text{ [J/kg]}$$

The enthalpy of vaporization for water is quite large ( $h_{LO} \approx 4200 \text{ J/kg}$ ) so that only a small counterflow of fluid is required to transport a large amount of heat with a negligible temperature gradient. The importance of a heat pipe does depend on the ability of water and vapor to move freely in a porous medium and is discussed in Section 2.2.1 of this report.

### A.3 THERMAL PROPERTIES DATABASES

The most important thermal properties for heat transfer calculations are (i) thermal conductivity, (ii) specific heat, and (iii) density. There has been some characterization of thermal properties at Yucca Mountain (DOE, 1988, 1990). The thermal conductivities are relatively uniform between the different rock units at Yucca Mountain and vary from approximately 1.0 to 2.0 W/(m-C). The principle factor influencing thermal conductivity has been reported to be whether the rock is dry or saturated (DOE, 1988). The conductivity is lower for dry conditions compared to saturated conditions. In the literature, either the linear or square-root functions of thermal conductivity as a function of saturation have been used (Pruess, 1987; among others)

$$k_T = k_T(S_L = 0) + S_L [k_T(S_L = 1) - k_T(S_L = 0)] \quad (\text{A-14})$$

or

$$k_T = k_T(S_L = 0) + \sqrt{S_L} [k_T(S_L = 1) - k_T(S_L = 0)] \quad (\text{A-15})$$

Similarly, variation of the heat capacity and density of tuffaceous rock are reported by DOE (1988). Buscheck and Nitao (1992), among others, note that much of the heat transfer at the proposed repository is expected to be conduction dominated. Hence, calculations are expected to be sensitive to both thermal properties and loading conditions.

Wollenberg et al. (1983) note that the thermal conductivity of dry rock can be much lower than saturated rock due to air having a much lower thermal conductivity than water, ( $k_{T,WATER} \approx 25 k_{T,AIR}$ ). For simple conductive analyses, tuff has been assumed to have the following characteristics:  $k_T \approx 1.4 - 1.8 \text{ W/(m-k)}$ ;  $\rho c \approx 2.0 \times 10^6 \text{ J/(m}^3\text{-K)}$  (DOE, 1990).

In the waste packages, the heat transfer may be due to a combination of conduction, natural convection, and thermal radiation. In order to include conduction heat transfer in an analysis, the thermal conductivity must be known. In order to include natural convection and/or thermal radiation, more information is typically required. Thermal radiative heat transfer from solid surface to solid surface requires knowledge of the surface emissivities. In a spent fuel assembly, thermal radiation can be the dominant heat transfer mechanism (Manteufel, 1991). In this case, the emissivity of interest would be that of heavily oxidized zircaloy cladding. The authors of MATPRO (Hohorst et al., 1990) have compiled material properties of interest in nuclear applications, which include oxidized zircaloy emissivity (see Figure A-3). The emissivity is frequently assumed to be 0.8, as shown in Figure A-3. The assumed value of emissivity becomes increasingly important as radiative heat transfer becomes dominant. Siegel and Howell (1981) list emissivities of various engineering materials which may be needed to analyze parts of the engineered barrier.

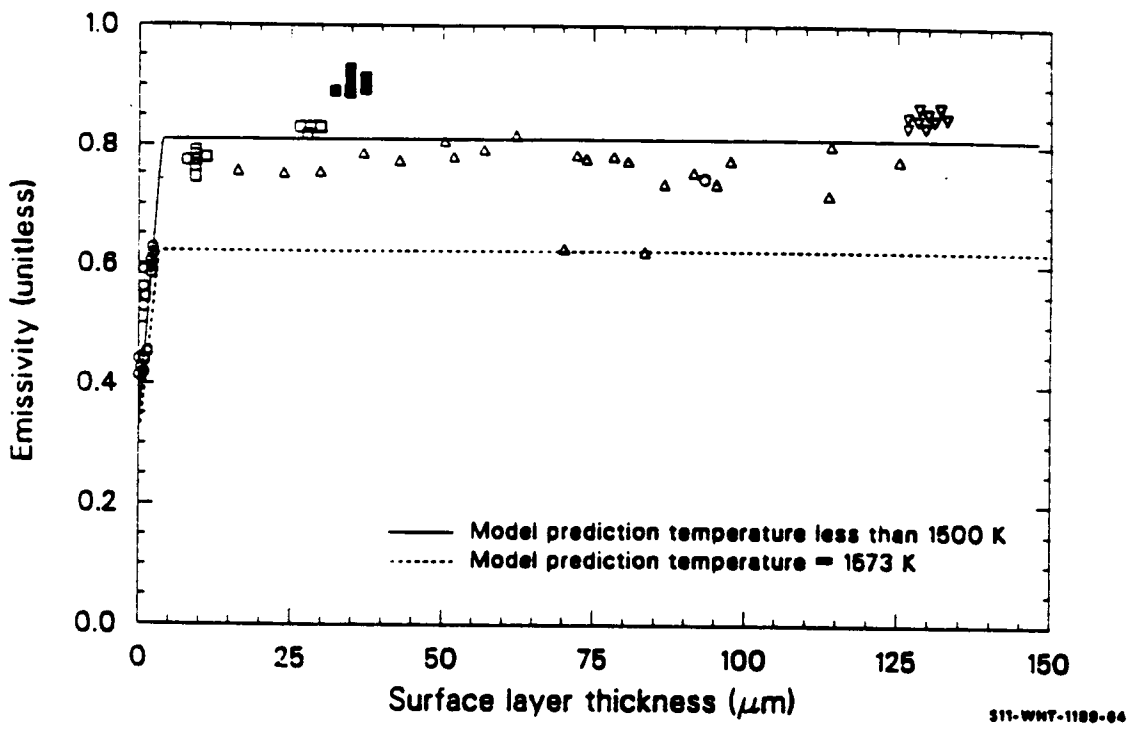


Figure A-3. Comparison of Experimental Measurements of the Emissivity of Oxidized Zircaloy (spent fuel rods) (Hohorst et al., 1990)

Natural convection is probably the most difficult heat transfer mechanism for which to compile a database of properties. This is because natural convection is primarily governed by the volume/geometry and imposed temperature boundary conditions. Natural convection may be important in large air gaps and analysts should consult texts for pertinent correlations (Incropera and DeWitt, 1981; Lienhard, 1987; Eckert and Drake, 1987; among others).

#### **A.4 COUPLINGS WITH OTHER PROCESSES**

In this section, the coupling with hydrologic, mechanical, and chemical processes are discussed as they are expected to influence heat transfer processes and the temperature distribution. Each are discussed in greater detail in Section 2 of this report.

Hydrologic processes can influence the heat transfer through (i) vaporization/condensation of water, (ii) liquid phase advection, and (iii) gas phase advection. The relative importance of fluid movement on heat transfer, however, may not be significant in many cases because conduction heat transfer in the porous medium may be dominant. For comparison, geothermal systems have large fluid flows so that the heat transfer may be convection dominated. For the partially saturated zone at Yucca Mountain, flow rates are expected to be sufficiently low so that it may be conduction dominated.

Mechanical processes can directly influence the heat transfer through (i) frictional generation of thermal energy or (ii) joint separation, which increases the resistance to heat conduction (possibly expressed as changes in the effective thermal conductivity of the rock mass). A frictional heat source may be present at joints which experience slipping. None of these couplings, however, are expected to have a large impact on thermal processes. Heat transfer is expected to influence mechanical processes through thermally-induced stresses (Hodgkinson and Bourke, 1980), which possibly leads to thermally-induced microfractures (i.e., cracks) (Wang et al., 1989).

Chemical processes can directly influence the heat transfer through the thermal energy source/sink term due to exothermic and endothermic chemical reactions. If the reaction is exothermic, this may be modeled as a thermal energy source. If the chemical reaction is endothermic, it may be modeled as a thermal energy sink. This effect will probably be minor compared to convective heat transfer. The presence of dissolved species may have an effect on fluid vapor pressures, fluid densities, and fluid and rock heat capacities.

**APPENDIX B**  
**HYDROLOGIC PROCESSES**

## HYDROLOGIC PROCESSES

Hydrologic processes in a fractured, porous medium are presented in this section. The subject of fluid flow in a porous medium is discussed by Bear (1972), Bear and Bachmat (1991), de Marsily (1986), Freeze and Cherry (1979), Hillel (1980a and 1980b), and Domenico and Schwartz (1990), among others. Thermally-driven hydrologic processes are of particular interest in this report and are discussed by Forsyth (1990), Forsyth and Simpson (1991), Whitaker (1977), Bixler (1985), Pollock (1982, 1986), and Pruess (1987, et al., 1990a,b). General references in the area of fluid mechanics include books by Bird et al. (1960), Fox and McDonald (1978), Potter and Foss (1982), and Todreas and Kazimi (1990).

The hydrologic processes important in underground disposal of HLW are those processes associated with fluid transport in both the gas and liquid phases, for both water and air in a fractured porous medium. In the literature, this is frequently referred to as two-phase (gas and liquid), two-component (air and water) mass transfer (Forsyth, 1990). Throughout this work, air is referred to as a component for modeling convenience, however, it is noted that air is a mixture of  $N_2$ ,  $O_2$ ,  $CO_2$ , and other gaseous species.

The mathematical model presented here focuses on fluid transport in a homogenous and isotropic porous medium. Additional mathematical models are required to represent fractures which are expected to be important at the proposed high-level waste repository.

### B.1 A MATHEMATICAL MODEL

The mathematical model for hydrologic processes in a homogenous and isotropic porous medium is based on the principles of (i) the balance of momentum and (ii) the conservation of mass (Fox and McDonald, 1978; Bear, 1972; Pruess, 1987; Forsyth, 1990; Whitaker, 1977; Pollock, 1982, 1986). In a porous medium, the balance of momentum is expressed as Darcy's law and is frequently considered as a constitutive equation. The conservation of mass equations are more general and provide the foundation for the mathematical model of hydrologic processes. The conservation equations will be discussed, followed by constitutive equations.

#### B.1.1 Conservation Equations

For this discussion the amount of air in the liquid phase is assumed negligible. The conservation equation for air can be written as:

$$\frac{\partial (\phi S_G \rho_{A,G})}{\partial t} = - \nabla \cdot \rho_{A,G} \vec{v}_G - \nabla \cdot \vec{j}_{A,G} + Q_{A,G} \quad (B-1)$$

for liquid water

$$\frac{\partial(\phi S_L \rho_{w,L})}{\partial t} = - \nabla \cdot \rho_{w,L} \bar{v}_L - Q_{w,LG} + Q_{w,L} \quad (\text{B-2})$$

and for water vapor

$$\frac{\partial(\phi S_G \rho_{w,G})}{\partial t} = - \nabla \cdot \rho_{w,G} \bar{v}_G - \nabla \cdot \bar{j}_{w,G} + Q_{w,LG} + Q_{w,G} \quad (\text{B-3})$$

where

- $\phi$  = porosity (m<sup>3</sup> void/m<sup>3</sup> medium) [dimensionless]
- $S$  = saturation (m<sup>3</sup> phase/m<sup>3</sup> void) [dimensionless]
- $\rho$  = density [kg/m<sup>3</sup>]
- $\bar{j}$  = diffusive mass flux [kg/(m<sup>2</sup>-s)]
- $Q$  = source/sink of mass [kg/m<sup>3</sup>-s]
- $\bar{v}$  = area-average fluid velocity [m/s]
- L = liquid [subscript]
- G = gas [subscript]
- W = water [subscript]
- A = air [subscript]

Equations (B-2) and (B-3) require a constitutive equation for the liquid-to-gas phase mass transfer,  $Q_{w,LG}$ . The phase densities and velocities can be functions of temperature, chemical composition, and mechanical stresses, leading to various types of couplings with other processes. If the equations are added, then a single mass conservation equation is generated:

$$\begin{aligned} \frac{\partial(\phi S_L \rho_{w,L} + \phi S_G \rho_{w,G})}{\partial t} = & - \nabla \cdot (\rho_{w,L} \bar{v}_L + \rho_{w,G} \bar{v}_G) \\ & - \nabla \cdot \bar{j}_{w,G} + Q_{w,L} + Q_{w,G} \end{aligned} \quad (\text{B-4})$$

Equation (B-4) is considered useful when the density of water in the gas phase,  $\rho_{w,G}$ , can be determined through a constitutive equation. Typically, the condition of local thermal-hydrologic equilibrium is assumed so that the amount of water in the gas phase is determined by the temperature and saturation (Edlefsen and Anderson, 1943). Equations (B-2) and (B-3) represent the case where the water in both the liquid and gas phase are not required to be in equilibrium and Eq. (B-4) represents the equilibrium case.

### B.1.2 Constitutive Equations

The constitutive equations need to be presented for the advective mass fluxes, the diffusive mass fluxes and the inter-phase mass transfer terms (for the non-equilibrium model). In this discussion, the components in each of the phases are assumed to be locally well-mixed so that each component travels at the same velocity. This appears to be a standard assumption that is made throughout the literature (Bear, 1972). The phase velocities are based on a modified Darcy's law which is assumed valid for partially saturated conditions (Bear, 1972; Hillel, 1980a)

$$\bar{v}_L = - \frac{k_{SAT} k_{REL,L}}{\mu_L} (\nabla P_L + \rho_L g \bar{k}) \quad (B-5)$$

$$\bar{v}_G = - \frac{k_{SAT} k_{REL,G}}{\mu_G} (\nabla P_G + \rho_G g \bar{k}) \quad (B-6)$$

where

- $k_{REL}$  = relative permeability [dimensionless]
- $k_{SAT}$  = saturated permeability [m<sup>2</sup>]
- $\mu$  = dynamic viscosity [N-s/m<sup>2</sup>]
- $P$  = pressure [N/m<sup>2</sup>]
- $\rho$  = density [kg/m<sup>3</sup>]
- $g$  = gravitational body force [ $g = 9.81 \text{ m/s}^2$ ]
- $\bar{k}$  = unit vector in direction of increasing elevation [dimensionless]

For partially saturated conditions,  $P_L$  should be considered as a "potential energy of liquid water per unit volume." The potential energy of water in a partially saturated medium is based on capillary and adsorptive forces. The gas pressure and liquid pressure are related through the capillary/adsorptive pressure:

$$P_{CAP/ADS} = P_G - P_L \quad (B-7)$$

where

$P_{CAP/ADS}$  = capillary/adsorptive pressure [N/m<sup>2</sup>]

The  $P_{CAP/ADS}$  is frequently characterized as a function of  $S_L$  using the van Genuchten model (van Genuchten, 1978; 1980). The molecular diffusion mass fluxes are given by Fick's law

$$\bar{j}_{W,G} = - \tau \phi S_G D_{WA,G} \rho_G \nabla m_{W,G} \quad (B-8)$$

$$\bar{j}_{A,G} = - \tau \phi S_G D_{WA,G} \rho_G \nabla m_{A,G} \quad (B-9)$$

where

- $\tau$  = tortuosity [dimensionless]
- $\phi$  = porosity [dimensionless]
- $S_G$  = gas saturation [dimensionless]
- $D_{WA,G}$  = molecular diffusion coefficient [m<sup>2</sup>/s]
- $\rho_G$  = gas density [kg/m<sup>3</sup>]
- $m_{W,G}$  = mass fraction [dimensionless].
- $m_{A,G}$  = mass fraction of air in the gas phase [dimensionless]

### B.1.3 Material Properties

The air and water densities ( $\rho_{A,G}$ ,  $\rho_{W,G}$ ,  $\rho_{W,L}$ ) are considered to be material properties that may depend on temperature, pressure, and, possibly, chemical composition.

The total gas pressure,  $P_G$ , is equal to the sum of component partial pressures

$$P_G = P_{A,G} + P_{W,G} \quad (B-10)$$

and the total gas density is equal to the sum of component densities

$$\rho_G = \rho_{A,G} + \rho_{W,G} \quad (B-11)$$

The air and water densities in the gas phase are normally determined through the ideal gas law

$$\rho_{A,G} = \frac{P_{A,G} M_A}{R T} \quad (B-12)$$

$$\rho_{W,G} = \frac{P_{W,G} M_W}{R T} \quad (B-13)$$

where

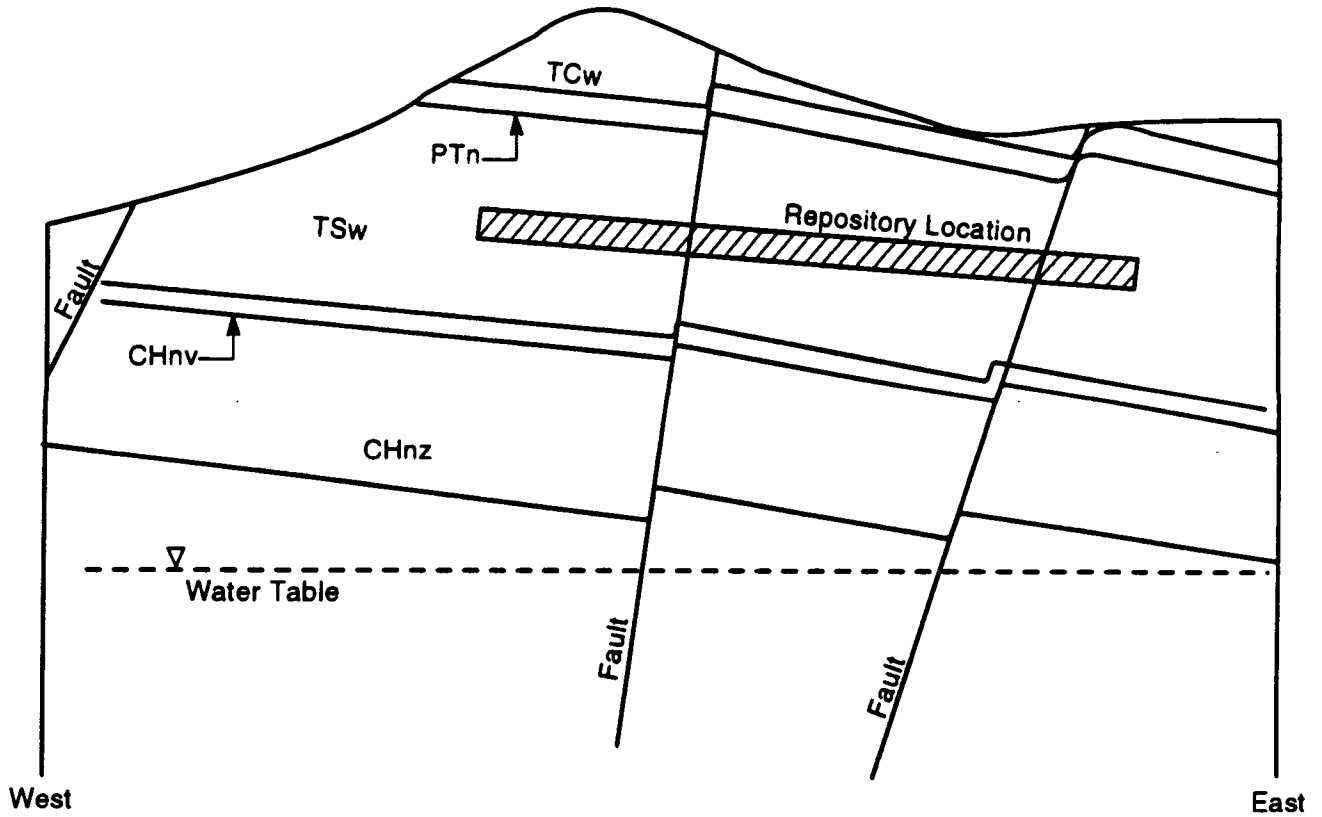
$P_{A,G}$ ,  $P_{W,G}$  = partial pressures of air and water in the gas [ $N/m^2$ ],  
 $M_A$ ,  $M_W$  = molecular weights [ $M_A = 28.97$  g/mole,  $M_W = 18.02$  g/mole],  
 $R$  = ideal gas constant [ $R = 8.314$  J/mole], and  
 $T$  = temperature [K].

## B.2 DATABASES FOR HYDROLOGIC PROPERTIES OF YUCCA MOUNTAIN

The hydrologic properties pertinent to the proposed HLW repository are discussed in a number of sources (Montazer and Wilson, 1984; Peters et al., 1984; DOE, 1988; Klavetter and Peters, 1986; and others). The primary quantities of interest are (i) location and dimensions of stratigraphic units, (ii) matrix permeability and porosity, (iii) fracture density, apertures, orientations, and connectivity, and (iv) moisture retention curves for matrix and fracture (i.e.,  $P_{CAP/ADS}$  versus  $S_L$  curves).

An east-west cross-sectional view of the proposed repository is illustrated in Figure B-1. The primary hydrogeologic units are: (i) Tiva Canyon welded (TCw), (ii) Paintbrush nonwelded (PTn), (iii) Topopah Spring welded (TSw), (iv) Calico Hills nonwelded vitric (CHnv), and (v) Calico Hills nonwelded zeolitic (CHnz) (DOE, 1988). The thicknesses of each unit vary and are approximately 0-150, 20-100, 290-360, 100-400, and 100-400 meters, respectively (Montazer and Wilson, 1984).

The proposed repository is to be located in the welded Topopah Spring unit at Yucca Mountain. The rock in this unit is reported to have a low porosity, a low permeability, and is densely fractured (Scott et al, 1982; Klavetter and Peters, 1986). The other units have varying hydrologic properties and



- TCw** Tiva Canyon Welded
- PTn** Paintbrush Nonwelded
- TSw** Topopah Spring Welded
- CHnv** Calico Hills Nonwelded Vitric
- CHnz** Calico Hills Nonwelded Zeolitic

**Figure B-1. East-West Cross-Sectional Illustration Highlighting the Different Hydrogeologic Units in the Unsaturated Zone at Yucca Mountain (adapted from DOE, 1988)**

are compared in Table B-1. The earliest and most extensive testing of tuffaceous materials was performed by Peters et al. (1984). The hydrogeologic units at Yucca Mountain generally fall into two categories: (i) welded tuffs and (ii) nonwelded tuffs. Typically the welded tuffs have low matrix permeability ( $\sim 10^{-18} \text{ m}^2$ ), low-to-medium matrix porosity, ( $\sim 10$  percent) and high fracture densities ( $> 10$  fractures/ $\text{m}^3$ ). Conversely, nonwelded tuffs have higher matrix permeability ( $\sim 10^{-14} \text{ m}^2$ ), high matrix porosity (30-40 percent) and low fracture densities ( $< 5$  fractures/ $\text{m}^3$ ). The majority of the fractures are "steeply dipping" and nearly vertical (DOE, 1990).

**Table B-1. Summary of Hydrogeologic Properties Relevant to Yucca Mountain (adapted from DOE, 1988)**

Hydrogeologic Unit <sup>a</sup>	Source of Data	Fracture Aperture (microns)	Fracture Density (no./ $\text{m}^3$ ) <sup>c</sup>	Matrix Porosity	Saturated Matrix Permeability ( $\text{m}^2$ )
TCw	(d)	ND <sup>b</sup>	10-20	0.12	$2 \times 10^{-18}$
	(e)	6.74	ND	0.08	$1 \times 10^{-18}$
PTn	(d)	ND	1	0.46	$1.0 \times 10^{-14}$
	(e)	27.00	ND	0.40	$4.0 \times 10^{-14}$
TSw	(d)	ND	8-40	0.14	$3.6 \times 10^{-18}$
	(e)	5.13	ND	0.11	$1.9 \times 10^{-18}$
CHnv	(d)	ND	2-3	0.37	$5.1 \times 10^{-15}$
	(e)	15.50	ND	0.46	$2.8 \times 10^{-14}$
CHnz	(d)	ND	2-3	0.31	$9.2 \times 10^{-18}$
	(e)	15.50	ND	0.28	$2.0 \times 10^{-18}$

<sup>a</sup> Hydrogeologic units are shown in Figure B-1  
<sup>b</sup> ND = no data  
<sup>c</sup> Scott et al. (1982)  
<sup>d</sup> Montazer and Wilson (1984)  
<sup>e</sup> Peters et al. (1984)  
 Note:  $1 \text{ m}^2$  (permeability)  $\approx 10^7$  m/s (hydraulic conductivity)

The stratification of rock units and the difference in permeability, porosity and fracture characteristics increase the complexity of predicting hydrologic processes. Wang (1992) reports that the variations in hydrologic parameters from tuff samples span 2 to 4 orders of magnitude for saturated permeability ( $k_{\text{SAT}}$ ), which highlights the uncertainties in hydrologic properties.

### B.3 FRACTURES

One major difficulty in predicting hydrologic processes is the characterization of fractures and fracture networks (Sagar and Gureghian, 1991; Ababou, 1991; Rasmussen and Evans, 1987, 1989; Klavetter and Peters, 1985; Wang and Narasimhan, 1986). By itself, the subject of flow in fractures has received much attention because fractures have different geometries and hydrologic properties from the matrix. Fractures are typically described as being two-dimensional with an aperture width typically of 0.1-1.0 mm. Sagar and Gureghian (1991) describe five candidate modeling approaches for predicting flow in a fractured, porous medium: (i) equivalent continuous porous medium model, (ii) double porosity model, (iii) discrete fracture network model, (iv) discrete fracture equilibrium model, and (v) discrete fracture non-equilibrium model. Only the first approach is discussed here. The reader is referred to Sagar and Gureghian (1991) for a more complete discussion of the different modeling approaches.

The equivalent continuous porous medium model has been used by Pruess, et al. (1987; 1990a,b), Rockhold et al. (1992), Nitao et al. (1992), Peters and Klavetter (1988), Nitao (1988), Buscheck and Nitao (1992), and others. The effective continuum approach uses an effective porosity

$$\phi_{EFF} = \phi_F + (1 - \phi_F) \phi_M \quad (B-14)$$

where

$\phi_{EFF}$  = effective continuum porosity,  
 $\phi_F$  = fracture porosity (based on a parallel plate model), and  
 $\phi_M$  = matrix porosity.

and an effective saturation

$$S_{EFF} = \frac{S_F \phi_F + S_M (1 - \phi_F) \phi_M}{\phi_{EFF}} \quad (B-15)$$

where

$S_{EFF}$  = effective continuum saturation,  
 $S_F$  = fracture saturation, and  
 $S_M$  = matrix saturation.

Klavetter and Peters (1986) describe a weighting procedure to calculate the effective matrix-fracture permeability

$$k_{EFF} = k_M (1 - \phi_F) + k_F \phi_F \quad (B-16)$$

where

$k_{EFF}$  = effective continuum permeability,  
 $k_F$  = fracture permeability, and  
 $k_M$  = matrix permeability.

The effective continuum approach yields characteristic curves for hydraulic conductivity (or permeability) as a function of pressure head (or capillary/adsorptive pressure). Figure B-2 shows the effective continuum permeability as a function of saturation, showing influences of matrix and fracture flow where the upper plateau represents the effect of the fractures and the lower plateau the effect of the matrix. At a pressure head near zero, both the fracture network and matrix are saturated. At higher pressure head, the fractures desaturate (dry-out), and the conductivity is reduced by approximately three orders of magnitude (the hump). As the pressure head increases, the matrix dries, and the conductivity is continually reduced. Typically, the effective continuum model predicts that the fractures quickly dry-out at an effective continuum saturation below 98 percent for the repository horizon at Yucca Mountain (e.g., Nitao, 1988). This implies that the fractured medium can sustain a considerable increase in liquid content before fracture flow occurs. The consensus in the literature is that the effective continuum approach is accurate as long as the hydrologic processes are sufficiently slow so that the fracture and matrix are in hydrologic equilibrium (Ababou, 1991; Gureghian and Sagar, 1991; Klavetter and Peters, 1986; Pruess et al., 1990a,b; and Nitao et al., 1992; among others).

Buscheck and Nitao (1992) compare calculated and measured liquid saturation profiles for various steady-state, one-dimensional recharge fluxes (see Figure B-3). The saturation data are from the Yucca Mountain Project Reference Information Base (DOE, 1990) and are shown in Figure B-3 as data points with error bars. The calculated liquid saturation profiles are based on an equivalent (or effective) continuum model (ECM). Buscheck and Nitao (1992) note that the ECM predictions and measurements are in good agreement in the low matrix permeability units (predominantly welded units). The ECM underpredicts the saturation in the high matrix permeability units (predominantly nonwelded) units. Nonequilibrium fracture flow through the welded units is a likely explanation of the differences (Buscheck and Nitao, 1992). Another explanation may be spatial variability of *in situ* saturation so that the measured values are biased due to localized sampling in boreholes. Another explanation is that the ground surface recharge flux is highly nonuniform so that episodic flows prevent Yucca Mountain from reaching a meaningful "steady-state" saturation profile. Regardless of a correct explanation, one possible explanation is that the ECM is not appropriate in low permeability units where episodic, fracture-dominated flow may dominate the hydrology. Wang and Narasimhan (1985), Peters and Klavetter (1988), Nitao (1991), and Nitao et al. (1992), among others have used and have noted limitations of the ECM. The consensus is that the ECM is valid under low fluxes and slow transients and cannot predict transient fracture flow that occurs before equilibration. Significant fracture flow occurs in the ECM model only when the matrix is nearly saturated; therefore, they severely under-predict the amount of fracture flow during episodic conditions, which are characterized by rapid regionally partially saturated transients and/or large infiltration rates.

The importance of fracture flow in a rock has been experimentally observed. Nitao, et al. (1992) reviewed experimental data that suggest that fracture-dominated flow has occurred at Yucca Mountain. The data include the detection of chlorine-36 as well as tritium at depths of 450-500 feet below the ground surface due to episodic rainfalls. Polymer-based drilling fluid flowed between adjacent boreholes (USW G-1 and USW UZ-1) indicating fluid movement in fractures occurred over a significant distance in less than three years.

In general, large fractures lead to larger fracture flow rates; however, more liquid is required to saturate the fracture. In many cases, a fracture may not be fully saturated, however, liquid may flow in the fracture. In this case, the terminology of liquid "dripping" in fractures may be more appropriate.

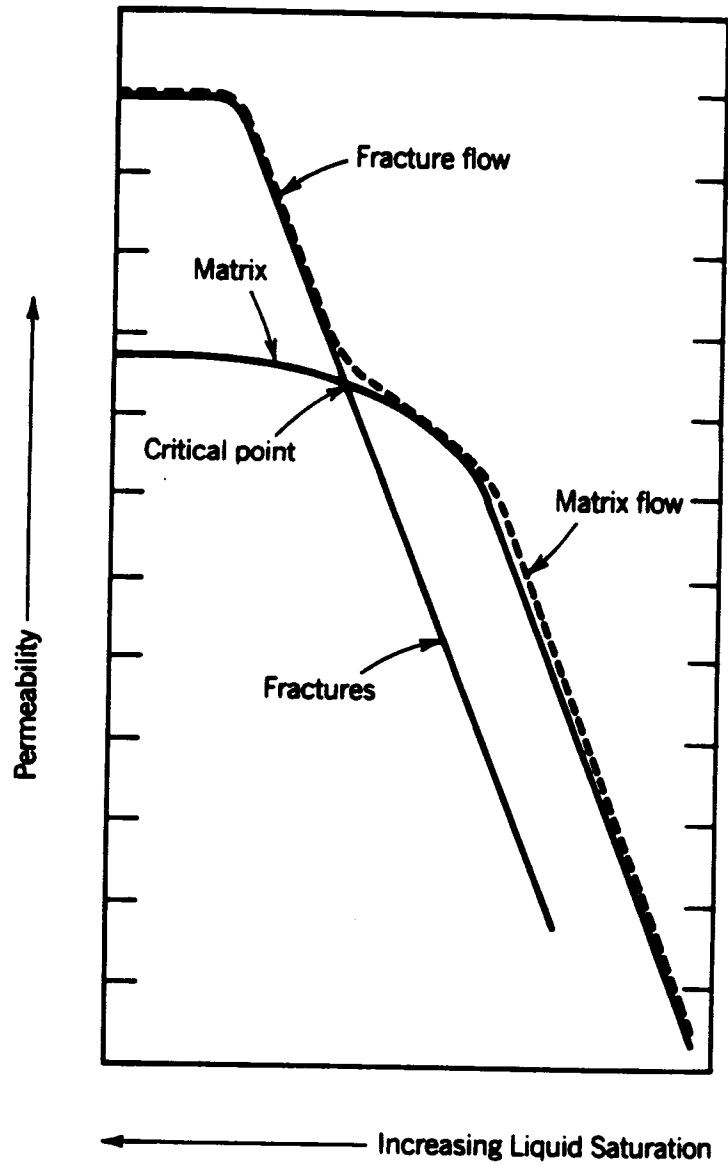


**Figure B-2. Effective Continuum Permeability as a Function of Saturation Showing Influences of Matrix and Fracture Flow (Montazer and Wilson, 1984; Domenico and Schwarz, 1990; among others)**

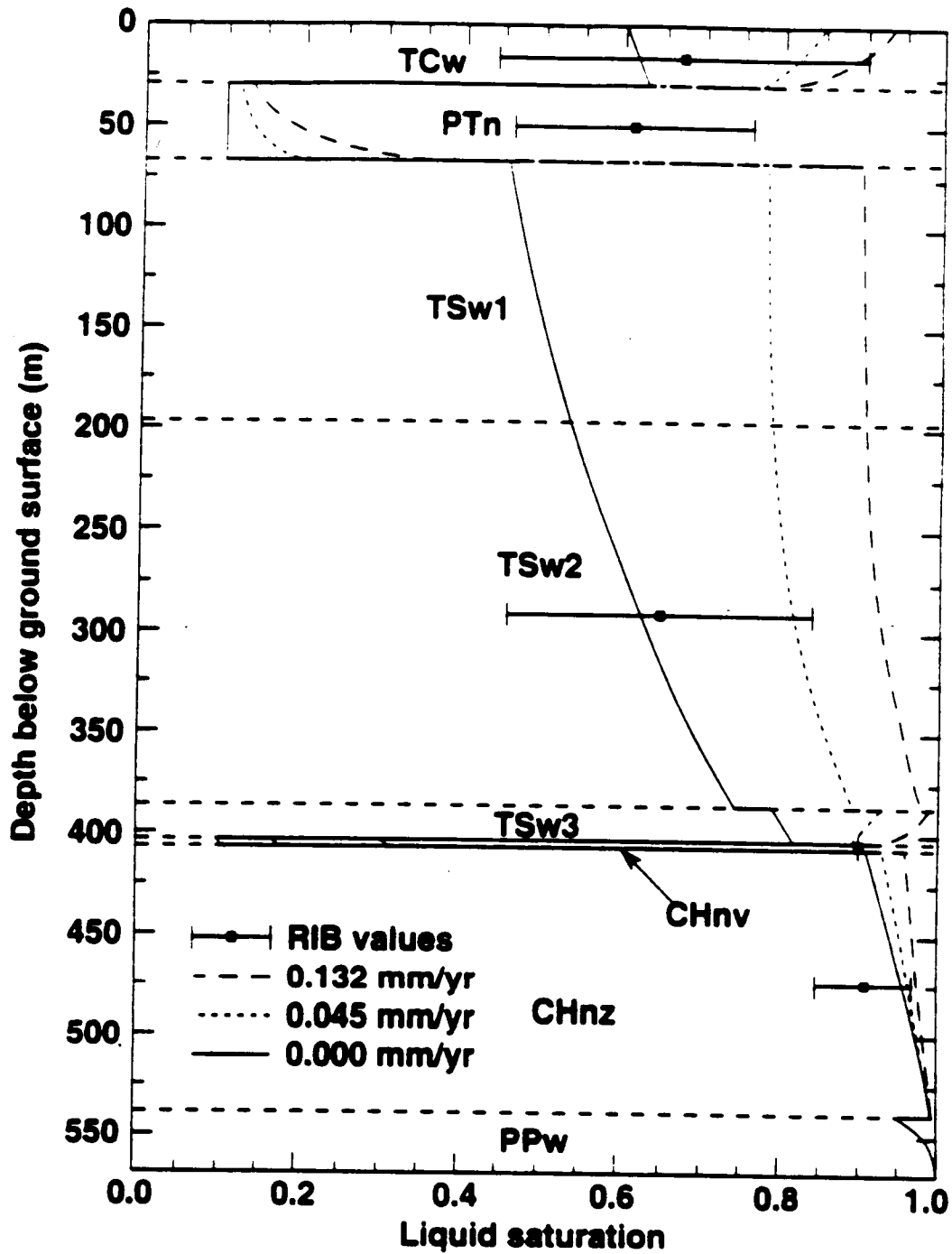


Figure B-3. Comparison of Calculated and Measured Liquid Saturation Profiles for Various Steady-State, One-Dimensional Recharge Fluxes (Buscheck & Nitao, 1992). Calculated Values Based on an Effective Continuum Model and Measured Values are from the Reference Information Base (RIB) (DOE, 1990).

Another consideration in predicting liquid flow in fractures is the connectivity of fracture networks. In general, a well connected network will lead to greater penetration (or travel) of liquid. Here, the emphasis is on vertical fractures where horizontal fractures may provide connectivity between vertical fractures.

#### **B.4 COUPLINGS WITH OTHER PROCESSES**

Hydrologic processes are widely expected to be important in the transport of radionuclides, hence they are expected to be considered in the study of chemical processes. The importance of chemical processes on hydrologic processes have been described mainly as dissolution and precipitation that may alter hydrologic properties, such as fracture aperture.

The couplings with thermal processes are also discussed in the literature; however, thermal processes are expected to influence hydrologic processes more than hydrologic affecting thermal. The noted exception is if there is a significant amount of liquid/vapor counterflow to transport heat in the reported "heat pipe" (Doughty and Pruess, 1988; 1990; 1991; 1992).

The hydrologic couplings with mechanical processes are not discussed in the literature as much as are other couplings. The mechanical properties of jointed rock may be described as a function of saturation; however, this effect continues to be investigated. The Early Site Suitability Evaluation suggests that compressive strength is 20-30 percent less for saturated versus dry samples. The changes in the mechanical stresses and strains in the rock are expected to change fracture apertures and influence flow.

**APPENDIX C**  
**MECHANICAL PROCESSES**

## MECHANICAL PROCESSES

Maintaining preclosure stability of the underground openings and postclosure stability of waste emplacement boreholes, in addition to allowing the option for waste retrieval, are key issues in the design of the repository. A typical rock mass can be viewed as a complex system of joints, faults, and intact rock. In some cases, the jointing may exist in several well defined orientations. However, in the vicinity of underground openings, additional excavation-induced fracturing can occur depending on the *in situ* stress conditions and type of excavation method, creating a complicated fracture and joint network. Also, anticipated and unanticipated natural phenomena, such as earthquake activity and underground nuclear testing, are particularly important at the proposed repository at Yucca Mountain and need to be taken into account in the design. Mechanical deformation within the rock mass consists of intact rock deformation, closure and shearing of joints, as well as movements along faults. Material properties of the intact rock at the proposed Yucca Mountain repository will most likely be heterogeneous due to the nature of their formation. Also, different sets of joints are likely to have different strengths and may also deform differently under various loading conditions.

Laboratory experimentation of the mechanical properties of the welded tuff at Yucca Mountain (Price et al. 1987) indicate that the intact rock is quite strong, with a uniaxial compressive strength of approximately 160 MPa and a high deformation modulus. Uncracked samples were shown to have stress-strain curves that show nearly elastic behavior up until failure. Samples with cracks exhibit nonlinear stress-strain behavior as expected when the applied stress is above 50 percent of the failure stress (Price, et al., 1987).

### C.1 CONTINUUM MATERIAL BEHAVIOR

Numerous textbooks describe the mechanics of continuous media, for example, Sokolnikoff (1956), Charlez (1991), Love (1944), and Timoshenko and Goodier (1970). It can be shown from momentum balance that the general equations of motion can be expressed as

$$\nabla \cdot \bar{\sigma} + \bar{f} = \rho \frac{d\bar{v}}{dt} \quad (C-1)$$

where

- $\bar{\sigma}$  = three dimensional stress tensor
- $\bar{f}$  = body force vector
- $\rho$  = solid density (kg/m<sup>3</sup>)
- $\bar{v}$  = velocity vector (m/s)
- $t$  = time (s)

When the inertial effects are negligible, Eq. (C-1) reduces to

$$\nabla \cdot \bar{\sigma} + \bar{f} = 0 \quad (C-2)$$

or alternatively using index notation as

$$\sigma_{ji,j} + f_i = 0 \quad (C-3)$$

where the repeated index (j) denotes a summation, and also, the comma preceding the index (j) denotes partial differentiation with respect to that index. Equation C-3 represents three equations for  $i = 1, 2,$  and  $3,$  known as the "equilibrium equations," which must be satisfied at any point within the medium. These equilibrium equations are used as the basis for solving elastostatic problems in rock mechanics.

The state of strain at a point in the body is specified by the components of the strain tensor. These components give the normal and shear strains for infinitesimal line elements originally parallel to the coordinate axes. The six equations for the strain components can be written in index notation as

$$e_{ij} = \frac{1}{2}(u_{i,j} + u_{j,i}) \quad (C-4)$$

where

$e_{ij}$  = normal strain components for  $i=j$  or shear strain components for  $i \neq j$   
 $u_i$  = three components of displacement ( $u_1, u_2, u_3$ )

Equation C-4 shows that the six strain components can be written in terms of the three displacements,  $u_1, u_2,$  and  $u_3.$  It follows that the strain components cannot be specified independently of one another and that some relationship must exist between them. It is possible using Eq. C-4 to establish a set of six relations between the strains known as "compatibility equations," (e.g., Charlez, 1991). These compatibility equations ensure that the strain field and the corresponding displacement field are continuous across the medium. Eqs. C-3 and C-4 or the corresponding compatibility equations are general and must be satisfied for any type of material. The six components of stress, six components of strain, and three components of displacement are thus written in terms of the three equilibrium (Eq. C-3) and six strain displacement equations (Eq. C-4), resulting in a set of nine equations for fifteen unknowns. The remaining six equations are provided by the constitutive relations between the stresses and strains and depend on the type of material behavior.

Intact rock behavior, especially that which exhibits high strength properties, such as the welded tuff at the proposed Yucca Mountain repository, can be approximated quite accurately by linear elastic behavior with the possible exception of those welded tuff units that have a very high porosity. This type of behavior is usually written in terms of the so-called generalized Hooke's Law which states that at each point in a three-dimensional, linearly elastic body, the six components of the stress tensor are linearly related to the six components of the strain tensor. These stress-strain relations for an isotropic, linearly elastic material can be written in index notation as

$$e_{ij} = \frac{1}{2G} \left[ \sigma_{ij} - \frac{\nu}{1+\nu} \sigma_{kk} \delta_{ij} \right] \quad (C-5)$$

where

$G$  = shear modulus ( $N/m^2$ )  
 $\nu$  = Poisson's ratio  
 $\delta_{ij}$  = Kronecker delta ( $\delta_{ij} = 1$  if  $i=j,$  and  $\delta_{ij} = 0$  for  $i \neq j$ )

In Eq. C-5,  $k$  is a dummy index, and, because it is repeated, denotes the sum of the three stress components. From moment equilibrium conditions, it is found that the stress tensor is symmetric,  $\sigma_{ij} = \sigma_{ji}$ , and, consequently, from Eq. C-5 the strain tensor is also symmetric.

## C.2 ROCK JOINT BEHAVIOR

In many situations, deformation along the rock joints in the form of normal and shear displacements plays a larger role in the deformation of the overall rock mass than just that of the intact rock. An example would be rock mass deformation in a competent, highly jointed rock mass under moderate to low *in situ* stresses (i.e., shallow depth). The proposed setting for the geologic repository at Yucca Mountain is in a well jointed, competent welded tuff at moderate depth, and thus, deformation along the joints and faults as a result of excavation as well as natural phenomena would be an important part of the overall response of the rock mass. Thus, accurate predictions of the mechanical behavior requires knowledge of the rock joint behavior.

Several joint models are currently being used to describe the normal and shear deformation along rock joints. These consist mainly of the Coulomb Friction, Barton-Bandis, and Continuously-Yielding joint models (Barton and Bandis, 1982; Barton et al, 1985; Cundall and Lemos, 1988), as well as ubiquitous or compliant joint models, which are based on a continuum description of the rock mass (Morland, 1974; Gerrard, 1982; Chen, 1986, 1990). The simplest joint model is the Coulomb-Friction model, which describes a linear relation between joint shear strength and joint normal stress. It assumes constant shear and normal stiffnesses and a constant angle of friction. The model can be presented in the following form

$$\tau = c + \sigma_n \tan \phi \quad (C-6)$$

where

- $\tau$  = joint shear strength (N/m<sup>2</sup>)
- $\sigma_n$  = joint normal stress (N/m<sup>2</sup>)
- $\phi$  = joint friction angle
- $c$  = cohesion (N/m<sup>2</sup>)

Once the shear strength is reached in the Coulomb-Friction model, perfectly plastic joint behavior is assumed. Also, if the joint is unloaded in shear after undergoing some permanent plastic displacement, the unloading slope, or shear stiffness, will be the same as that during loading.

Mechanical experimentation of single rock joints shows the deformation to be non-linear and inelastic (Bandis, et al., 1983). Barton et al. (1985) have proposed a joint model that describes the normal and shear responses based on testing of single jointed rock specimens. This model is referred to as the Barton-Bandis joint model. The model takes into account the hysteresis that occurs during joint normal loading-unloading, as well as permanent inelastic closure that takes place after repeated loading and unloading of the joint. The model also allows for dilation of the joint to occur during shearing, as observed in laboratory experiments. The joint shear strength envelope proposed by Barton and Bandis can be expressed using Eq. C-6 with a variable  $\phi$  angle. This  $\phi$  angle is intended to take into account joint damages and reduction in the dilation angle during joint shear. In the Barton-Bandis model, the angle of friction ( $\phi$ ) is assumed to be constant, provided the normal stress is constant, during the process of

shearing until a peak joint shear displacement corresponding to the peak shear resistance is exceeded. The peak angle of friction of a joint can be expressed in terms of joint roughness and wall strength parameters, as follows

$$\phi_{\text{peak}} = \text{JRC}_{\text{peak}} \cdot \log_{10} (\text{JCS}/\sigma_n) + \phi_r \quad (\text{C-7})$$

where

- $\phi_{\text{peak}}$  = peak or maximum friction angle
- $\text{JRC}_{\text{peak}}$  = empirically determined initial joint roughness coefficient (dimensionless)
- $\text{JCS}$  = empirically determined joint wall compressive strength ( $\text{N}/\text{m}^2$ )
- $\phi_r$  = joint residual friction angle

Substituting Eq. C-7 back into Eq. C-6 and assuming no cohesion, gives the following relation for the peak shear stress

$$\tau_{\text{peak}} = \sigma_n \tan[\text{JRC}_{\text{peak}} \cdot \log_{10}(\text{JCS}/\sigma_n) + \phi_r] \quad (\text{C-8})$$

The gradual reduction of the shear strength in the post-peak phase is caused by a decline in the effective contribution of roughness due to surface mismatch and wear. This behavior can be modeled by using different values for the roughness,  $\text{JRC}_{\text{mob}}$ , that will be activated once the joint becomes mobilized. Barton et al. (1985) also proposed an empirical expression defining the joint closure under normal stress as

$$\sigma_n = \frac{\Delta V_j}{a - b\Delta V_j} \quad (\text{C-9})$$

where  $\Delta V_j$  is the joint closure, and  $a$  and  $b$  are empirical constants.

The Continuously-Yielding joint model was formulated by Cundall and Lemos (1988) to take into account non-linear compression, non-linearity and dilation in shear, and a non-linear limiting shear strength criterion. This model suggests that at any state of normal stress,  $\sigma_n$ , the joint shear strength is given by

$$\tau = \sigma_n \tan \phi_m \sin(\Delta u_s) \quad (\text{C-10})$$

where

- $\phi_m$  = current friction angle of the joint
- $\Delta u_s$  = joint shear displacement increment

As damage accumulates, the current friction angle,  $\phi_m$ , is continuously reduced by the following equation

$$\Delta \phi_m = \frac{1}{R} (\phi_m - \phi_r) \Delta u_s^p \quad (\text{C-11})$$

where

R = roughness parameter for the joint surface (m)  
 $\Delta u_s^p$  = plastic joint shear displacement which is a fraction of  $\Delta u_s$

Joint stiffnesses for the Continuously-Yielding model are normal stress dependent according to

$$K_n = a_n \sigma_n^{e_n} \quad (C-12)$$

$$K_s = a_s \sigma_n^{e_s} \quad (C-13)$$

where  $K_n$  is the joint normal stiffness,  $K_s$  is the joint shear stiffness, and  $a_n$ ,  $e_n$ ,  $a_s$ , and  $e_s$  are empirical constants.

### C.3 MATHEMATICAL MODELING OF MECHANICAL PROCESSES

There are numerous computational methods currently available for modeling the mechanical deformation of rock. These consist of continuum methods such as finite difference (Forsythe and Warsaw, 1960), finite element (Zienkiewicz, 1979; Cook, 1981), and boundary element (Brebbia, 1978) methods. Other approaches consist of discontinuum modeling techniques that include the discrete element method (Cundall, 1971), modal method (Williams, et al., 1985), discontinuous deformation analysis method (Shi and Goodman, 1988), and moment exchange method (Hahn, 1988). It has been common in engineering practice to model the far-field rock mass behavior using continuum modeling techniques. In this region, one is interested in more of the macroscopic mechanical behavior of the rock mass, or perhaps, deformation along a major structural feature, such as a fault. Discontinuum methods have been used in modeling the near-field mechanical behavior of the rock, where one is more interested in the deformation along individual joints or fractures that may intersect, for example, underground openings or waste emplacement boreholes. Hybrid modeling techniques, combining both continuum and discontinuum techniques, have also been used for excavation problems involving infinite and semi-infinite regions. A brief discussion of each of these modeling approaches and computer codes is given below.

#### C.3.1 Continuum Analysis

The continuum modeling techniques describe the rock mass as a continuous solid, within which displacements and stresses are defined in terms of governing differential equations. In finite difference and finite element methods, a mesh of elements that are interconnected at the nodes is constructed. Displacement compatibility is required along the edges of the elements. The system of equations is written for the entire assemblage of elements, including the constraints and boundary conditions. Each element of the discretized medium is assigned a constitutive material behavior representative of the medium. Both finite element and finite difference methods are well established for continuum modeling and can be used to model complex material behavior.

In boundary element formulations, only the boundary of the medium (i.e., surface of the excavation or ground surface) is discretized. As a result, the dimension of the problem is reduced by one. The numerical solution is first obtained along these surfaces, and then the solution at different points within the medium is obtained from the solution at the boundary. From a computational point of view, the boundary element leads to a much smaller system of algebraic equations than a finite element solution

for the same problem. In addition, the boundary element method is especially well suited to problems involving infinite and semi-infinite regions, such as those occurring in underground excavation design, since the boundary conditions at infinity are met analytically. However, currently available "infinite elements" now allow problems involving semi-infinite and infinite regions to be accurately modeled using the finite element method. The main disadvantage of the boundary element method, is that it does not have the capability to model complex material behavior as can be done with finite element and finite difference methods.

A discontinuum medium, such as a fractured and jointed rock medium, can be analyzed by continuum methods, such as finite element, finite difference, and boundary element methods, by approximating the medium as an equivalent continuum, considering the effective properties in shear and in compression. As the spacing of the joints increases and/or the joints become stiffer both in compression and in shear, the properties of the rock mass approach the intact rock properties. In such a case, the effect of joint discontinuity is neglected, and the rock mass is modeled as a medium of intact rock. However, with decreasing joint spacing and/or with decreasing joint stiffness both in shear and in compression, the ratio of rock mass properties to intact rock properties decreases. For these fractured rock masses, the concept of "effective" or macroscopically averaged properties is used (Fossum, 1985; Amadei and Goodman, 1981; Duncan and Goodman, 1968). This means that one seeks to determine the effective properties which govern the macroscopic behavior of the discontinuous rock masses in terms of the properties of the intact rock and joints and the geometric nature of their combination.

Many finite element (Key, 1987; Whirley, 1991; Hallquist, 1988), boundary element (Banerjee and Ahmad, 1985), and finite difference (Hoffman, 1981) programs have interface elements or "slide lines" that enable them to model discontinuous materials to some extent. However, their formulation is usually restricted in one or more of the following ways (Cundall and Hart, 1989). First, the logic may break down when many intersecting interfaces are used; second, there may not be an automatic scheme for recognizing new contacts; third, the formulation may be limited to small displacements and/or rotations. Such programs are usually adapted from existing continuum programs.

### C.3.2 Discontinuum Analysis

Discontinuum modeling techniques have been recently introduced for simulating the complete behavior of a fractured and jointed rock medium where the discontinuities play a critical role in determining the deformation which includes rigid body motion. These techniques model the properties of both joints and the intact rock explicitly. The discrete element models have two distinguishing features compared to continuum models: (i) the behavior of the geologic system is described by both a continuum material description of the intact rock and a discontinuum material model for major discontinuities (i.e., joints, faults, etc.) and (ii) the deformation mechanisms include large displacement (i.e., joint slip and separation) and block rotation. The discrete element method is similar to the finite element or finite difference method in that the problem domain is divided into a system of solid elements (blocks). The principal difference is that the discrete element method also permits the geometry of the elements to be defined by the spacing and orientation of the discontinuities in the rock mass, thereby allowing blocks to interact (or disconnect) from neighboring blocks. The discrete element method includes not only continuum theory representation for the blocks but also force displacement laws that specify forces between blocks and a motion law that specifies motion of each block due to unbalanced forces acting on the block.

In the discrete element method, blocks may be rigid or deformable. The rigid block formulation represents the medium as a set of discrete blocks which do not change their geometry as a result of applied loading and only the joints can deform. Consequently, the formulation is most applicable to problems in which the deformation of the system is primarily a result of deformation or slip along the discontinuities and where elastic properties of the intact material may be ignored. Such conditions arise in low-stress environments and/or where the intact material possesses high strength and low deformability. At the site of the proposed geologic repository at Yucca Mountain, although the welded tuff is considered to possess high strength, the waste emplacement horizon is at sufficient depth to induce some elastic block deformation around the underground openings. For these situations, the deformation of individual blocks cannot be reasonably ignored; that is, blocks cannot be assumed to be rigid. In this case, arbitrary deformation of blocks is permitted through internal discretization of blocks into finite element or finite difference zones, in addition to the rigid-body modes associated with each block of the jointed rigid block formulation.

### **C.3.3 Hybrid Analysis**

Hybrid modeling techniques can also be used for analysis of the mechanical behavior in underground excavation problems, which usually involve infinite or semi-infinite regions. Development of this computational scheme is based on a recognition of different deformation modes that occur in rock surrounding an excavation. The far-field away from the excavation experiences only small deformations and is represented reasonably well as an elastic continuum using a boundary element scheme or an infinite element (Bettess and Zienkiewicz, 1977; Zienkiewicz and Morgan, 1983) scheme. The near-field rock in the vicinity of the excavation experiences larger displacements along joints or fractures and possibly non-linear material behavior, and is better modeled by finite element, finite difference, or discrete element methods. In the hybrid modeling approach, the near-field scheme (finite element, finite difference, or discrete element) is coupled with the far-field scheme (boundary element or infinite element) by satisfying the condition of continuity of displacements and stresses on the interface between the near-field and the far-field domain.

## **C.4 COUPLING WITH OTHER PROCESSES**

Mechanical processes will, in general, be coupled with thermal, hydrologic, and chemical processes. It is expected that thermal loading as a result of waste emplacement will have significant effect on the mechanical state within the rock mass, inducing additional stresses and displacements as a result of thermal expansion. The thermal effect will most likely peak after the first few hundred years and then begin to approach an asymptote. Changes in chemistry of the rock as a result of thermal heating may cause additional mechanical degradation of the rock around the underground openings and emplacement boreholes.

For the proposed Yucca Mountain site, mechanical processes will likely have a significant effect on the hydrologic characteristics in the near-field repository region, mainly due to changes in the hydraulic apertures around the excavations and emplacement boreholes. However, due to the partially saturated nature of the Yucca Mountain site which may introduce gas and/or vapor phases, and the fact that flow in the fractures may only occur periodically, the mechanical hydrologic coupling is not well understood at this time.

**APPENDIX D**  
**CHEMICAL PROCESSES**

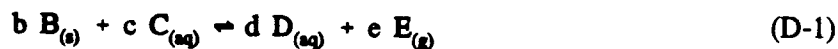
## CHEMICAL PROCESSES

The performance of both the engineered and natural barriers of a geologic high-level radioactive waste (HLW) repository can be affected significantly by the operation of chemical processes in response to a variety of external and internal changes. The following section is intended as a brief summary of the principles and applications of equilibrium and kinetic chemical processes pertinent to the proposed HLW repository at Yucca Mountain, Nevada. The discussion closely follows the developments by Rubin (1983), Yeh and Tripathi (1989), and Mangold and Tsang (1991). The reader is referred to a variety of textbooks (e.g., Garrels and Christ, 1965; Lasaga and Kirkpatrick, 1981; Stumm and Morgan, 1981; Drever, 1982; Hem, 1985) for a more extensive and complete treatment of equilibrium and kinetic chemistry. The first subsection deals with equilibrium chemical processes. Nonequilibrium reaction kinetics will be discussed in more detail later in this appendix.

The laws of thermodynamics and conservation of energy, mass, and charge are the basic tools for modeling chemical processes (Mangold and Tsang, 1991), and the degree to which chemical equilibrium has been achieved is of critical importance (Rubin, 1983). A primary distinction is drawn between those processes that are both reversible and "fast enough" to justify an assumption of equilibrium and those that are slow and/or irreversible, requiring consideration of nonequilibrium reaction kinetics (Figure C-1). Within both equilibrium and nonequilibrium classes of reactions, a secondary distinction is made between homogeneous reactions (single-phase) and heterogeneous (multiple-phase) reactions. A final division can be made for heterogeneous reactions where surface (sorption, ion exchange) and "classical" (precipitation/dissolution, redox) processes are discriminated. The ensuing discussion is generally concerned only with the high-order distinction between equilibrium and nonequilibrium chemical processes.

### D.1 EQUILIBRIUM CHEMICAL PROCESSES

A geochemical system can generally be represented by a series of reactions (homogeneous or heterogeneous, surface or classical) of the general form



where

B, C, D, and E = phases involved in the reaction [solid(s), aqueous(aq), gas(g)]  
b, c, d, e = stoichiometric reaction coefficients

By convention, these reactions are written so that the forward reaction proceeds from left to right, and the reverse reaction proceeds from right to left.

For the  $i$ th component in reactions of the type presented in Eq. (D-1), the mass balance is constrained such that

$$m_{i,j} = \sum v_i m_{s,i} \quad (D-2)$$

where

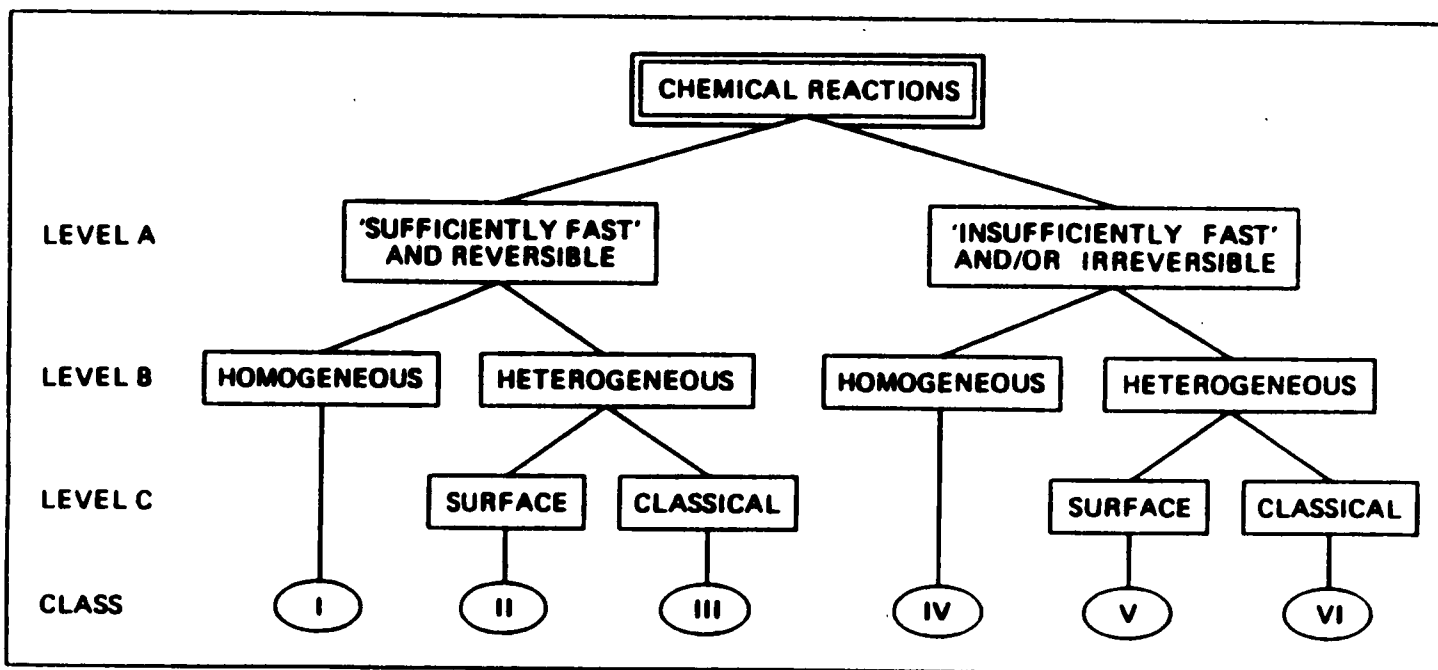


Figure D-1. Distinctions Between Classes of Chemical Reactions (after Rubin, 1983)

- $m_{t,i}$  = total molality (moles/kg H<sub>2</sub>O) of component I  
 $m_{s,i}$  = molality of species S containing component I  
 $\nu_i$  = the stoichiometry of component I in species S

In a similar fashion, charge balance in electrolyte solutions is constrained such that

$$\sum Z_s m_s = 0 \quad (D-3)$$

where

Z = the charge of the subscripted species

Based on an assumption of equilibrium, reactions of the form given in Eq. (D-1) can be represented by mass-action equations of the form

$$K = \frac{(a_D)^d (f_G)^g}{(a_B)^b (a_C)^c} \quad (D-4)$$

where

- K = thermodynamic equilibrium constant (dimensionless) which is a function of temperature and pressure  
 $(f_G)^g$  = fugacity (bars) of a gas phase G raised to the power of its reaction coefficient g [e.g.  $(f_G)^g$ ]  
 $(a_s)^s$  = the thermodynamic activity (dimensionless) of aqueous species, solid, or liquid S raised to the power of its reaction coefficient, s [e.g.  $(a_D)^d$ ]

For pure solids and liquids,  $(a_s) = 1$ , and at low pressures, the fugacity of a gas (in this case, gas G) can be approximated by its partial pressure, p, such that  $[p(G)]^g \approx (f_G)^g$ . For aqueous species, however, activity is a function of pressure, temperature, and solution composition, and the activity/molality relationships are generally of the form

$$(a_s)^s = m_s \gamma_s \quad (D-5)$$

where

- $\gamma_s$  = the activity coefficient of species S (kg H<sub>2</sub>O/ mole S)  
 $m_s$  = the molality of species S (mole S/ kg H<sub>2</sub>O)

$\gamma_s$  also varies as a function of temperature, pressure, and solution composition, and is either determined experimentally or defined by one of several approximations, such as the mean-salt method or the Debye-Hückel and Davies equations (Stumm and Morgan, 1981). The validity of these approximations is generally limited to relatively dilute solutions. Recent studies (Pitzer, 1973, 1979; Harvie et al., 1984; Plummer et al., 1988; Pabalan and Pitzer, 1990) have developed a set of virial equations (Pitzer equations) to calculate solution properties for concentrations ranging from dilute electrolyte solutions to highly concentrated brines. All activity/concentration relations require additional thermodynamic data, however, and in the absence of experimental data, frequently an activity coefficient of 1 is assumed, and simple concentrations are substituted for activities in Eq. (D-4).

The driving force for a chemical reaction, the Gibbs free energy of reaction  $\Delta G_R$  (J/mole), is defined as the difference between the free energy of the products and the reactants. A function of pressure and temperature,  $\Delta G_R$ , can also be used (Mangold and Tsang, 1991) to describe chemical equilibrium through the relationship

$$\Delta G_R = \Delta G_R^\circ + RT \ln \left( \frac{(a_D)^d [p(E)]^e}{(a_B)^b (a_C)^c} \right) = \Delta G_R^\circ + RT \ln (Q) \quad (D-6)$$

where

- R = the ideal gas constant (8.314 J/K-mole) '
- T = the absolute temperature in Kelvin
- $\Delta G_R^\circ$  = the standard free energy change of the reaction (J/mole)
- Q = the activity product or the reaction quotient

Analogous to  $\Delta G_R$ ,  $\Delta G_R^\circ$  is defined as the difference between the sum of the standard state energies of formation of the products and that of the reactants (e.g.,  $\Sigma \Delta G_{F^\circ}^{\text{products}} - \Sigma \Delta G_{F^\circ}^{\text{reactants}}$ ).

Because the reaction will tend towards a minimum energy state, a negative value for  $\Delta G_R$  will favor the forward reaction; a positive value favors the reverse reaction. As the reaction progresses in the favored direction at a given temperature and pressure, the free energy of reaction ( $\Delta G_R$ ) will approach zero. At equilibrium,  $\Delta G_R = 0$ ,  $Q = K$ , and  $\Delta G_R^\circ = -RT[\ln(K)]$ . Using thermodynamic relations such as the Maxwell and van't Hoff equations (Garrels and Christ, 1965), and standard state thermodynamic properties (e.g., heat capacity ( $c_p$ ), enthalpy (H), and entropy (S)) for the reactant and product phases to calculate the effects of changing conditions on  $\Delta G_R^\circ$ , it is possible to calculate equilibrium constants as a function of pressure and temperature from Eq. (D-6). Values for  $\Delta G_R^\circ$  are tabulated in a number of thermodynamic databases for a wide variety of liquids, gases, solids, and aqueous species.

Acid-base and redox reactions can also be written in a form analogous to Eq. (D-1), involving either the transfer of a proton (acid-base) or an electron (redox) (Mangold and Tsang, 1991). A mathematical construction similar to Eqs. (D-4) and (D-6) can then be used to express these types of reactions as functions of hydrogen ion activity (pH) and oxidation potential (Eh) or electron potential [ $pE = (F/2.303RT)Eh$ , where F is the Faraday constant =  $96.4935 \times 10^4$  J/volt equiv].

## D.2 NONEQUILIBRIUM CHEMICAL PROCESSES

Equilibrium thermodynamics is useful to tell the direction in which an overall reaction should proceed. Most chemical reactions, however, occur in a series of steps, one or more of which may require the input of energy into the system. This results in a series of energetic barriers that needs to be overcome for the reaction to run to completion. The rate at which equilibrium is approached will depend on a variety of properties. High temperature and pressure, as well as elevated concentrations of dissolved species and high surface area all contribute to supply the energy necessary to overcome kinetic barriers and tend to favor faster rates of reaction. In addition, the reaction rate is faster for systems that are far out of equilibrium, and it tends to decrease as the equilibrium state is approached. If enough time is available in a closed system with constant temperature and pressure conditions, an elementary reaction

of the form given by Eq. (D-1) will eventually reach equilibrium, and the development given in Eqs. (D-2) through (D-6) is appropriate. In many systems, however, the time available is not sufficient to overcome the kinetic barriers and allow the reaction to reach a steady-state equilibrium condition. Under these conditions, chemical kinetics are used to examine the rate at which chemical reaction occurs.

An elementary one-step chemical reaction of the form given in Eq. (D-1) is composed of a forward (f) reaction component (left to right by convention) and a reverse (r) reaction component. The overall rate of reaction,  $r$  (moles/sec), is the difference between the rate of these two components (i.e.,  $r = r_f - r_r$ ). Each direction of the reaction is also described by a rate constant. At equilibrium, rate constants are related to the equilibrium constant such that

$$K = \frac{k_f}{k_r} \quad (D-7)$$

where

$$\begin{aligned} k_f &= \text{the forward reaction rate constant (sec}^{-1}\text{)} \\ k_r &= \text{the reverse reaction rate constant (sec}^{-1}\text{)} \end{aligned}$$

Through this relationship, rate constants are expressed as a function of temperature according to the Arrhenius equation

$$k = A_p \exp\left(-\frac{E_a}{RT}\right) \quad (D-8)$$

where

$$\begin{aligned} A_p &= \text{a pre-exponential constant} \\ E_a &= \text{the activation energy (J/mole) for the reaction} \end{aligned}$$

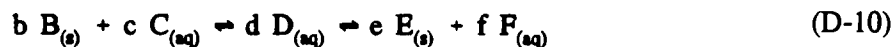
Reactions can be either reversible with comparable values for both  $k_f$  and  $k_r$  or irreversible if  $k_r$  is small relative to  $k_f$ . Generally determined experimentally through a set of time-series experiments, these constants are incorporated into mathematical expressions to define the progress of the reaction according to a rate law. The form that the mathematical expression takes is referred to as the *order* of the rate law. Defined as the change in concentration of a species  $S$ , of interest, the rate law takes the general form

$$\frac{dm_s}{dt} = k m_s^n \quad (D-9)$$

where  $m_s$  is molality. The order of the reaction with respect to a single reactant (or product) is referred to as the partial order of the reaction and is equal to the exponent  $n$  in Eq. (D-9) (e.g., if  $n_B = 2$ , the reaction is second-order with respect to B). The overall order of the reaction is the sum of all of the partial orders (Richardson and McSween, 1989).

Reaction progress generally consists of several steps. These include the transport of reactants to each other at an interface, the chemical reaction of these reactants, and the transport of the products

away from the interface. The slowest of these steps will become the rate-limiting step for the progress of the chemical reaction. In addition, each one of these steps may be comprised of one or more pathways that lead to either sequential or parallel formation of intermediate compounds, through a series of reactions such as



In this case, B and C react to form products, E and F, through the intermediate compound, D.

### D.3 REACTION PROGRESS MODELS

One critical aspect of a chemical system is the transfer of mass between the solid, gas, and liquid phase during chemical reactions. Using the principles outlined above, an approach has been developed (e.g., Helgeson, 1970) to model reaction progress in the natural system.

As discussed in the next section, several large thermodynamic databases exist for geologic materials (e.g., Robie et al., 1978; Helgeson et al., 1978; Parkhurst et al., 1980; Ball et al., 1987; Phillips et al., 1988; Wolery et al., 1990). Although the relationships outlined in Eqs. (D-1) through (D-12) are well understood, the data needed, particularly for the radionuclides, to support the modeling of chemical processes are frequently nonexistent. Also, the nonlinear nature of most chemical processes presents a challenge in adapting numerical methods to chemical modeling. In addition, where equilibrium processes can be expressed by a set of algebraic equations, kinetically controlled processes involve partial differential equations. Equilibrium thermodynamic treatment also offers the advantage of determining the chemical status of the overall status of the system when our knowledge of the specific mechanisms involved is limited. Due to this simplicity, equilibrium is often assumed at one or more scales in the treatment of chemical processes.

Reaction progress models are a way of monitoring the approach to equilibrium through a series of sequential homogeneous equilibrium reactions. Helgeson (1979) notes that the assumption of partial equilibrium accepts that, although the system under consideration is likely to be out of equilibrium with respect to one or more processes, it can also be considered to exist in equilibrium with respect to at least one process. In a similar fashion, an assumption of local equilibrium assumes that, at small scales of time and space, chemical reactions maintain homogeneous equilibrium.

Based on the assumptions of partial and/or local equilibrium, the chemical affinity ( $A^*$ ) has been defined for the process of interest (De Donder and van Rysselberghe, 1936; Prigogine, 1955; Helgeson, 1979) such that

$$A^* = RT \ln[K/Q] = - \left( \frac{\partial G}{\partial \xi} \right)_{P,T} \quad (D-11)$$

where R, T, G, K, and Q are as defined above. The higher the chemical affinity, the more favored the reaction. At equilibrium,  $A^* = 0$ .  $\xi$  is a measure of the degree to which the rate-limiting reaction in the process has proceeded and represents the total number of moles of reactants converted into products divided by the appropriate stoichiometric coefficient of the reactant in the reaction being considered. Since the rate-limiting reaction controls the rate of the overall reaction, changing  $\xi$  through a series of small

but finite steps allows reaction progress to be monitored through a series of homogeneous, equilibrium reactions. From this approach, the reaction rate near equilibrium can be expressed such that

$$r = \frac{\partial \xi}{\partial t} = \frac{k_f A^*}{RT} \quad (\text{D-12})$$

#### D.4 THERMODYNAMIC DATABASES

A great deal of effort has been made to determine experimentally the thermodynamic properties necessary for the modeling of chemical processes. There have been many compilations of data which vary in the amount of attention paid to the quality and internal consistency of the data, completeness of the dataset, and the pressure and temperature ranges over which the data are valid. Several recent studies (Baes and Mesmer, 1976; Krupka et al., 1988; Phillips et al., 1988; Serne et al., 1990) have outlined strategies and selection criteria for evaluating chemical data for inclusion in a comprehensive database. There are also approaches for estimating thermodynamic data for some less well characterized compounds (Phillips et al., 1988). Some authors (Haas, 1974; Helgeson et al., 1978) have used statistical regression analyses to derive internally consistent databases. With respect to more common elements and phases, abundant experimental data are available. These data have been refined through application in a wide variety of chemical environments, and the agreement between different data sources is often good over a broad range in temperatures and pressures. However, for many trace elements, such as the chemically complex transuranic elements important in high-level waste disposal, available data are sparse, and agreement is frequently poor.

Table D-1 (after Serne et al., 1990) is a listing of the more commonly used compilations of thermodynamic data. Special emphasis is placed on those data related to geochemical reaction codes. The reader is referred to the original reference (and the references therein) for specifics on how the data were generated and selected.

#### D.5 COUPLING WITH OTHER PROCESSES

Through changes in fluid, gas, and solid properties, thermal, mechanical and hydrological processes in the repository environment will be affected through coupling with chemical reactions of the forms given in Eqs. (D-1) and (D-12). These effects will be discussed in more detail in Section 2. In a general sense, however, these changes may include the following:

- Fluids — The presence of aqueous species in solution can affect a variety of fluid properties, including density, viscosity, vapor pressure (boiling curve), heat capacity, and the degree of saturation with respect to different solid phases. In addition, molecular diffusion along chemical gradients may lead to solute transport in the absence of advection. Similarly, diffusion of uncharged water molecules across semipermeable clay layers in response to salinity gradients can result in an osmotic pressure gradient which, in turn, can affect fluid flow.

**Table D-1. Examples of Tabulations of Thermodynamic Data (Modified from Serne et al., 1990)**

<b>TITLE</b>	<b>REFERENCE</b>
The Hydrolysis of Cations	Baes and Mesmer (1976)
JANAF Thermochemical Tables. 3rd Edition. Part I (Al-Co); Part II (Cr-Zr)	Chase et al. (1985a,b)
CODATA: Key Values for Thermodynamics	Cox et al. (1989)
Summary and Critique of the Thermodynamic Properties of Rock-Forming Minerals	Helgeson et al. (1978)
Standard Potentials in Aqueous Solutions	Bard et al. (1985)
Handbook of Thermodynamic Data	Naumov et al. (1974)
The Chemical Thermodynamics of Actinide Elements and Their Compounds. Part 1 (The Actinide Elements); Part 2 (The Actinide Aqueous Ions); Part 3 (Miscellaneous Actinide Compounds), and others	Oetting et al. (1976) Fuger and Oetting (1976) Cordfunke and O'Hare (1978)
Thermodynamic Tables for Nuclear Waste Isolation: Aqueous Solutions Database	Phillips et al. (1988)
Chemical Thermodynamics of Technetium	Rard (1989)
Thermodynamic Properties of Minerals and Related Substances at 298.15 K and 1 Bar ( $10^5$ Pascals) Pressure and at Higher Temperatures	Robie et al. (1978)
Selection of Standard Free Energies of Formation for Use in Soil Chemistry	Sadiq and Lindsay (1979, 1981) Elrashidi and Lindsay (1984)
Critical Stability Constants. Volume 4: Inorganic Complexes	Smith and Martell (1976)
The NBS Tables of Chemical Thermodynamic Properties. Selected Values for Inorganic and $C_1$ and $C_2$ Organic Substances in SI Units	Wagman et al. (1982)
NEA-TDB: Chemical Thermodynamics of Uranium	Grenthe et al. (1992)
A Tabulation of Thermodynamic Data for Reactions Involving 58 Elements Common to Radioactive Waste Package Systems	Benson and Teague (1980)
Revised Chemical Equilibrium for Major Water-Mineral Reactions and Their Limitations	Nordstrom et al. (1990)
The CHEMVAL Database	Read and Broyd (1989)
SUPCRT92: A Software Package for Calculating the Standard Molal Thermodynamic Properties of Minerals, Gases, Aqueous Species, and Reactions from 1 to 5000 bars and 0 to 1000 °C.	Johnson et al (1991) Tanger and Helgeson (1988) Shock and Helgeson (1988, 1990) Sverjensky et al. (1991)
Thermodynamic Values at Low Temperature for Natural Inorganic Materials: An Uncritical Summary	Woods and Garrels (1987)

- Solids — Determined by the solubility of the mineral of interest, precipitation, and dissolution of different solid phases as reactions progress can affect porosity and permeability of the medium. In addition, the production of intermediate species through incongruent mineral dissolution may produce significant changes in properties, such as volume and sorptive capacity, depending on the phase produced. Mechanical properties of a medium can also be affected by chemical processes, such as oxidation or aqueous corrosion of metals, or weakening of natural materials through dissolution and weathering. Through reaction, solid phases can act as a buffer on the composition of fluids (e.g., pH, Eh, and ionic strength). Electrolytes can also be removed (or added) from solution either by the precipitation/dissolution of stoichiometric compounds or by the inclusion of electrolytes as trace impurities in other solid phases. In addition to precipitation/dissolution, solids can also act as a source or a sink through a variety of surface reactions, such as ion exchange, adsorption/desorption, and matrix diffusion.
- Gases - Each gas phase present in a system will reach equilibrium with the liquid phase through the exchange of molecules across the gas/water interface. Changes in gas partial pressures will set up pressure gradients, and lead to a new set of equilibrium conditions if time is sufficient. Gas is produced through biological or chemical reactions and can lead to increased pressures and buffering of solution pH, Eh, and composition. Since several radionuclides are thought to occur as gas phases ( $^{14}\text{C}$ ,  $^{129}\text{I}$ ), an increased gas flux could lead to increased radionuclide migration to the accessible environment.

Equations (D-6) and (D-12) demonstrate some of the temperature dependence of equilibrium chemistry and reaction rates. In addition, a variety of chemical parameters (log K, rate constants, pH, activity/concentration relationships) vary as a function of temperature. In a natural system, hydrologic conditions can also have a significant effect on system chemistry. Fluid flow will determine, to a large extent, whether or not the system is open or closed to different given solid, aqueous, or gas phases. Flow rates will determine the time available for a reaction to approach equilibrium. Fluid flow paths determine fluid compositions and which minerals are involved in chemical reactions.

Based on analyses of the anticipated thermal loading at Yucca Mountain (Pruess and Wang, 1987), temperature is likely to be one of the primary couples to affect system chemistry. Fluid flow and saturation (Turner, 1991) are also critical in applying chemical principles to modeling the transport of radionuclides from the repository to the accessible environment. Clearly, chemistry is closely coupled with the temperature and fluid flow regimes of the repository environment. Understanding the complex feedbacks between these regimes is an important step in evaluating the ability of the repository to successfully isolate high-level radioactive waste. Mechanical effects are likely to be less direct, involving aspects such as pulse inputs due to barrier failure, or providing access for fluids and gases to the waste package.